

REPORT DOCUMENTATION PAGE

Form Approved
OMB No. 074-0188

Public reporting burden for this collection of information is estimated to average 1 hour per response, including the time for reviewing instructions, searching existing data sources, gathering and maintaining the data needed, and completing and reviewing this collection of information. Send comments regarding this burden estimate or any other aspect of this collection of information, including suggestions for reducing this burden to Washington Headquarters Services, Directorate for Information Operations and Reports, 1215 Jefferson Davis Highway, Suite 1204, Arlington, VA 22202-4302, and to the Office of Management and Budget, Paperwork Reduction Project (0704-0188), Washington, DC 20503.

1. AGENCY USE ONLY (Leave blank)		2. REPORT DATE August 28, 2001	3. REPORT TYPE AND DATES COVERED Final Technical Report: 01/01/98 to 09/30/98
4. TITLE AND SUBTITLE "SHOCK PROPAGATION AND SUPERSONIC DRAG IN LOW TEMPERATURE PLASMAS" Support for AFOSR-SPONSORED WORKSHOP: "Understanding and Control of Ionized High-Speed Flows." Held at Princeton University, Princeton, NJ, Feb. 26-27, 1998		5. FUNDING NUMBERS AFOSR Grant #F49620-97-1-0497 P00002	
6. AUTHOR(S) Professor Richard B. Miles			
7. PERFORMING ORGANIZATION NAME(S) AND ADDRESS(ES) Princeton University Dept. Mechanical & Aerospace Engrg. Olden St. Princeton, NJ 08544		8. PERFORMING ORGANIZATION REPORT NUMBER	
9. SPONSORING / MONITORING AGENCY NAME(S) AND ADDRESS(ES) AFOSR/NA 801 North Randolph St. Room 732 Arlington, VA 22203-1977		10. SPONSORING / MONITORING AGENCY REPORT NUMBER	
11. SUPPLEMENTARY NOTES			
12a. DISTRIBUTION / AVAILABILITY STATEMENT Approved for public release; distribution is unlimited.			12b. DISTRIBUTION CODE
13. ABSTRACT (Maximum 200 Words) This grant supported an Air Force-sponsored workshop, "Understanding and Control of Ionized High-Speed Flows," which was conducted at Princeton University, February 26-27, 1998. In recent years, there has been a great deal of interest in the formation mechanisms and properties of air plasmas. This interest is, in part, motivated by experiments conducted in Russia and in the United States which indicate shock propagation in weakly ionized air plasmas is at a higher velocity than would be predicted by presently understood models. If this is, indeed, the case, such plasmas could be used for supersonic/hypersonic drag reduction. In addition, atmospheric plasmas could influence flow control devices, electromagnetic attenuation, and hypersonic propulsion systems. As a consequence, the formation of such plasmas in atmospheric pressure environments, and the study of the properties of these plasmas, are of significant national interest.			
14. SUBJECT TERMS Air plasmas, Weakly ionized air plasmas, AFOSR workshop			15. NUMBER OF PAGES 2 plus 1 Appendix
			16. PRICE CODE
17. SECURITY CLASSIFICATION OF REPORT Unclassified	18. SECURITY CLASSIFICATION OF THIS PAGE Unclassified	19. SECURITY CLASSIFICATION OF ABSTRACT Unclassified	20. LIMITATION OF ABSTRACT UL

NSN 7540-01-280-5500

Standard Form 298 (Rev. 2-89)
Prescribed by ANSI Std. Z39-18
298-102

20010905 179

FINAL TECHNICAL REPORT (Dated 8/28/01)

AFOSR GRANT #F4920-97-1-0497, P00002
(150-6756)

**"SHOCK PROPAGATION AND SUPERSONIC DRAG IN
LOW TEMPERATURE PLASMAS"**

SUPPORT FOR:

**AFOSR-SPONSORED WORKSHOP ENTITLED:
"Understanding and Control of Ionized High-Speed Flows"**
Princeton University
Princeton, NJ 08544
February 26-27, 1998

ABSTRACT

This grant supported the costs of an Air Force-sponsored workshop, "Understanding and Control of Ionized High-Speed Flows," which was conducted at Princeton University, February 26-27, 1998. In recent years, there has been a great deal of interest in the formation mechanisms and properties of air plasmas. This interest is, in part, motivated by experiments conducted in Russia and in the United States which indicate shock propagation in weakly ionized air plasmas is at a higher velocity than would be predicted by presently understood models. If this is, indeed, the case, such plasmas could be used for supersonic/hypersonic drag reduction. In addition, atmospheric plasmas could influence flow control devices, electromagnetic attenuation, and hypersonic propulsion systems. As a consequence, the formation of such plasmas in atmospheric pressure environments, and the study of the properties of these plasmas, are of significant national interest.

DISCUSSION

The purpose of the workshop was to highlight the basic science issues involved with controlling high-speed flows using weakly-ionized plasmas. The specific objectives of the two-day meeting were to review recent experimental/theoretical research in this area, and to exchange ideas/understanding on the basic flow physics of the problem, and to discuss future research directions. Princeton University was a natural location for this workshop since work is underway here to examine both drag characteristics and electron discharge physics associated with weakly ionized plasmas.

Sixty individuals, each of whom is considered a leading authority on this issue, attended the two-day workshop (a full listing of the participants is located in Appendix A). The first day of the workshop consisted of four sessions on an agenda of twelve speakers and covered the following topics:

Session I: "Introduction to the Problem" (presentations by B. Ganguly of AFRL and A. Auslender of NASA LaRc).

Session II: "Aerodynamics of Ionized Flow" (presentations by R. Miles of Princeton University, J. Shang of AFRL, N. Malmuth and V. Soloviev of Rockwell Science, and V. Subramanian of The Ohio State University).

Session III: "Theory and Computation of Ionized Flows" (presentations by G. Karniadakis of Brown University, K. Powell of the University of Michigan, and S. Nazarenko of the University of Arizona).

Session IV: "Plasma Generation and Maintenance" (Presentations by S. Kuo of Polytechnic University, J. Kline of Research Support Instruments, and W. Rich of The Ohio State University).

The second day of the workshop, the participants were divided into four separate working groups for further discussion, followed by debriefings and laboratory tours at Princeton.

Appendix A is a complete record of the two-day workshop and includes the final agenda for the meeting, the complete list of participants and their contact information, as well as copies of each of the presentations for all of the four topic areas listed above.

Appendix A

Princeton University

School of Engineering and Applied Science
Department of Mechanical and Aerospace Engineering
P.O. Box CN5263
Princeton, New Jersey 08544-5263



FINAL AGENDA

AFOSR-SPONSORED WORKSHOP:

"UNDERSTANDING AND CONTROL OF IONIZED HIGH-SPEED FLOWS"

February 26-27, 1998

MEETING LOCATION: Convocation Room (C217) Engineering Quadrangle
Olden Street, Princeton, NJ 08544

THURSDAY, FEBRUARY 26, 1998:

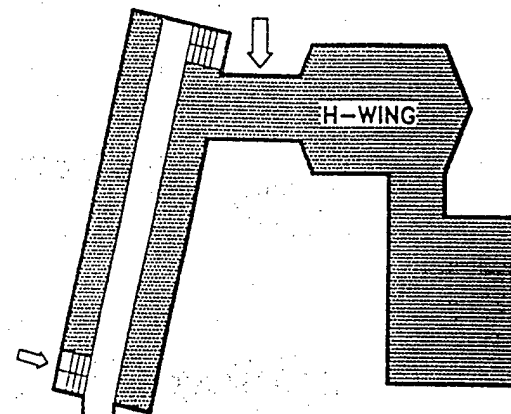
7:30 AM	SIGN-IN/COFFEE
8:00 AM	OPENING REMARKS: G.L. Brown--Chairman, MAE Dept., Princeton R. Miles--Princeton S. Walker--AFOSR
8:30 AM	SESSION I: INTRODUCTION TO THE PROBLEM B. Ganguly--AFRL, A. Auslender--NASA LaRC
9:30 AM	DISCUSSION
10:00 AM	BREAK
10:30 AM	SESSION II: AERODYNAMICS OF IONIZED FLOW R. Miles--Princeton, J. Shang--AFRL, N. Malmuth/V. Soloviev--Rockwell Science V. Subramanian--OSU
11:30 AM	DISCUSSION
12:00 PM	LUNCH
1:30 PM	SESSION III: THEORY AND COMPUTATION OF IONIZED FLOWS G. Karniadakis--Brown U., K. Powell--UM, S. Nazarenko--UA
2:30 PM	DISCUSSION
3:00 PM	BREAK
3:30 PM	SESSION IV: PLASMA GENERATION AND MAINTENANCE S. Kuo--Polytechnic Univ., J. Kline--RSI, W. Rich--OSU
4:30 PM	DISCUSSION
5:00 PM	FIRST DAY WRAP-UP
6:00 PM	RECEPTION, Prospect House

FRIDAY, FEBRUARY 27, 1998:

7:30 AM	SIGN-IN/COFFEE
8:00 AM	OPENING REMARKS
8:15 AM	WORKING GROUPS
10:30 AM	BREAK
11:00 AM	GROUP DEBRIEFINGS
12:00 PM	LUNCH/LABORATORY TOUR

ENGINEERING QUADRANGLE

A-WING	Chemical Engineering
B-WING	Electrical Engineering
C-WING	SEAS Faculty Lounge
D-WING	Mechanical & Aerospace Engineering
E-WING	Civil Engineering and Operations Research
G-WING	Energy Research Lab
H-WING	Von Neumann Hall
J-WING	POEM/EE/MAE
COS	Computer Science



Elevators

Entrances/Exits

● Handicapped Access

G-WING

Room #3 (Rm. G-201)
Eisenhart Conference Room

Room #2 (Rm. J-223)
MAE Faculty Lounge

A-WING

Main Meeting (Room C-217)
Convocation Room

Room #1 (Rm. C-222)
Dean's Conference Room

LIBRARY

B-WING

C-WING

E-WING

Main Entrance

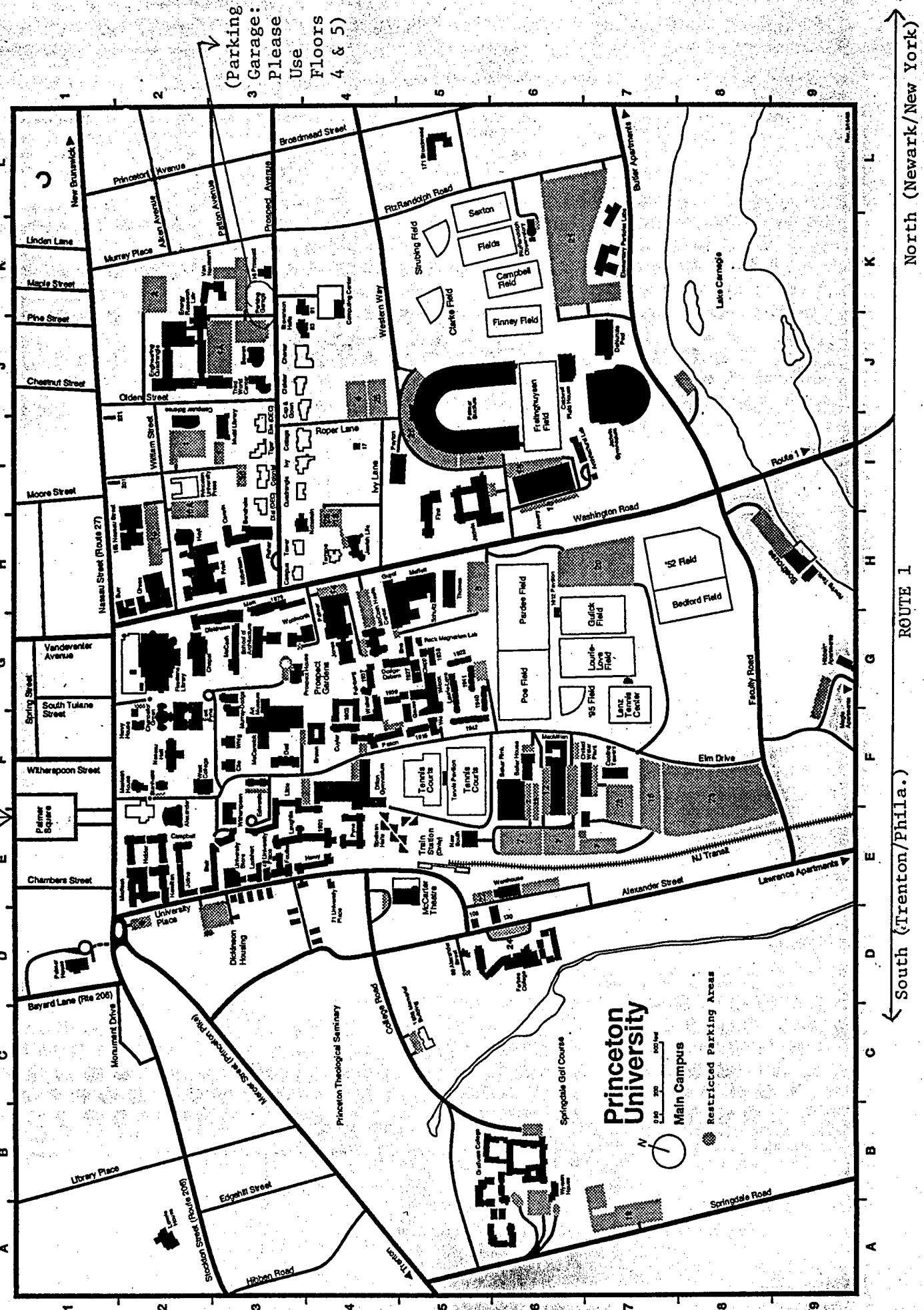
Olden Street

COMPUTER SCIENCE BUILDING

Restrooms are located in the corners
of the building where 2 wings meet.

CAMPUS MAP

Nassau Inn



North (Newark/New York)

ROUTE 1

← South (Trenton/Phila.)

PARTICIPANT LIST

AFOSR-SPONSORED WORKSHOP: "UNDERSTANDING & CONTROL OF IONIZED HIGH-SPEED FLOWS"

PRINCETON UNIVERSITY
FEBRUARY 26-27, 1998

NAME	ADDRESS	PHONE/FAX NUMBERS	E-MAIL
ADAMOVICH, Igor	The Ohio State University Dept. Mechanical Engineering 2019 Robinson Laboratory 206 West 18 th Avenue Columbus, OH 43216	614-292-0561 (P) 614-292-3163 (F)	Adamo@mps.ohio-state.edu
AUSLENDER, Aaron	NASA-Langley Research Center MS 168 Hampton, VA 23681	757-864-6545 (P)	A.H.Auslander@LaRC.NASA.GOV
BAILEY, William	AFIT/ENP, Dept. of Physics 2950 P Street Wright-Patterson AFB, OH 45433	937-255-3636 x4501 (P) 937-255-2921 (F)	wbailey@afit.af.mil
BAIN, Lee	AFRL/PR Bldg. 18 1950 Fifth St., Suite 10 WPAFB, OH 45433-7251	937-255-1237 (P) 937-656-4659 (F)	Bainwl@wl.wpafb.af.mil
BARKER, Robert	AFOSR/NE 110 Duncan Ave., Suite B115 Bolling AFB, DC 20332	202-767-5011 (P) 202-767-4986 (F)	Robert.barker@afosr.af.mil
BERMAN, Michael	AFOSR/NL 110 Duncan Avenue, Suite B115 Bolling AFB, DC 20332	202-767-4963 (P) 202-404-7475 (F)	Michael.berman@afosr.af.mil
BEUTNER, Thomas J.	WL/FIMO 2145 5 th Street Aero-Diagnostics Research Section Wright-Patterson AFB, OH 45433-7005	219-872-5694 (P)	
BRANDENBURG, John	Research Support Instruments 4325-B Forbes Blvd. Lanham, MD 20706	301-306-0010 (P) 301-306-0295 (F)	Rsidc@mindspring.com

NAME	ADDRESS	PHONE/FAX NUMBERS	E-MAIL
BROWN, Garry L.	Princeton University MAE Dept., Rm D-216 E-Quad Olden Street Princeton, NJ 08544	609-258-6083 (P) 609-258-6109 (F)	Glb@princeton.edu
BUSHNELL, Dennis M.	NASA Langley Research Center MS-197 Hampton, VA 23665-5225	757-864-8987 (P) 757-864-8980 (F)	d.m.busnell@larc.nasa.gov
CAMBIER, Jean-Luc	MSE Technology Applications, Inc. PO Box 4078 220 North Alaska Street Butte, MT 59702	406-494-7304 (P) 406-494-7230 (F)	
CAPPELLI, Mark	Stanford Univresity Mechanical Engineering Dept. Stanford, CA 94305-3032	650-725-2020 (P) 650-723-1748 (F)	cap@leland.stanford.edu
CARTER, Campbell D.	Innovative Scientific Solutions, Inc. 2786 Indian Ripple Road Dayton, OH 45440-0001	937-255-8704 (P) 937-656-4652 (F)	Cartered@possum.appl.wpafb.af.mil
CHASE, Raymond L.	ANSER, Inc. Crystal Gateway 1215 Jefferson Davis Highway Arlington, VA 22202-3251	703-416-3290 (P) 703-416-3329 (F)	Chaser@answer.org
CHOUEIRI, Edgar	Princeton University MAE Dept., Rm D-432 E-Quad Olden Street Princeton, NJ 08544	609-258-5220 (P) 609-258-6109 (F)	Choueiri@princeton.edu
DRYER, Frederick L.	Princeton University MAE Dept., Rm D-316 E-Quad Olden Street Princeton, NJ 08544	609-258-5206 (P) 609-258-1939 (F)	Fdryer@phoenix.princeton.edu
EFTHIMION, Philip	Princeton Plasma Physics Laboratory Princeton University B244 C-Site PPPL Princeton, NJ 08544	609-243-3212 (P) 609-243-2874 (F)	Pefthimion@pppl.gov
GAITONDE, Datta	AFRL/VAAC Rm A-120, Bldg 450 2645 Fifth St., Suite 7 WPAFB, OH 45433-7913	937-255-7127 (P) 937-656-4210 (F)	Datta@fim.wpafb.af.mil

NAME	ADDRESS	PHONE/FAX NUMBERS	E-MAIL
GANGULY, Bish	AFRL/PR 2645 Fifth St., Suite 13 Wright-Patterson AFB, OH 45433-7919	937-255-2923 (P) 937-476-4095 (F)	Gangulbn@possum.appl.wpafb.af.mil
GARSCADDEN, Alan	AFRL/PR Building 18 1950 Fifth St., Suite 10 Wright-Patterson AFB, OH 45433-7251	937-255-2246 (P) 937-255-6641 (F)	Garscaa@wl.wpafb.af.mil
JACKSON, Thomas A.	AFRL/PR Building 18 1950 Fifth St., Suite 10 Wright Patterson AFB, OH 45433-7251	937-255-1234 (P) 937-656-4659 (F)	Jacksonta@wl.wpafb.af.mil
JAHN, Robert	Princeton University MAE Dept., Rm. D-334 E-Quad Olden Street Princeton, NJ 08544	609-258-4550 (P) 609-258-6109 (F)	Rjahn@princeton.edu
KARNIADAKIS, George	Brown University Center for Fluid Mechanics Division of applied Mathematics Providence, RI 02912	401-863-1217 (P)	Gk@cfm.brown.edu
KEEFER, Dennis	Univ. Tennessee Space Institute Gas Diagnostics Research Division Tullahoma, TN 37388-8897	931-393-7475 (P) 931-454-2271	Dkeefer@utsi.edu
KIMMEL, Roger	AFRL/VAAA Bldg. 450 2645 Fifth St., Suite 7 WPAFB, OH 45433-7913	937-255-2193 (P) 937-656-7868 (F)	Kimmelr@fim.wpafb.af.mil
KLINE, John	Research Support Instruments 4325-B Fores Blvd. Lanham, MD 20706	301-306-0295 (P)	
KORETZKY, Edward	Polytechnic University		
KUO, Spencer	Polytechnic University Route 110 Farmingdale, NY 11735	516-755-4301 (P) 516-755-4404 (F)	Spkuo@poly.edu

NAME	ADDRESS	PHONE/FAX NUMBERS	E-MAIL
KUSHNER, Mark J.	University of Illinois Dept. of Electrical & Computer Engrg. 1406 W. Green St. Urbana, IL 61801	217-244-7096 (P) 217-244-7097 (F)	Mjk@uiuc.edu
LAM, Sau-Hai	Princeton University MAE Dept., Rm. D-302C E-Quad Olden Street Princeton, NJ 08544	609-258-5133 (P) 609-258-6109 (F)	Lam@princeton.edu
LAW, C.K.	Princeton University MAE Dept., Rm D-323 E-Quad Olden Street Princeton, NJ 08544	609-258-5271 (P) 609-258-6233 (F)	Cklaw@princeton.edu
LAWLESS, John	Redwood Scientific, Inc. 1005 Terra Nova Blvd. Pacific, CA 94044	650-738-8083 (P) 650-738-8086 (F)	70262.363@comuserve.com
LEONE, Stephen	University of Colorado Campus Box 440 Boulder, CO 80309-0440	303-492-5128 (P) 303-492-5504	Srl@jila.colorado.edu
MACHERET, Sergey	Princeton University, MAE Dept. Room D-414 E-Quad Olden St. Princeton, NJ 08544	609-258-5130 (P) 609-258-1139 (F)	Macheret@princeton.edu
MALMUTH, Norman	Rockwell Science Center 1049 Camino Dos Rios Thousand Oaks, CA 91360	805-373-4154 (P) 805-373-4775 (F)	Ndm@norman.risc.rockwell.com
McMICHAEL, James	DARPA/TTO 3701 N. Fairfax Drive Arlington, VA 22203-1714	703-696-2377 (P)	JmcMichael@darpa.mil
MICCI, Michael M.	Pennsylvania State University Dept. of Aerospace Engineering 233 Hammond Building University Park, PA 16802	814-863-0043 (P) 814-865-7092 (F)	Micci@henry2.aero.psu.edu
MILES, Richard	Princeton University MAE Dept., Rm D414 EQ Olden Street Princeton, NJ 08544	609-258-5131 (P) 609-258-1139 (F)	Miles@hepcat.princeton.edu

NAME	ADDRESS	PHONE/FAX NUMBERS	E-MAIL
MORRIS, Robert	AFRL/VSBP 29 Randolph Road Hanscom AFB, MA 01731	617-377-8758 (P) 617-377-1148 (F)	Morris@plh.af.mil
MURTHY, S.N.B.	Purdue University Thermal Sciences & Propulsion Center School of Mechanical Engineering 1003 Chaffee Hall West Lafayette, IN 47907-1003	765-494-1501 (P) 765-494-0530 (F)	
NACHMAN, Arje	AFOSR/NM 110 Duncan Avenue Bolling AFB, DC 20332	202-767-4939 (P) 202-404-7496 (F)	Arje.nachman@afosr.af.mil
NAZARENKO, Sergey	University of Arizona Dept. of Mathematics 617 N. Santa Rita Ave. Tucson, AZ 85721		
NELSON, Gordon	MSE Technology Applications, Inc. PO Box 4078 220 North Alaska Street Butte, MT 59702	406-494-7403 (P) 406-494-7230 (F)	Gnelson@buttenet.com
PETERKIN, Robert E.	AFRL/DEHE 3550 Aberdeen Ave., SE Kirtland AFB, NM 87117-5776	505-846-0259 (P)	Bob@ppws07.plk.af.mil
POGGIE, Jonathan	US Air Force Research Laboratory AFRI/VAAA 2645 Fifth St., Suite 7 WPAFB, OH 45433-7913	937-255-5464 (P) 937-656-7868 (F)	Poggiej@fm.wpafb.af.mil
POWELL, Kenneth	University of Michigan Dept. of Aerospace Engineering Ann Arbor, MI 48109-1248	313-764-3331 (P) 734-763-0578 (F)	Powell@engin.umich.edu
RABITZ, Herschel	Princeton University Dept. of Chemistry 129 Frick Lab Princeton, NJ 08544	609-258-3917 (P) 609-258-6746 (F)	Hrabitz@chemvax.princeton.edu
RICH, William	The Ohio State University Robinson Laboratory 206 W. 18 th Avenue Columbus, OH 43210-0001	614-292-6309 (P) 614-292-3163 (F)	Rich.2@osu.edu

NAME	ADDRESS	PHONE/FAX NUMBERS	E-MAIL
SCHRECK, Scott	AFOSR/NM 110 Duncan Avenue, Suite B115 Bolling AFB, DC 20332	202-767-7902 (P) 202-404-7496 (F)	Scott.schreck@afosr.af.mil
SHANG, Joseph	AFRL/VA Building 450 2645 Fifth St., Suite 7 Wright-Patterson AFB, OH 45433-7913	937-255-6156 (P)	
SHEROHMAN, John	Lawrence Livermore National Laboratory PO Box 808, L-377 Livermore, CA 94551	510-422-1059 (P) 510-422-4563 (F)	Sherohman1.llnl.gov
SHUMLAK, Uri	University of Washington Aeronautics & Astronautics Dept. Box 352250 Seattle, WA 98195-2250	206-616-1986 (P) 206-543-4719 (F)	Shumlak@aa.washington.edu
SMITS, Alexander	Princeton University MAE Dept., Rm. D-302D E-Quad Olden St. Princeton, NJ 08544	609-258-5117 (P) 609-258-6109 (F)	Asmits@princeton.edu
SOLOVIEV, Victor	Rockwell Science Center 1049 Camino Dos Rios Thousand Oaks, CA 91360		Vics@post.mipt.rssi.ru
SUBRAMANIAM, Vish V.	The Ohio State University Dept. of Mechanical Engineering 2087 Robinson Lab 206 West 18 th Avenue Columbus, OH 43210	614-292-6096 (P) 614-292-3163 (F)	Subramaniam.1@osu.edu
TISHKOFF, Julian	AFOSR/NA 110 Duncan Avenue, Suite B115 Bolling AFB, DC 20332	202-767-0465 (P) 202-767-4988 (F)	Julian.tishkoff@afosr.af.mil
TURCHI, Peter	AFRL/DE Kirtland AFB, NM		Turchi.1@osu.edu
VAN WIE, David	Johns Hopkins 11100 Johns Hopkins Road Bldg. 10A, Room 115 Laurel, MD 20723-6099	301-953-5194 (P) 410-792-5850 (F)	David.vanwie@jhunapl.edu

Understanding and Control of Ionized High-Speed Flows

AFOSR-Sponsored Workshop

Princeton University

26-27 Feb 98



NEW WORLD VISTAS (NWW)

- **41 Technologies Identified By AFMC And The Air Force Scientific Advisory Board**
- **32 NWW Technologies To Receive Basic Research Support**
- **\$14.8M Budget For FY 1997**

HYPERSONICS

Objectives

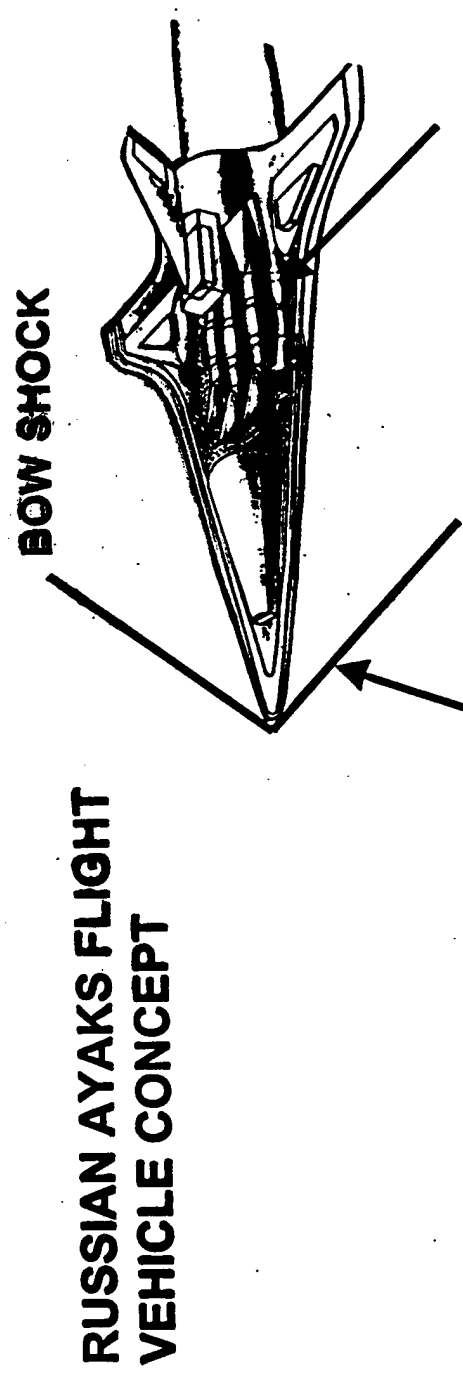
- Investigate Advanced Propellants And Cooling Concepts To Enable Hydrocarbon-Fueled Mach 8+ Aeropropulsion And Combined Cycle Propulsion
- Examine Electromagnetic Manipulation Of Ionized Flowfields To Improve Hypersonic Vehicle Performance



NEW WORLD VISTAS POWER PROJECTION AND MOBILITY

TOPIC 08 - HYPERSONICS

RESEARCH ISSUE: IMPACT OF WEAKLY IONIZED FLOWS ON
VEHICLE/PROPULSION SYSTEM PERFORMANCE



MEASUREMENTS INDICATE THAT
UNSTEADY ANALYSIS IS REQUIRED
TO DESCRIBE ENERGY TRANSFER
BETWEEN SHOCKS AND NONEQUILIBRIUM
MEDIA (GANGULY, AFRL/PR)

EXPERIMENTAL RESULTS SHOW THAT
REACTION WITH IONIZED AIR CAUSES
HYDROCARBON FUEL COMPONENTS
TO DECOMPOSE AND FORM REACTIVE
FREE RADICALS (MORRIS, AFRL/VSS)

Background

- Many experiments have shown large changes in shock strength, speed, and stand-off distance in weakly-ionized flows
- Complete analysis of proposed mechanisms for the observed shock dynamics is lacking
- US interest/research is increasing - USAFA June 97 workshop



Purpose of Workshop

- Highlight basic science issues involved with controlling high-speed flows using weakly-ionized plasma
 - Review recent basic research in the area
 - Technical exchange on flow physics
 - Discuss future directions



FINAL AGENDA

AFOSR-SPONSORED WORKSHOP:

"UNDERSTANDING AND CONTROL OF IONIZED HIGH-SPEED FLOWS"

February 26-27, 1998

MEETING LOCATION: Convocation Room (C217) Engineering Quadrangle
Olden Street, Princeton, NJ 08544

THURSDAY, FEBRUARY 26, 1998:

7:30 AM	<i>SIGN-IN/COFFEE</i>
8:00 AM	<u>OPENING REMARKS:</u> G.L. Brown--Chairman, MAE Dept., Princeton R. Miles--Princeton S. Walker--AFOSR
8:30 AM	<u>SESSION I: INTRODUCTION TO THE PROBLEM</u> B. Ganguly--AFRL, A. Auslender--NASA LaRC
9:30 AM	DISCUSSION
10:00 AM	<i>BREAK</i>
10:30 AM	<u>SESSION II: AERODYNAMICS OF IONIZED FLOW</u> R. Miles--Princeton, J. Shang--AFRL, N. Malmuth/V. Soloviev--Rockwell Science V. Subramanian--OSU
11:30 AM	DISCUSSION
12:00 PM	LUNCH
1:30 PM	<u>SESSION III: THEORY AND COMPUTATION OF IONIZED FLOWS</u> G. Karniadakis--Brown U., K. Powell--UM, S. Nazarenko--UA
2:30 PM	DISCUSSION
3:00 PM	<i>BREAK</i>
3:30 PM	<u>SESSION IV: PLASMA GENERATION AND MAINTENANCE</u> S. Kuo--Polytechnic Univ., J. Brandenburg--RSI, W. Rich--OSU
4:30 PM	DISCUSSION
5:00 PM	FIRST DAY WRAP-UP
6:00 PM	<i>RECEPTION, Prospect House</i>

FRIDAY, FEBRUARY 27, 1998:

7:30 AM	<i>SIGN-IN/COFFEE</i>
8:00 AM	OPENING REMARKS
8:15 AM	WORKING GROUPS
10:30 AM	<i>BREAK</i>
11:00 AM	GROUP DEBRIEFINGS
12:00 PM	LUNCH/LABORATORY TOUR

Rules of Engagement



- Let's keep this science-oriented but relevant; we'll let someone else actually build AJAX
- Let's really attempt to better understand this stuff before we leave
- Let's critique the work, but not criticize the people
- Please don't say, "It's just a thermal effect"; prove it.
- Don't be afraid to ask questions; we have people from many diverse technical backgrounds here
- Government people never say stupid things (by default)
- Please treat the second day as your collective chance to shape the future AF basic research investment in this area
- Let's have fun - 2 days without email, voice mail, dept. chairs, supervisors, etc.

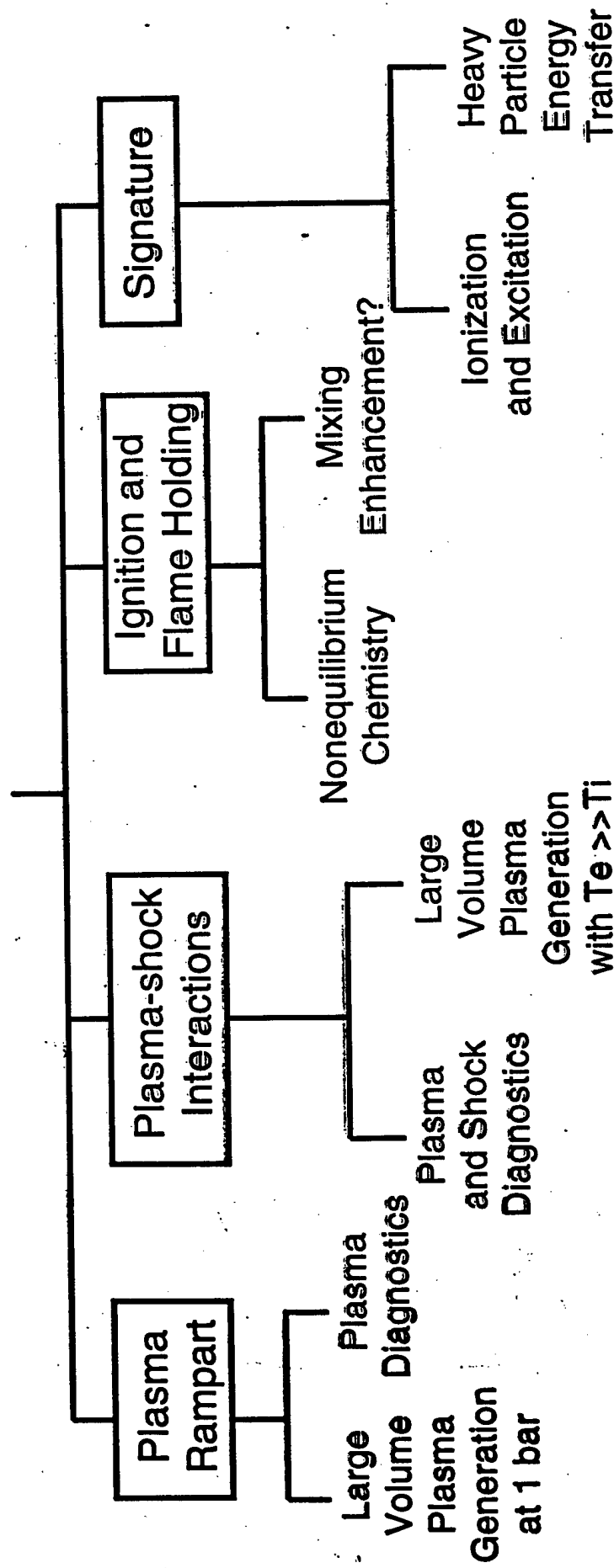
AFOSR
Workshop

Princeton Univ

Feb 26, 1998

Dr. Bish Ganguly

Nonequilibrium Air Plasma



POTENTIAL PAYOFFS OF NONEQUILIBRIUM PLASMAS TO HYPERSONICS

- Thermal problem minimized - shock wave dissipation by nonequilibrium plasmas
- Combustion efficiency improvement - mixing enhancement by plasma interactions
- Drag reductions through boundary layer control
- Improve ignition and flame holding for subsonic to hypersonic combustor by nonequilibrium plasma chemistry

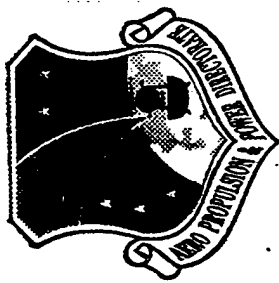
EXPERIMENTAL OBSERVATIONS OF PLASMA-SHOCK INTERACTIONS

- Shock wave dispersion, damping and velocity increase (super thermal) are observed in glow discharges of both atomic and molecular gases
 - a. fractional ionization - 10^{-7} to 10^{-3}
 - b. gas temperature - 300 to 1400 K
- Similar features are not observed in thermal plasmas
- Weak magnetic field impacts sound velocity
- Sound velocity change depends on Te
- UV illumination of the plasma is claimed to increase speed of sound in plasma

CURRENT STATUS OF THE RESEARCH RESULTS

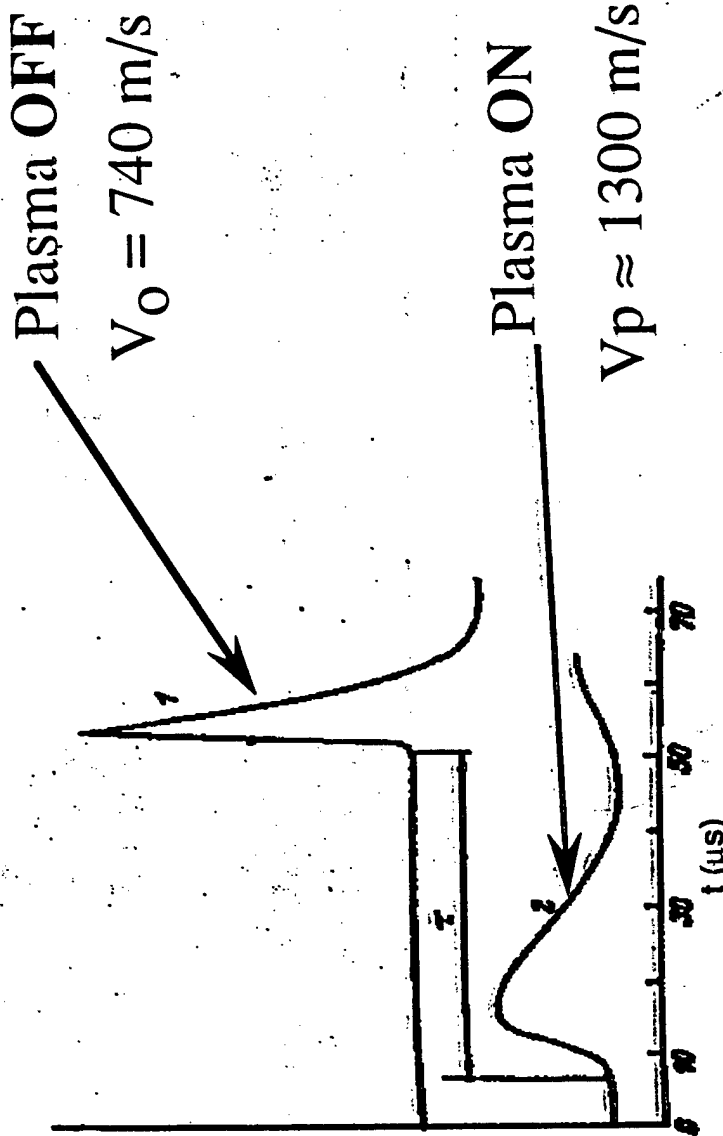
- SEVERAL GROUPS HAVE REPORTED INCREASED DISPERSION AND DAMPING OF SHOCK WAVES IN WEAKLY IONIZED PLASMAS, ALSO HIGHER SHOCK PROPAGATION VELOCITIES
- SOME OF THE RESEARCHERS ASCRIBED THE EFFECTS TO THE NONÉQUILIBRIUM PLASMAS, OTHERS TO THE TEMPERATURE GRADIENT FORMED IN PLASMAS
- ACCURATE THÉORÉTICAL MODEL EXISTS FOR SMALL AMPLITUDE AUDIO FREQUÊNCY ACOUSTIC WAVE PROPAGATION IN PLASMAS
- ACCURATE MODEL DOES NOT EXIST FOR SHOCK WAVE PROPAGATION IN NÔNÉQUILIBRIUM PLASMAS

Shock Wave Propagation in a Weakly Ionized Low-pressure Discharge



Plasma Parameters

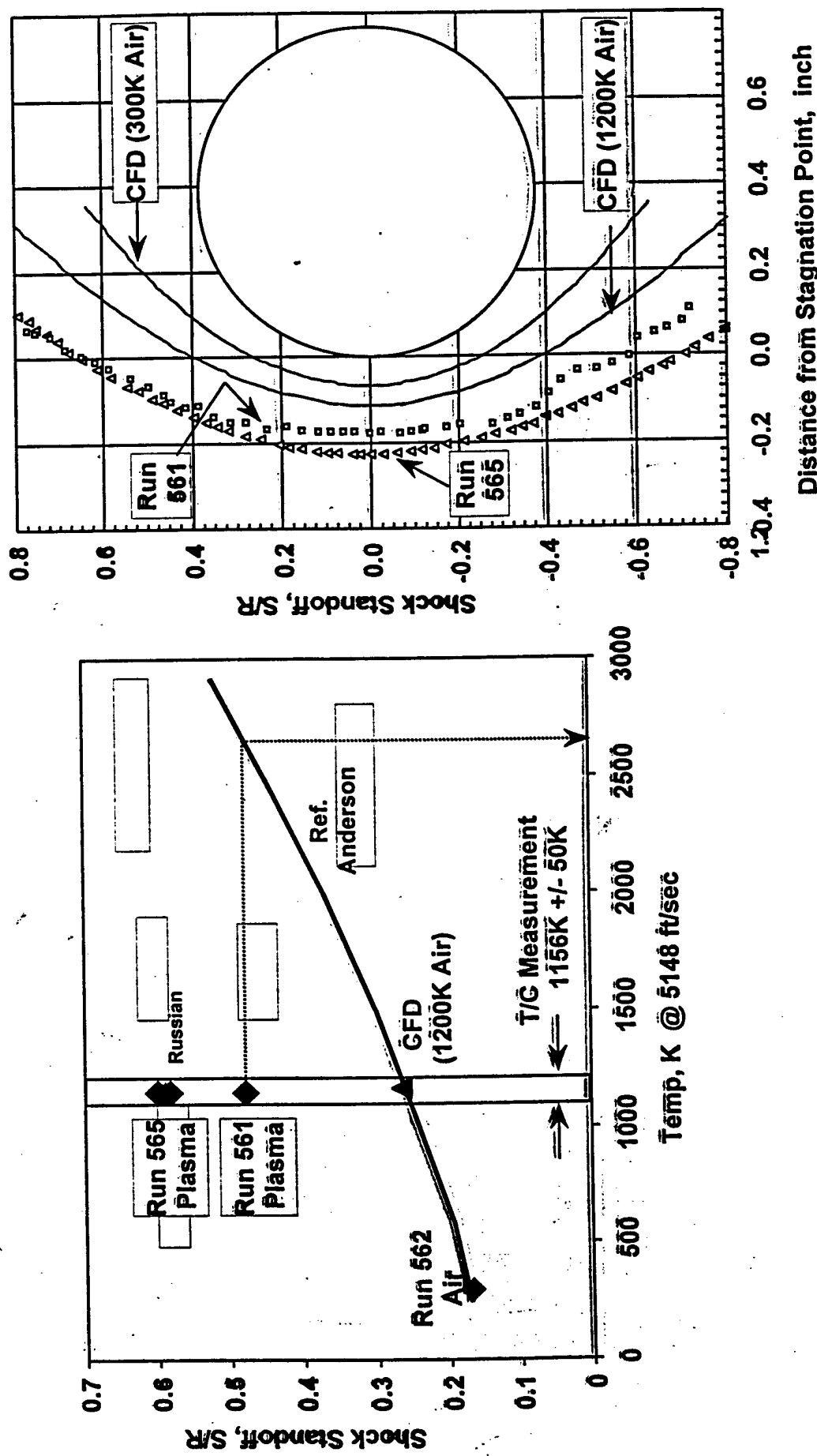
$P = 30 \text{ torr}$
 $J = 3 \text{ mA/cm}^2$
 $T_g = 800 \text{ K}$



A. I. Klimov et al., Sov. Tech. Phys. Lett. **8**, 192 (1982)

Shock Standoff Comparison to Predictions

(0.75 in. diam, 30 torr)



RESEARCH TOPICS OF INTEREST

- MACH NO. DEPENDENT SHOCK WAVE ATTENUATION AND DISPERSION
VS. GAS PRESSURE AND CURRENT DENSITY

SIMULTANEOUS MULTIPONT MÉASURÉMENTS

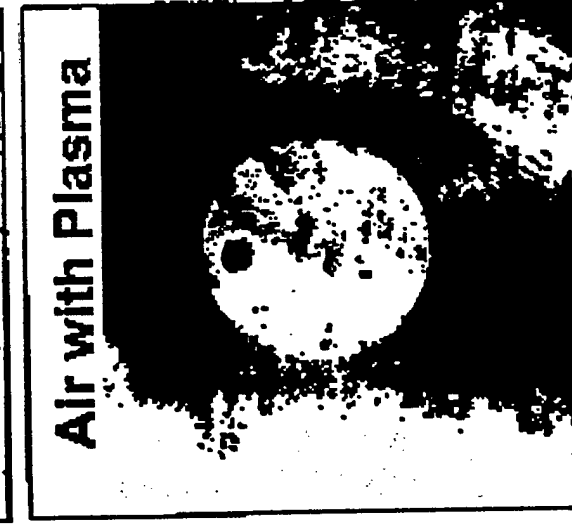
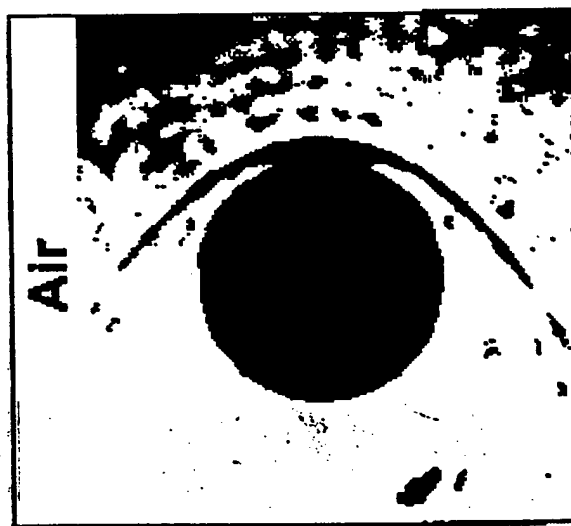
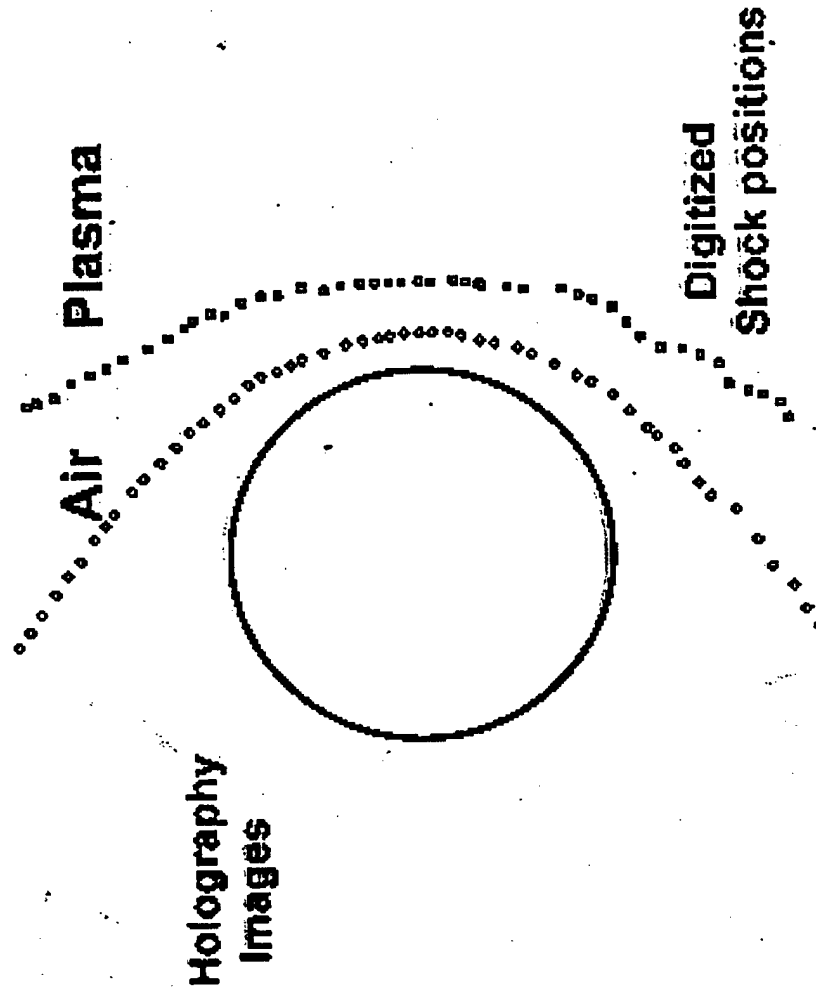
- GAS HEATING EFFECTS
- LINEAR/NONLINEAR ENERGY COUPLING
- ENERGY TRANSFER MÉCHANISM

ENERGY EXCHANGE MÉCHANISMS

- CHARGE EXCHANGE EFFÉCTS
- ELECTRON ENERGY ENHANCÉMENT BY AMBIPOLAR ELECTRIC FIELD
- KINETIC TO ELECTROSTATIC ENERGY TRANSFÉR

Initial Replication of Russian Results at AEDC

(0.75-in diam sphere, 30 torr)

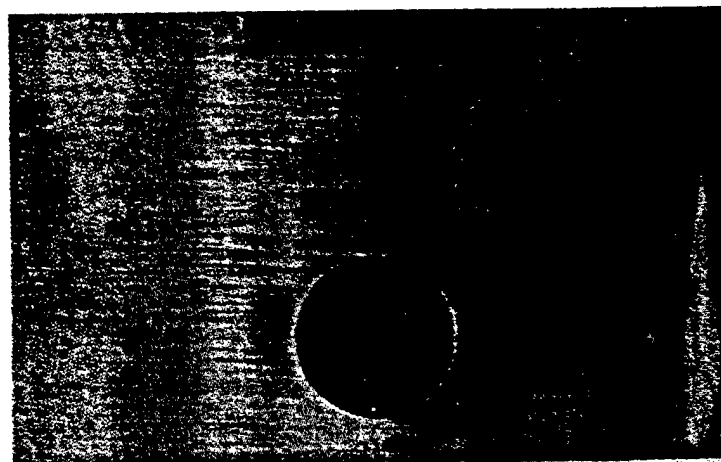


Weakly Ionized Gas Research

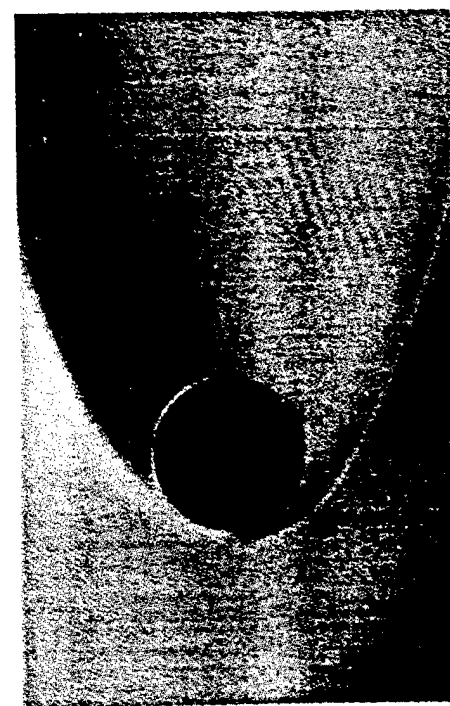
Russian Ballistic Tests (G. Mishin & A. Kilmov, 1978)

- Effect of pre-ionization on the flow around a sphere at Mach 6 in air

(b) With Pre-ionization

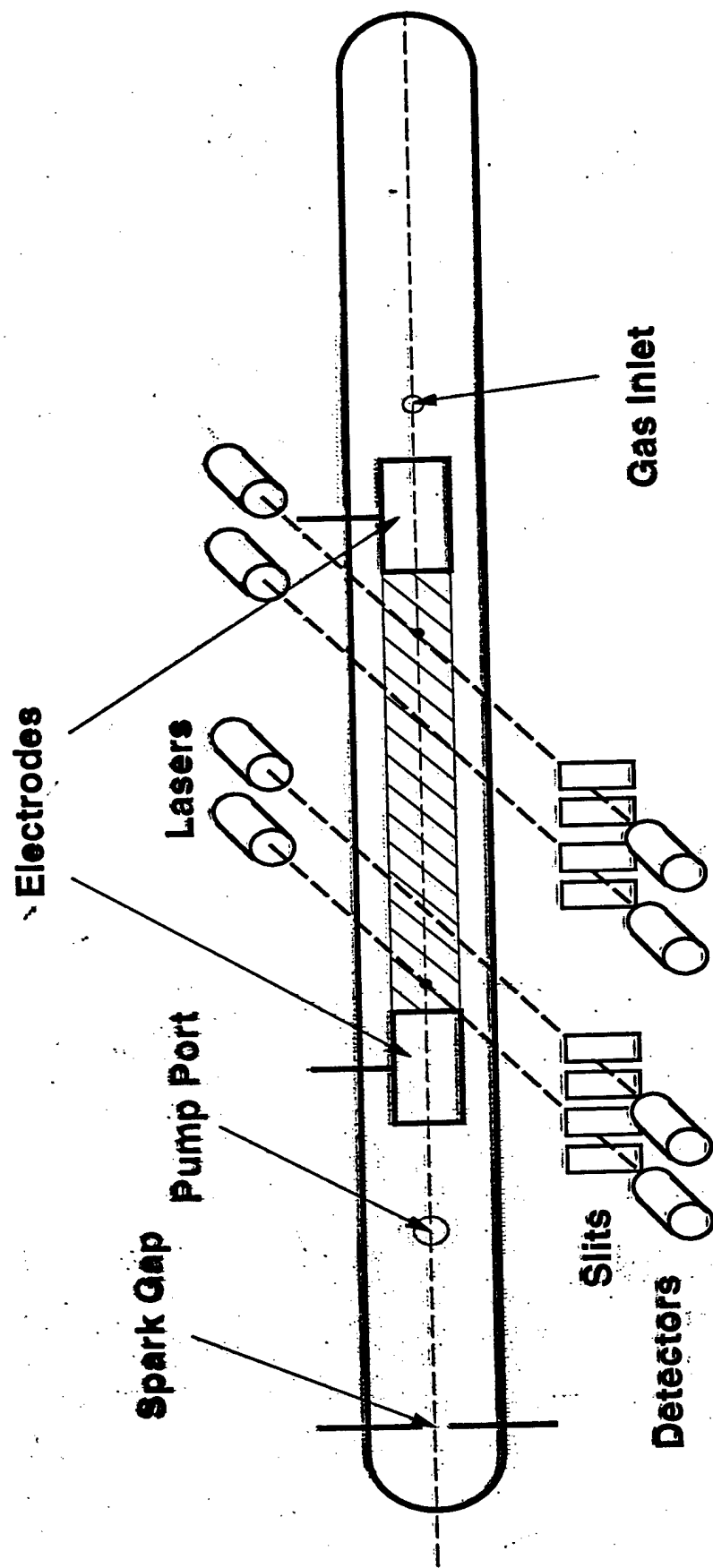


(a) Without Pre-ionization

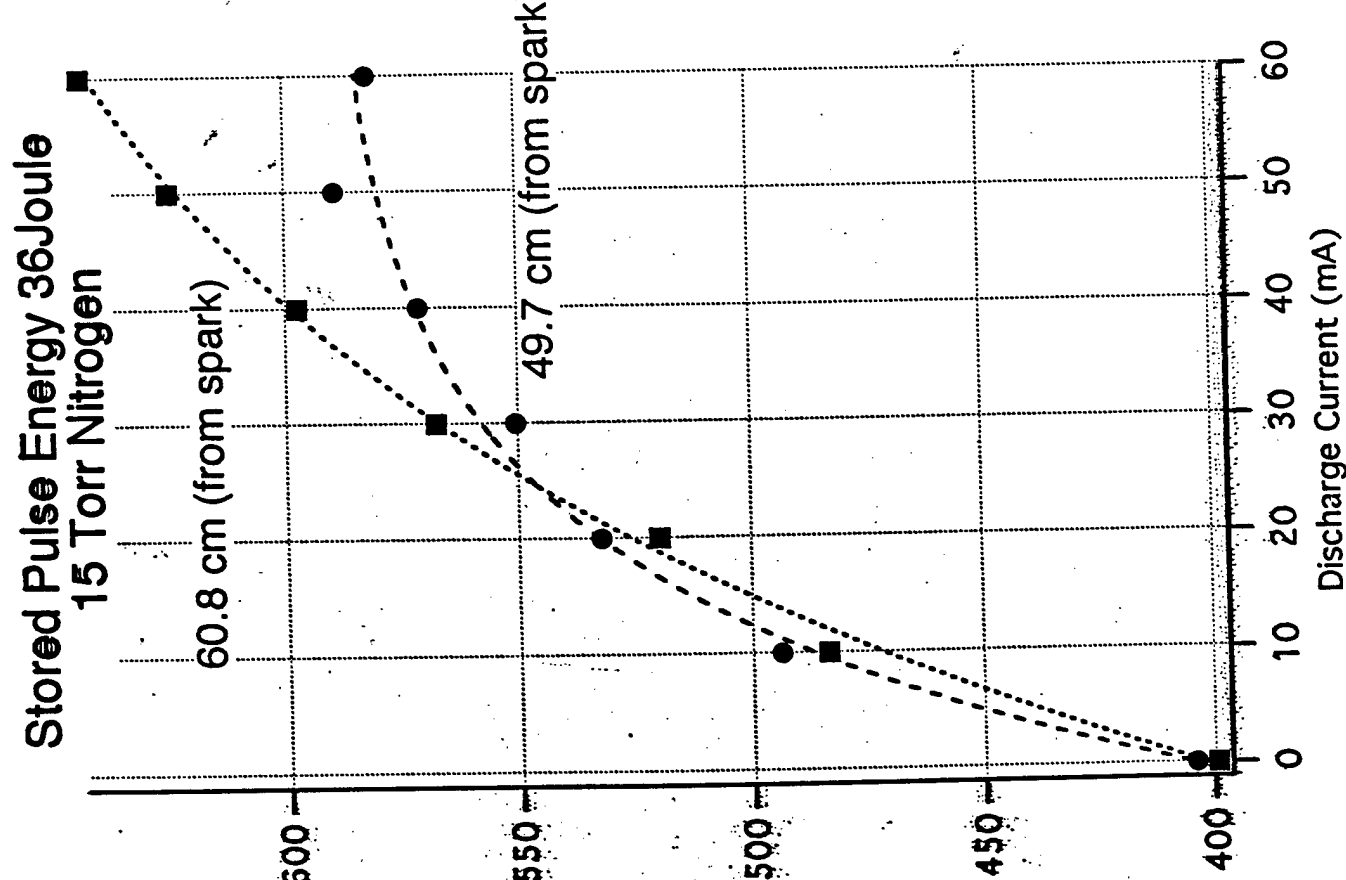
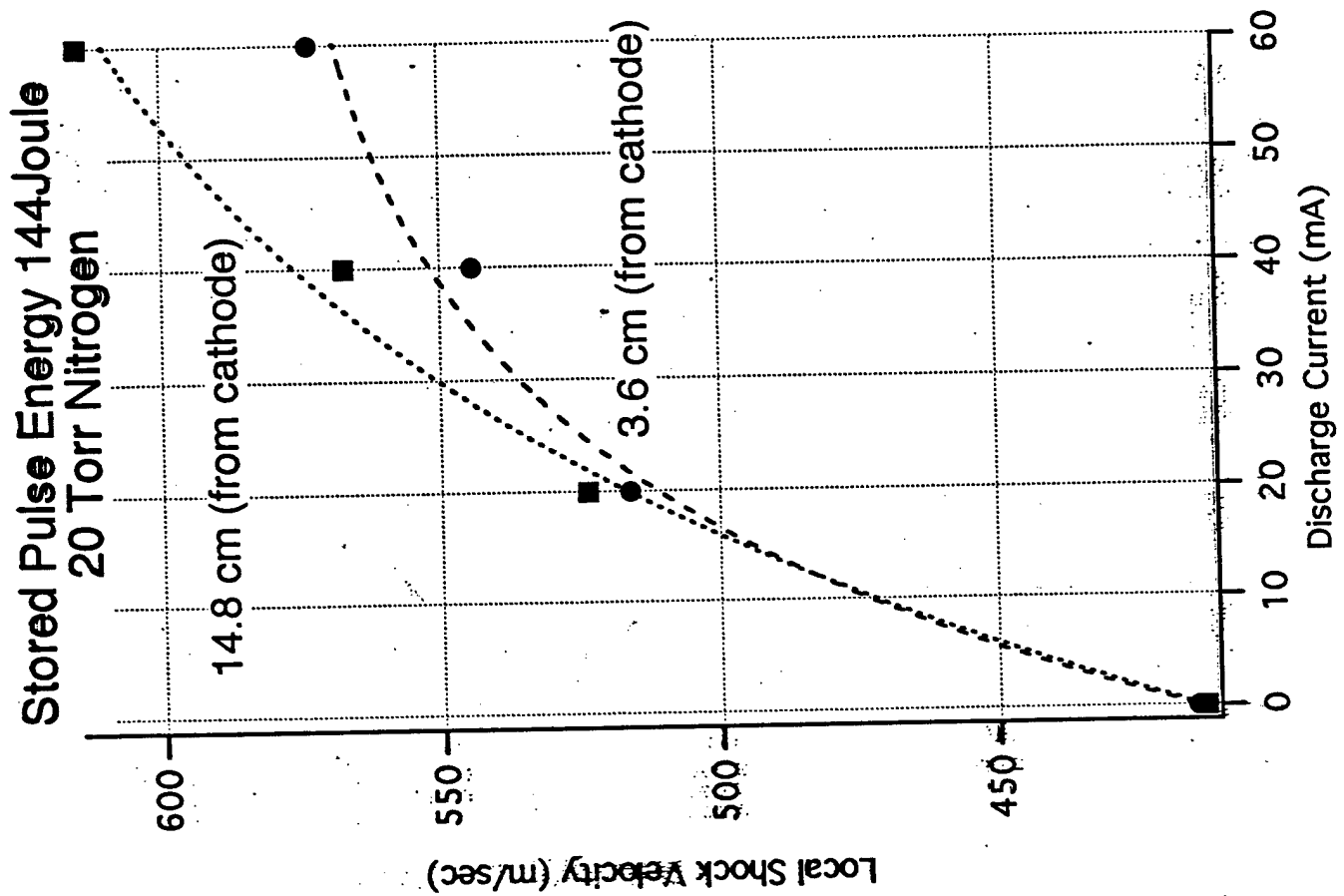


M = 6 →

Schematic of Experiment



Local Velocity in Discharge as Function of Discharge Current



SHOCK WAVE INTERACTIONS WITH WEAKLY IONIZED GASES

- Confirmed shock wave relaxation in nonequilibrium plasmas
- Occurs even at 10^{-7} fractional ionization
- Measurements demonstrated highly non-linear interactions of acoustic shock wave with non-equilibrium weakly ionized plasmas
- Measurements need to be performed to quantify interaction mechanisms and energy balance
- Data will be required to permit energy efficiency analysis of plasma based drag reduction and shock wave amplitude control

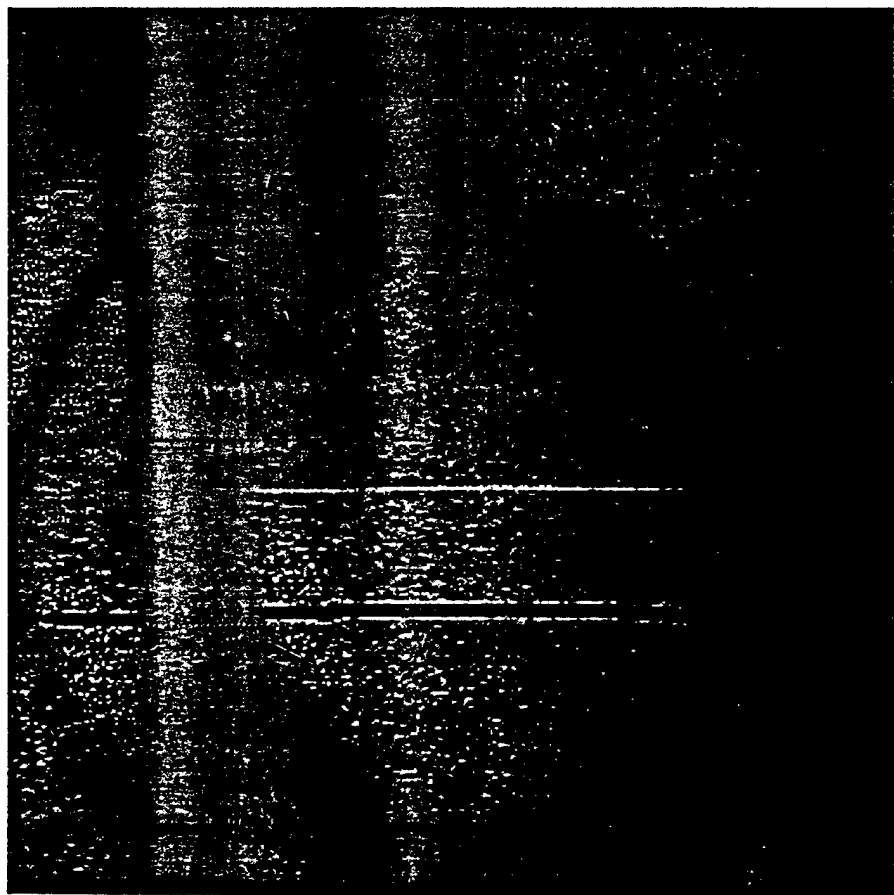
OUR PLANNED RESEARCH FOR FY98-99

- Simultaneous multi-point local shock wave velocity measurements.
- Spectroscopic measurement of gas temperatures.
- Shock wave structure recovery in decaying plasma and neutral gas.
- 2-D Schlieren imaging of shock profiles.
- Spectroscopic measurement of shock wave density profile.
- Shock dispersion measurements in pulsed and radio frequency discharges.
- Shock propagation in double layer plasmas.
- Shock induced electric field modulation measurements.

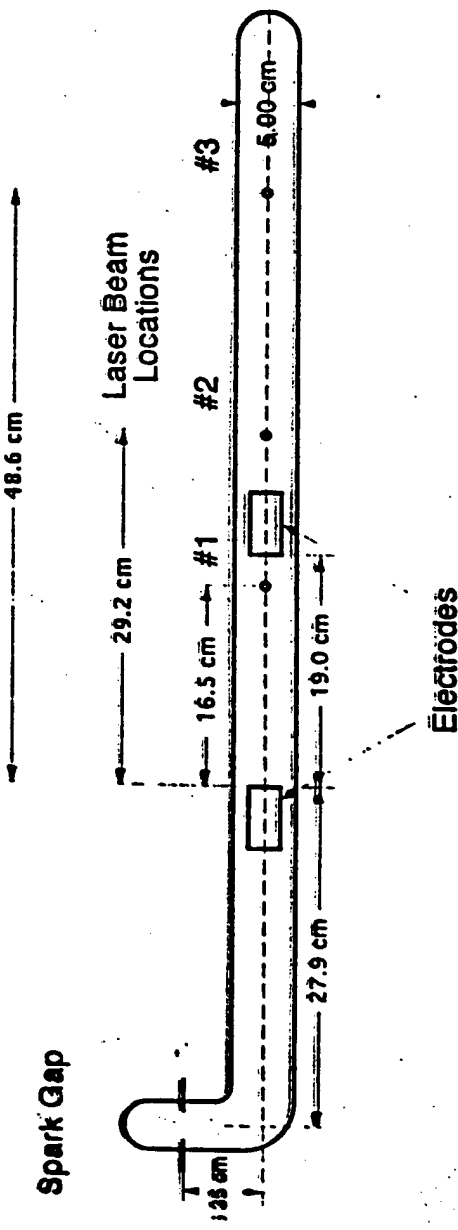
SUMMARY

- Data show the dissipation of supersonic shock waves is nonlinearly dependent on amplitude in weakly ionized nonequilibrium plasmas
- Spatially resolved measurements indicate that shock propagation velocity change and dispersion cannot be explained by gas heating only
- Shock wave dispersion and damping are dependent on the gas number density and fractional ionization
- The energy coupling mechanisms are not understood at present
- Plasma energy density and single particle collision frequency are inadequate to explain the observed phenomena
- Long range cooperative interactions may be important

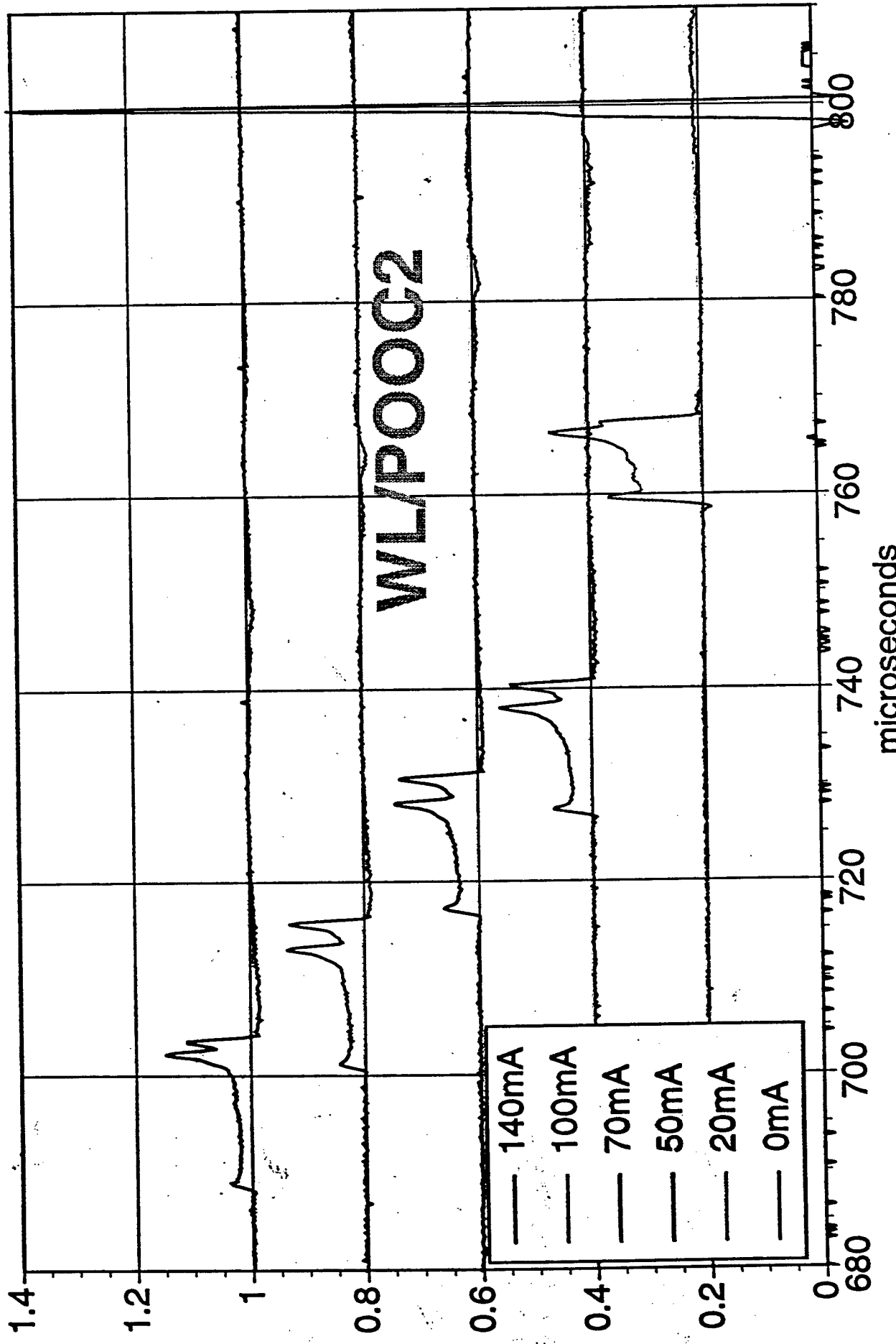
A Comparison of the Shock Thickness With a 0.8 mm
Diameter Wire , 30 Torr Argon , Pulser Voltage 9kV



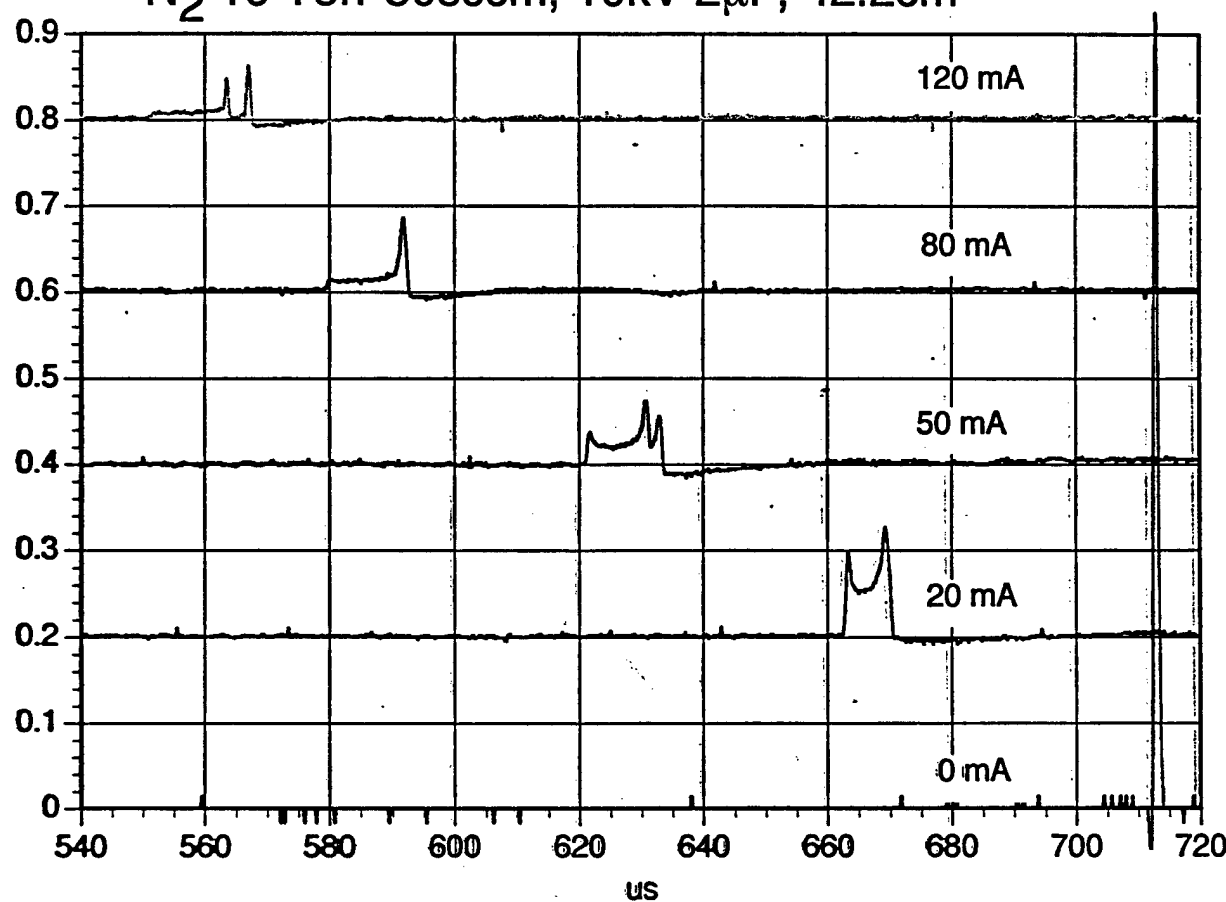
Discharge Tube Dimensions and Location of Laser Beams



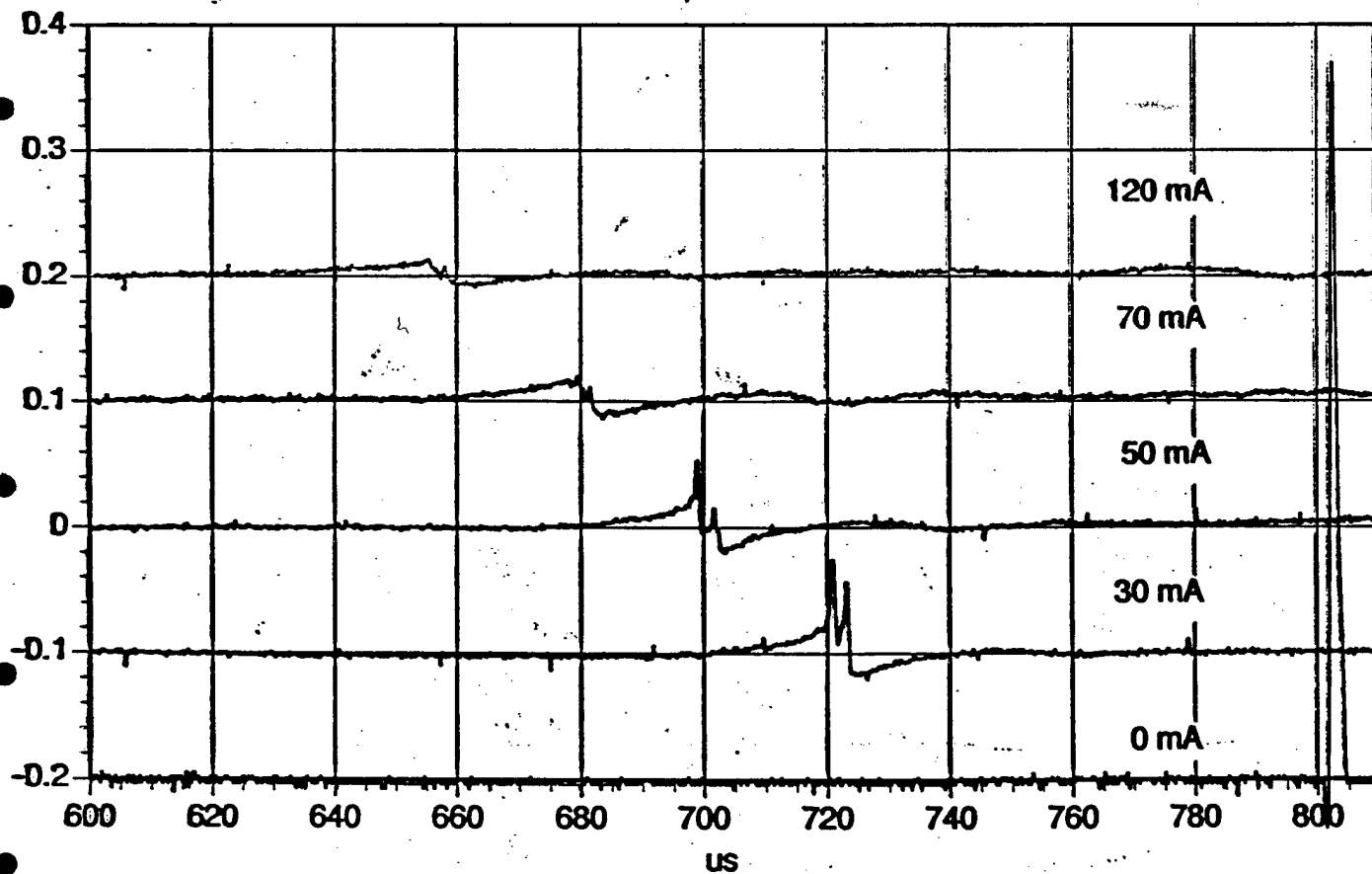
Argon 30 Torr, 10kV 2 μ F, 42.2cm



N_2 10 Torr 50sccm, 10kV 2 μ F, 42.2cm



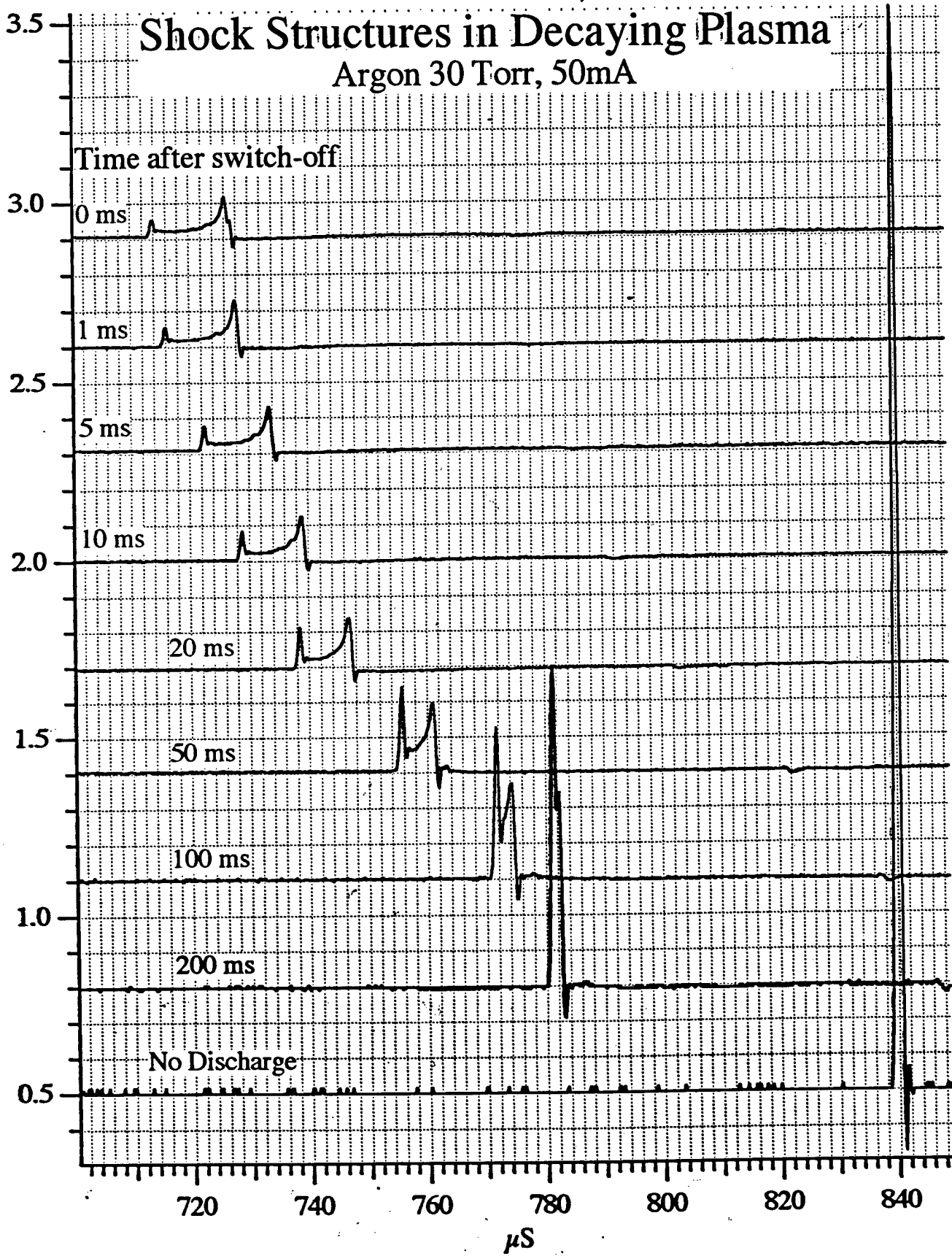
50 Torr, 42.2cm



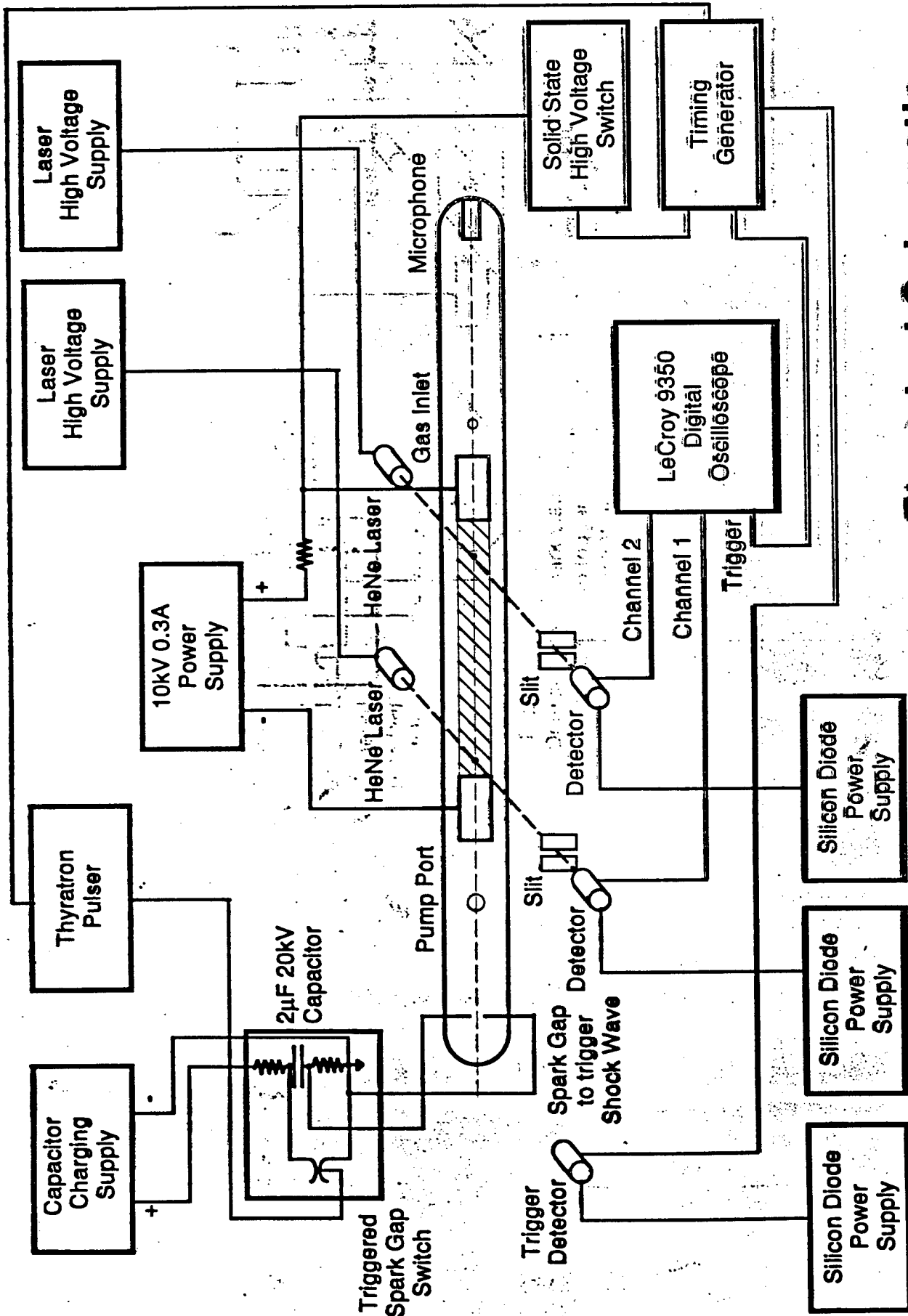
Shock Structures in Decaying Plasma

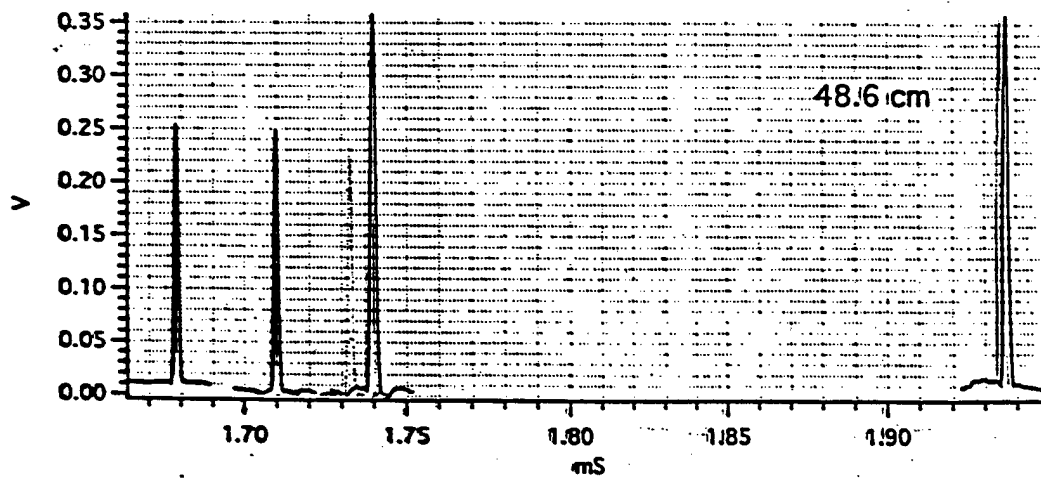
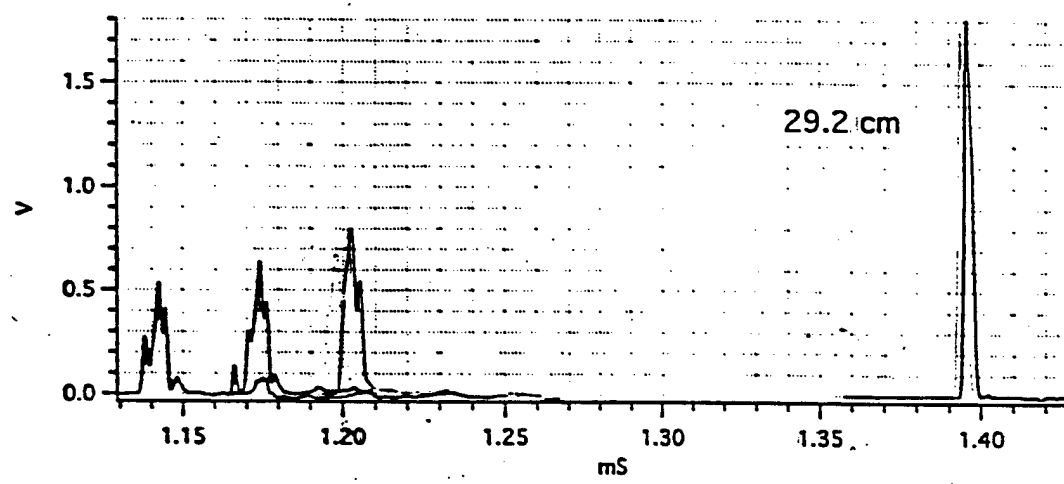
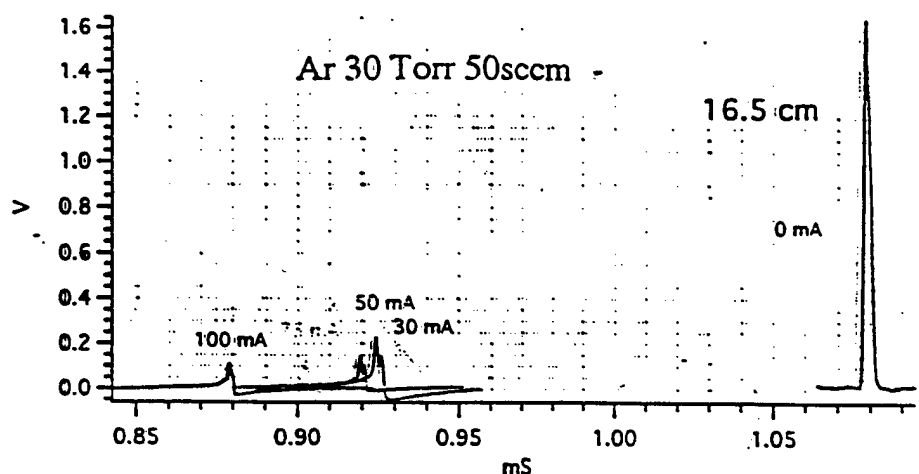
Argon 30 Torr, 50mA

Time after switch-off

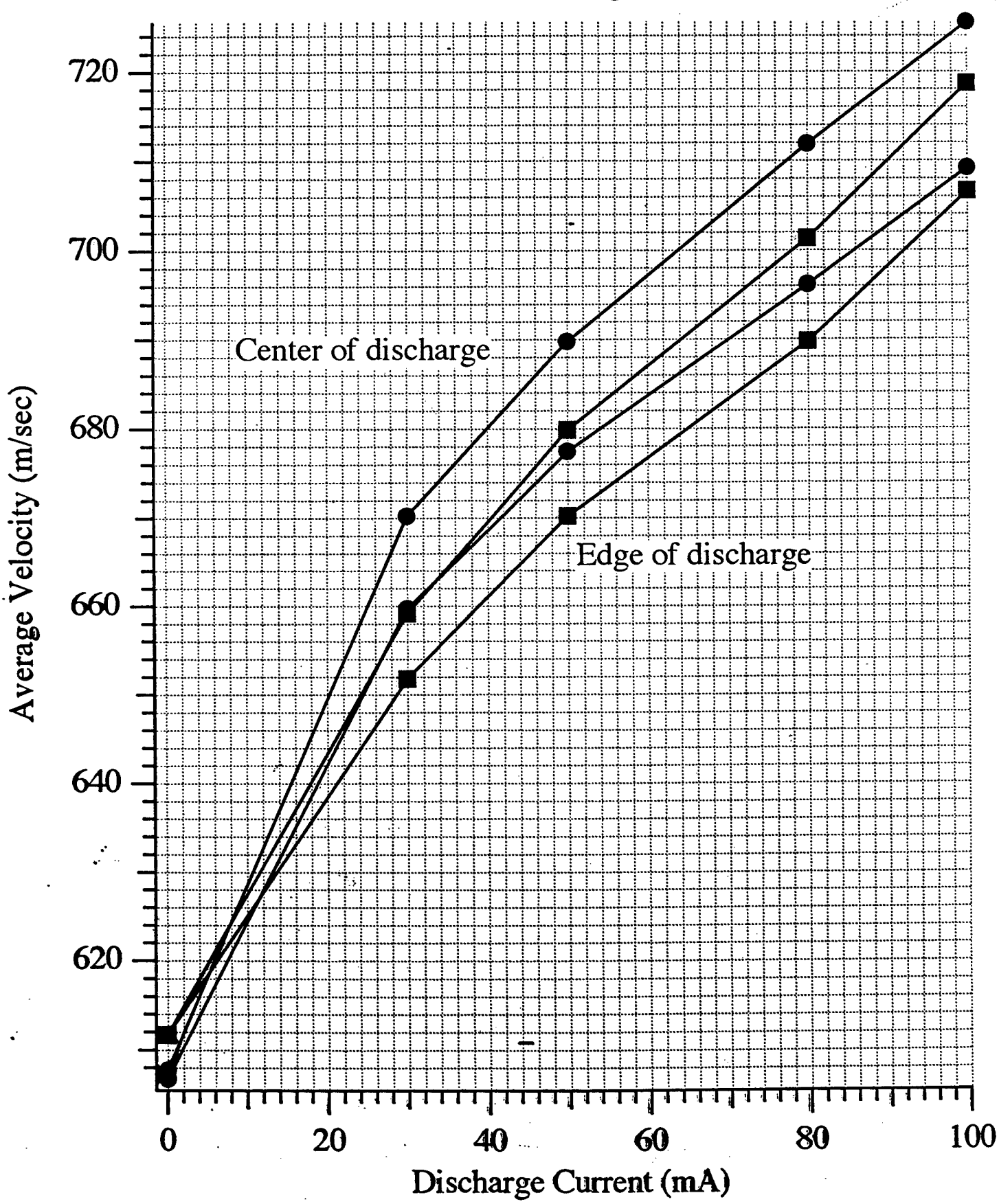


Electrical Schematic for typical measurement



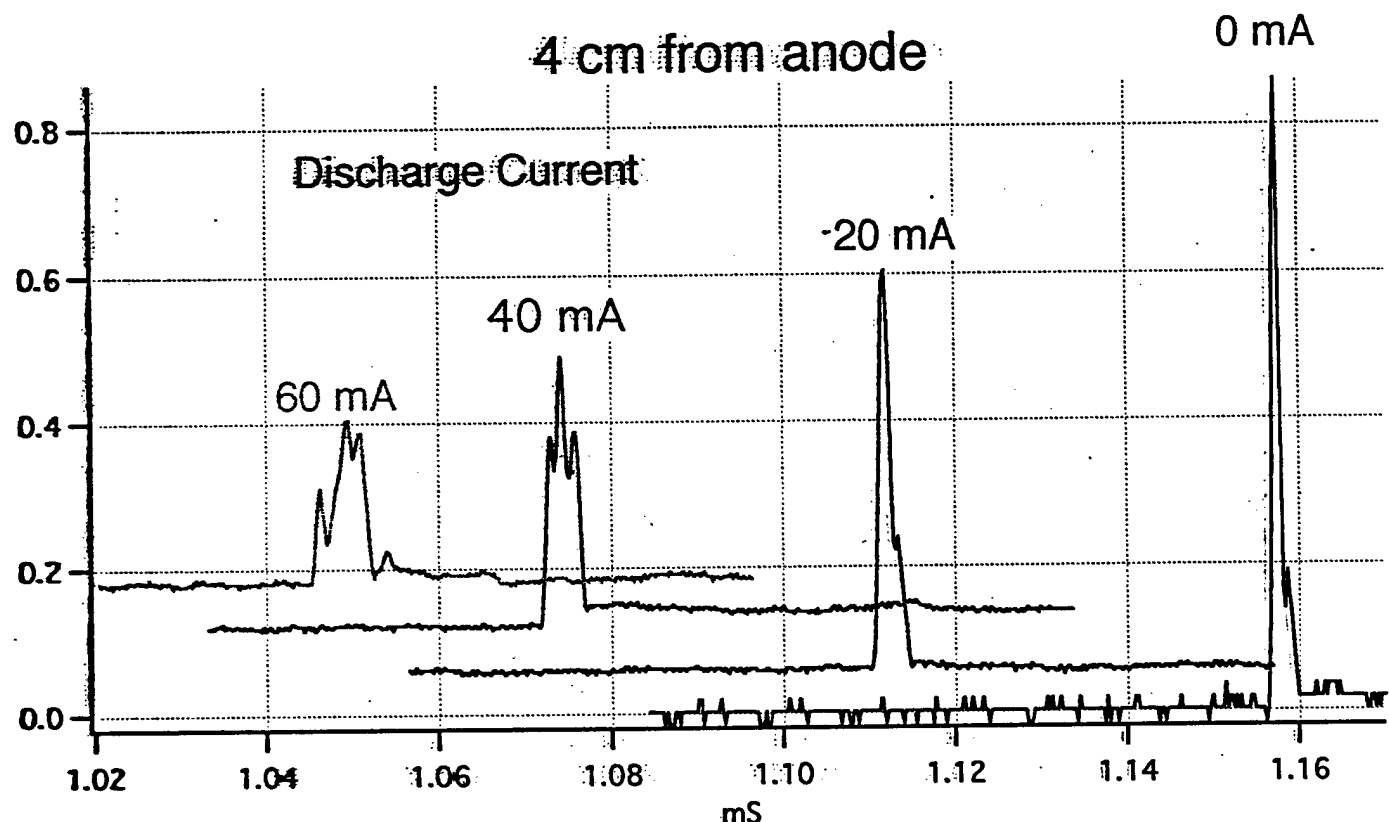


Average Velocity of Front and Back Boundaries
of Shockwave at Center and Off-Axis
as Function of Discharge Current

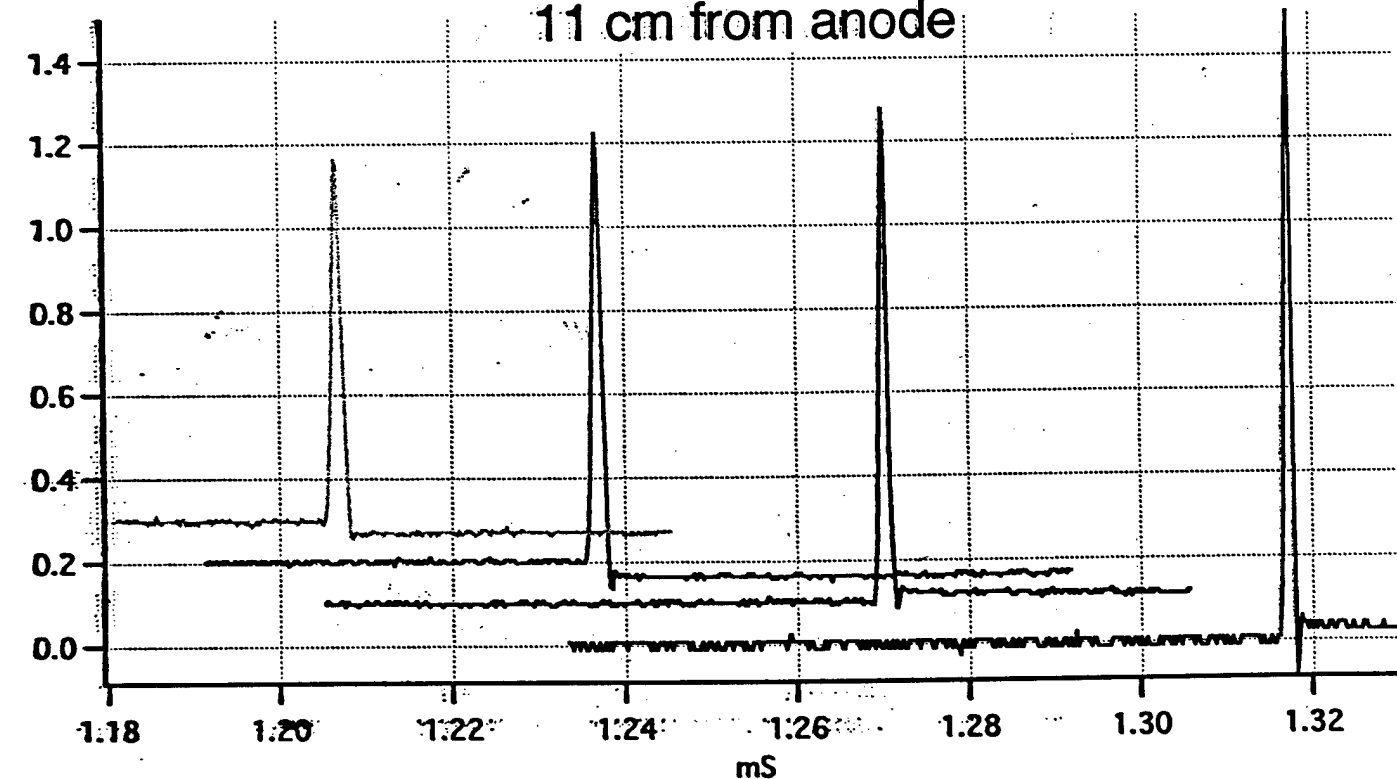


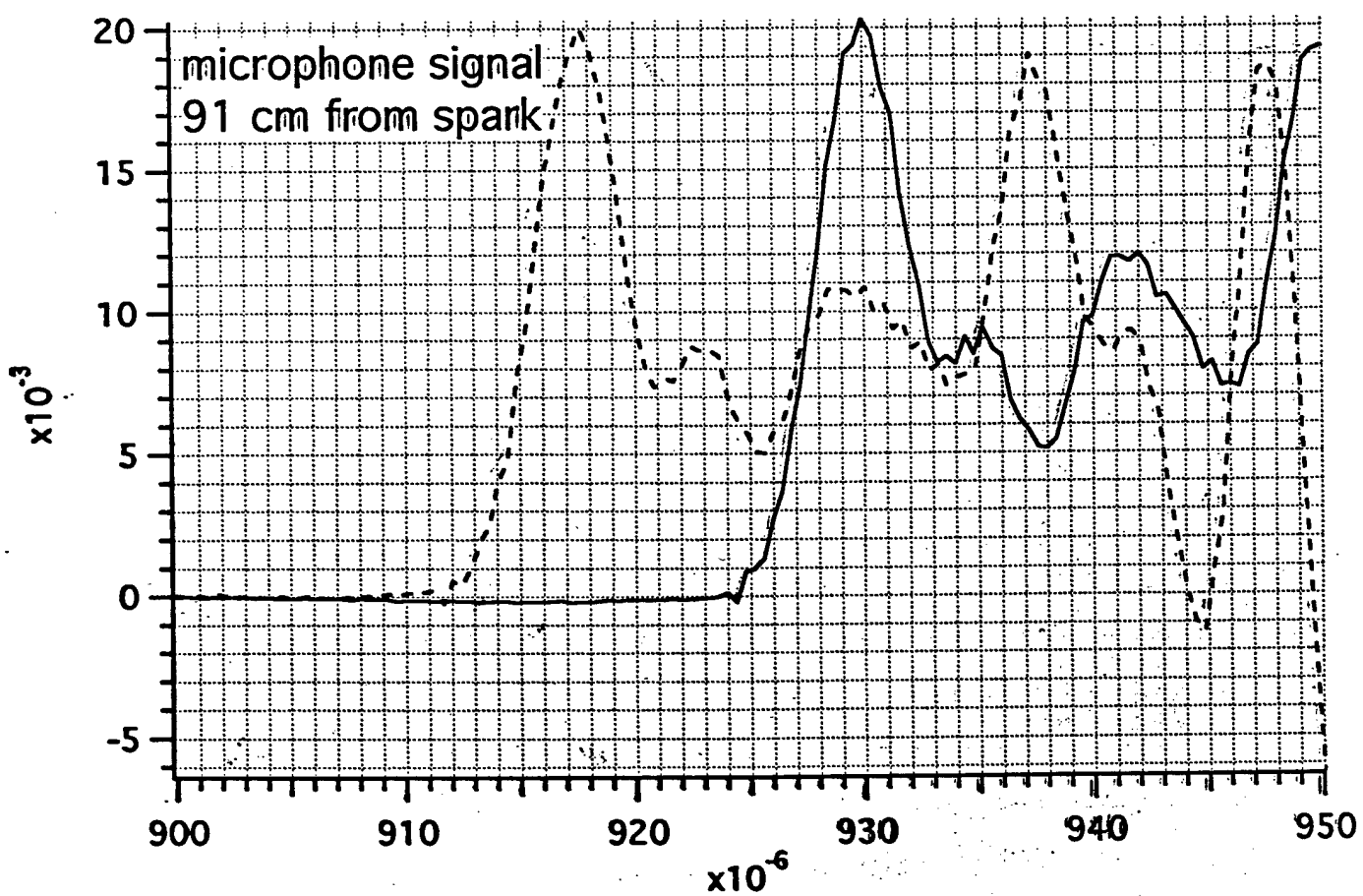
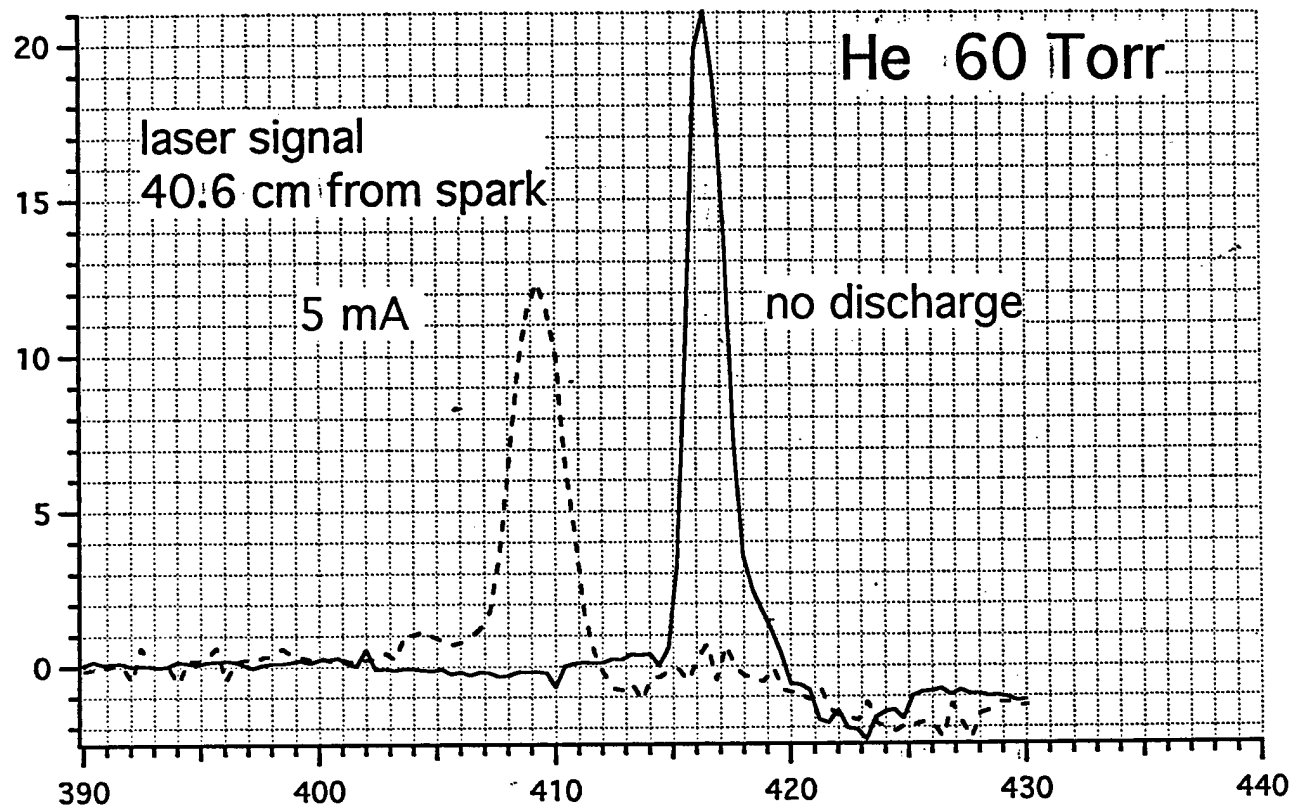
Deflection Signals Downstream of Discharge

Pulse Energy 81 Joule



11 cm from anode





UNDERSTANDING AND CONTROL OF IONIZED
HIGH-SPEED FLOWS

AFOSR WORKSHOP
PRINCETON UNIVERSITY
FEBRUARY 26-27, 1998

Plasma Drag Reduction — An Overview of the Issues
Aaron Auslender
NASA Langley Research Center

OUTLINE

- Problem Statement and Related Issues
- Present Research Focus — NASA/LaRC and ICASE
- Analysis of Air Force Experiments — ODU
- Ballistic Range Mechanisms — ODU
- Onboard-Microwave Experiments — NASA/LaRC
- Shock Tube Experiments — FA&M

Flow around a sphere moving supersonically in a gas-discharge plasma

G. I. Mishin, Yu. L. Serov, and I. P. Yavor

(Submitted April 11, 1991)

Pis'ma Zh. Tekh. Fiz. 17, 65-71 (June 12, 1991)

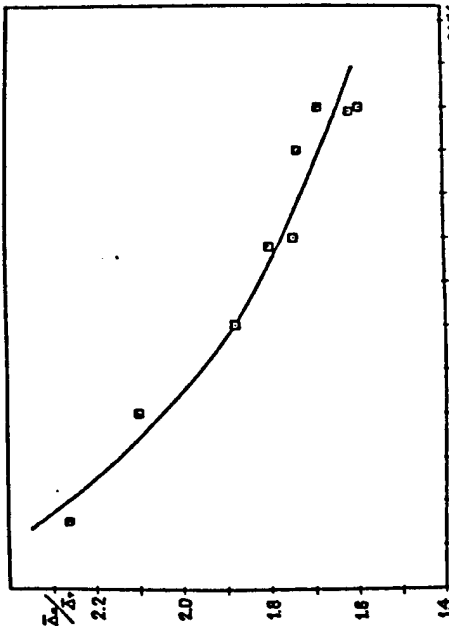


FIG. 2. Ratio of experimentally determined relative standoff distance of the bow shock from a sphere moving through a glow-discharge plasma to the corresponding calculated value of the relative standoff distance in air at the same temperature as the plasma ($\tilde{\Delta}_p$ is the relative standoff distance of the bow shock in the plasma, $\tilde{\Delta}_r$ is the relative standoff distance in air at $T = 1350$ K, and v is the velocity of the sphere).

414 Sov. Tech. Phys. Lett. 17(6), June 1991

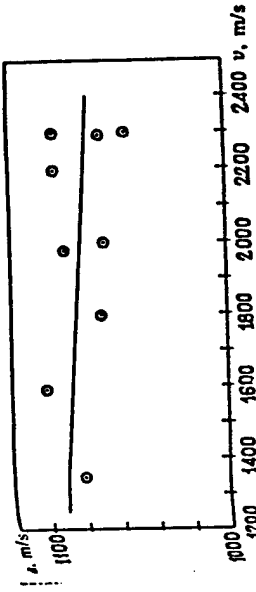
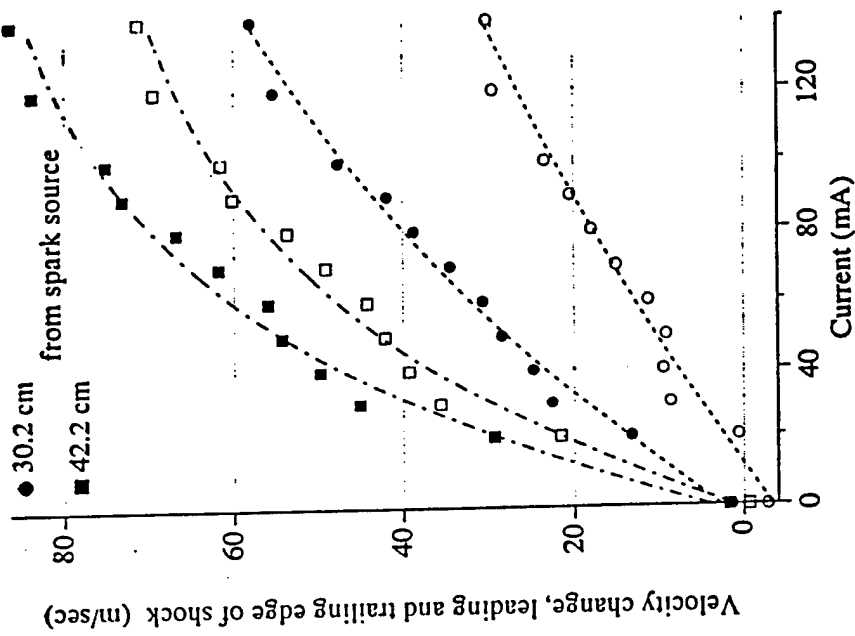


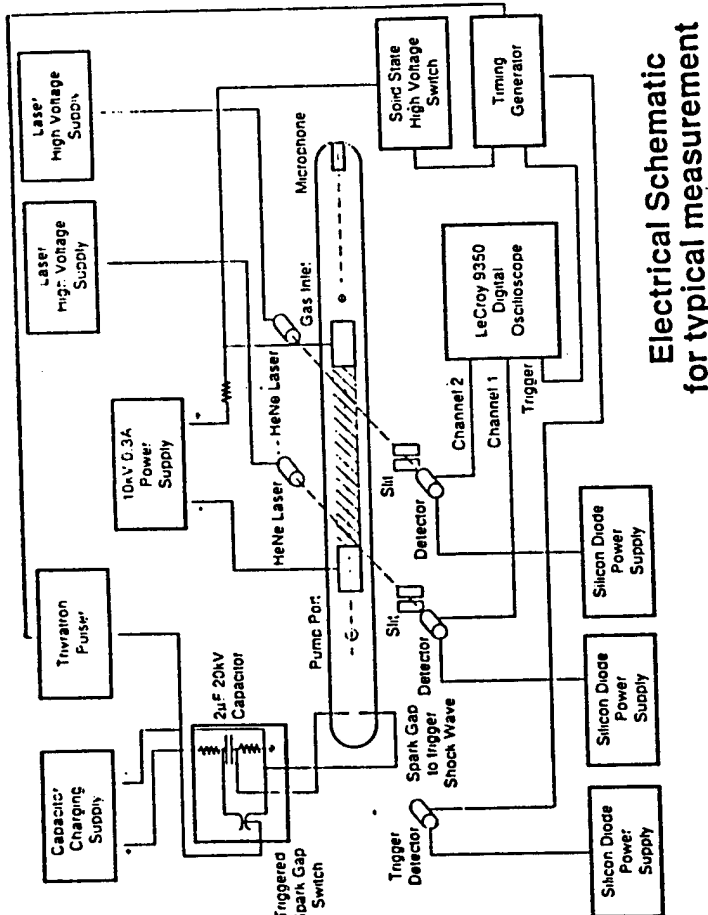
FIG. 3. "Effective" (governing the flow pattern) sound velocity in a plasma in the range of velocities of a spherical model 1350–1300 m/s (a is the effective sound velocity, and v is the velocity of the sphere).

The main series of experiments was carried out in a steadily burning discharge at a gas pressure of 40–50 torr and a discharge current density of 25–50 mA/cm². The electron density was $\approx 10^{11}$ – 10^{12} cm⁻³, the ionization coefficient was $\alpha = 10^{-5}$ – 10^{-6} , and the electron temperature was $T_e = 1$ – 4 eV. The gaskinetic temperature T_a of the plasma was determined by several techniques: by measuring the density of the gas from interferograms, by means of Chromel-Alumel thermocouple, by radiation pyrometry, and from the electron vibration—rotation spectra of the molecules.² The measurements showed that the temperature distribution along the diameter is bell-shaped, with $T_a \leq 1400$ K on the axis of the discharge.

NASA Langley Research Center



Velocity change, leading and trailing edge of shock (m/sec)



Electrical Schematic
for typical measurement

ACOUSTIC SHOCK WAVE PROPAGATION IN NONEQUILIBRIUM NITROGEN AND ARGON PLASMAS

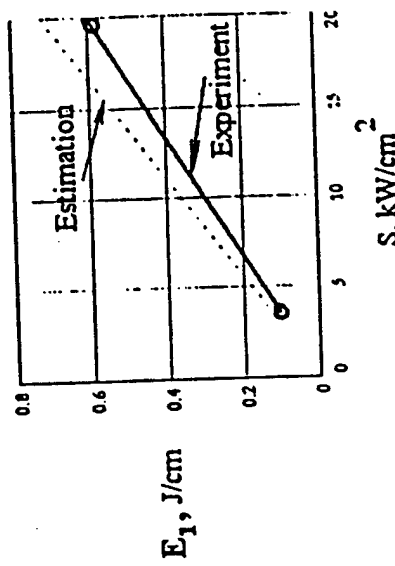
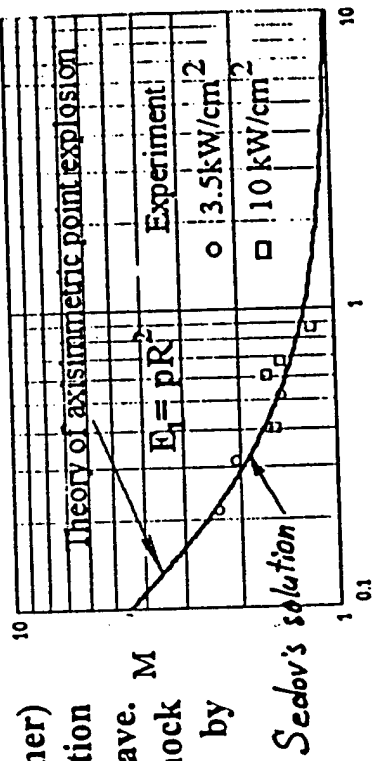
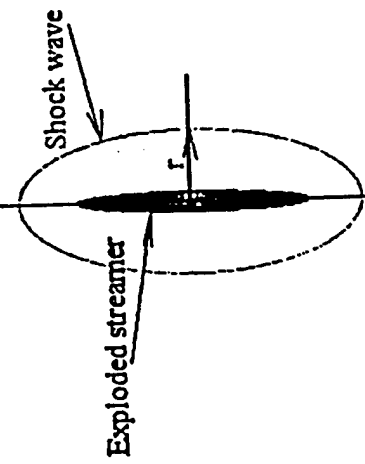
B. N. GANGULY AND P. BLETZINGER
WRIGHT LABORATORY, WRIGHT-PATTERSON AFB

Physics of the
Undercritical Microwave Discharge
and Its Influence on the
Supersonic Aerodynamics and
Shock Waves

K. Khodataev (MRTI)

Absorption Ability of the Microwave Streamer Discharge

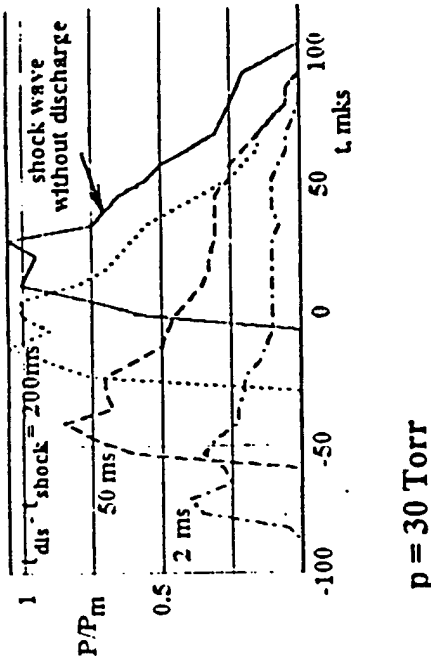
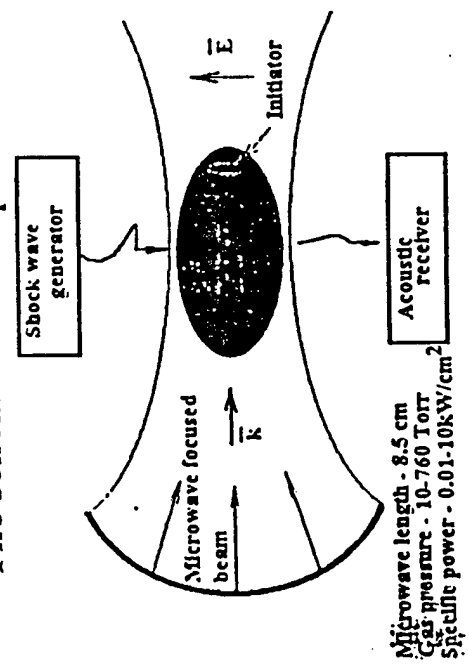
Each filament element (streamer) being heated by microwave radiation explodes and generates the shock wave. M The phase trajectory $M(r)$ of the shock wave gives the energy absorbed by filament length unit E_1



The net of the microwave discharge filaments absorbs whole radiation flux.

The Experimental Data about a Shock Wave Attenuation in a Microwave Discharge

The scheme of the experiment



$P = 30 \text{ Torr}$

The typical oscilloscopes

The measurements show that discharge region:

- attenuates the pulse shock waves,
- increases the pulse shock wave time duration,
- the memory time of discharge region equals more than 0.1 s.

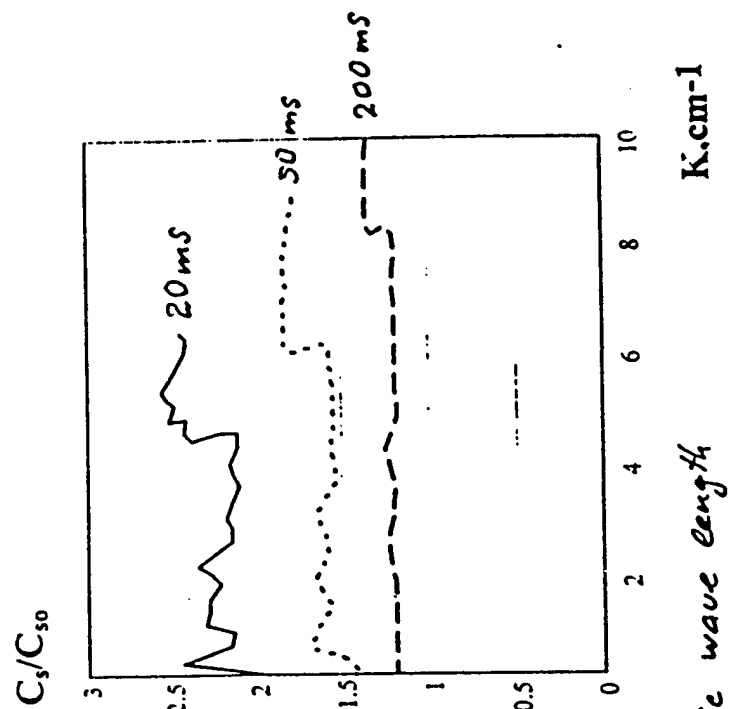
The Acoustic Interferometry Study of the Microwave Discharge Region

The sound velocity dependence
on wave number $C_s(k)$ in the
decaying microwave discharge
plasma.

The delay time after discharge:
20 ms -solid, 50 ms -dot, 200 ms-dash
line.

The dependence show that:
the discharge region

- is heated in average,
- has microscale hot
inhomogeneities,
- has a memory time up to
0.2s.



$$H = \frac{2\pi}{\lambda} - \text{acoustic wave length}$$
$$\text{K.cm}^{-1}$$

$$\begin{aligned}
 \frac{\partial \mathbf{v}_n}{\partial t} &= -c_n^2 \nabla \rho_v / \rho_{0v} - \omega_{ni} (\mathbf{v}_n - \mathbf{v}_i) \\
 \frac{\partial \rho_v}{\partial t} &= -\rho_{0v} \nabla \cdot \mathbf{v}_n \\
 \frac{\partial \mathbf{v}_i}{\partial t} &= -c_i^2 \nabla \rho_u / \rho_{0u} - \omega_{in} (\mathbf{v}_i - \mathbf{v}_n) \\
 \frac{\partial \rho_u}{\partial t} &= -\rho_{0u} \nabla \cdot \mathbf{v}_i
 \end{aligned} \tag{1}$$

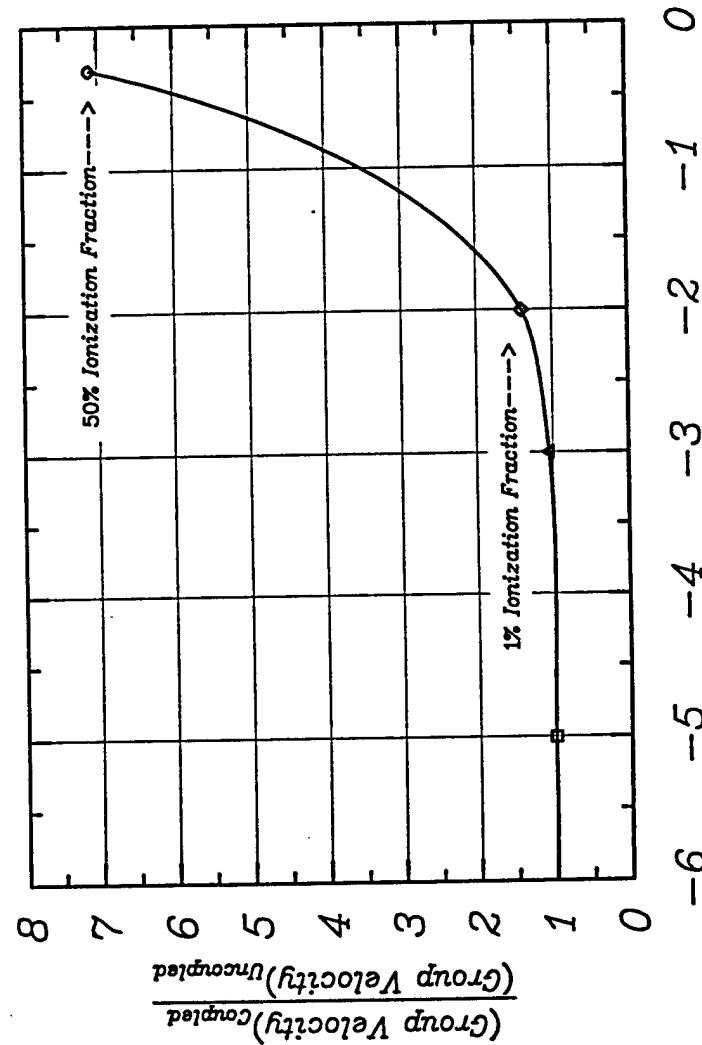
$$\begin{aligned}
 \mathbf{v}_n &= \nabla \phi_n \\
 \mathbf{v}_i &= \nabla \phi_i
 \end{aligned} \tag{2}$$

$$\begin{aligned}
 \frac{\partial^2 \phi_n}{\partial t^2} - c_n^2 \nabla^2 \phi_n + \omega_{ni} \left(\frac{\partial \phi_n}{\partial t} - \frac{\partial \phi_i}{\partial t} \right) &= 0 \\
 \frac{\partial^2 \phi_i}{\partial t^2} - c_i^2 \nabla^2 \phi_i + \omega_{in} \left(\frac{\partial \phi_i}{\partial t} - \frac{\partial \phi_n}{\partial t} \right) &= 0
 \end{aligned} \tag{3}$$

$$\begin{vmatrix}
 -\omega^2 + c_n^2 k^2 - i\omega \omega_{ni} & i\omega \omega_{ni} \\
 i\omega \omega_{in} & -\omega^2 + c_i^2 k^2 - i\omega \omega_{in}
 \end{vmatrix} = 0 \tag{4}$$

- Analysis assumed:
 - (1) Uncoupled Speed-of-Sound Ratio "Fast-Wave" to the "Slow-Wave" equals ten
 - (2) Ionization Fraction is constant

- Conclusion:
 - (1)"Slow-Wave" only propagates in the long-wave-length limit
 - (2) Large Ionization Fractions are required ("Slow-Wave")



$\log_{10} [\text{Ionization Fraction}]$

Plasma Drag Reduction Physics

NASA Langley Research Center

PRESENT RESEARCH EFFORTS

- Kinetics
 - Excited State —> reactions —> “hot” electron production
 - Metastable States —> “long-lived” neutrals
- Far-From Equilibrium Effects —> neutral particle stationary solutions of the Boltzmann kinetic equation having sources/sinks (fluxes)
 - > influences speed-of-sound
 - > yields mass/momentun/energy fluxes in the shock region (OSU)
- Far-From Equilibrium Effects (OSU, NASA/LaRC and ICASE)
 - DSMC Modelling (NASA/LaRC and ICASE) employing a central forcing function of the class: $Force = \alpha_0 e^{-(X-X_{SHOCK})^2/\alpha_1}$ to assess the magnitude of the required mechanism(s)
 - Development of related mechanism(s) and analysis of the relevant “fluid” equation set (OSU)

Shock-Wave Structure in a Rigid Sphere Gas¹

G. A. BIRD²
Department of Mechanics of Fluids, University of Manchester, Manchester, England

Translational Equilibrium in a Rigid Sphere Gas

G. A. Bird
Department of Aeronautical Engineering, University of Sydney,
Sydney, Australia
(Received 10 May 1963)

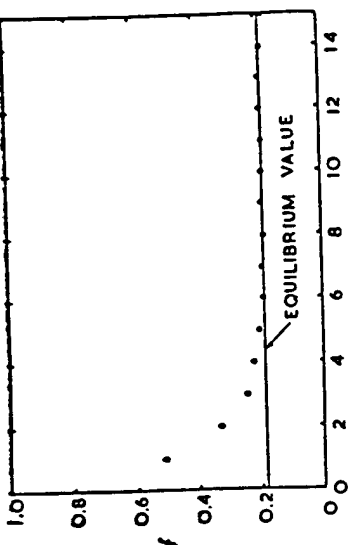


FIG. 1. Fraction of molecules in range 0.9 to 1.1 n_e .

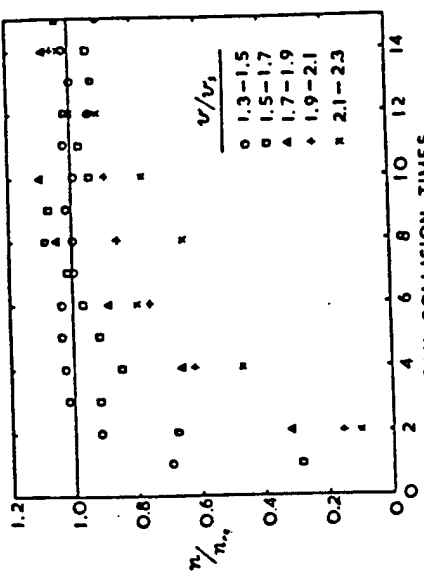


FIG. 2. Fraction of molecules in range 0.9 to 1.1 n_e .

Exact power-law solutions of the particle kinetic equations

A. V. Kats, V. M. Kontorovich, S. S. Moiseev, and V. E. Novikov
Kharkov Research Institute for Metrology,
Institute for Radiophysics and Electronics, Ukrainian Academy of Sciences,
and Physico-technical Institute, Ukrainian Academy of Sciences
(Submitted November 21, 1975)
Zh. Eksp. Teor. Fiz. 71, 177-192 (July 1976)

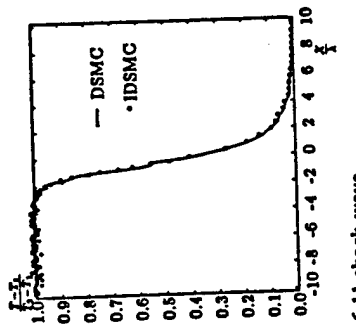


FIG. 3. Approach to equilibrium in higher speed ranges.

ODU Research Activity

- Analysis of planar-wave experiments
 - shock front propagation
- Analysis of ballistic range experiments
 - standoff distance
- Determination of underlying physical mechanisms
 - distribution of internal energy
 - collisional dynamics during relaxation
 - influence of double electric layer on charged and excited particles
 - nonequilibrium effects
- Shock dispersion experiments and plasma generation
(future work)

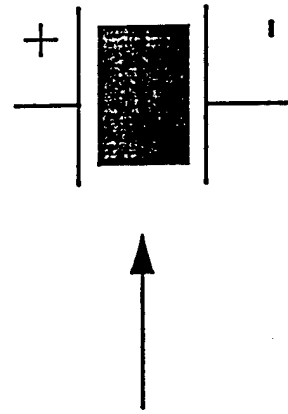
“Anomalous” Effects in Atomic & Molecular Gases at $T_e \gg T_n$

- Not observed at $T_e = T_n$.
- Not dependent on direction of applied electric field.
- Reduced/nonexistent at transverse magnetic field of below/above ~ 500 G.
- Increase with ultraviolet irradiation.
- Rise-time from plasma inception ~ 100 μ s.
- Afterglow decay time depends on gas species.
Can be > 100 ms.

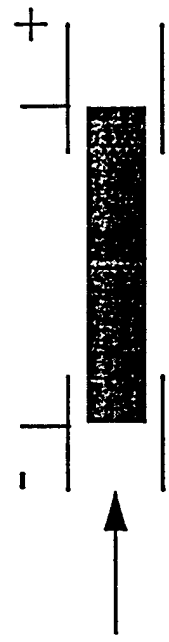
Generic Experiments

- A. Shock wave propagation through a DC glow discharge
 1. parallel-plate transverse propagation
 2. cylindrical coaxial propagation
- B. Supersonic flow in weakly ionized gas around a spherical model (ballistic range experiments)

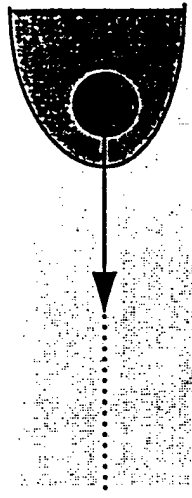
A. 1.



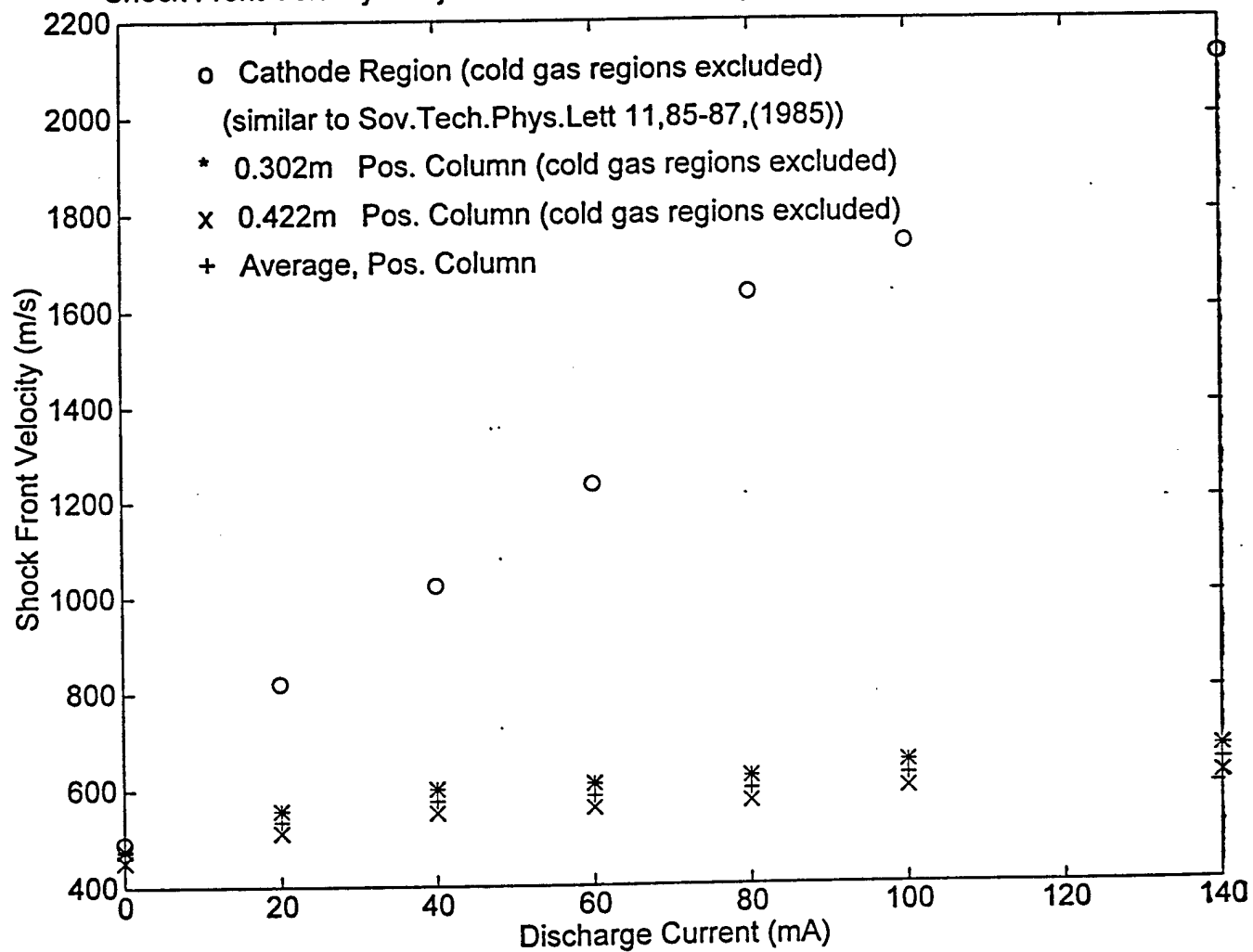
A. 2.

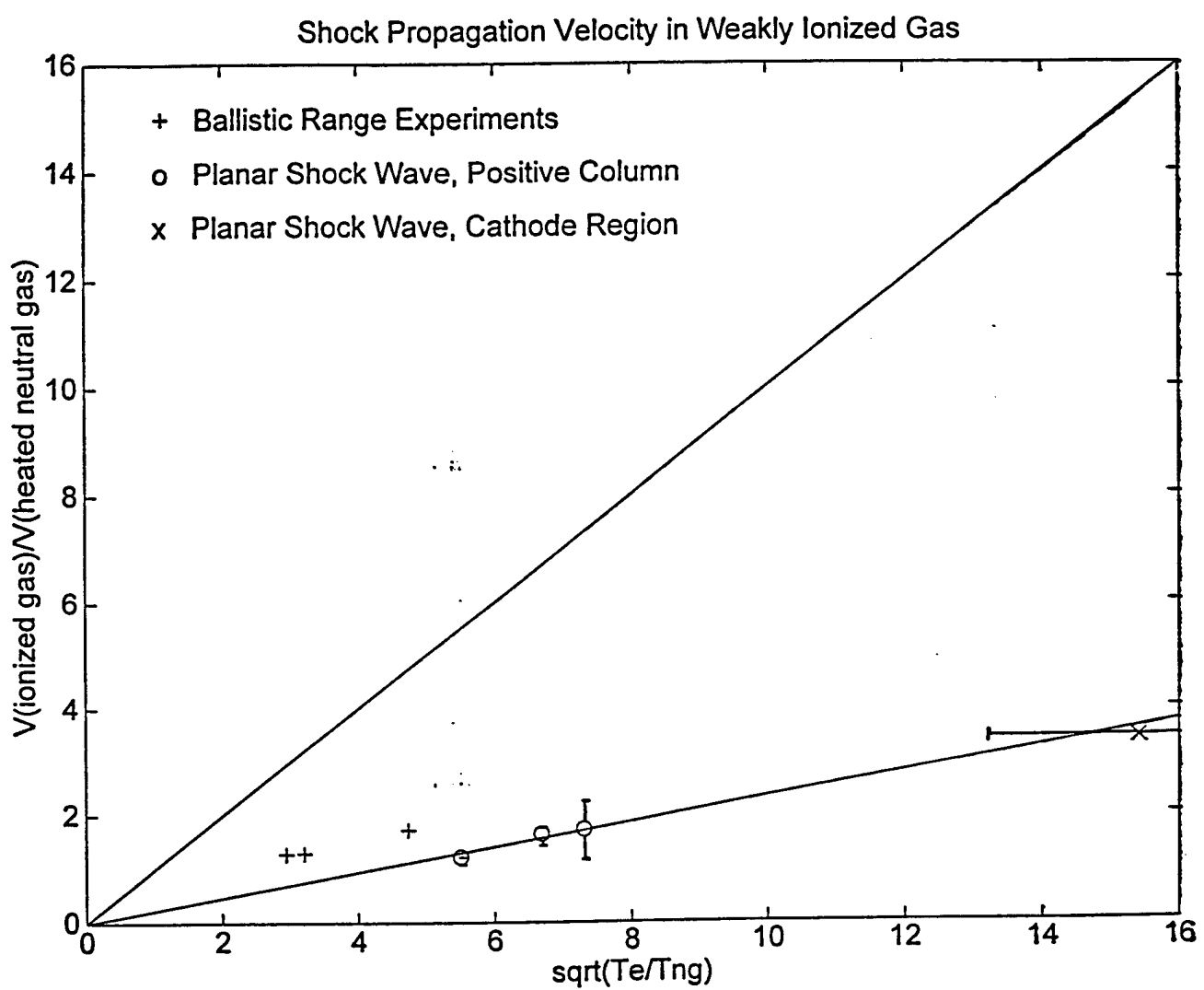


B.



Shock Front Velocity in Cylindrical Glow Discharge [Phys. Lett., A230, 218-222 (1997)]





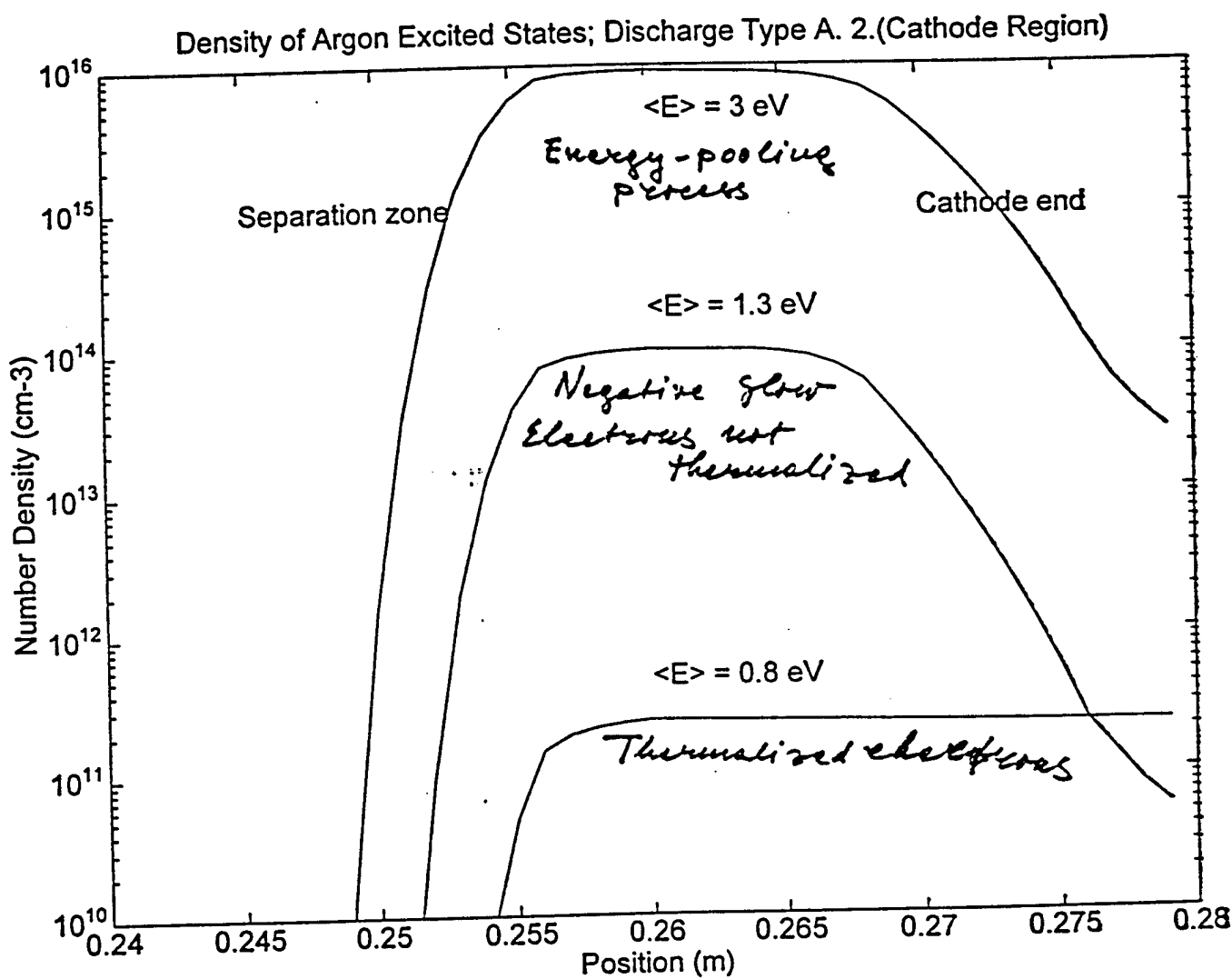
Metastable States

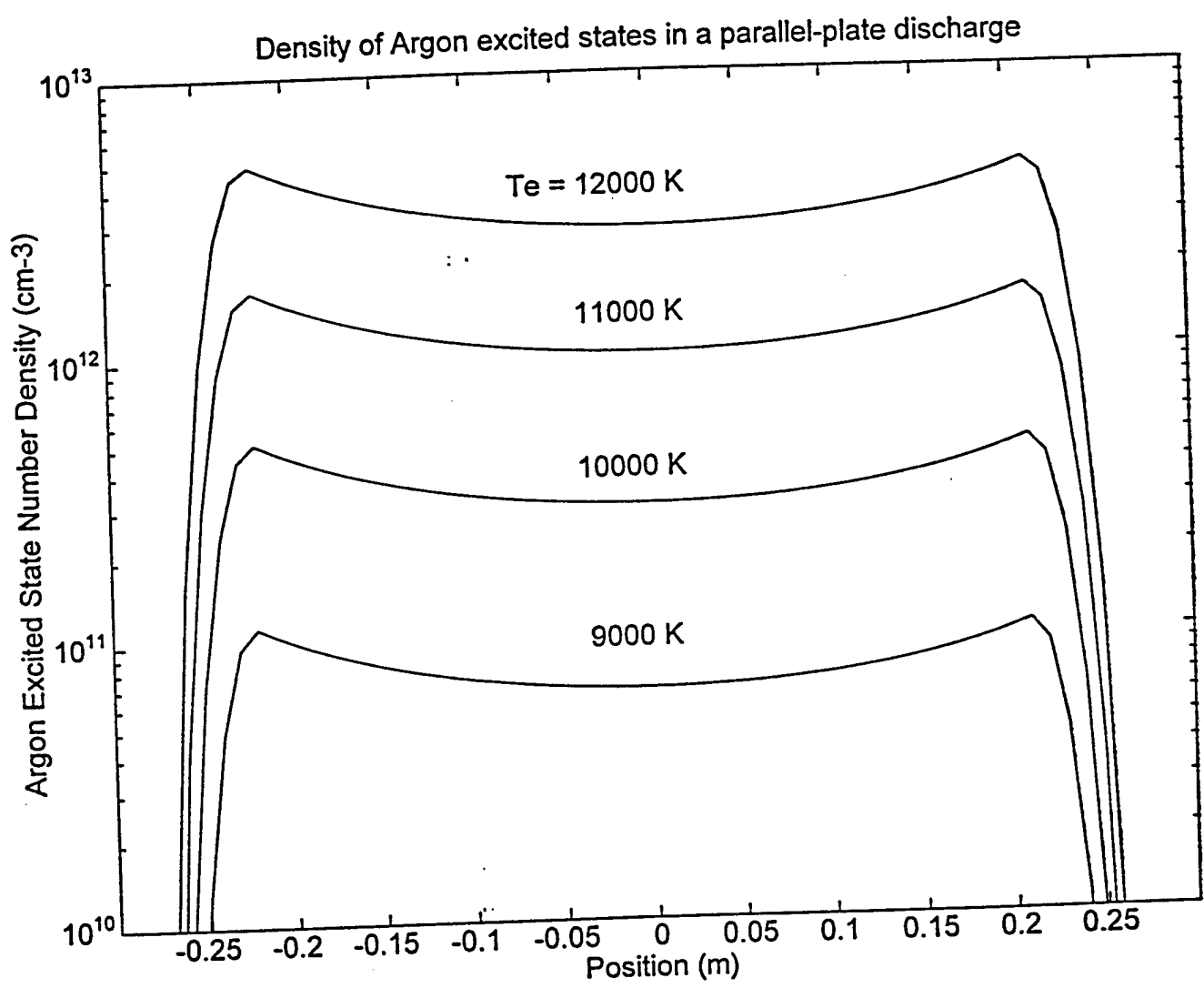
- Oxygen $a^1\Delta_g$ (0.97 - 5) eV
- Nitrogen $A^3\Sigma_u^+$ (6.17 - 8.83) eV
- Argon $1S_{3,5}$ 11.55 eV & 11.72 eV
- 2p (12.91 - 13.48) eV

Relevant Collision Processes

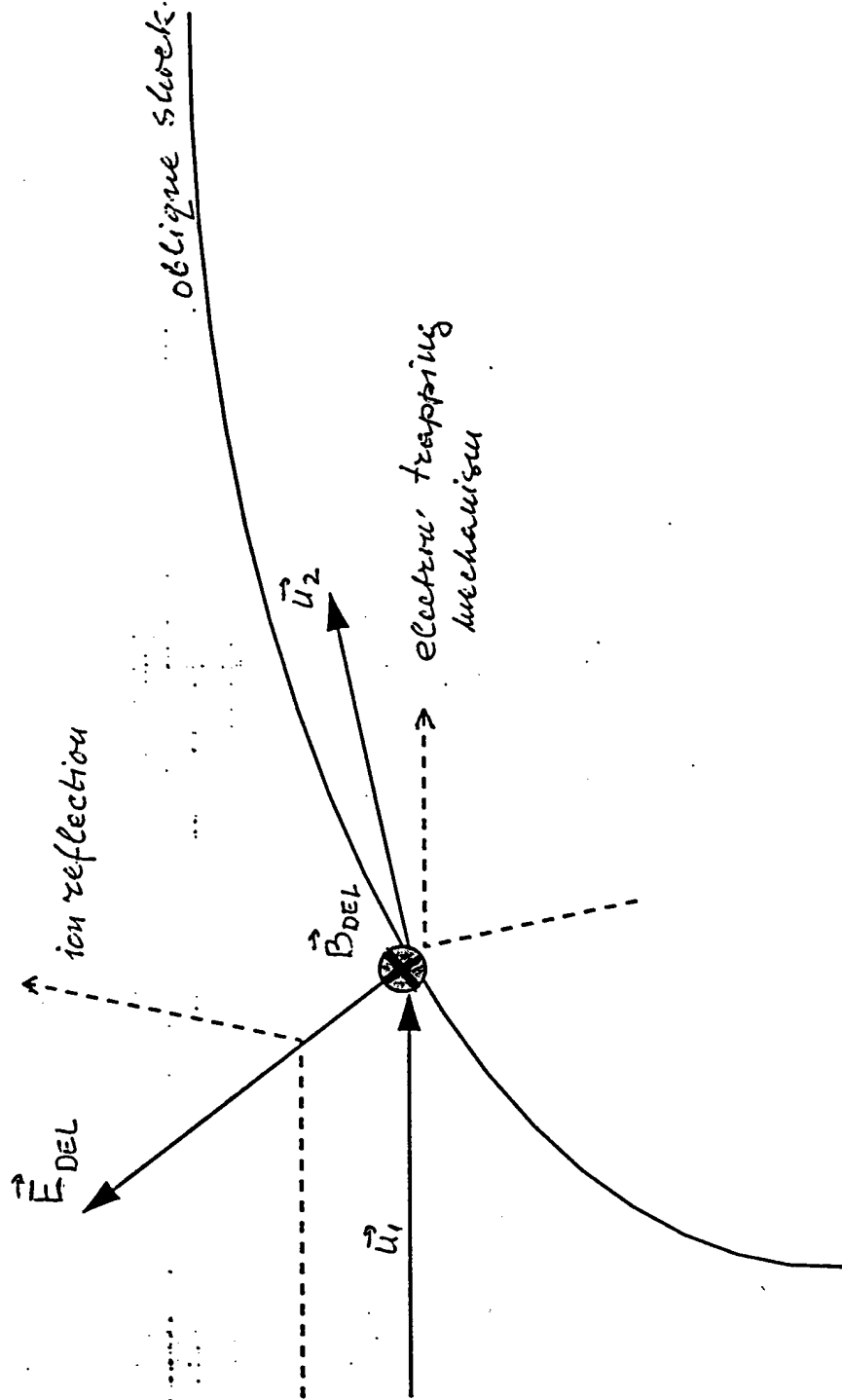
- Electron impact ionization
 - Dominant ionization mechanism at high pressures.
 $\text{Ar}^* + e^- \Rightarrow \text{Ar}^+ + e^-$ (0 to 4 eV)
- Energy pooling reactions
 - Dominant ionization mechanism at medium pressures.
- Charge Transfer
 - $\text{Ar}^* + \text{Ar}^* \Rightarrow \text{Ar} + \text{Ar}^+ + e^-$ (5 to 15 eV)
 $\Rightarrow \text{Ar}^* + \text{Ar}^+ + \text{Ar}^+ + e^-$ (0 to 4 eV)
 - (Density breakdown, “oven effect” of Rydberg states).

$$\text{Ar}^*(\text{fast}) + \text{Ar} \Rightarrow \text{Ar}(\text{fast}) + \text{Ar}^+$$

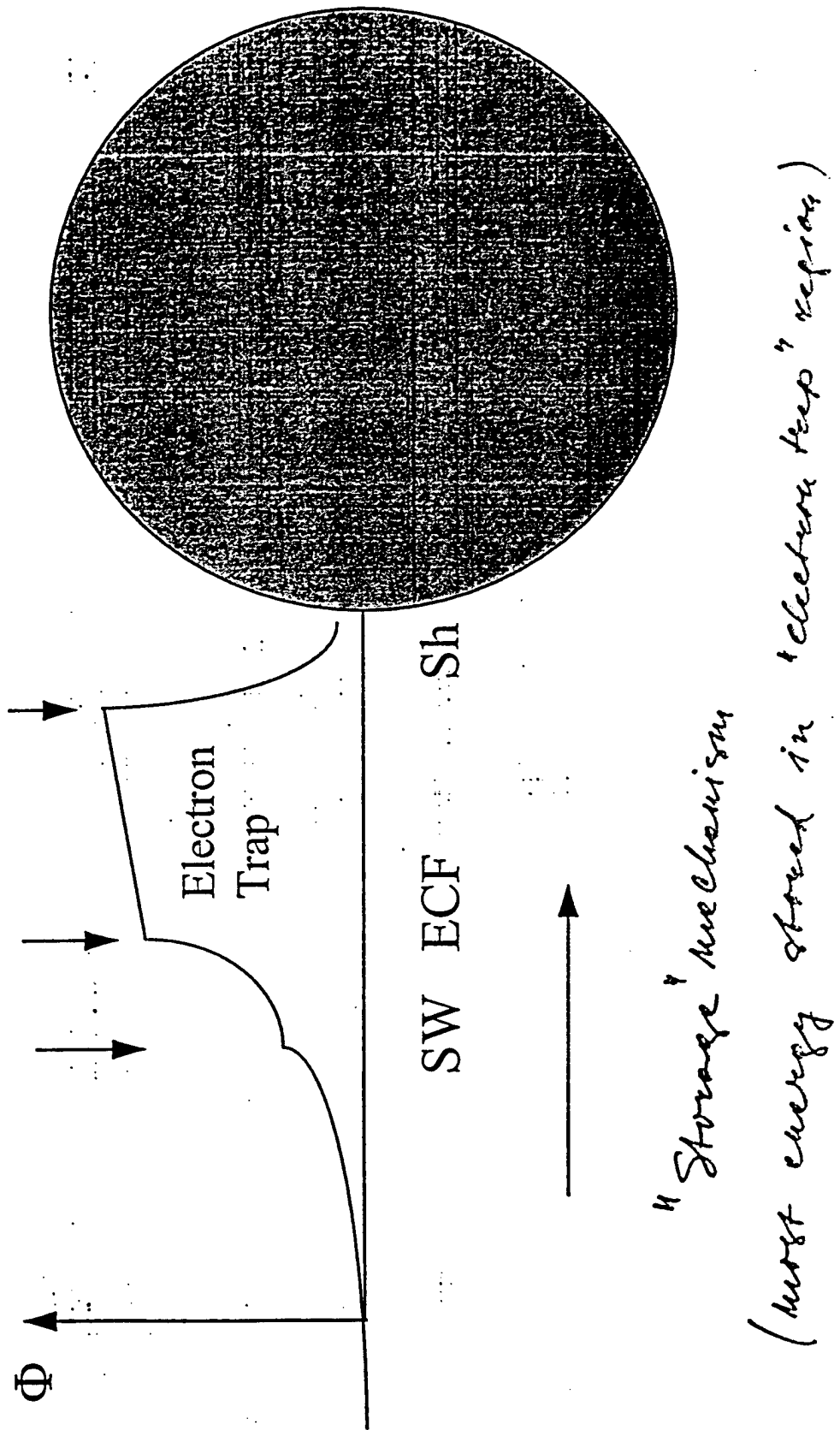




EM Field at DEL



Electric Potential Distribution on the Centerline



Shock Structure

Relaxation (ECF)

“Residual”

Shock wave (SW)

“Precursor”

Centerline

Precursor

“Leader”

Effects which Follow Initial Perturbation

– Ion dynamics

- Shock wave generates a Double Electric Layer (DEL).
- DEL generates an ion acoustic wave.
- Local increase of ion density traveling with the wave.
- Slow ions reflected from DEL.

– Electron dynamics

- Moving DEL induces transversal B field.
- B field confines slow electrons.
- Fast electrons escape DEL.
- Most electrons trapped in relaxation zone
- Electrons heated by inverse bremsstrahlung.

Precursor

- Fast Ions reflected and accelerated on DEL
 - able to excite and ionize atoms and molecules
- Fraction of hot electrons heated by:
 - *inverse bremsstrahlung* (observed difference in population of resonant and metastable states)
 - *energy pooling reactions*
- Mechanisms:
 - A. Ion-acoustic wave
 - B. Ionization wave generated by heavy particles (fast ions and neutrals)?
 - C. Onset of turbulence by angular momentum transfer in energy pooling reactions?

ON-BOARD GENERATION OF A "PRECURSOR" MICROWAVE
PLASMA AT MACH 6: EXPERIMENT DESIGN

R. J. EXTON

NASA AERONAUTICS AND SPACE ADMINISTRATION
LANGLEY RESEARCH CENTER

MACH 6 PLASMA/DRAG REDUCTION TEAM

MEMBER

PRIMARY RESPONSIBILITY

R. J. EXTON	EXPERIMENT DEFINITION
R. J. BALLA	VISUALIZATION/LASERS
G. J. BRAUCKMANN	MODELS/FACILITY
M. DIFULVIO	FACILITY
W. E. LIPFORD	OPTICAL SUPPORT
J. FUGITT*	MICROWAVE (EXPERIMENT)
M. C. BAILEY	MICROWAVE (THEORY)
W. C. KELLIHER	NUCLEAR SOURCES
I. A. CARLBERG	NUCLEAR SOURCES
G. C. HERRING	ELECTRON DENSITY
B. SHIRINZADEH	NEUTRAL DENSITY
P. D. BABB	SAFETY
A. H. AUSLENDER	CPD
D. B. RHODES	SCHLIEREN
S. JONES	SCHLIEREN

*DOE JEFFERSON LAB

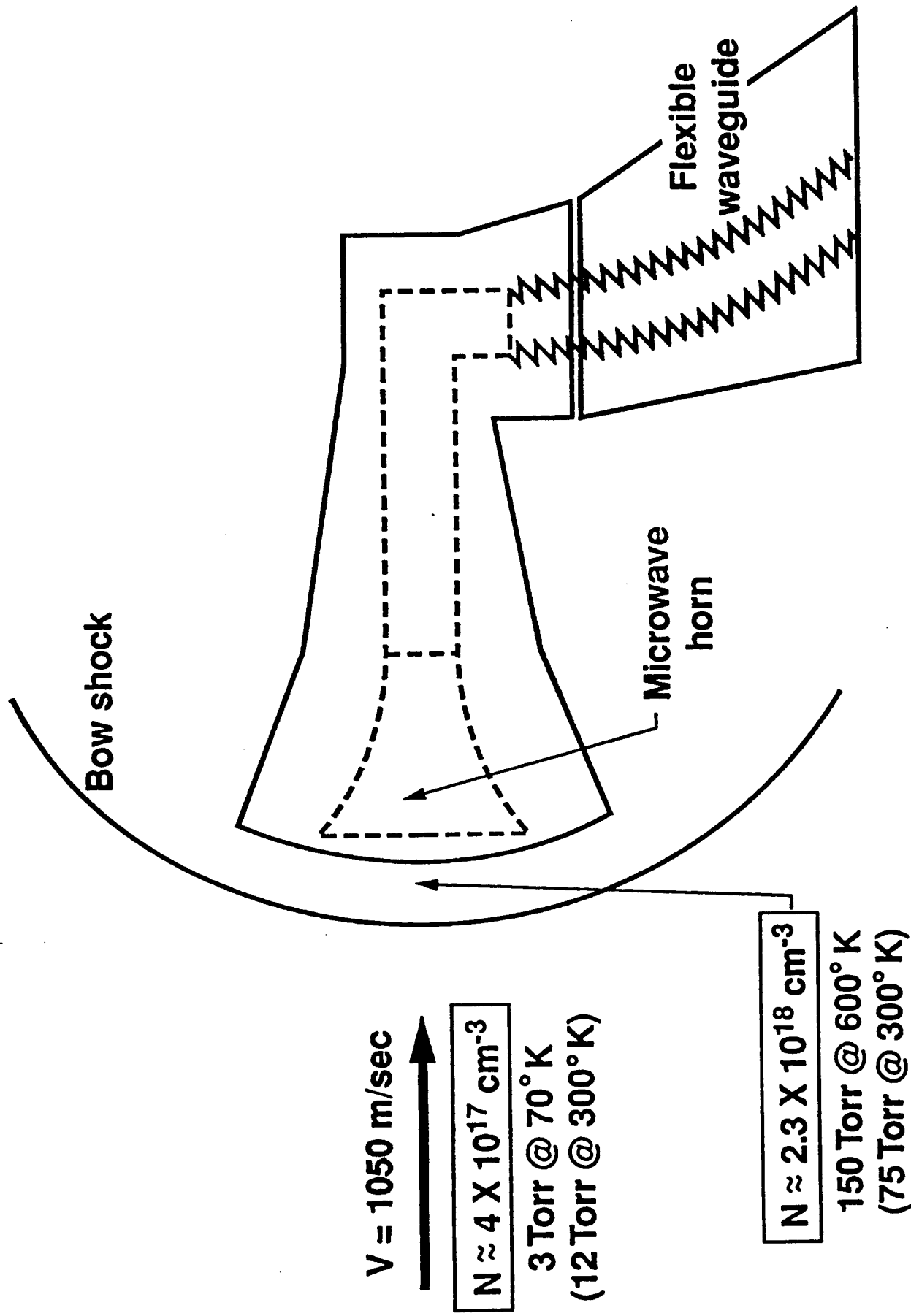
OBJECTIVES:

1. Experimentally demonstrate a concept for on-board generation of a microwave plasma;
2. Develop plasma diagnostic techniques for low density (cold) plasmas;
3. Clarify the physics underlying the phenomenon in conjunction with a parallel CFD effort.

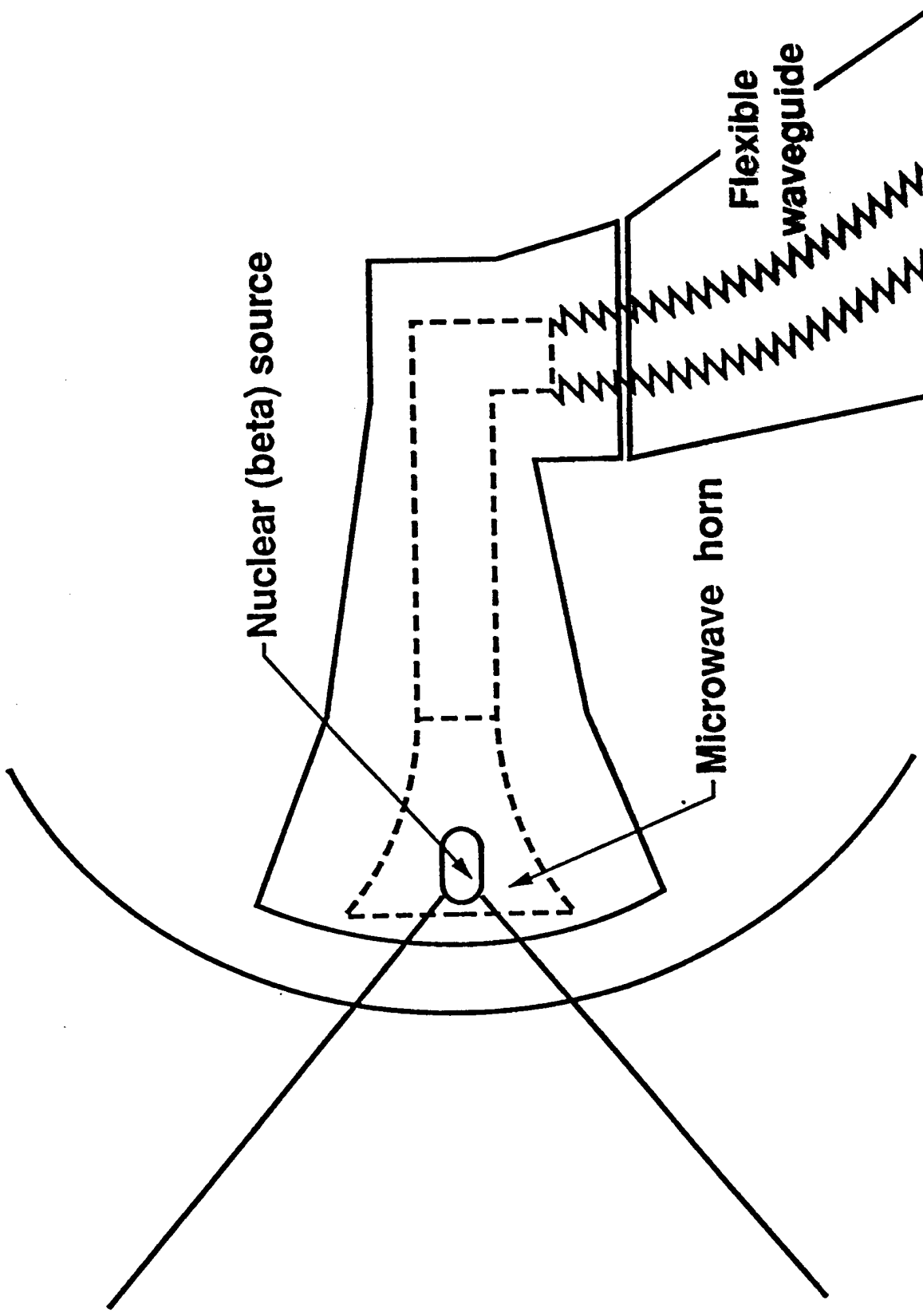
APPROACH

- Design model/microwave horn for Mach 6 facility conditions
- Measure the forces on the model (plasma on/off)
- Characterize the plasma flow field (shock standoff and shape, electron density and temperature, neutral density profile)
- Investigate both cw and pulsed microwave power amplifiers as plasma generators

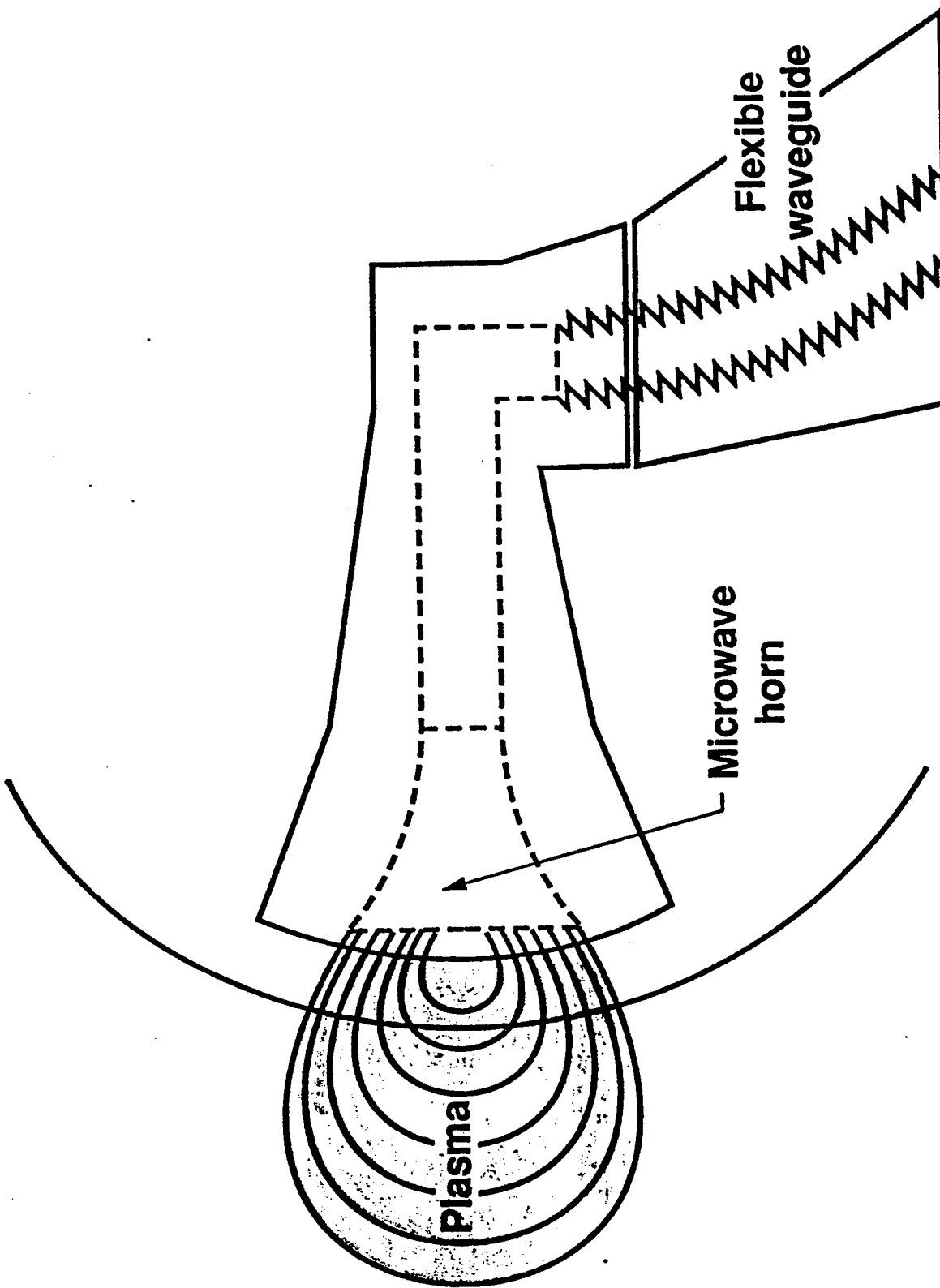
"Precursor" Microwave Plasma at Mach 6



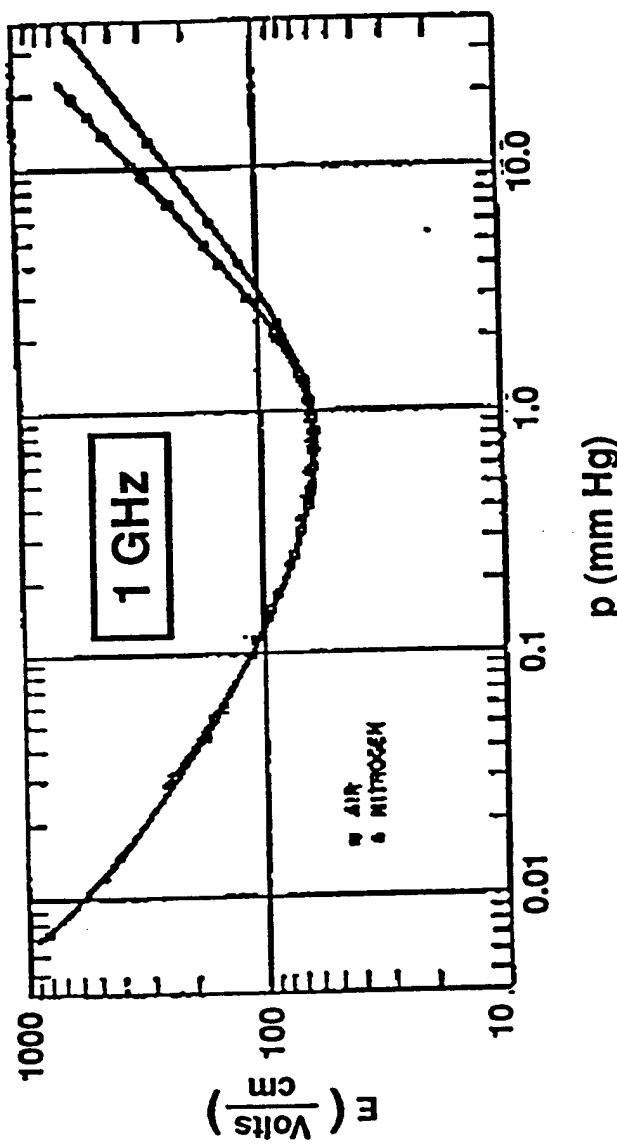
"Precursor" Microwave Plasma at Mach 6



"precursor" Microwave Plasma at Mach 6



Microwave Breakdown in Air, O₂, and N₂

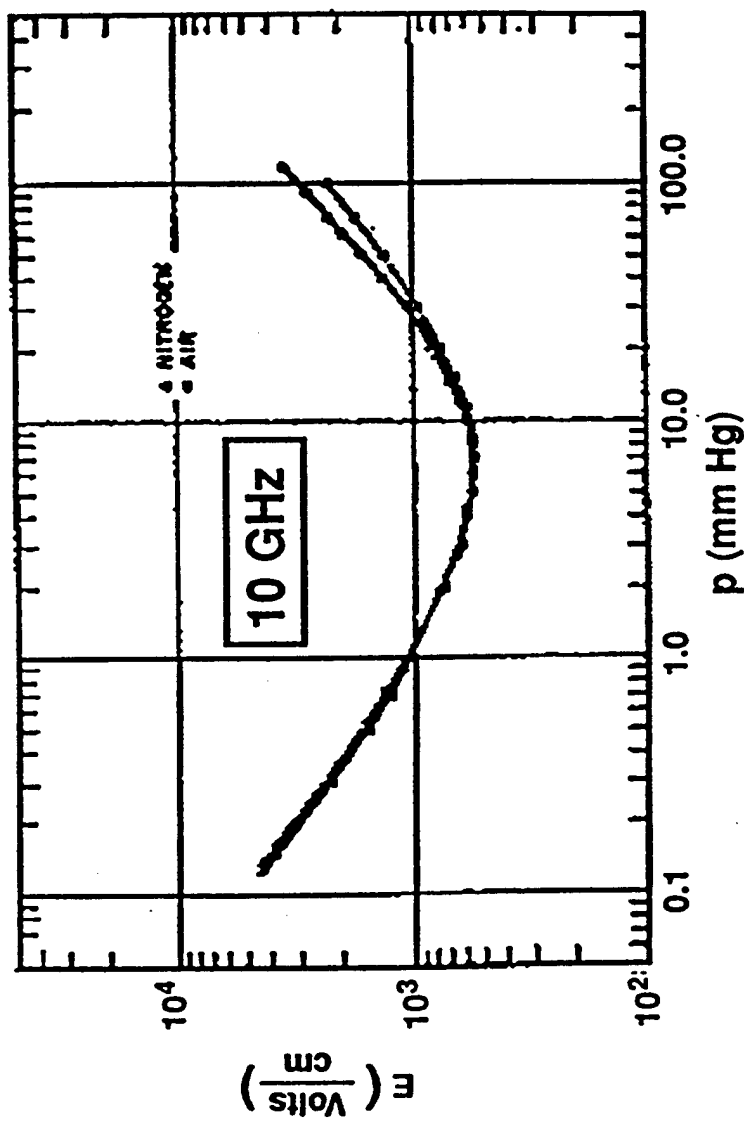


Cw breakdown fields for air and nitrogen at a frequency of 994 Mc/sec.

(Characteristic diffusion length $A = 2.65 \text{ cm}$)

A. D. MacDonald et. al. Phys. Rev. 130, 1841 (1963)

Microwave Breakdown in Air, O₂, and N₂

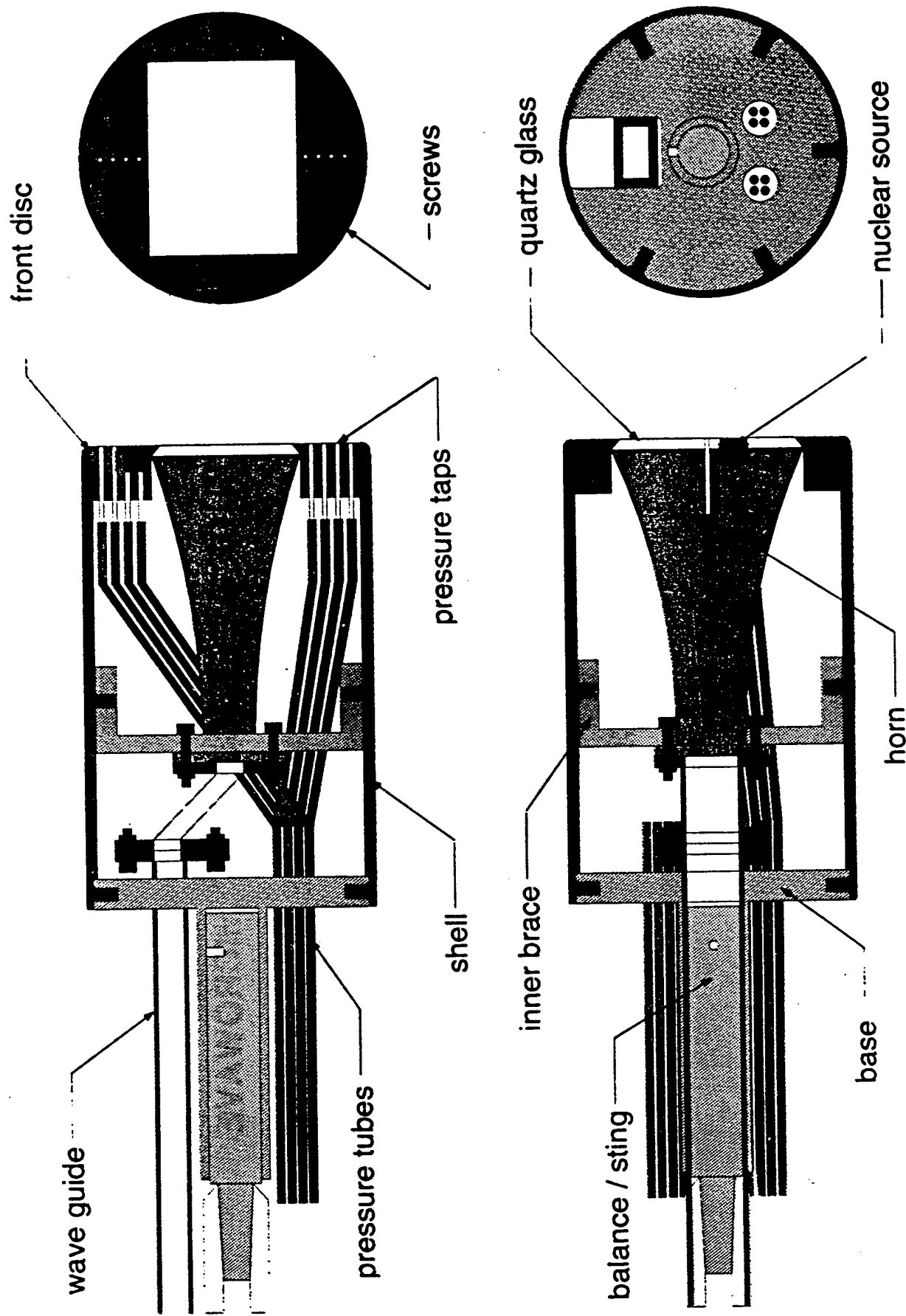


Cw breakdown fields for air and nitrogen at a frequency of 9.4 kMc/sec.

(Characteristic diffusion length $A = 0.22$ cm)

A. D. MacDonald et. al. Phys. Rev. 130, 1841 (1963)

PLASMA DRAG REDUCTION MODEL



DIAGNOSTICS

INITIAL ENTRY

- o PULSED, DIGITAL SCHLIEREN
- o GATED, CCD CAMERA
- o OPTICAL MULTICHANNEL ANALYZER
(200-900 NM)

FUTURE ENTRIES

- o EXCIMER LASER (NEUTRAL PROFILE)
- o LASER/MICROWAVE INTERFEROMETRY
(ELECTRON DENSITY)

SCHEDULE-MACH 6

SCHEDULE/MICROWAVE POWER

INITIAL ENTRY ~AUG 97

POWER AMPLIFIERS (AVAILABILITY)

<u>CW</u>	0	200 W, 8-18 GHz (AVAILABLE)
*	*	500 W, 8-18 GHz (POSSIBLE LOANER)
*	*	2 kw @ 14 GHz (COMMERCIAL)
*	*	10 kw @ 18 GHz (?????)
<u>PULSED</u>	0	26 kw PEAK, X-BAND (8.2-12.4 GHz) 5% DUTY 1.3 kw AVG. (POSSIBLE LOANER)
*	*	100 kw PEAK, X-BAND (8.2-12.4 GHz)
*	*	100 kw PEAK, KU-BAND(POSSIBLE (12.4-18.0 GHz) 3 MICROSEC PULSE 100 Hz

2ND ENTRY..FY98

CONCERNS

- o SUFFICIENT FIELD STRENGTH FOR BREAKDOWN
(~700 V/cm @ 10-15 TORR)
- o PLASMA EXTENT SUFFICIENT TO ATTAIN "PRECURSOR"
- STATUS
- o ELECTRON DENSITY AND TEMPERATURE ADEQUATE TO
 BRING ABOUT SHOCK MODIFICATION

SOLUTION

MORE POWER

Program Overview

Shock Wave Dynamics in Weakly Ionized Plasmas at Laboratory for Modern Fluid Physics, Florida A&M University (FAMU), Tallahassee, FL

Prof. J. A. Johnson III, Distinguished Prof. of Science and Engineering
Dr. Richard Appartaim, Research Associate in Physics
Mr. Kester Thompson, Graduate Student, Mechanical Engineering

Overall FAMU Purpose

To determine the roles which turbulence and/or nonequilibrium effects in weakly ionized gases play in shock wave transport dynamics through:

- (a) comprehensive optical diagnostics of the interactions of shock waves with turbulence and/or nonequilibrium plasmas in the low supersonic and hypersonic regimes;
- (b) rigorous analyses of the associated physics, including quantummechanical as well as classical phenomena;
- (c) explorations of potential modalities for the implementation of plasma drag reduction of operational aircraft.

Recent FAMU Achievements

- > Evidence of shock wave strength reduction from a turbulence manipulated nonequilibrium flow in a pressure ruptured shock tube;
- > Preliminary evidence of shock wave acceleration in our new Supersonic Shocked Plasma Facility where a Mach 2 shock wave moves from a plasma free region into one with a weak plasma;
- > Preliminary evidence from our Hypersonic Arc Driven Shock Tube of highly localized energy transfer from small scale turbulent nonequilibrium fluctuations into large scale flow of the sort which can weaken the strength of a resident shock wave.
- > Preliminary experimentally testable explanations of the influence of turbulence and/or nonequilibrium effects on standard macroscopic transport quantities

Specific Immediate FAMU Plans

- > Modifications of our current Supersonic Shocked Plasma Facility to afford a wider variety of manipulations in the shock wave-plasma interaction, including the introduction of seed molecules and microwave probes;
- > System-specific modelling of the plasma and atomic processes so as to determine the underlying physics along with a full range of test modalities, including those relevant to ballistic ranges, flight, and other configurations different from our own;
- > The implementation of a new Turbulent Stark Velocimetry as a program of development of relevant portable diagnostics suitable for possible near term introduction on operational airframe platforms.

AERODYNAMIC APPLICATIONS OF WEAKLY IONIZED PLASMAS

R. Miles, S. Macheret, S.H. Lam, P. Efthimion, L Martinelli
Princeton University

- Drag Reduction
- Plasma Ramparts
- Flow Control
 - By Localized Energy Addition
 - By $J \times B$ forces
- Control and Initiation of Chemical Processes
- Power Extraction
 - MHD in an engine inlet (AJAX)
 - MHD in ionized flow
- Hypersonic Wind Tunnel Drivers
 - By Energy Addition through microwaves
 - By MHD acceleration
- Suppression of shock strength and sonic boom

SUSTAINING A PLASMA IN HIGH SPEED FLOW

Important for Drag reduction, Plasma Ramparts, Flow Control,
Shock Suppression, MHD, and Combustion Initiation and Control

- Discharge may be blown out
- Thermal (equilibrium) plasma will need to be reinitiated -
a thermal plasma cannot propagate at supersonic speed
- Nonequilibrium plasma will require high electric field and high power
- A filamentary plasma may serve the purpose and will require less
power (a small portion of the volume is ionized)
- Filaments may be guided by laser or electron beams
- A high power microwave may be the preferred source.

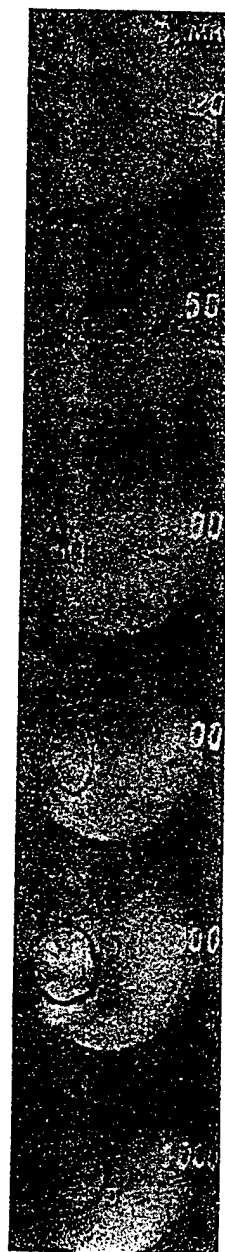
SUSTAINING MICROWAVE DRIVEN PLASMAS IN ATMOSPHERIC PRESSURE AIR

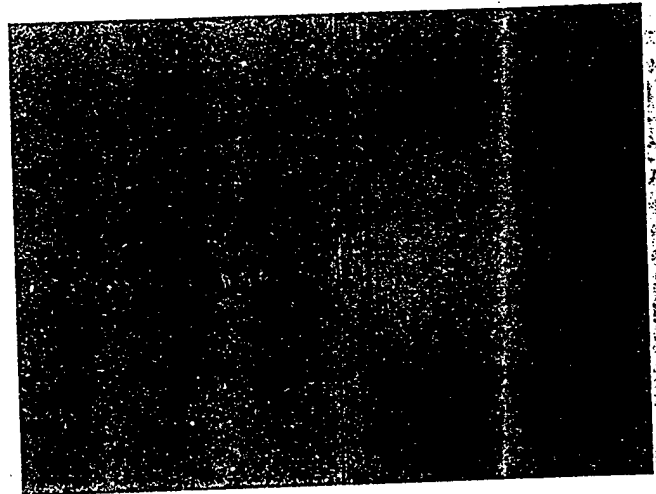
Thermal Regime

- Requires $T_{min} > 4000K$
- Needs relatively low microwave power (kilowatts/cm^2)
the power offsets the thermal losses
- Long lifetime (cooling time)

Nonequilibrium Regime

- Requires high power microwaves to overcome the electron recombination and attachment rates
- Diffuse plasma (low pressure)
 - Low temperature neutral species
- Filamentary discharge (high pressure)
 - High temperature localized streamers

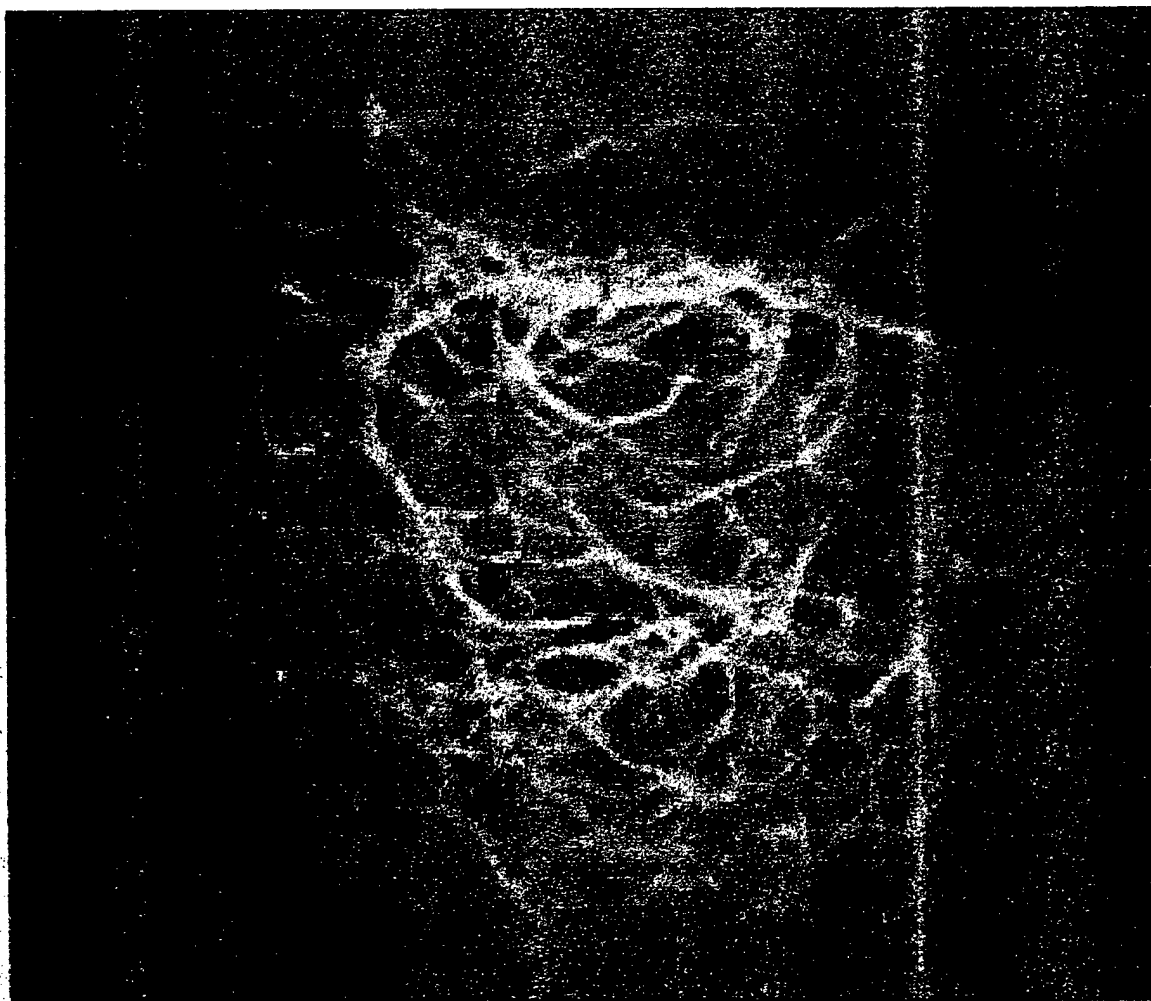




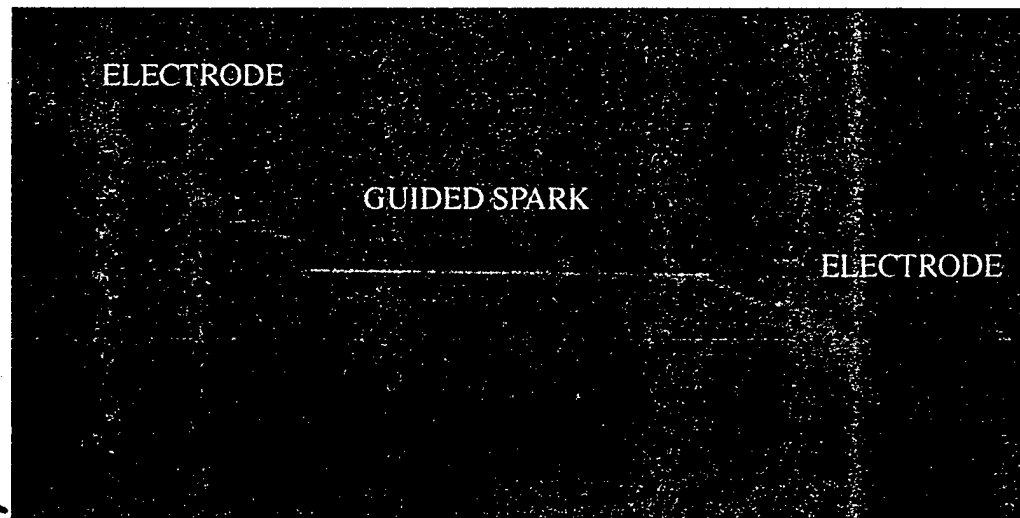
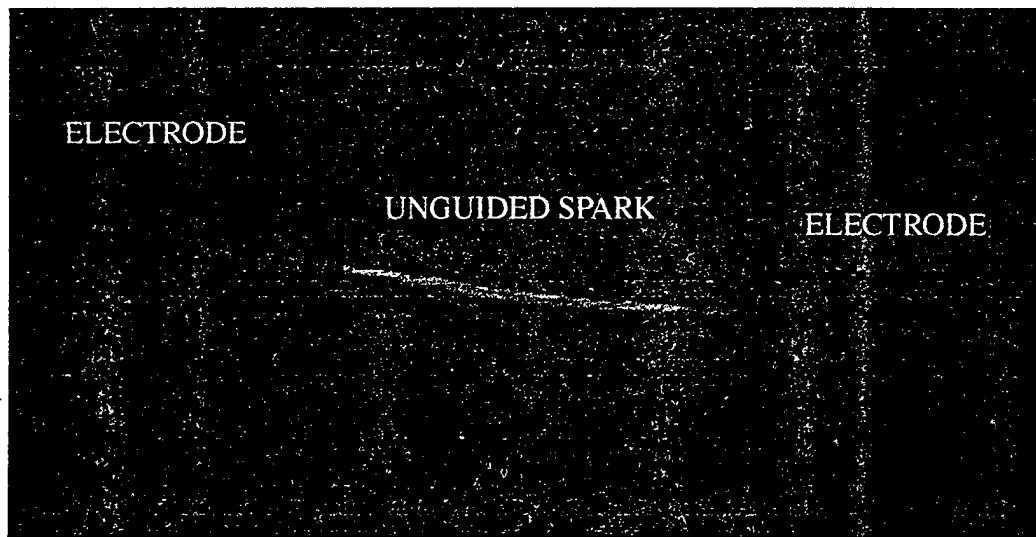
FILAMENTATION OF ATMOSPHERIC
MICROWAVE DRIVEN PLASMA

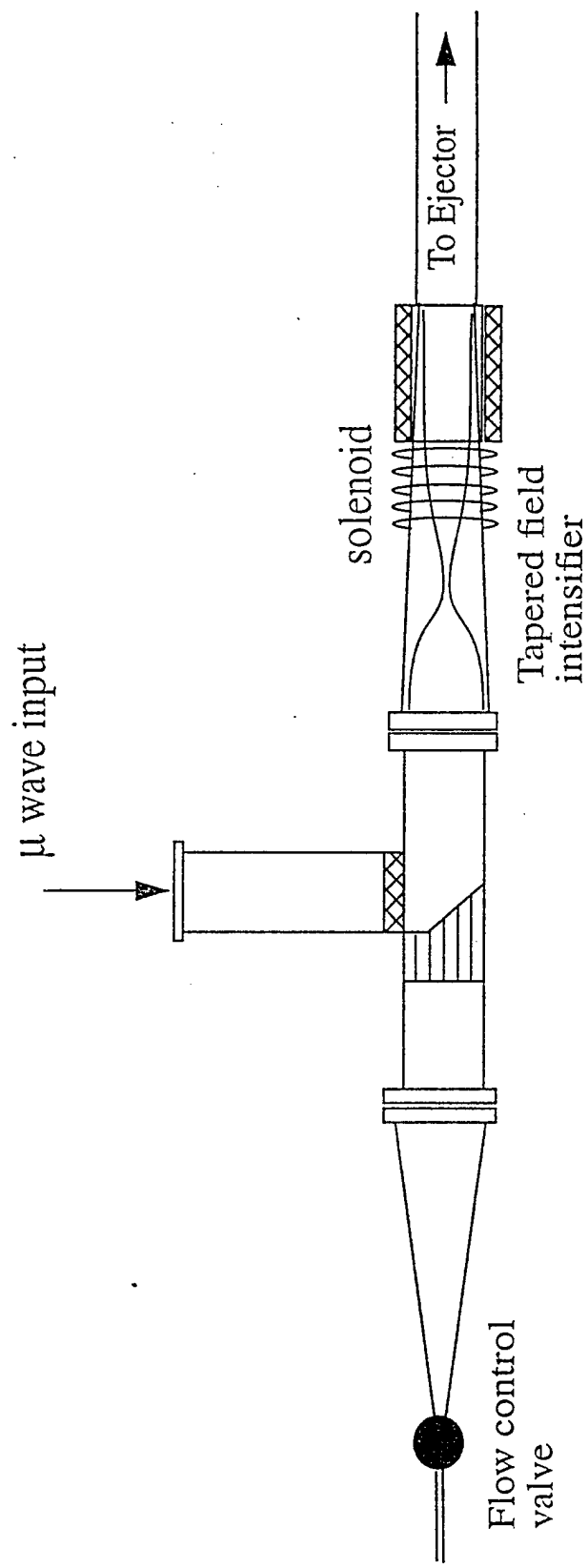
Grachev, Esakov, Mishin and Khodataev

Moscow RadioTechnical Institute



LASER GUIDED ARC FORMATION





DRAG REDUCTION

Experimental Observations

Shocks Accelerate Upon Entry Into Plasmas From Neutral Gas

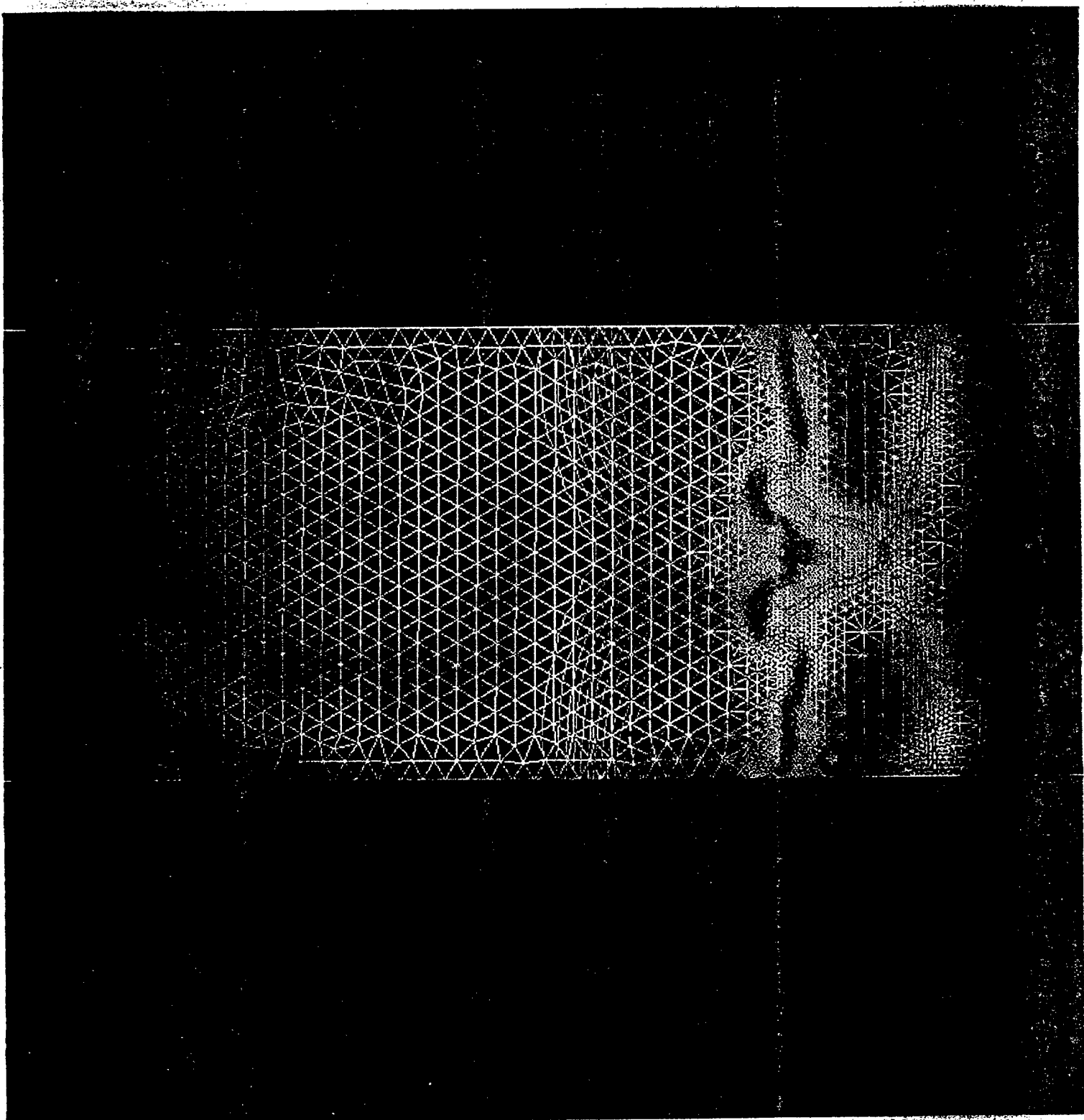
Dramatic Changes In Structure:

- Shock Front Broadens
- Amplitude Decreases
- Shock Typically Splits Into Two or Three

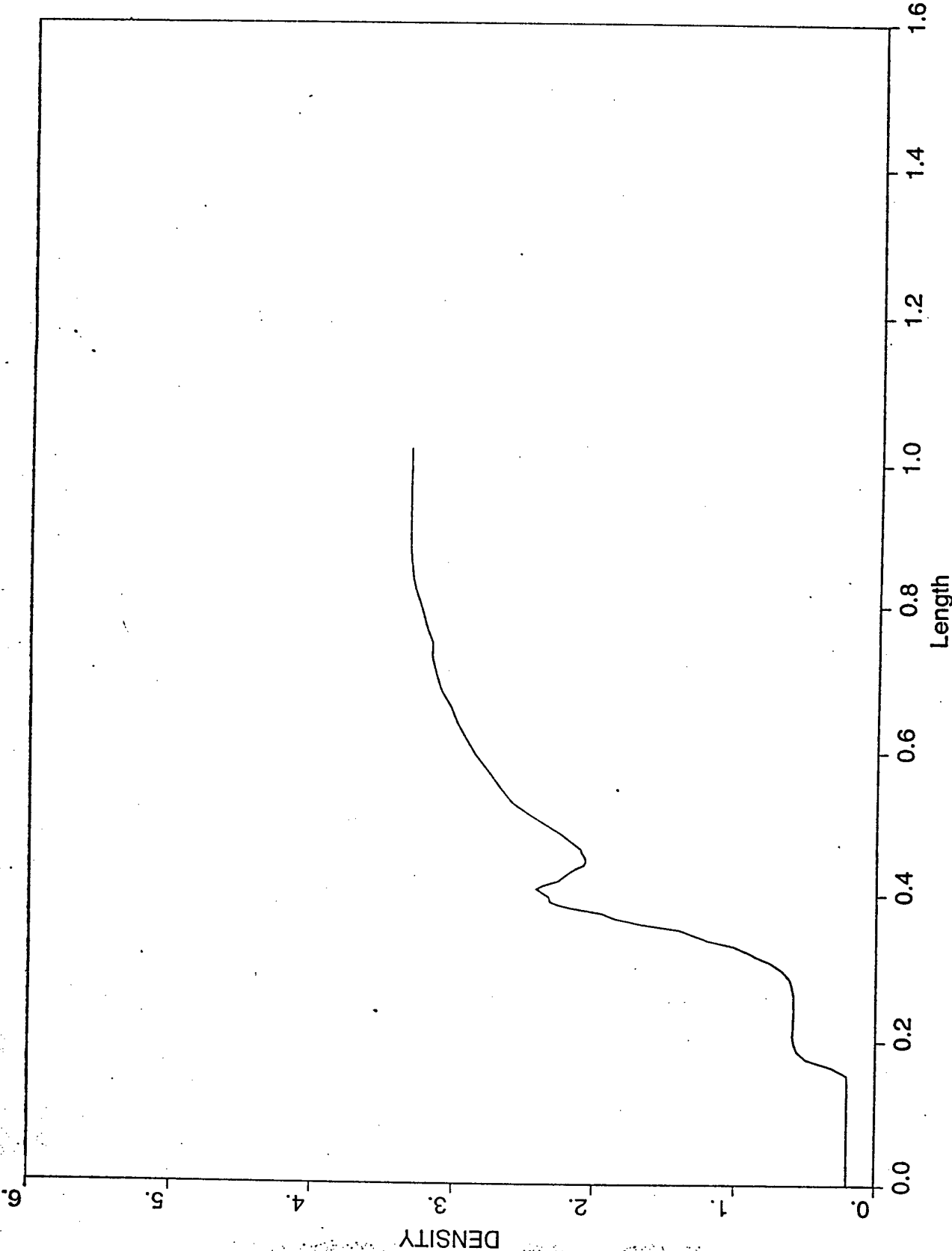
Effect Persists for Quite a Long Time (up to 1 - 10 msec)

Observations Were Made In Various Discharges (Longitudinal And Transverse), In Various Gases (Air, Argon, Hydrogen, Helium, Etc.) Using Various Diagnostics.

Ballistic Range Experiments Seem to Imply a Change in the Effective Speed of Sound, and Show Decrease in Supersonic Drag.

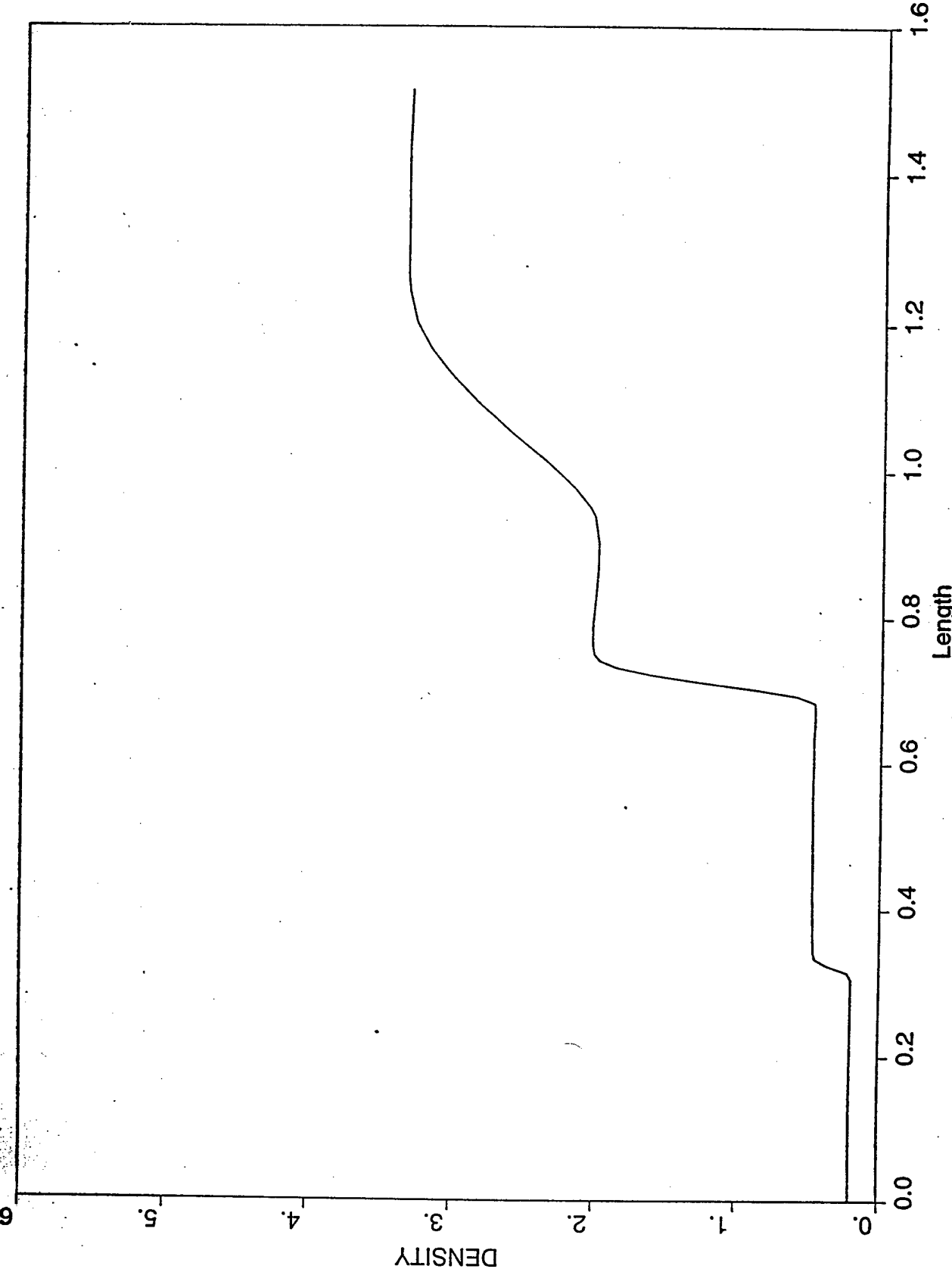


DENSITY PROFILE ACROSS THE SHOCK IN "THERMAL DIAPHRAGM" CASE
(CURVED BOUNDARY BETWEEN HOT AND COLD REGIONS)
CUT ALONG THE CENTER LINE.

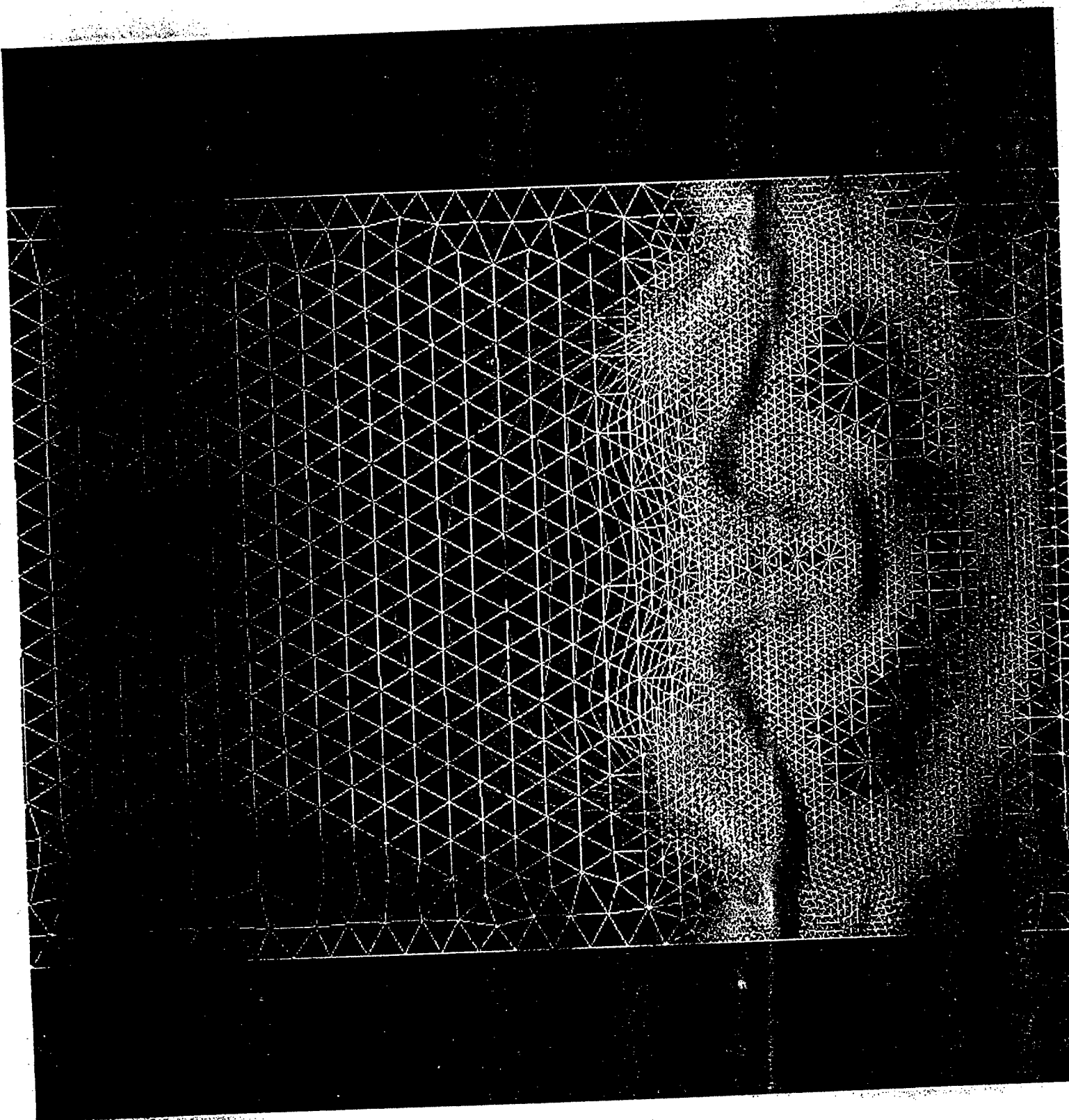


Planar Cut @ (0.83, -0.24, 0.25)(0.83, 0.74, 0.25)(1.82, -0.24, 0.25)

DENSITY PROFILE ACROSS THE SHOCK IN "THERMAL DIAPHRAGM" CASE
(CURVED BOUNDARY BETWEEN HOT AND COLD REGIONS)
SIDE CUT



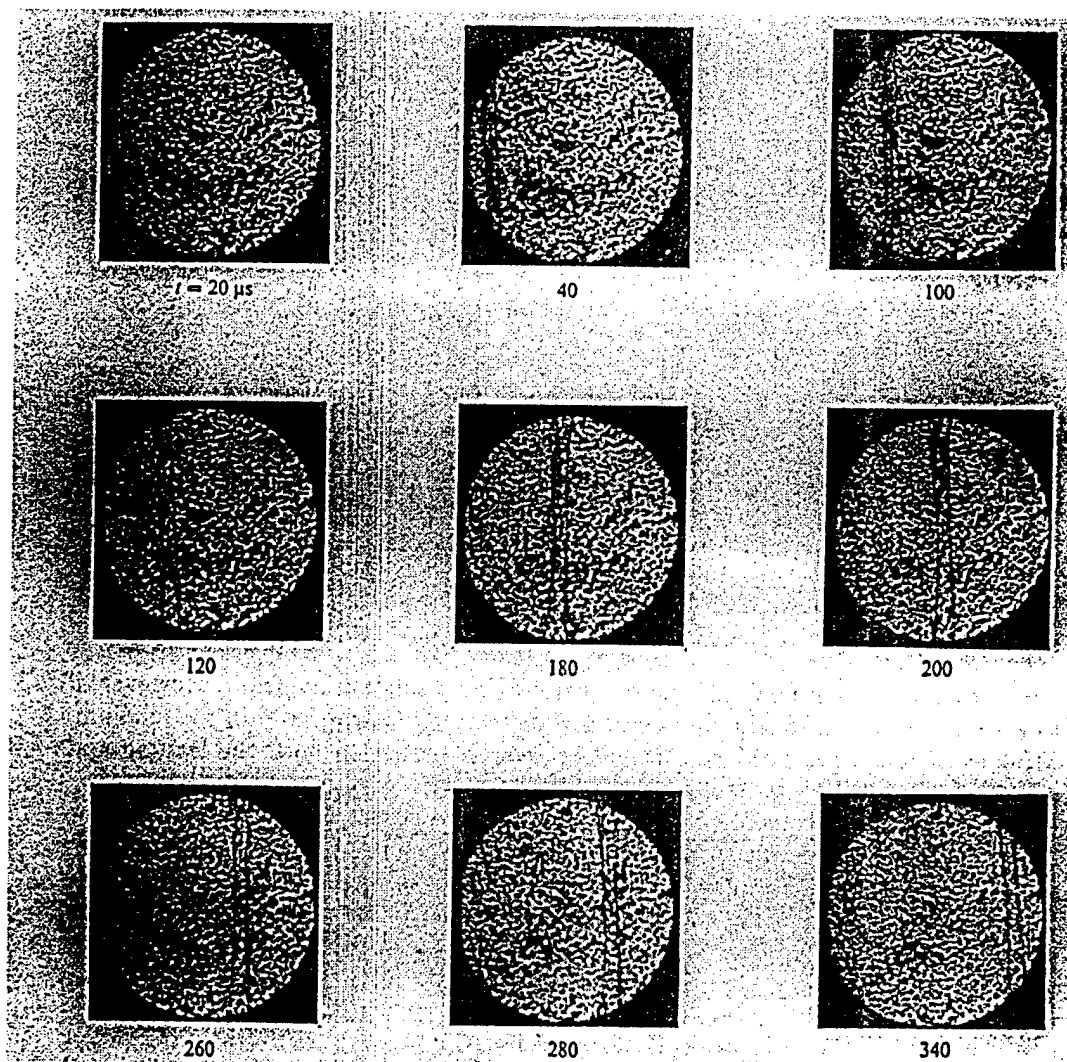
Planar Cut @ (1.01, -0.28, 0.25)(1.01, 1.26, 0.25)(2.55, -0.28, 0.25)



EXPERIMENTAL CONCERNS

- Temperature
 - In all the experiments, the temperature of the neutral gas has not been directly measured.
- Temperature Profile
 - A transverse temperature profile or a curved thermal boundary will lead to complex shock structure. This may occur as the shock passes through the hot cathode or anode fall regions of the discharge. (Well away from the centerline of the experiment)
 - Models indicate the apparent shock splitting and the density rise echo experimental observations
- Nonuniform Temperature Field
 - Shock splitting has been seen in turbulent mixtures of gases. If the plasma has hot and cold regions, a similar shock break-up may occur.

M = 1.03 SHOCK PROPAGATION THROUGH
HE + R 12 TURBULENT MIXTURE
Hesselink and Sturtevant



CONCLUSIONS ON DRAG REDUCTION

- All the experimental phenomena we examined are consistent with thermal gradient effects
- Ballistic range data needs to be studied in more detail
- Accurate temperature and density measurements need to be made
- There may be some effects of thermal gradients, unsteady phenomena, vorticity, and random or flickering heat addition.

PRINCETON PROGRAM

- Development of new diagnostics for temperature and density imaging
- New World Vistas
 - Sustaining microwave driven plasmas in a Mach 3 flow
 - Plasma effects on the bow shock in a Mach 3 flow.
 - Study of basic mechanisms of acoustic wave interactions and shock dynamics in stationary plasmas
- Plasma Ramparts
 - Experimental studies of the control of plasma filamentation
 - Kinetic model development for pulsed ionized air plasmas
 - Modeling nonequilibrium molecular processes
 - High power microwave driven discharge dynamics
 - Stabilizing and extending microwave driven plasmas with magnetic fields
- Mariah II (Radiatively Driven Wind Tunnel augmented by MHD)
 - Sustaining conductivity in atmospheric pressure air with electron beams
 - Acceleration and deceleration of supersonic flows in MHD channels
 - Energy coupling into high pressure air
 - MHD acceleration with filamentary discharges

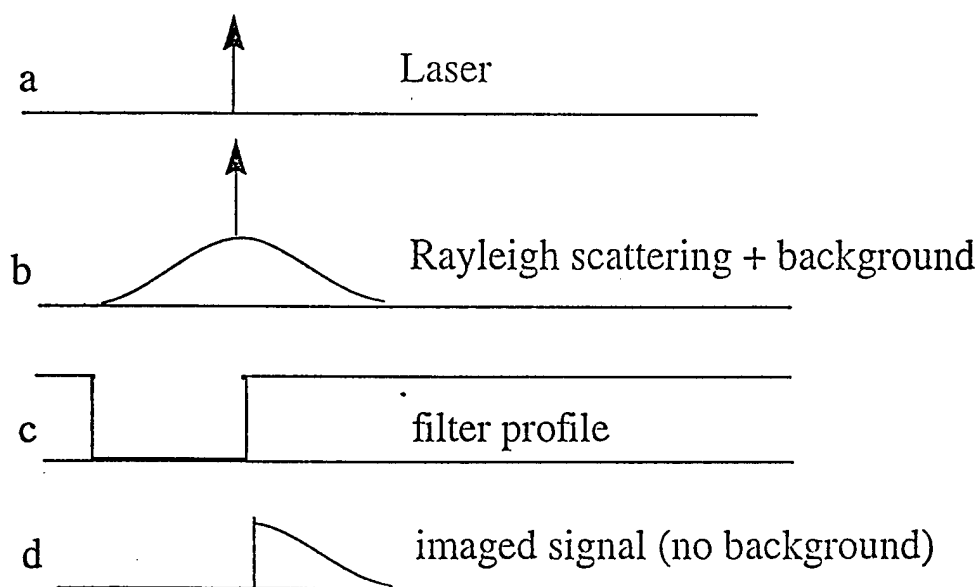
PLASMA TEMPERATURE MEASUREMENT BY FILTERED RAYLEIGH SCATTERING

Rayleigh Scattering

- Total Scattering is Proportional to Density
- Linewidth is proportional to \sqrt{T}
- Signal is weak
- Background scattering is at nearly the same frequency

Filtered Rayleigh Scattering

- Eliminates Background Scattering
- Permits Measurement of Linewidth



FILTERED RAYLEIGH SCATTERING IMPLEMENTATION

Source

- Tunable Ultraviolet, Injection Locked Laser
- Ti:sapphire with "Ramp and Lock" Technology
(Schwartz Electro-Optics)

Filter

- Atomic Mercury Vapor
- 2" Diameter Cell Held at 40°C with a
hot water bath (vapor pressure 1 Torr)

Camera

- UV Sensitive, Intensified CCD (Princeton
Instruments)

SEQUENTIAL RAYLEIGH IMAGES OF MACH 2.5
SHOCKWAVE / BOUNDARY LAYER INTERACTION
AT A 14° WEDGE

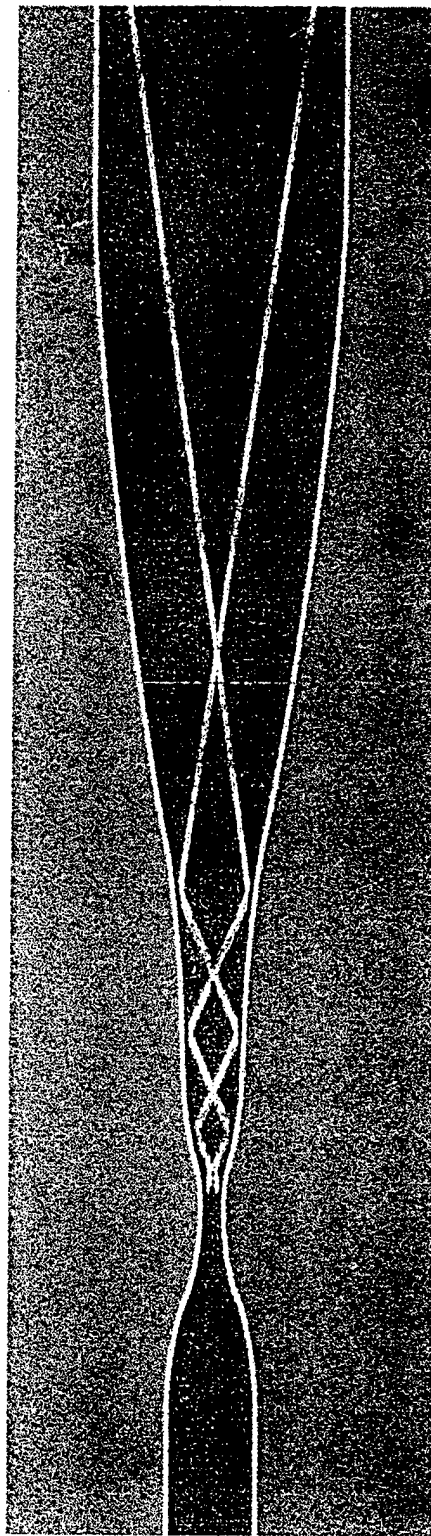


Framing rate is 500,000 images per second

Mariah II

- No wind tunnel can at present be run to accurately simulate flight conditions at higher than Mach 8
 - 240K, (120,000 ft) requires 2800K, 8 atm in plenum
 - NO contamination
 - Low static T or low static P (enthalpy too low or entropy too high)
 - Short time operation
- Radiatively Driven concept adds energy downstream of the throat in the supersonic section
 - Static temperature stays low
 - Low temperature but high pressure in the plenum
 - Concept is driven by lasers or electron beams
 - Demonstrated with 10KW laser in December at Wright Labs
- MHD section is to be added to further accelerate the flow after the Radiative section
 - Reduces the front end pressure requirement
 - Extends the envelope of the tunnel
 - Requires electron beam sustained conductivity
 - Must operate at close to room temperature and at pressures on the order of .1 atm.

Energy Addition by Lasers



RDHWT Review April 23 - 24, 1997

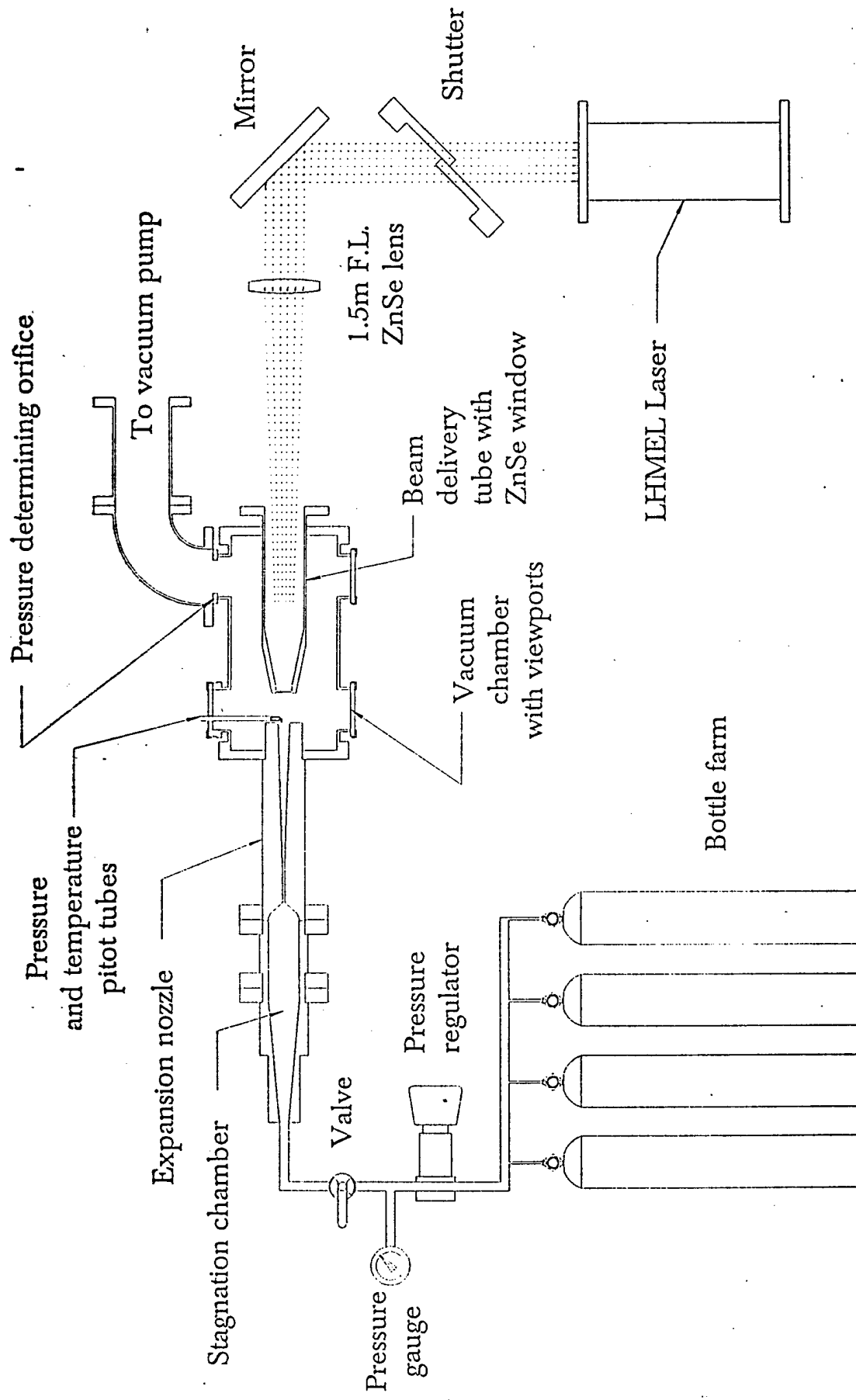
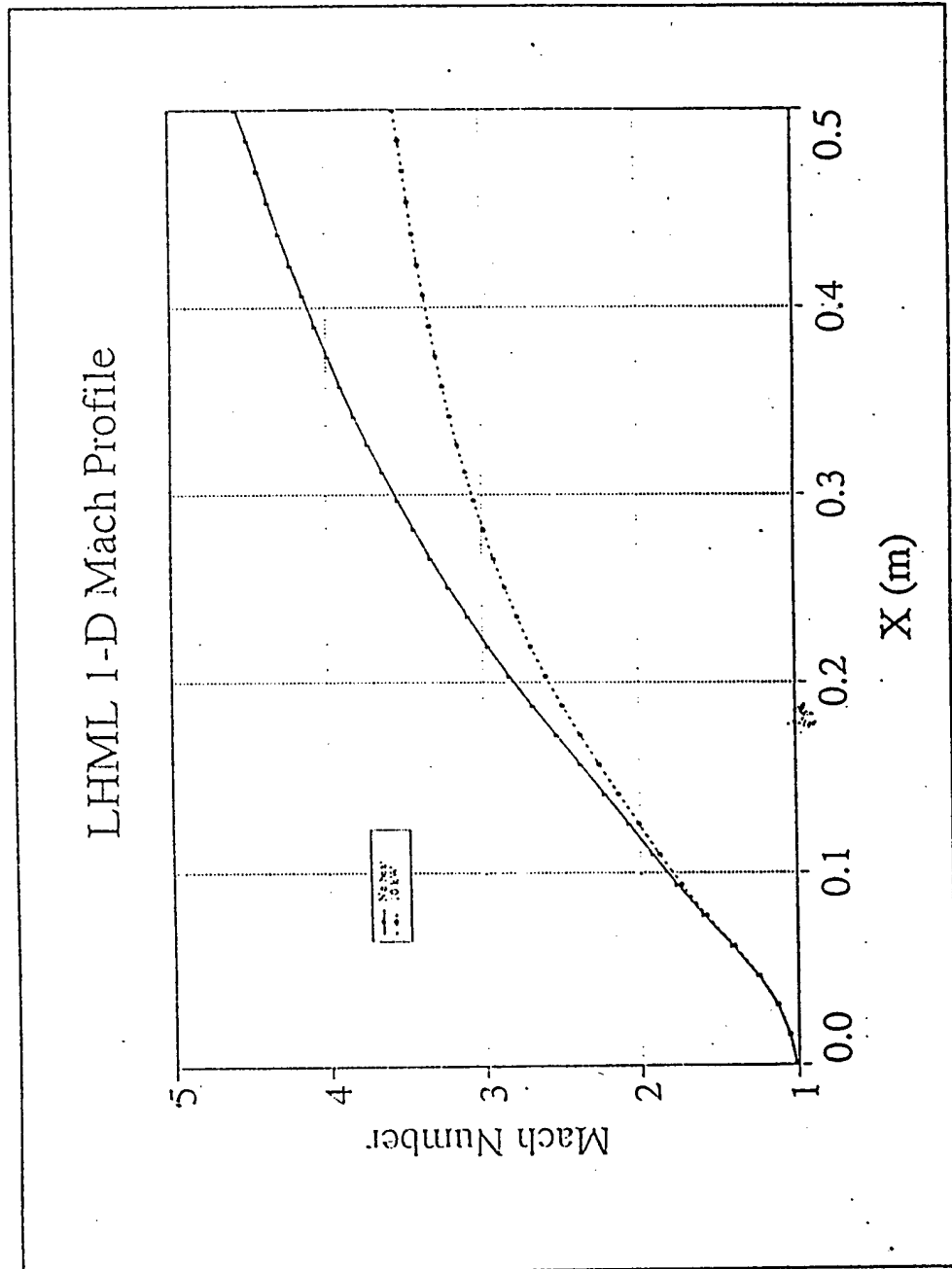


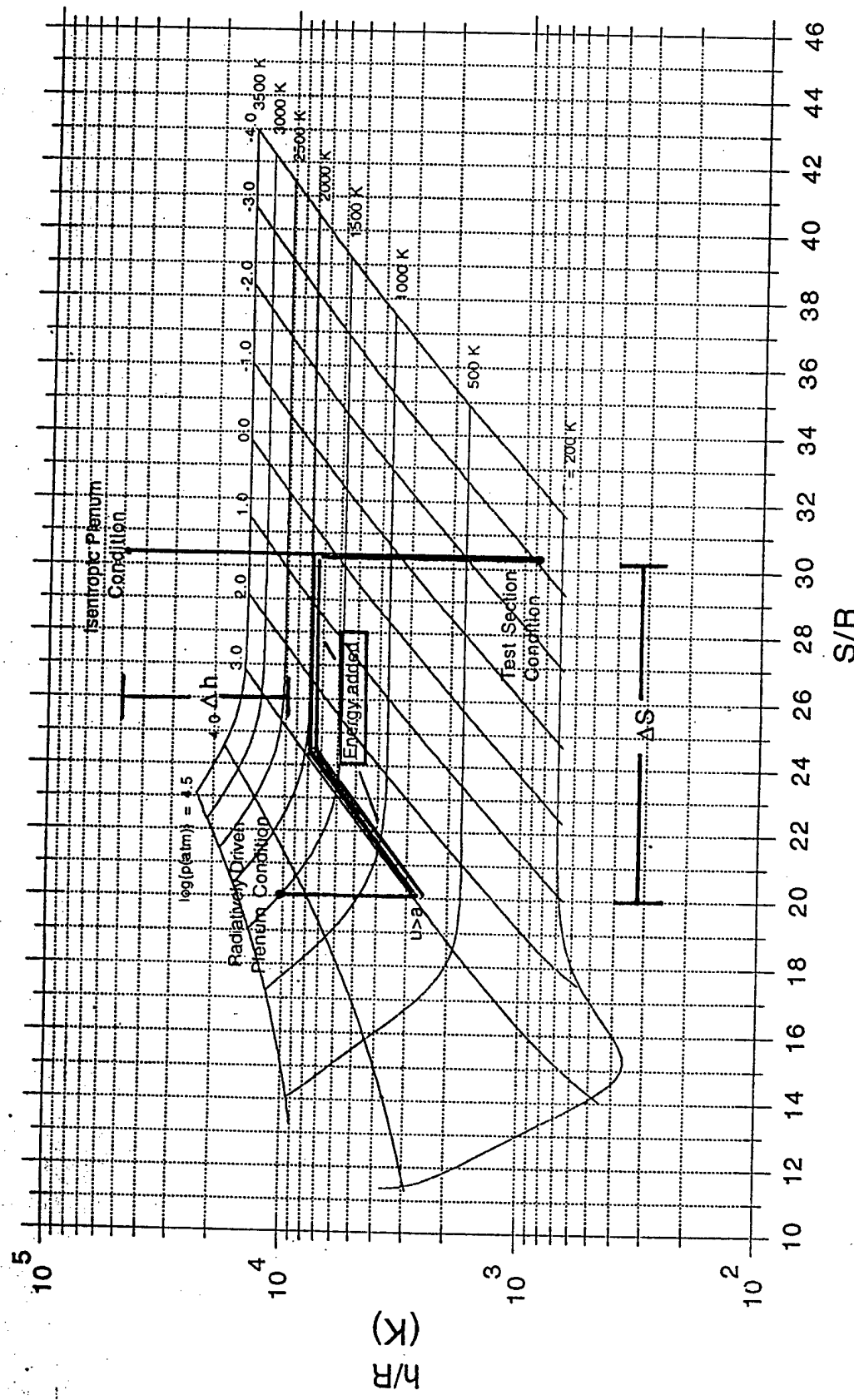
Figure 1. Diagram of 10 kw laser energy addition experiment

CFD - Energy Addition

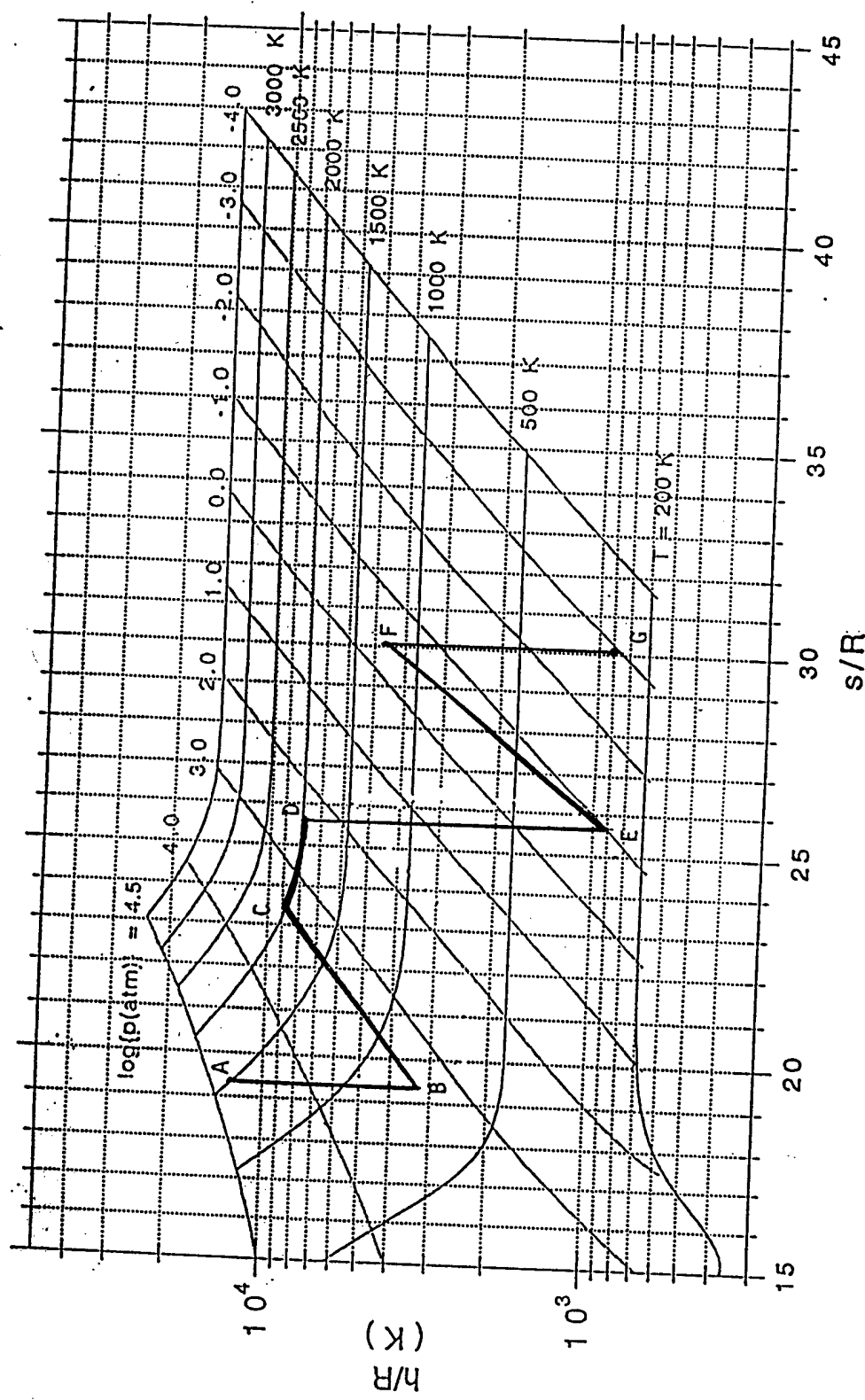
- ◆ At exit $\Delta M \sim 1$



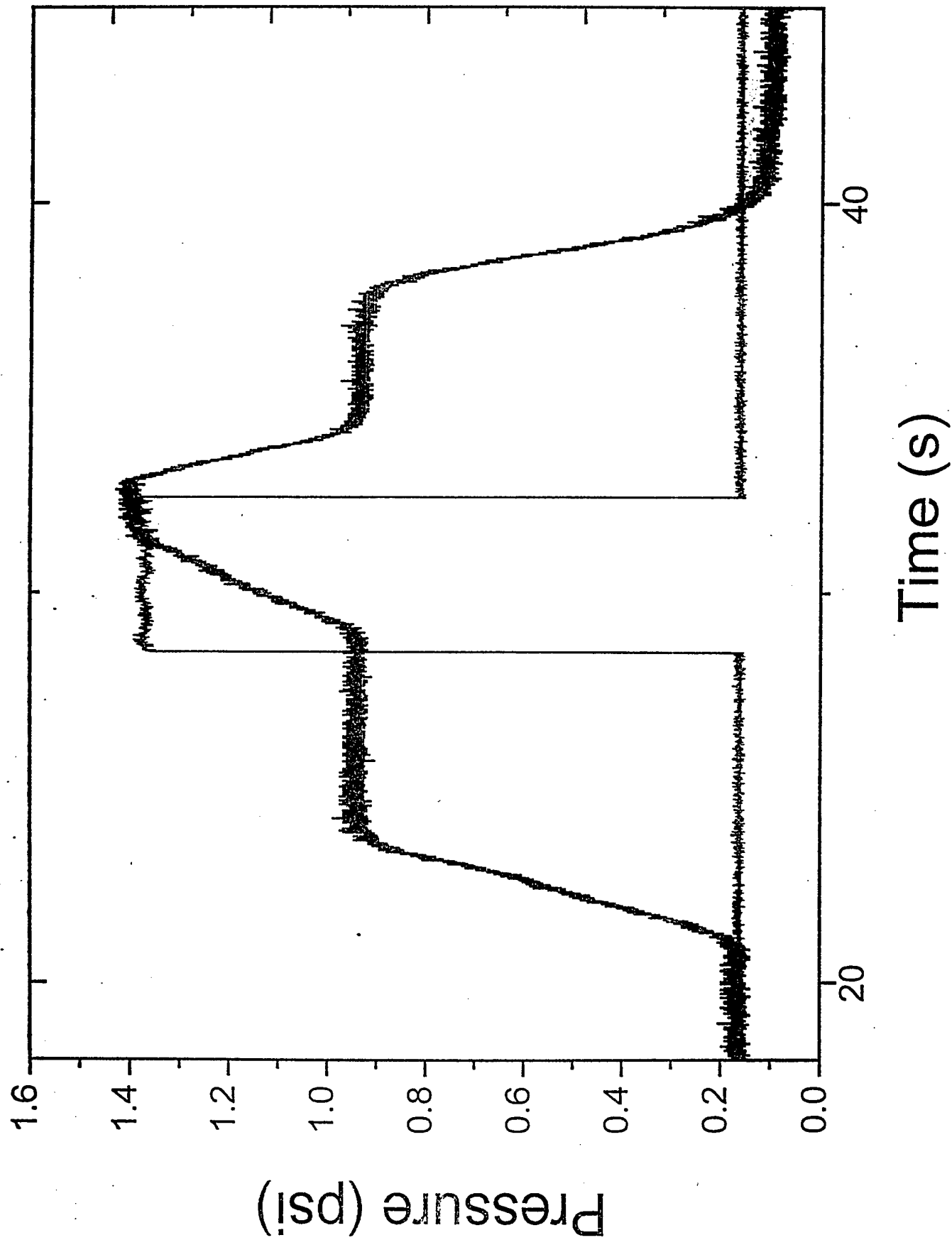
Thermodynamic Comparison of Philosophies



Energy equal to the energy deficit between the two plenum conditions is added along the highlighted path which is determined by the tunnel profile. An effective temperature, $\Delta h/\Delta s$, indicates the mean temperature at which the enthalpy must be coupled. Note that real gas effects are significant in the plenum region so that enthalpy is a function of pressure.



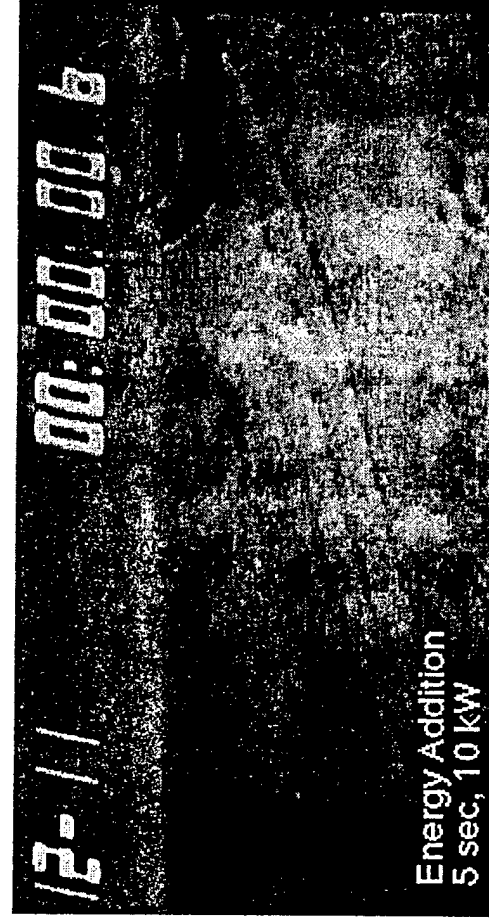
Static 1 inch from exit



Flow Around Probe



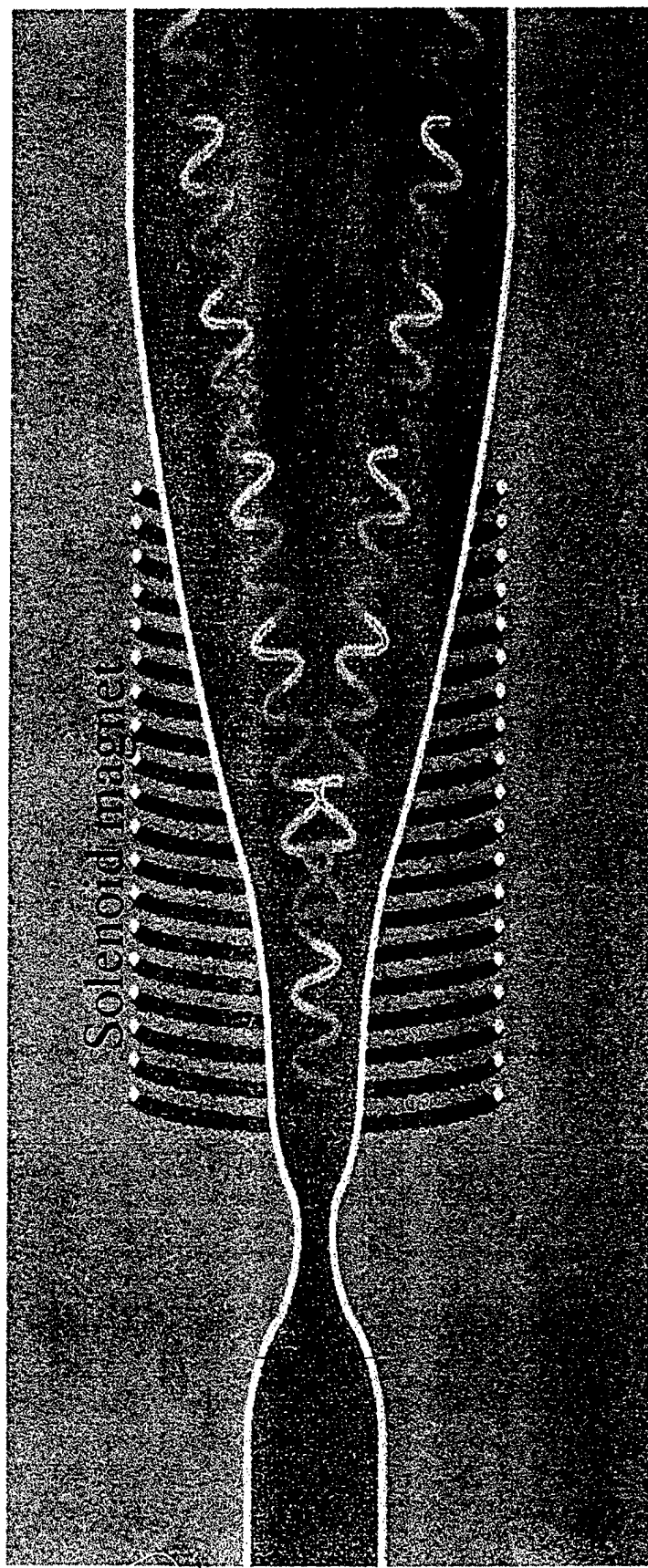
Laser Off
 $M = 4.3$



Laser On
 $M = 3.9$

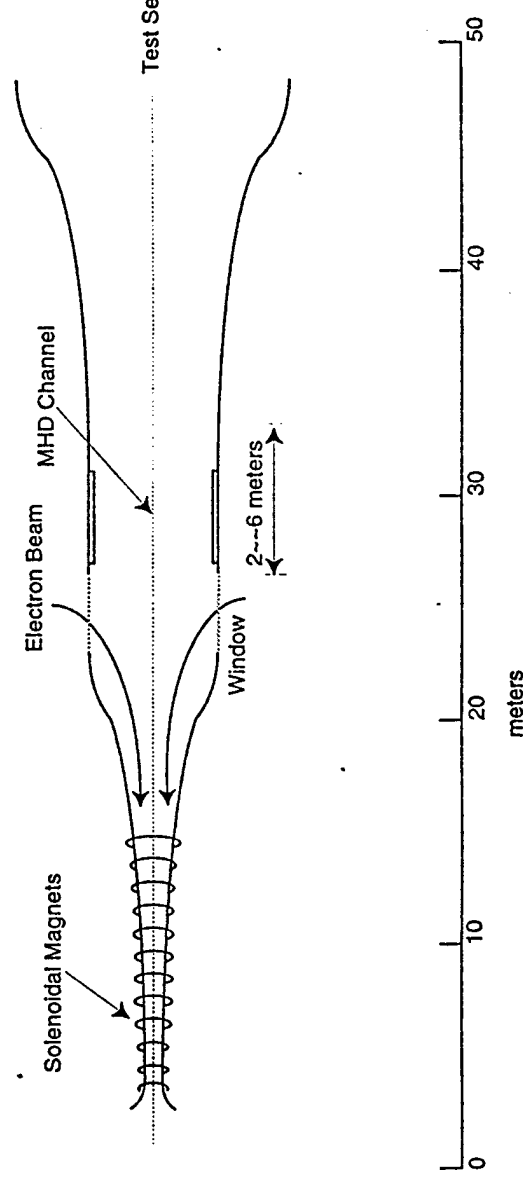
Results verified by Pitot Measurements

Energy Addition by Electron Beams



RDHWT Review April 23 - 24, 1997

Hybrid Hypersonic Wind Tunnel with E-beam Heating and MHD Acceleration
Mach 14, 3.0-m Exit Diameter



Thermodynamic limit of RDHWT:

$$\Delta h = T_a \Delta s$$

T_a can't be extremely high (erosion, chemistry);
minimum s is defined by incompressibility;
maximum s is defined by test section requirements.

THERMODYNAMIC ADVANTAGE OF MHD

Total enthalpy augmentation:

$$\Delta h_t = \frac{K}{K-1} T \Delta s$$

where $K \equiv E/(uB) =$ (Energy added)/(Push work)

The best thermodynamically:

when $K \rightarrow 1$, Δh_t can be large even for small $T \cdot \Delta s$
(non-entropy-generating energy addition).

However, when $K \rightarrow 1$, $j = \sigma \cdot (E - uB) \rightarrow 0$,
and to add

$$\Delta h_t = \sigma K(K-1)uB^2L/\rho ,$$

very large conductivity, σ , and/or length, L , would be required

AJAX

Proposed by Russians in 1990

(Vladimir Freistadt -

State Hypersonic Systems Scientific Research Enterprise
St. Petersburg)

MHD converter in the inlet connected to MHD accelerator in the nozzle to by-pass free stream kinetic energy and reduce the entropy rise in the inlet.

- Reduces the flow to subsonic in the combustor
- MHD conditions almost the same as Mariah II
- Requires some method to sustain conductivity

Reduction in vehicle drag by cold plasma injection at the nose

Increase of combustion volume and efficiency within the engine by plasma injection or injection of materials ahead of the fuel injectors

Reforming of kerosene and water into hydrogen and CO for fuel.

Computational Hypersonics Initiative
in
Air Force Research Laboratory

J. S. Shang
Air Vehicle Directorate
Air Force Research Laboratory
Wright-Patterson Air Force Base, Ohio 45433

Objective

- Rekindle a multidisciplinary computational modeling and simulation research to support the USAF New World Vista Vision.
- Develop an enabling critical simulation technology for aerospace vehicle in hypersonic flight regime.
- Research the potential of electromagnetics/shock interaction as a new flow-field control mechanism.

Scientific "Findings" in Plasma/Shock Interaction

- Appearance of a shock precursor and increase standoff distance of bow shock wave in weakly ionized gas.
- Shock propagation velocity increases and shock front disperses in plasma medium.
- Intermingled reflected compression and rarefaction waves propagation in inhomogeneous plasma media.
- Aerodynamic drag and heat transfer to solid surface are modified by weakly ionized gas.
- Magnetic field suppresses laminar-turbulent transition bypass.

Macroscopic Conservation Equations

$$\begin{aligned}
 \frac{\partial \rho \alpha_i}{\partial t} + \nabla \cdot (\rho \alpha_i \bar{u} + \rho \alpha_i \bar{u}_i) &= \dot{r}_i \\
 \frac{\partial \rho}{\partial t} + \nabla \cdot (\rho \bar{u}) &= 0 \\
 \frac{\partial \rho \bar{u}}{\partial t} + \nabla \cdot (\rho \bar{u} \bar{u} - \bar{\tau}) &= \rho \sum \bar{f}_i \\
 \frac{\partial \rho e}{\partial t} + \nabla \cdot (\rho e \bar{u} + \bar{u} \bar{\tau} - k \nabla T + \rho \sum \alpha_i h_i \bar{u}_i + \dot{q}_r) &+ \sum_i r_i \Delta h_i^o \\
 &= \rho \sum \alpha_i \bar{f}_i (\bar{u} + \bar{u}_i)
 \end{aligned}$$

In numerical simulations of hypersonic flows, this system of conservative equations is usually written in strong conservation form.

$$\frac{\partial U}{\partial t} + \frac{\partial F}{\partial x} + \frac{\partial G}{\partial y} + \frac{\partial H}{\partial z} = 0$$

Arrhenius equation

In order to apply the law of mass action, the rate of reactions is assumed to be independent of whether or not the system is in equilibrium. This commonly accepted assumption is consistent with the local equilibrium approach. The rate constant is given as $K_{c,j} = K_{f,j}/K_{b,j} = \Pi(X_i)^{\nu_{i,j}''}/\Pi(X_i)^{\nu_{i,j}'}$. Only when the gas mixture is in chemical equilibrium, the forward and reverse reactions are in dynamic balance, and the net rate of change in composition vanishes.

$$\left(\frac{dX_i}{dt}\right)_j = (\nu_{i,j}'' - \nu_{i,j}') K_{f,j} \left[\Pi(X_i)^{\nu_{i,j}'} - \frac{1}{K_{c,j}} \Pi(X_i)^{\nu_{i,j}''} \right]$$

The so-called rate constant has been experimentally recognized as

$$K_{c,j} = C \exp\left(-\frac{\epsilon_a}{KT}\right)$$

This is the well-known Arrhenius equation, and the constant ϵ_a is often referred to as the Arrhenius activation energy. This equation has been modified to better fit to measurements as

$$K_{c,r} = CT^n \exp\left(-\frac{\epsilon_a}{KT}\right)$$

Internal Degree of Excitation of Gas Medium

The partition function of a microscopic particle is fundamentally important in relating atomic/molecular structure, which influence the energy level, and thermodynamic behavior.

$$Z = \sum_i g_i \exp \left\{ -\frac{\epsilon_i}{kT} \right\}$$

Usually, the coupling of internal degrees of freedom of gas medium is neglected, this assumption leads to the factorization property of partition functions.

$$Z = Z_{trs} \cdot Z_{rot} \cdot Z_{vib} \cdot Z_{el}$$

The energy of different internal degree of excitations is additive, the total internal energy is then found by summing the translational, rotational, vibrational, and electronic modes.

$$E_i = E_t + E_r + E_v + E_e$$

Partition Functions of Internal Degree of Freedom

Translational DOF	$Z_{trs} = \left(\frac{2\pi mkT}{h^2}\right)^{\frac{3}{2}} V$
Rotational DOF	$Z_{rot} = \frac{T}{\sigma\theta_r}$
Vibrational DOF	$Z_{vib} = \frac{1}{1 - \exp\left\{\frac{\theta_v}{T}\right\}}$
Electronic DOF	$Z_{el} = g_o + \sum_i g_i \exp\left(-\frac{\theta_{e,i}}{T}\right)$

Shortcomings in Computational Hypersonics

- Inadequate description of transport property.
- Unreliable non-equilibrium kinetic models for vibration-vibration and vibration-translation energy transfer.
- Marginal numerical accuracy and low computational efficiency.
- Sparse or non-existent verification data base.

Langevin's Formula

Mobility of Charged Particles

$$D = \frac{3}{8} \sqrt{\frac{\pi}{2}} \frac{1}{nS_D} \left(\frac{m+M}{mM} kT \right)^{\frac{1}{2}}$$

$$\frac{u}{E} = \frac{3}{8} \sqrt{\frac{\pi}{2}} \frac{q}{nS_D} \left(\frac{m+M}{mM} \frac{1}{kT} \right)^{\frac{1}{2}}$$

Mobility of Heavy Ions

$$D = \frac{3}{8} \sqrt{\pi} L \left(\frac{m+M}{mM} kT \right)^{\frac{1}{2}}$$

$$\frac{u}{E} = \frac{3}{8} \sqrt{\pi} q L \left(\frac{m+M}{mM} \frac{1}{kT} \right)^{\frac{1}{2}}$$

$$L = \frac{1}{\sqrt{2nS_d}}$$

Mobility of Free Electrons

$$\frac{u_e}{E} = \frac{2}{3} \sqrt{\frac{2}{\pi}} \frac{eL_e}{(mkT)^{\frac{1}{2}}}$$

$$L_e = 4\sqrt{2}L$$

Understanding and Control of Ionized High-Speed Flows

AFOSR Workshop

Plasma Aerodynamics Studies

N. Malmuth, V. Soloviev, H. Hornung, V. Bytchkov
V. Krivstov, A. Konchakov, A. Tseskis and V. Velikodnyi

February 26, 1998



Other Team Members

- W. Beaulieu, Boeing Aircraft and Missile Systems
- P. Bellan, Caltech
- A. Fedorov, Moscow Institute of Physics and Technology
- I. Goldberg, Rockwell Science Center
- A. Klimov, Moscow Technical Club
- K. Lee, Rockwell Science Center
- S. Leonov, Moscow Technical Club
- D. Ota, Rockwell Science Center
- S. Palinswamy, Metacomp
- S. Ramakrishnan, Rockwell Science Center



Plasma Aerodynamics Objectives/Approach

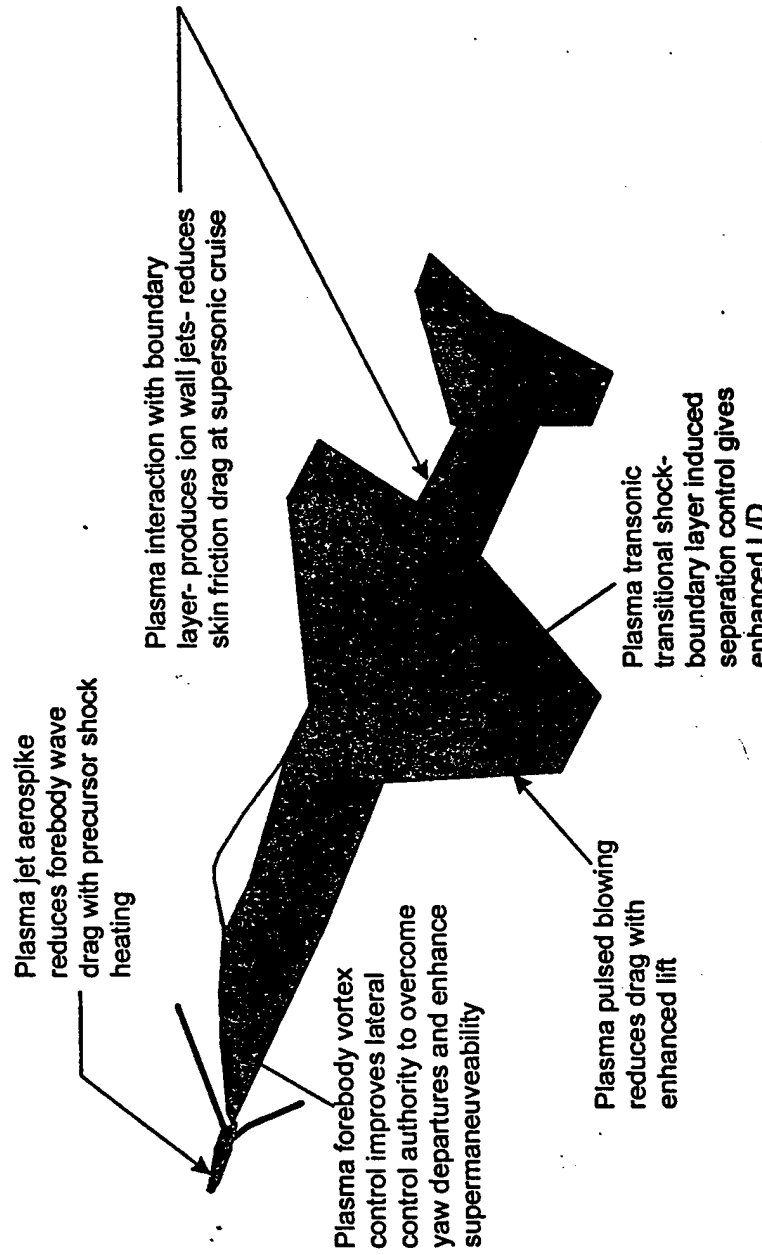
- Program Objectives
 - Determine basic physical processes of plasma aerodynamic augmentation
 - Develop analytical and computational models of these processes
 - Provide links with experiments
- F-15 flight test
 - Ground and on-board flight instrumentation
 - Plasma generator technology
- Wind tunnel, ballistic range, discharge tube and other ground tests
 - coupling with analytical model development, e.g. cross-validations
 - design and interpretation of experiments

Objectives/Approach (cont'd)

- Approach
 - Study importance of key physical mechanisms in flow such as:
 - plasma energy addition to flow such as Joule heating
 - anomalous dispersion
 - ion-acoustic waves
 - non-equilibrium phenomena
 - second viscosity and other transport parameter modification
 - electromagnetic effects such as induced B fields and Lorentz forces
 - Use solutions of unit problems such P1-P4 (for which limited experimental databases exist) to isolate these important mechanisms
 - Interface with experiments
 - Design new experiments
 - Compare evolving theoretical models with previous datasets

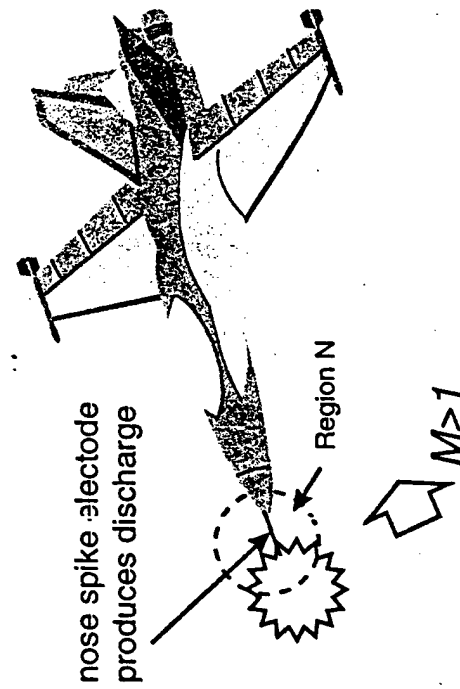
Supercruise Fighter

Plasma Aerodynamic Enhancements



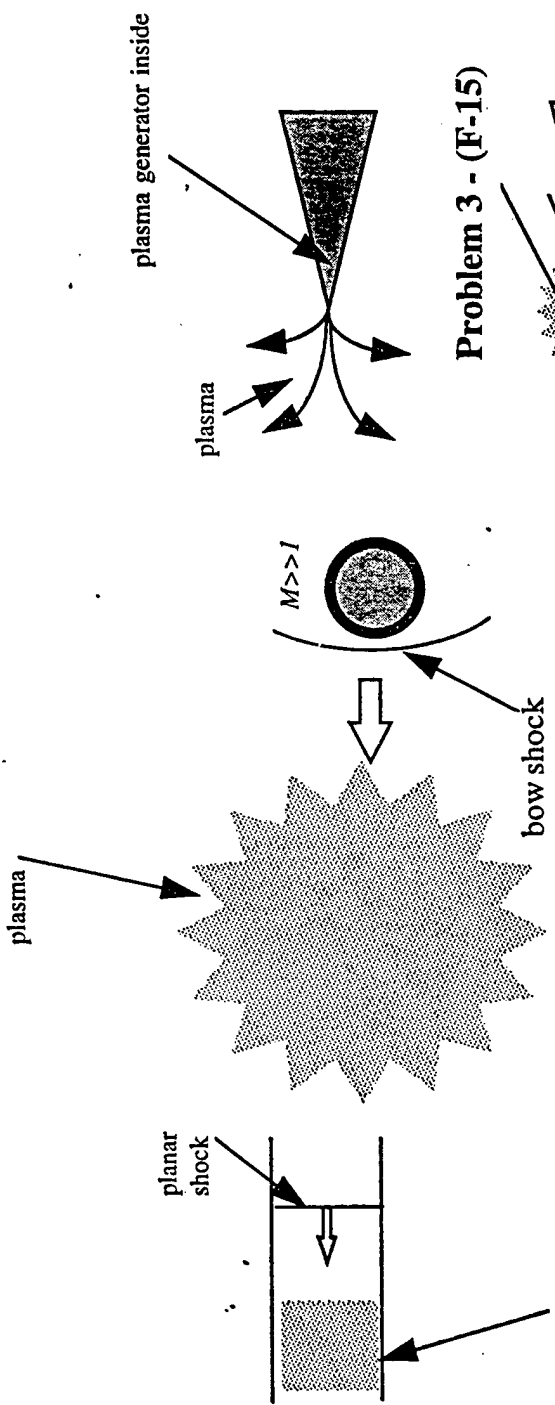
Noseboom Plasma Flow Control (Problem P4)

- Basic hypotheses:
 - dissipative processes in plasma lead to
 - Joule heating that reduces pressure drag
 - control of nose separation and nose shocks
- Problem is a useful departure point for treatment of:
 - Problem 3: erosive plasma + RF discharge on F-15
 - 1-D shock structure
 - hypersonic applications
- P4 study useful since experimental dataset available to test models



Problems

3



Problem 1

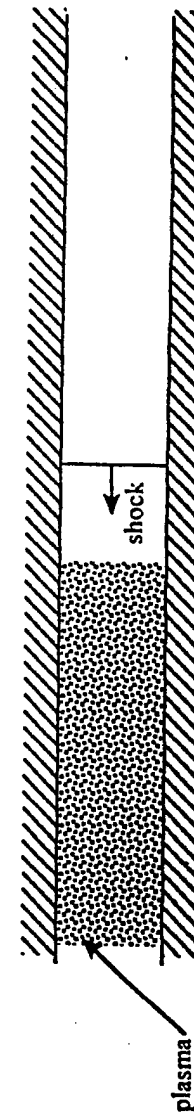
Problem 2

Problem 3 - (F-15)

Problem 3a - (F-15)

Plasma Shock Structure

- Modify 1-D Navier Stokes equations to model
 - electric field and other plasma terms
 - second viscosity
 - relaxation
 - anomalous dispersion
- Examine scaling of shock thickness with strength from Russian experiments



1-D shock propagating into a plasma

Perfect Gas Shock-Layer Problem

Equations of Motion

Continuity

$$\frac{d}{dx}(\rho u) = 0$$

Momentum

$$\rho u \frac{du}{dx} + p \frac{dp}{dx} = \frac{d}{dx} \left(\mu'' \frac{dh}{dx} \right)$$

Energy

$$\rho u'' \frac{du}{dx} - u'' \frac{dp}{dx} = \frac{d}{dx} \left(\frac{\mu''}{Pr''} \frac{dh}{dx} \right) + \mu'' \left(\frac{dh}{dx} \right)^2$$

$\mu'' \approx 2\mu + \lambda$, $\mu \equiv$ shear viscosity, $\lambda \equiv$ "second" viscosity, $Pr'' \equiv$ Prandtl Number

Boundary conditions

$$\frac{du}{dx}, \frac{dh}{dx} \rightarrow 0 \text{ as } x \rightarrow \pm\infty$$

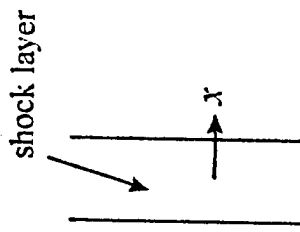
Solution for Shock Thickness

$$\delta = \frac{32 \left(\gamma + (\gamma - 1) \left(\frac{1}{Pr''} - 1 \right) \right) V_f'}{3(\gamma + 1)(V_f' - V_i')}$$

$\delta \equiv$ viscous shock layer thickness

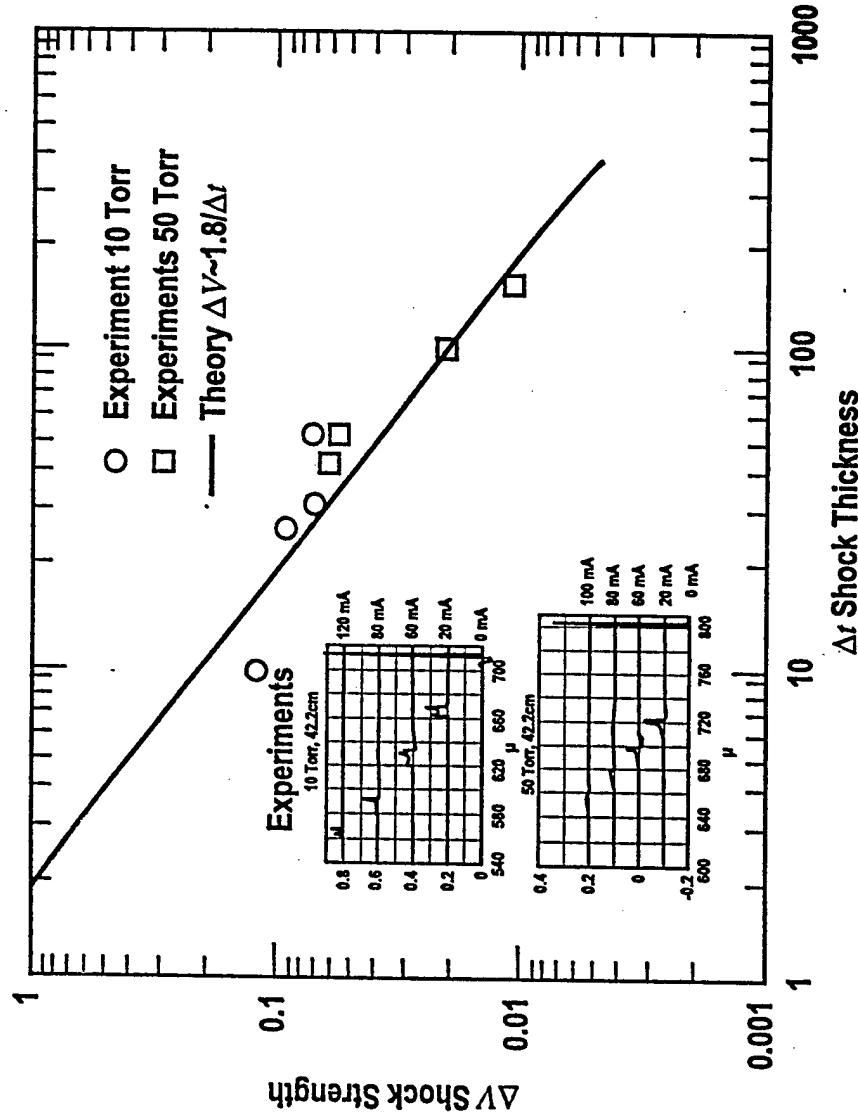
$V_f' - V_i' \equiv$ shock strength

$\gamma \equiv$ specific heat ratio



Scaling of Shock Attenuation with Thickness in a Plasma

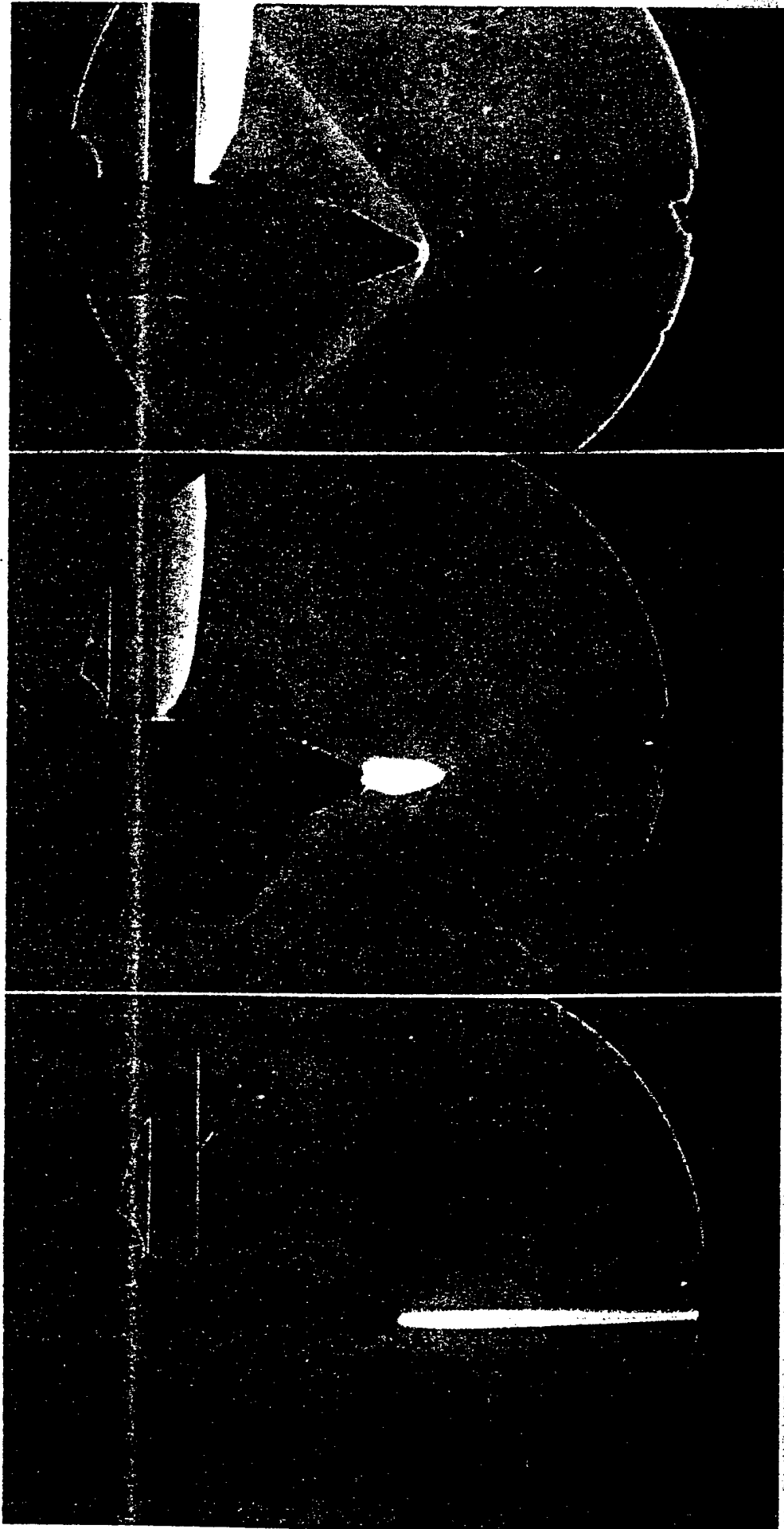
SC.4052CS.022398



BOEING®

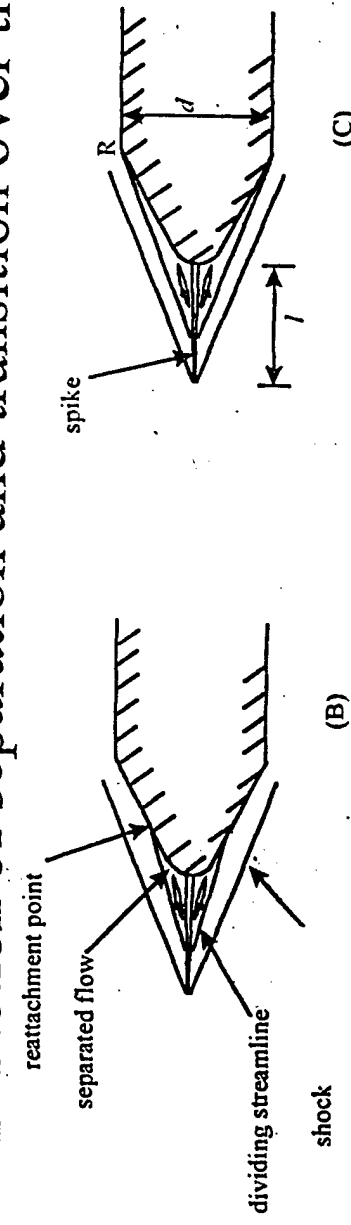
Rockwell

Science Center

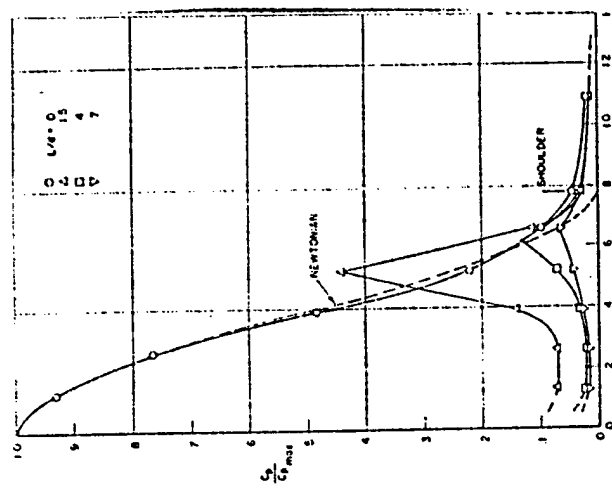


Drag Reduction Mechanisms

- Plasma jet aerospike extension
 - aerospike reduces drag by making a shallow oblique shock out of blunt nose detached almost normal shock
 - creates low pressure separation in front of blunt nose to give a net suction thrust increment
- Transverse shock due to plasma heating leading to rarefaction of separation region
- Interaction of separation and transition over the aerospike



Aerospike Effect on Pressures



Bogdanoff and Vas JAS 1959

- Spike produces peak in pressures near reattachment point
- Peak attenuates with increasing spike length reducing drag
- Needs to be traded against high heat transfer near peak
- Plasma heating can affect reattachment and therefore pressure peak

Estimate of Drag Reduction

Approximate formula based on Newtonian on blunt nose and cone part

$$C_p = 2 \left(\sin^2 \varepsilon + \frac{1}{M_\infty^2} \right) (1 - \alpha^2) + \frac{P_{\text{plateau}} \alpha^2}{q} - \frac{2}{M_\infty^2} \left(1 - \left(\frac{r_{\text{head}}}{r_d} \right)^2 \right)$$

P_{plateau} ≡ pressure in separation region

$$r_d \equiv \frac{d}{2}$$

$$\alpha \equiv \frac{r_j}{r_d}$$

r_j ≡ radius at junction of spherical nose tip with cone portion

ε ≡ cone semiaxis angle

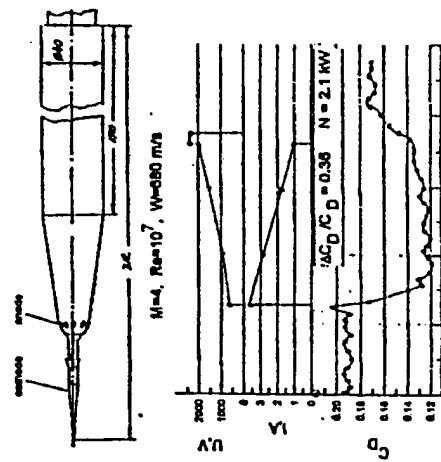


Figure 3 Wind Tunnel Experiments of the Electric Discharge Influence on Drag at TMC

	Experiment	Estimated	Remarks/assumptions in separation zone
current off	.19	.216	plateau pressure = 1/2 normal shock value
current on	.12	.07	vacuum due to plasma

Plasma On

16.03.00 0.6264f+03 0.2001e+03 0.0101S 6:30:58

11.200000	12.000000	13.000000	14.000000	15.000000	16.000000
11.000000	12.000000	13.000000	14.000000	15.000000	16.000000
10.800000	11.800000	12.800000	13.800000	14.800000	15.800000
10.600000	11.600000	12.600000	13.600000	14.600000	15.600000
10.400000	11.400000	12.400000	13.400000	14.400000	15.400000
10.200000	11.200000	12.200000	13.200000	14.200000	15.200000
10.000000	11.000000	12.000000	13.000000	14.000000	15.000000

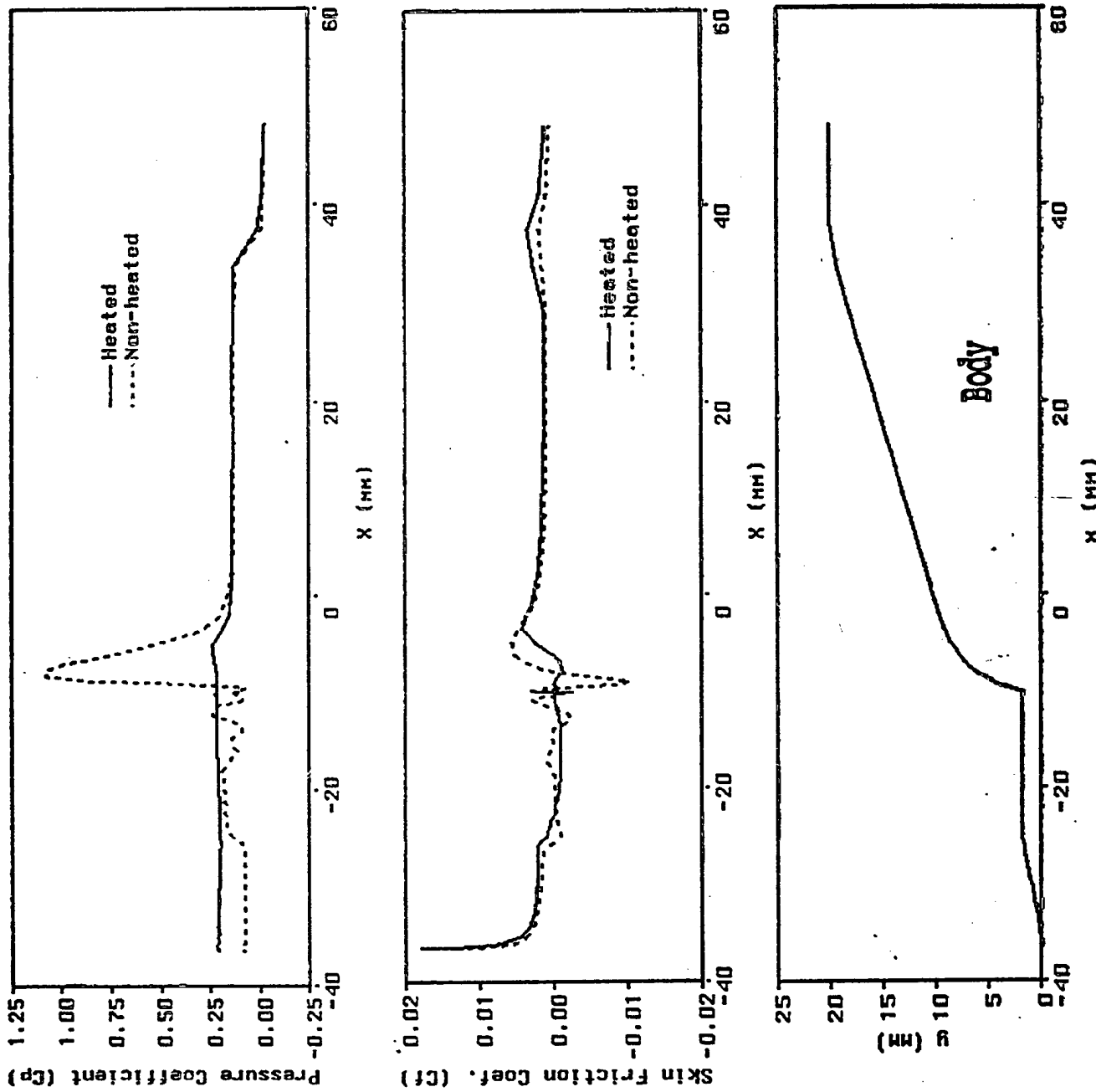
Plasma off

5/6/97 SIGHT PRESSURE CONDENSER GASES

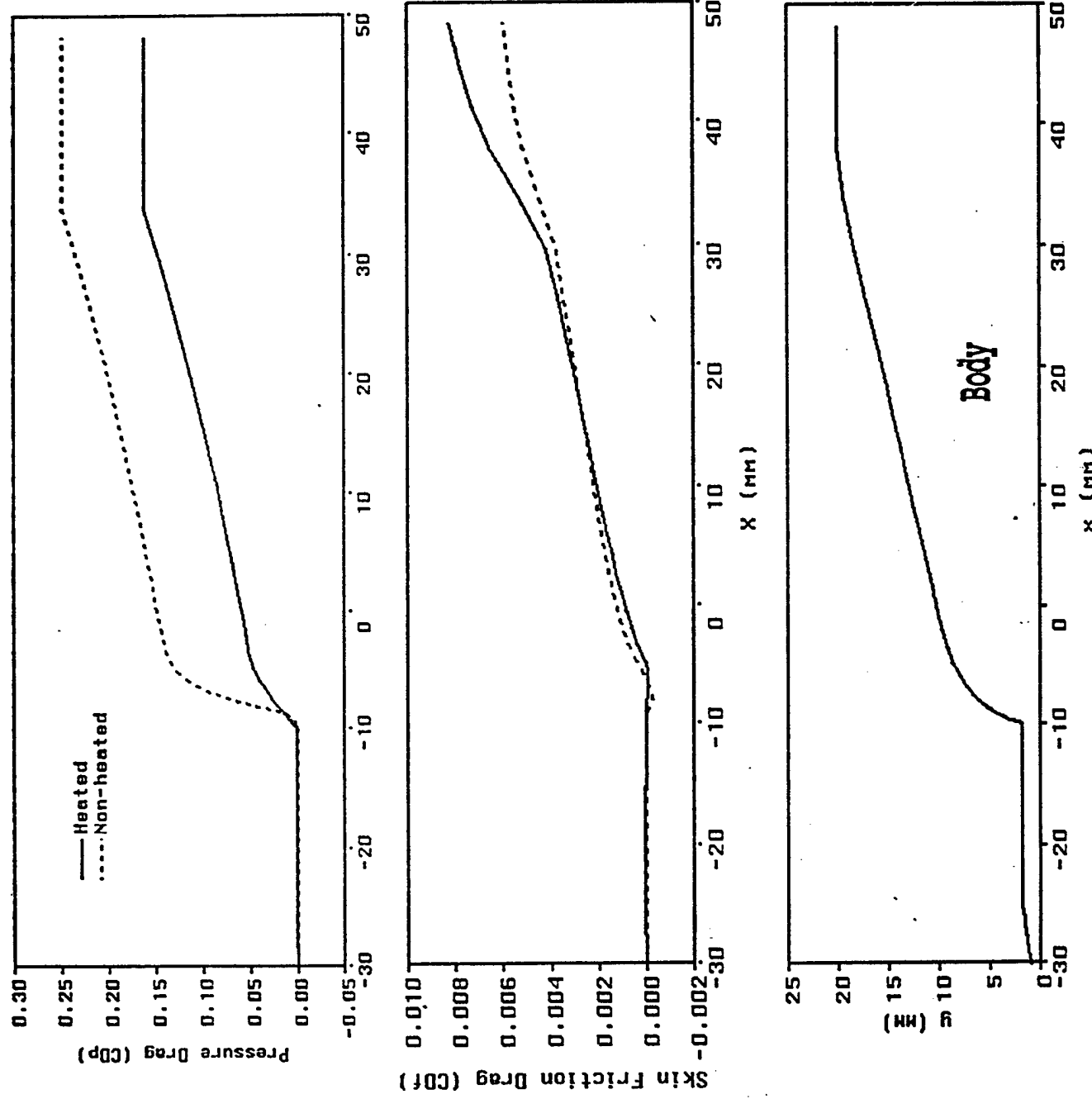
0.0200 0.0200 0.0200 0.0200

1.0000
1.2000
1.4000
1.6000
1.8000
2.0000
2.2000
2.4000
2.6000
2.8000
3.0000
3.2000
3.4000
3.6000
3.8000
4.0000
4.200000
4.400000
4.600000
4.800000
5.000000
5.200000
5.400000
5.600000
5.800000
6.000000
6.200000
6.400000
6.600000
6.800000
7.000000
7.200000
7.400000
7.600000
7.800000
8.000000
8.200000
8.400000
8.600000
8.800000
9.000000
9.200000
9.400000
9.600000
9.800000
10.000000

Pressure and Skin Friction Distributions With Plasma Heating



Cumulative Pressure and Skin Friction Drag with Plasma Heating



Comparison of Predicted Drags With Russian Experiments

	Rockwell Science Center Computation*	Russian Experiment
C_D (Plasma off)	0.254	0.220
C_D (Plasma on)	0.170	0.180
$\Delta C_D / C_D$	0.33	0.18

*Laminar Navier Stokes model with plasma power uniformly distributed over spike electrode surface

- Discrepancies above within experimental errors
- Heat source model may give dominant physics of spike electrode problem
- Computed relative drag changes agree with experimental order of magnitude

Forebody drag of a cone-cylinder with counterflow jet in supersonic flow

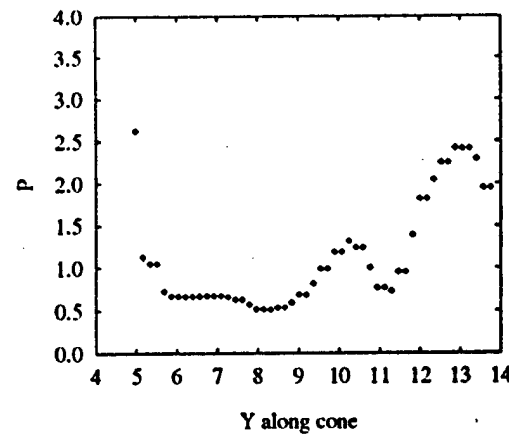
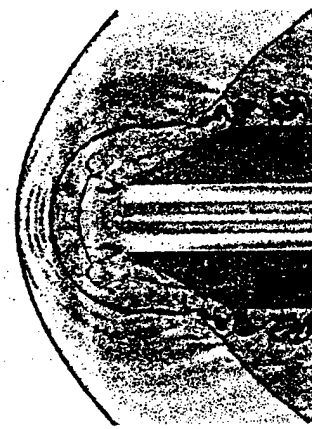
Temp. Tech area Jiv Nov 11, 12

- Objectives
 - Study competition of jet momentum drag with surface pressure drag
 - Study basic physical mechanisms
 - Relate to plasma jet effects

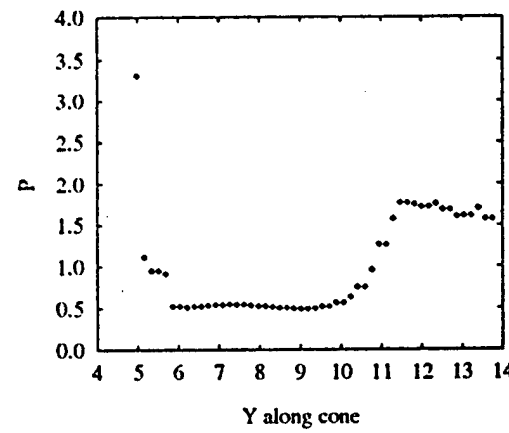
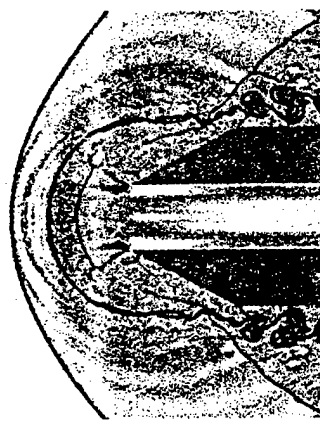


Rockwell

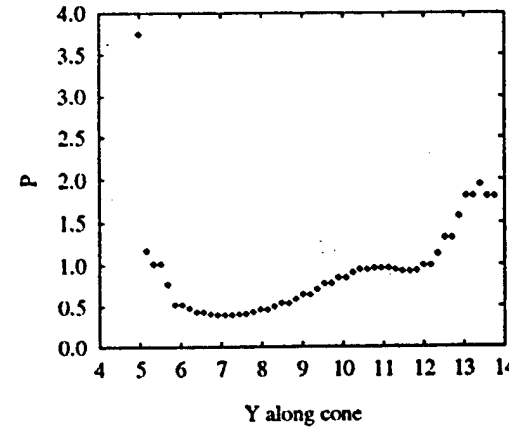
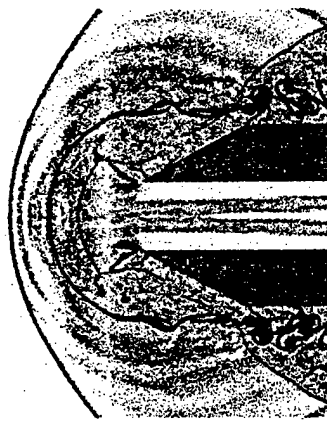
Science Center



$$p_4/p_\infty = 15.0, C_{D_e} = 0.395, C_{D_t} = 0.462, C_D = 0.857$$



$$p_4/p_\infty = 18.0, C_{D_e} = 0.342, C_{D_t} = 0.553, C_D = 0.895$$



$$p_4/p_\infty = 21.0, C_{D_e} = 0.312, C_{D_t} = 0.646, C_D = 0.957$$

Counterflow jet, $M_\infty = 2.0, T_4/T_\infty = 10, \gamma = 1.4.$

Forebody drag of a cone-cylinder with counterflow jet in supersonic flow

Temp_techarea_jv_Nov 11, 12

- Flow field features
 - Small pressure ratios < 12, (subsonic jets)
 - jet insufficiently powerful to counter freestream, contact surface is an effective blunt body
 - leads to saddle point singularity from which contact interface issues
 - jet separation over body causing a low pressure region giving a thrust
 - Large pressure ratios > 12, (supersonic jets)
 - Goes through normal shock prior to impingement with freestream
 - Free shear layer stagnates on shoulder, leading to eddies, baroclinic vorticity, multiple secondary shocks and instabilities



Rockwell

Science Center

17

Forebody drag of a cone-cylinder with counterflow jet in supersonic flow

Temp_techarea_jtv_Nov 11, 12

- Conclusions
 - Two competing tendencies
 - Jet momentum flux- increases drag
 - Pressure thrust on forebody-decreases drag
 - Drag can be lower than the forebody drag of an equivalent sharp cone or cone frustum
 - Minimum drag occurs when the jet to freestream pressure ratio is approximately 1.1



Rockwell

Science Center

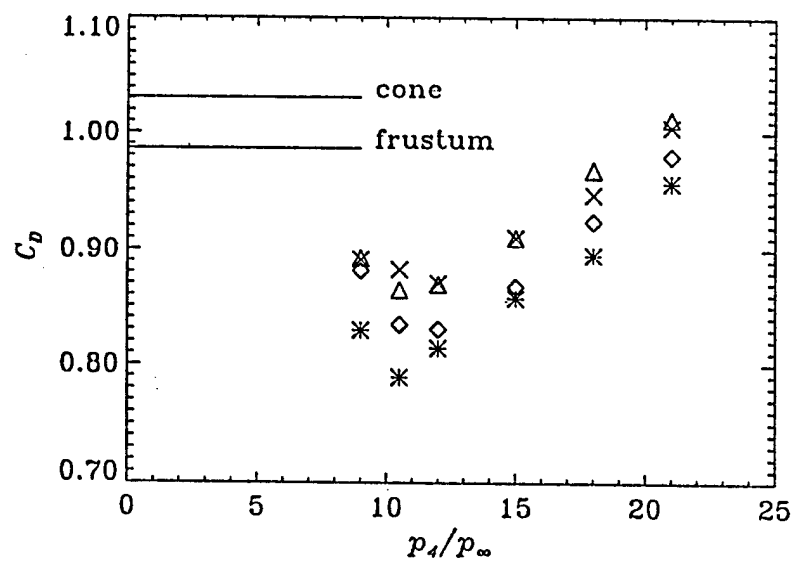


Figure 7: Forebody drag coefficient as a function of p_4/p_∞ for different values of T_4/T_∞ as follows: crosses:1, triangles:3, diamonds:6, asterisks:10. The forebody drag coefficients of the sharp cone and the cone frustum are shown as lines for reference. $M_\infty = 2, \gamma = 1.4$

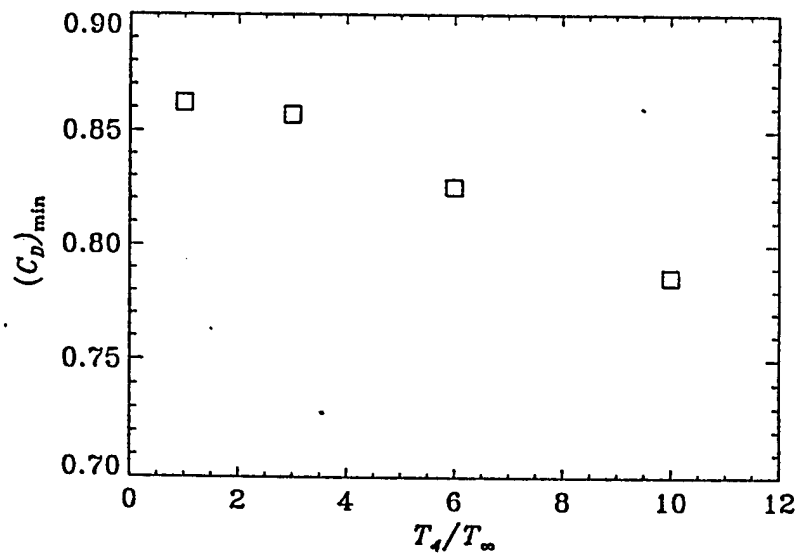


Figure 8: The minimum value of the forebody drag coefficient as a function of T_4/T_∞ . $M_\infty = 2, \gamma = 1.4$

Propagation of 1-D Shock Waves Through Weakly Ionized Plasmas

V.R.Soloviev, V.M.Krivtsov, A.M.Konchakov
Moscow Institute of Physics and Technology, Russia

N.Malmuth
Rockwell Science Center, CA, USA

Main topics of the model

- Hugoniot relations on a shock wave (SW) in a weakly ionized plasma
- Estimations of the energy stored in different excited states for glow discharge plasma
- The existence of high situated metastable states in Ar and N₂, which serve as a ‘new ground state’ for higher states excitation by electron impact
- Highly excited atomic and/or molecular states store sufficient energy to produce SW acceleration and attenuation
- Inclusion of highly excited atom energy release behind the SW front dramatically improves agreement of theory with experiment for 1-D shock penetrating into a plasma and hypersonic sphere entering a plasma

Hugoniot relations on a shock wave (SW) in a weakly ionized plasma

A set of gas mass, momentum and energy conservation equations in SW coordinates

$$\frac{\partial \rho}{\partial t} + \frac{\partial(\rho u)}{\partial \xi} = 0,$$

$$\frac{\partial(\rho(u+D))}{\partial t} + \frac{\partial}{\partial \xi}(\rho u(u+D) + p) = \frac{\partial}{\partial \xi}\left[\frac{4}{3}\mu\frac{\partial u}{\partial \xi}\right] + f_\xi,$$

$$\begin{aligned} \frac{\partial}{\partial t}\left[\rho\left(h + \frac{(u+D)^2}{2}\right) - p\right] + \frac{\partial}{\partial \xi}\left[\rho u\left(h + \frac{(u+D)^2}{2}\right)\right] &= \frac{\partial}{\partial \xi}\left[\frac{\lambda}{c_p}\frac{\partial h}{\partial \xi}\right] + \\ &+ \frac{4}{3}\mu\frac{\partial^2}{\partial \xi^2}\left(\frac{(u+D)^2}{2}\right) + f_\xi(u+D) + Q_r \end{aligned}$$

$$h = c_p T_a = \frac{\gamma}{\gamma-1} \frac{p}{\rho},$$

ρ, p, h are density, pressure and enthalpy of the gas; v is its velocity;

λ, μ are thermal conductivity and dynamic viscosity coefficients;

c_p, γ are specific heat at a constant pressure and the ratio of specific heats;

D is the SW velocity;

The f_ξ and Q_r terms describe the plasma influence on the gas.

Hugoniot relations

$$\rho_1 u_1 = \rho_0 D,$$

$$\rho_1 u_1^2 + p_1 = \rho_0 D^2 (1 - \varepsilon_{u1}) + p_0,$$

$$h_1 + \frac{u_1^2}{2} = h_0 (1 + \varepsilon_h) + \frac{D^2}{2} (1 - 2\varepsilon_{u2}),$$

where

$$\varepsilon_{u1} = \frac{1}{\rho_0 D^2} \int_{-\infty}^{\infty} f_\xi d\xi, \quad \varepsilon_{u2} = -\frac{1}{\rho_0 D^3} \int_{-\infty}^{\infty} f_\xi u d\xi, \quad \varepsilon_h = \frac{1}{\rho_0 D h_0} \int_{-\infty}^{\infty} Q_r d\xi$$

- To produce a plasma effect on SW propagation it is necessary $\varepsilon_{u1}, \varepsilon_{u2}$, or ε_h to be of the order of 1.

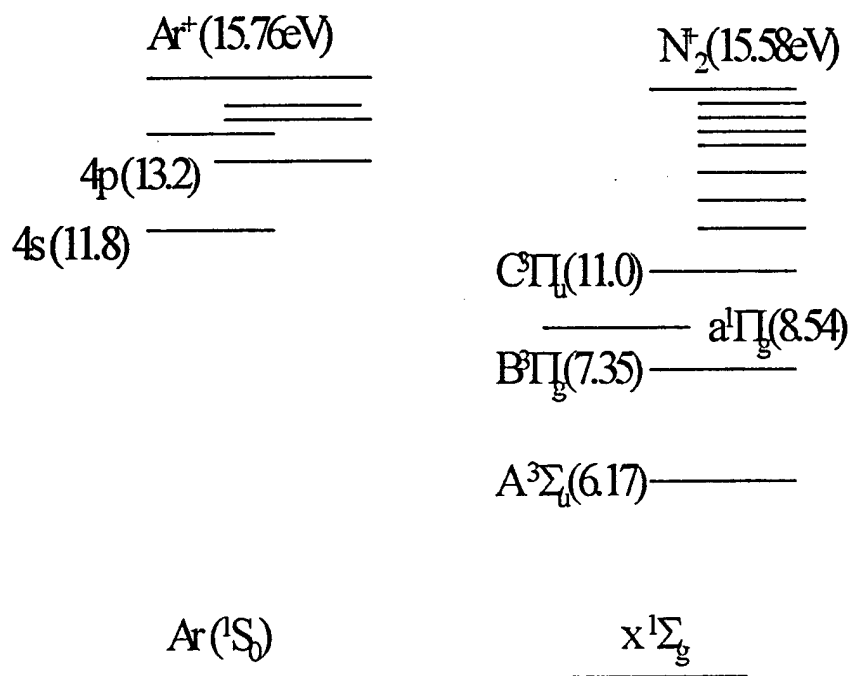
The typical cold glow discharge plasma parameters in SW - discharge interaction experiments

gas pressure (gas density)	$p \approx 3 - 30 \text{ Torr} (\text{N} \approx 10^{17} - 10^{18} \text{ cm}^{-3})$
gas temperature	$T \approx 300 \text{ K}$
current density	$j \approx 1 - 100 \text{ mA/cm}^2$
electric field strength	$E \approx 100 \text{ V/cm}$
E/N value	$(2 - 10) \times 10^{-16} \text{ V} \cdot \text{cm}^2$
discharge specific power	$W \approx 0.1 - 10 \text{ W/cm}^3$
electron temperature	$T_e \approx 1 - 3 \text{ eV}$
electron density	$n_e \approx 10^{10} - 10^{12} \text{ cm}^{-3}$
metastable atom (or molecule) density	$N_m \approx 10^{11} - 10^{13} \text{ cm}^{-3}$

The energy stored in different excited states

- freestream gas enthalpy $h_0 = N c_p T \sim 10^{16} \text{ eV/cm}^3$
- ionization $n_i E_i \sim 10^{12} \text{ eV/cm}^3, \quad \epsilon_h = n_i E_i / N c_p T \sim 10^{-4}$
- metastable atoms (or molecules) $N_m E_m \sim 10^{14} \text{ eV/cm}^3, \quad \epsilon_h = N_m E_m / N c_p T \sim 10^{-2}$
- specific discharge energy supply
during the time of unit length SW pass $\epsilon_h = W \times 1 \text{ cm} / D N c_p T \sim 10^{-2} - 10^{-1}$
- the vibrational energy is shown to be unsuitable to explain the SW anomalous propagation effects because of large vibrational-translational relaxation time $\tau_{VT} \sim 10^{-3} \text{ s}$

The scheme of Ar and N₂ electronic excited states



Ar(4s) and N₂(A³Σ) are the metastable states

The Ar metastable state quenching and building up

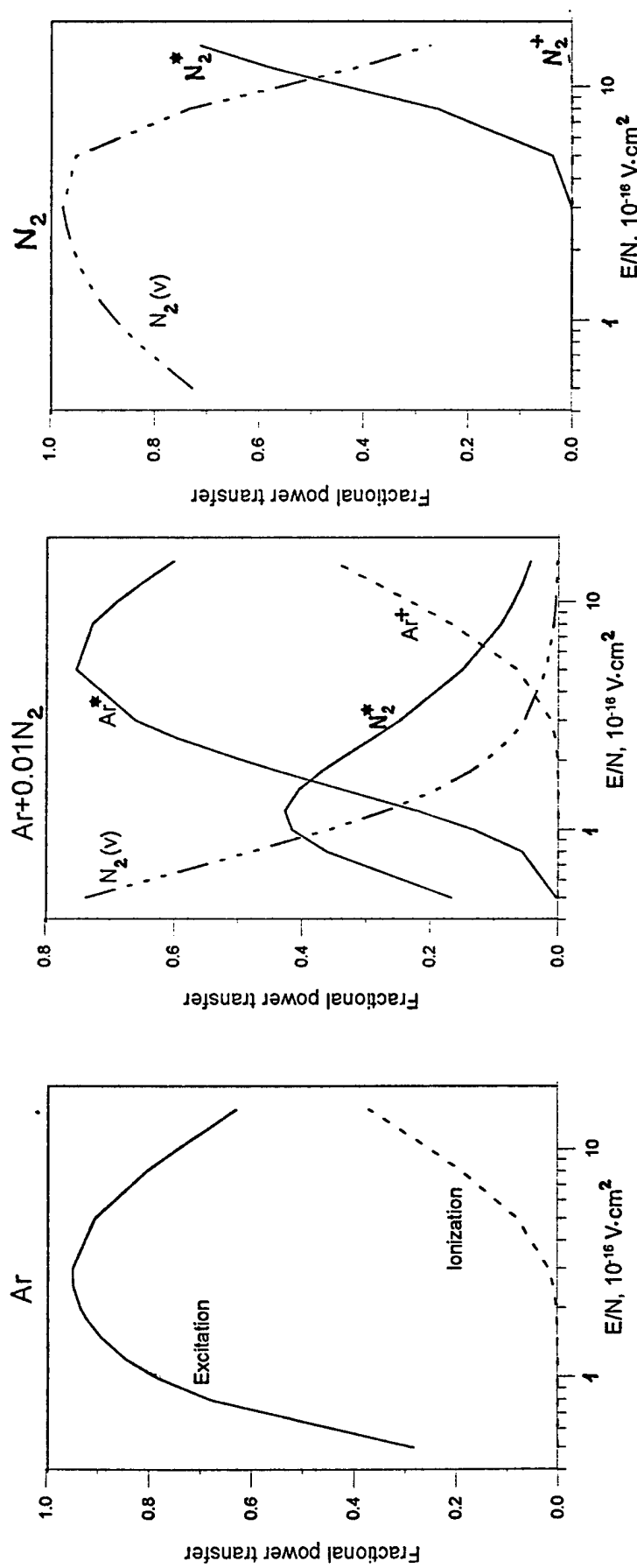
Process	Rate constant	Quenching time for p=10 Torr, n _e =10 ¹¹ cm ⁻³ and 1% N ₂ diluent in Ar
Ar(4s) + 2Ar → Ar [*] ₂ + Ar	10 ⁻³² cm ⁶ /s	0.8 ms
Ar(4s) + e → Ar + e + 11.8ev	10 ⁻⁸ cm ³ /s	1ms
Ar(4s) + N ₂ → Ar + N ₂ (C, B, ...)	3.6×10 ⁻¹¹ cm ³ /s	0.01ms
Ar(4s) + Ar(4s) → Ar ⁺ + Ar + e	10 ⁻⁹ cm ³ /s	1ms×(10 ¹² /n(4s)[cm ⁻³])
Ar(4p) + Ar → Ar(4s) + Ar	~ 10 ⁻¹¹ - 10 ⁻¹² cm ³ /s	0.3 - 3mcs
Ar(4p) → Ar(4s) + hν	3.2×10 ⁷ s ⁻¹	0.03mcs

The N₂(A³Σ) metastable state quenching and building up

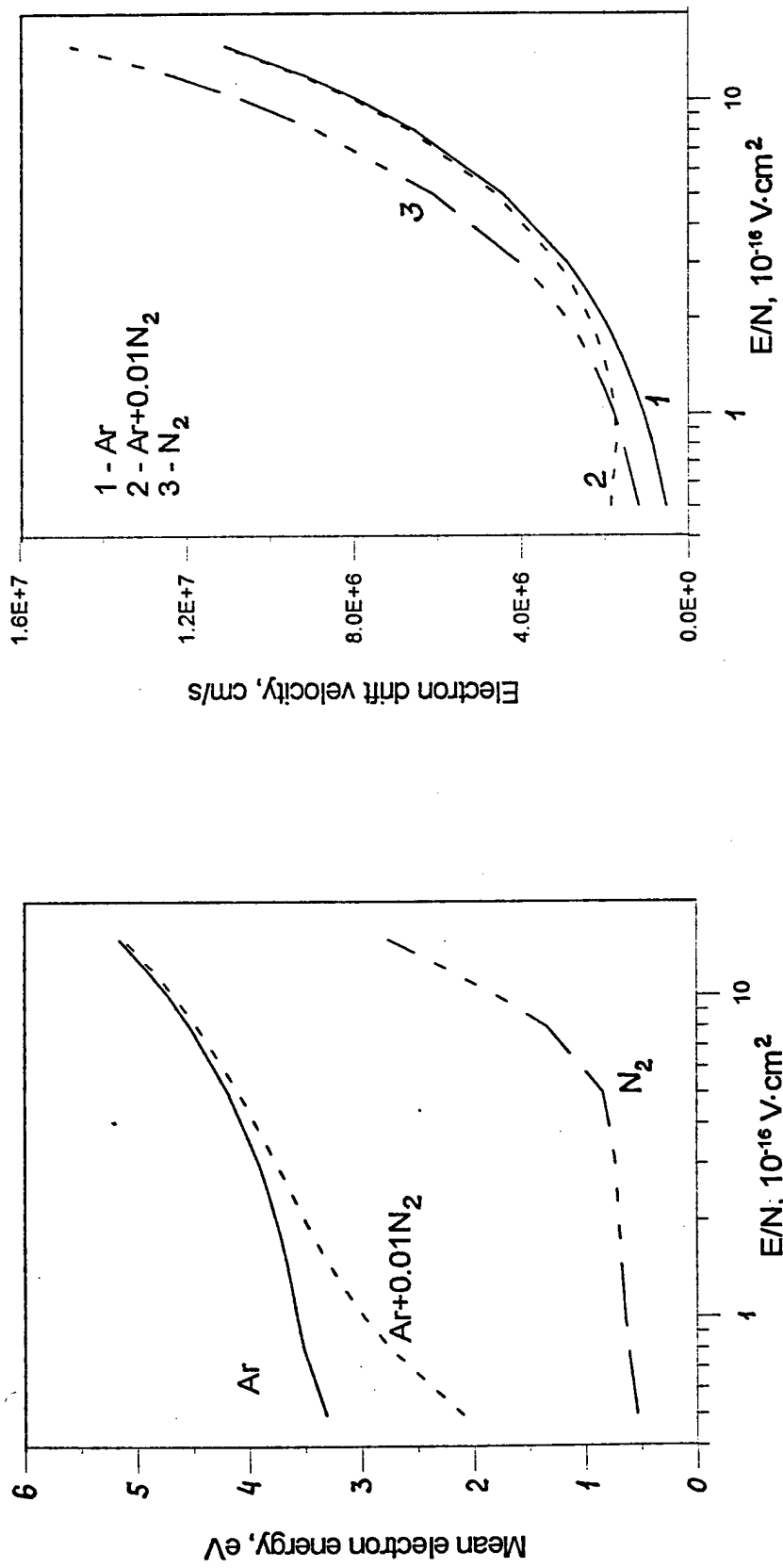
N ₂ (A ³ Σ) + Ar → N ₂ (X) + Ar	<4×10 ⁻¹⁴ cm ³ /s	> 0.1ms
N ₂ (A ³ Σ) + N ₂ (X) → 2 N ₂ (X)	<4.5×10 ⁻¹⁷ cm ³ /s	>100ms
N ₂ (A ³ Σ) + O ₂ → N ₂ (X) + O ₂	3.6×10 ⁻¹² cm ³ /s	4mcs (for air composition)
N ₂ (A ³ Σ) + N ₂ (X,v) → N ₂ (B ³ Π) + N ₂ (X)	~ 10 ⁻¹⁰ cm ³ /s	
N ₂ (A ³ Σ) + N ₂ (A ³ Σ) → N ₂ (B,C,...) + N ₂ (X)	10 ⁻⁹ cm ³ /s	1ms×(10 ¹² /n(A)[cm ⁻³])
N ₂ (B ³ Π) + N ₂ (X) → N ₂ (A ³ Σ) + N ₂ (X)	2×10 ⁻¹¹ cm ³ /s	0.15mcs
N ₂ (B ³ Π) → N ₂ (A ³ Σ) + hν	1.5×10 ⁵ s ⁻¹	6.5mcs
N ₂ (C ³ Π) → N ₂ (A,B) + hν	2.7×10 ⁷ s ⁻¹	0.037mcs

The discharge fractional power input into different excited states for Ar, N₂ and Ar-N₂ mixture

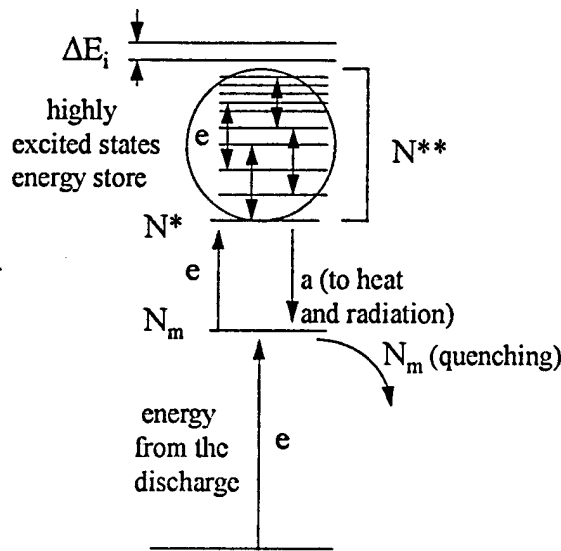
E-is electric field strength, N - is gas number density



The mean electron energy (electron temperature) and electron drift velocity versus E/N value for Ar, Ar+0.01N₂ and N₂ discharges



The kinetic model of energy storing in highly excited states



The system of balance equations for excited states

$$\frac{\partial N_m}{\partial t} = \frac{W\eta}{E_m} - N_m(k_p N_m + \frac{1}{\tau_q}) - k_e n_e N_m + N^*(k_q N + A_R \theta)$$

$$\frac{\partial N^*}{\partial t} = k_e n_e N_m - N^*(k_q N + A_R \theta)$$

$$N^{**} = \sum_{n=n^*}^{n_j} N^* \frac{g_n}{g_{n^*}} \exp\left(-\frac{E_n - E_{n^*}}{T_e}\right), \quad \text{for } n > n^* \quad k_e n_e \gg k_q N \frac{\Delta E_{n,n+1}}{T_e},$$

$$\Delta E_{n,n+1} \approx \frac{2Ry}{n^3}, \quad n^* \approx \sqrt[3]{\frac{2Ry}{T_e} \frac{k_q N}{k_e N_e}} \approx 4-5, \quad E_i - E^* \approx 0.5-1 \text{ eV}$$

$Ry = 13.6 \text{ eV}$ is the Rydberg constant

$W = jE$ - is the discharge specific power;

$\eta \sim 1$ - is the discharge fractional power input into excitation;

E_m, E_n - are the energies of the different states excitation from the ground state;

k_p - is the metastable atom Penning process rate constant;

τ_q - is the metastable state quenching time in other processes;

k_e - is the electron excitation rate constant from metastable to N^* states;

k_q - is the gas quenching rate constant for N^* states;

A_R - is the radiative decay rate for N^* states;

θ - is the probability of radiation trapping;

ΔE_i - is the decrease of ionization potential due to excited atom electron - ion interaction;

For the tube radius R

$$\theta = \frac{1}{3\sqrt{\pi\sigma_{abs}N_m R}}$$

For Ar(4p) \rightarrow Ar(4s) transitions $\theta \approx 3 \times 10^{-2} (10^{12}/N_m)^{0.5}$ followed by

$$A_R \theta \ll k_q N$$

The steady state values of N_m and N^* :

$$N_m \approx \sqrt{\frac{W\eta}{k_p E_m}} \approx 2.5 \times 10^{13} \sqrt{W[W/cm^3]}, \text{ cm}^{-3}$$

$$N^* \approx N_m \frac{k_e n_e}{k_q N} \approx 3.5 \times 10^{12} \frac{\sqrt{W[W/cm^3]}}{p[\text{Torr}]}, \text{ cm}^{-3}$$

The equilibrium highly excited hydrogen-like states population

$$n_f \approx \sqrt{\frac{Ry}{\Delta E_i}} \approx \sqrt{\frac{Ry}{e^2 N_i^{\frac{1}{3}}}}$$

- the upper limit of principle quantum number for hydrogen-like states;

$$n_f \approx 100 \text{ for } N_i \approx 10^{11} \text{ cm}^{-3}$$

$$N^{**} \approx N^* \frac{2n_f^3}{3g^*} \exp\left(-\frac{E_i - E^*}{T_e}\right) \sim 10^4 N^*$$

$g^* \sim 30$ is the degeneracy of N^* state

The energy stored in highly excited states

$$\varepsilon^{**} \approx (E^* - E_m) \frac{n_f^3}{g^*} \frac{k_e N_e}{k_q N} \sqrt{\frac{W\eta}{E_m k_p}} \exp\left(-\frac{E_i - E^*}{T_e}\right)$$

$$\varepsilon^{**} \approx 10^{17} \frac{\sqrt{W[W/cm^3]}}{p[Torr]}, \frac{eV}{cm^3},$$

$$\frac{\varepsilon^{**}}{c_p N T} \approx 1$$

The energy released to heat behind the shock wave

$$\Delta \varepsilon \approx \varepsilon^{**} \left(1 - \frac{N_0 N_{e1}}{N_1 N_{e0}}\right)$$

0 and 1 indexes correspond to the gas and plasma parameters before and behind the shock

The relaxation length behind the SW front

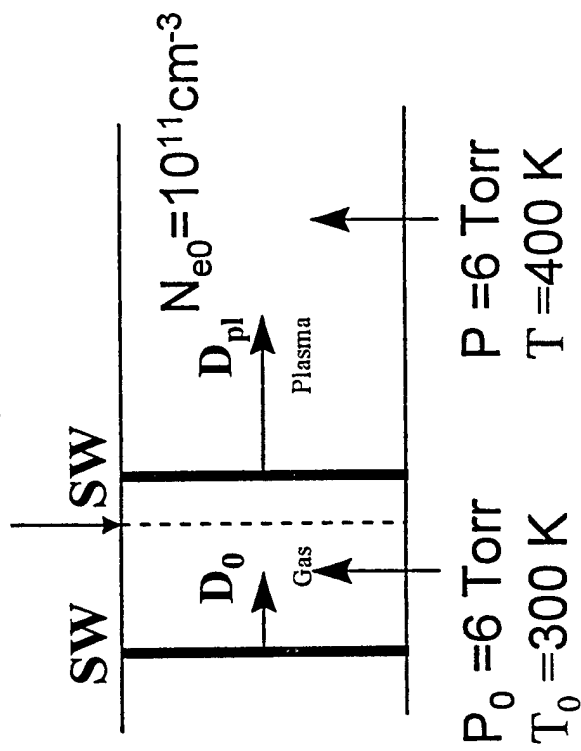
$$\xi_r \approx D \frac{N_0}{N_1} \frac{1}{k_p N_m} \approx 4 \times 10^{-5} \frac{N_0}{N_1 \sqrt{W[W/cm^3]}} D[cm/s], \quad cm$$

Inclusion of Plasma Effects Dramatically Improves Agreement of Theory with Experiment for 1-D Shock Penetrating Into a Plasma

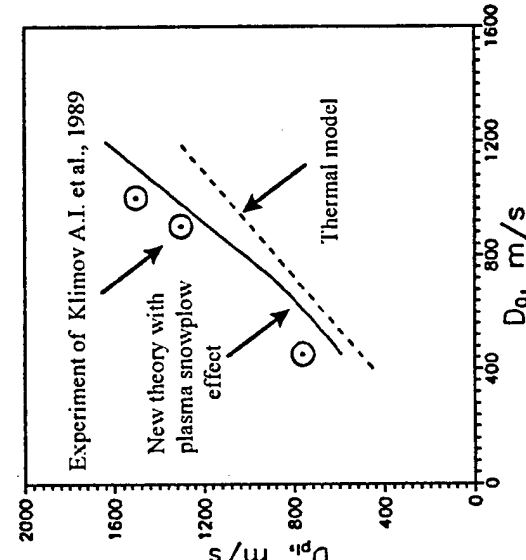
Physical System

$1.3 < M < 3.5$, $M = D_0/a_0$,
 a_0 =sound velocity

Gas-Plasma
boundary



Dependence of shock speed in plasma D_{pl} versus the initial shock speed D_0 in undisturbed gas.

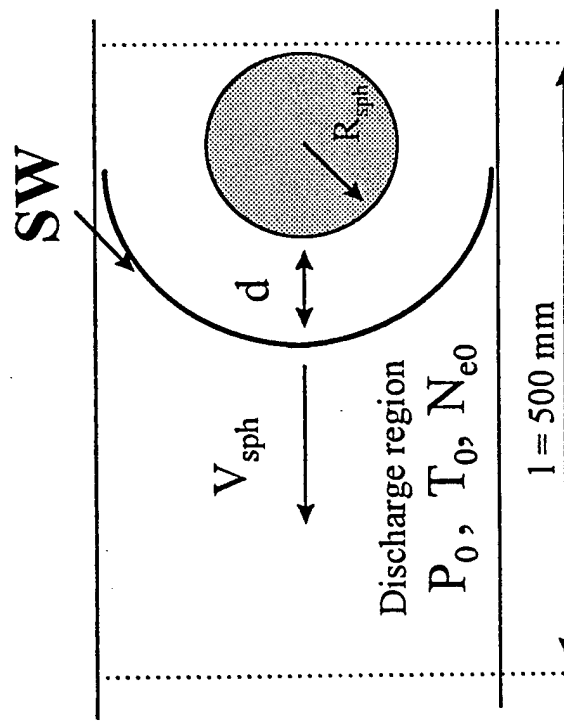
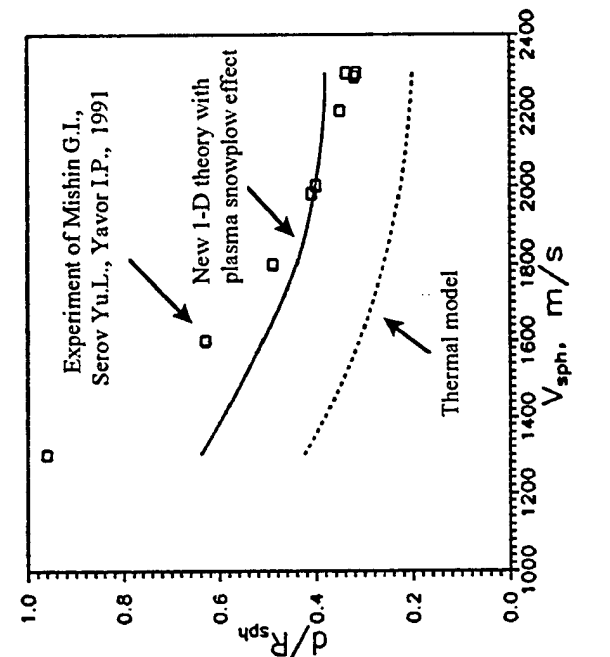


Inclusion of Plasma Effects Dramatically Improves Agreement of Theory with Experiment for Hypersonic Sphere Entering a Plasma

Physical System

$P_0 = 45 \text{ Torr}$, $T_0 = 1350 \text{ K}$, $N_{e0} = 10^{11} \text{ cm}^{-3}$,
 $1.7 < M < 3.2$, $M = V_{\text{sph}}/a_0$, $R_{\text{sph}} = 20 \text{ mm}$

Dependence of relative shock standoff distance d/R_{sph} from the sphere versus the speed of the sphere V_{sph} .



Conclusions

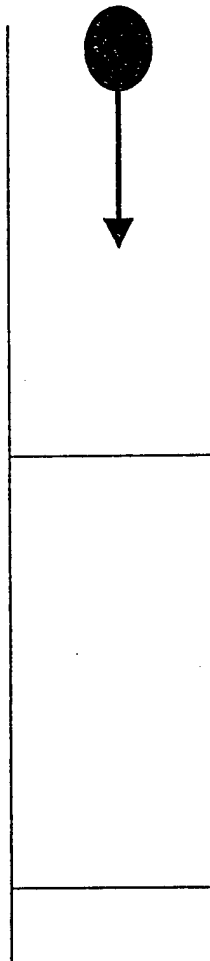
- The mechanism of shock wave (SW) acceleration and attenuation due to interaction with a weakly ionized plasma really exists
- Preliminary calculations of 1-D SW speed in plasma are in a good agreement with experimental results when the highly excited states energy release behind the SW front is taken into account
- SW acceleration is accompanied by decrease of density and velocity jump with a small increase of static pressure jump through the SW front
- The foregoing results in a decrease of dynamic pressure jump through the SW front
- The creation of a discharge plasma IN FRONT OF the shock wave courses the SW attenuation and drag reduction for supersonic and hypersonic vehicles
- More detailed kinetic analysis is necessary to obtain more precise results

Anomalous Behavior of Shocks in Weakly Ionized Gases - Theory & Modeling

Vish V. Subramaniam
Department of Mechanical Engineering
and Chemical Physics
The Ohio State University
Columbus, Ohio 43210

- Anomalous effects seen in two different types of experiments:

- (1) Ballistic range

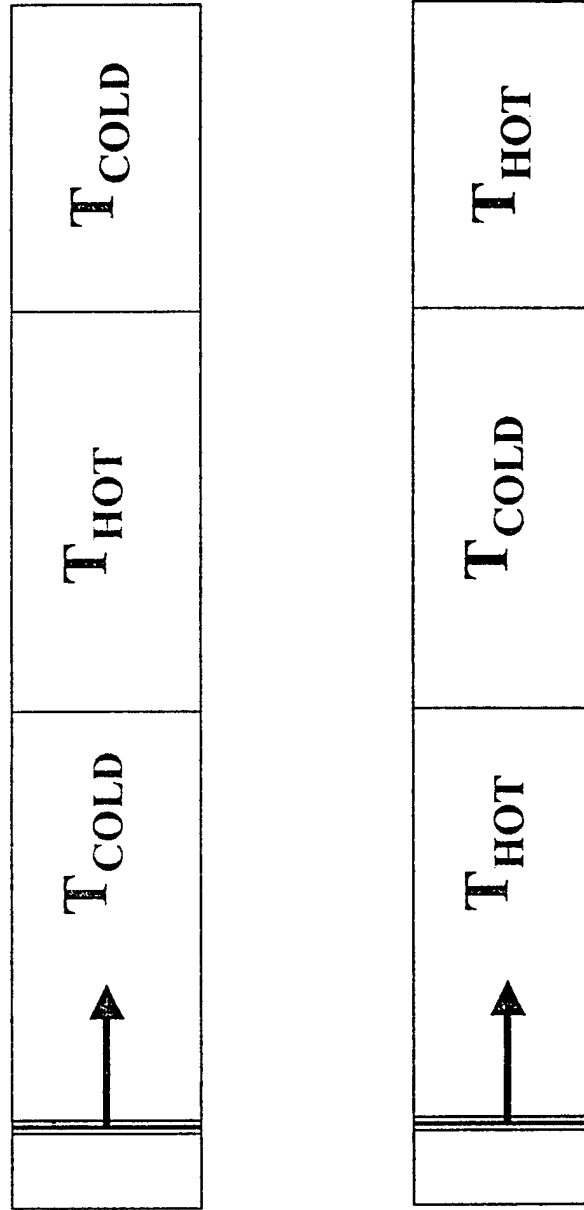


- (2) Spark-generated shock launched into a glow discharge (WPAAFB)



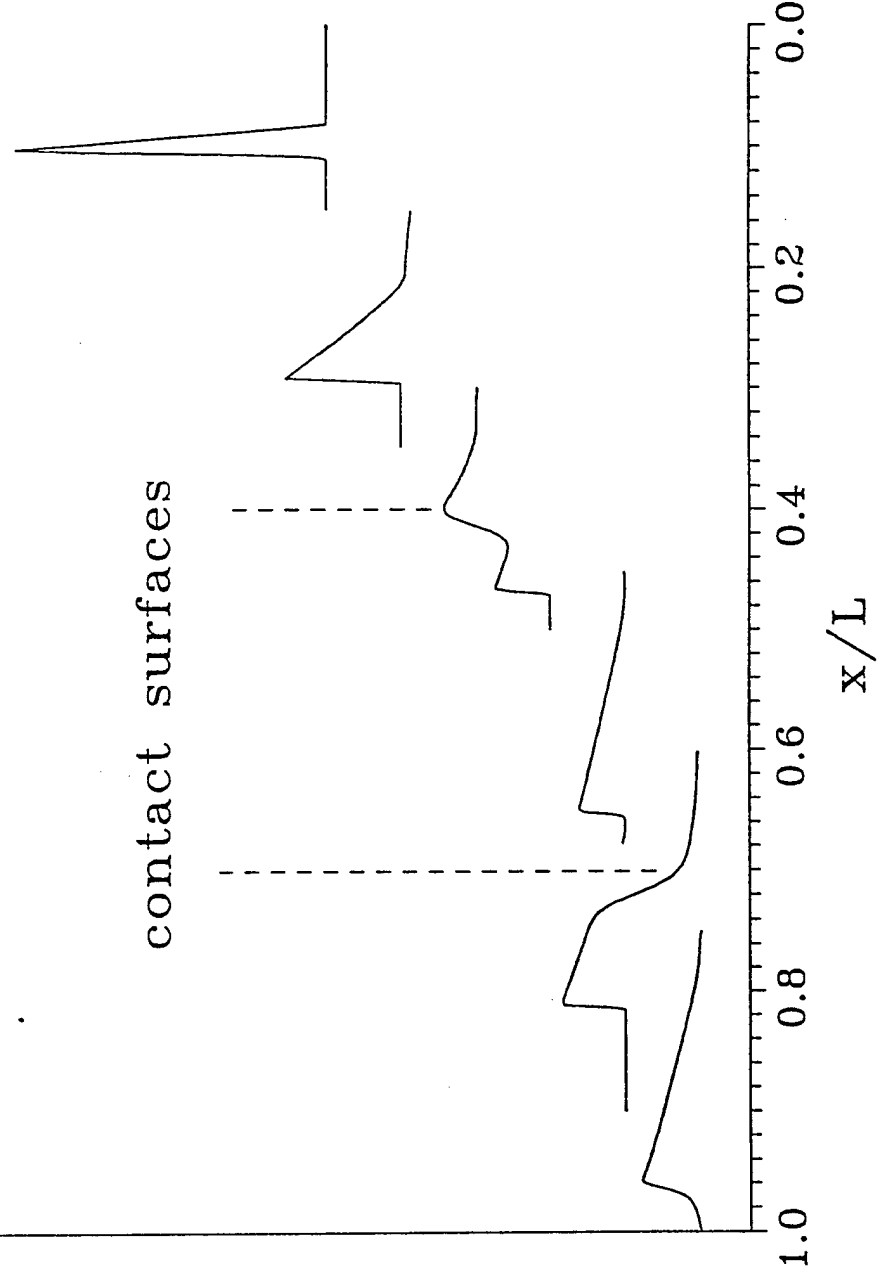


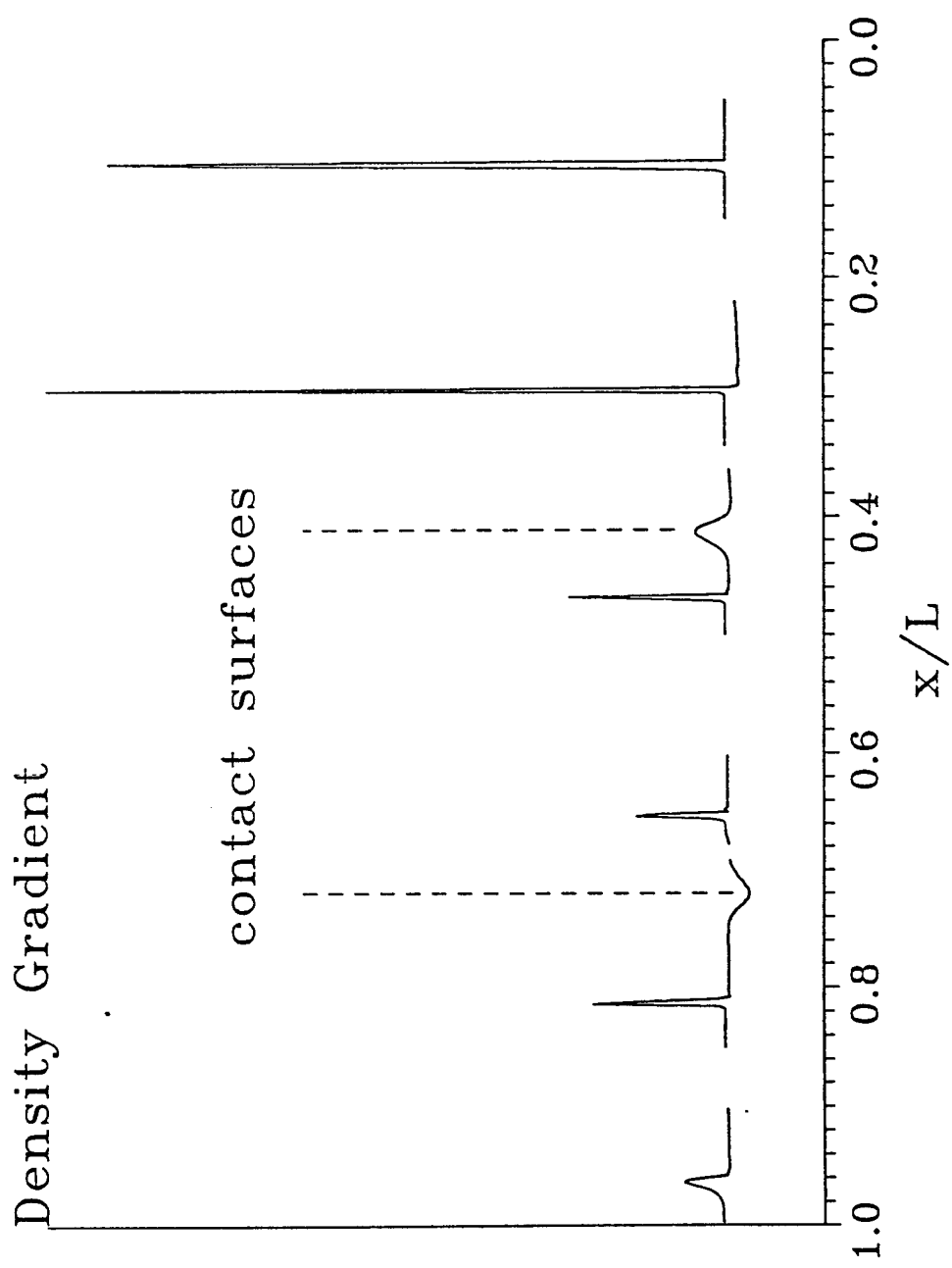
Effects of purely axial thermal gradients

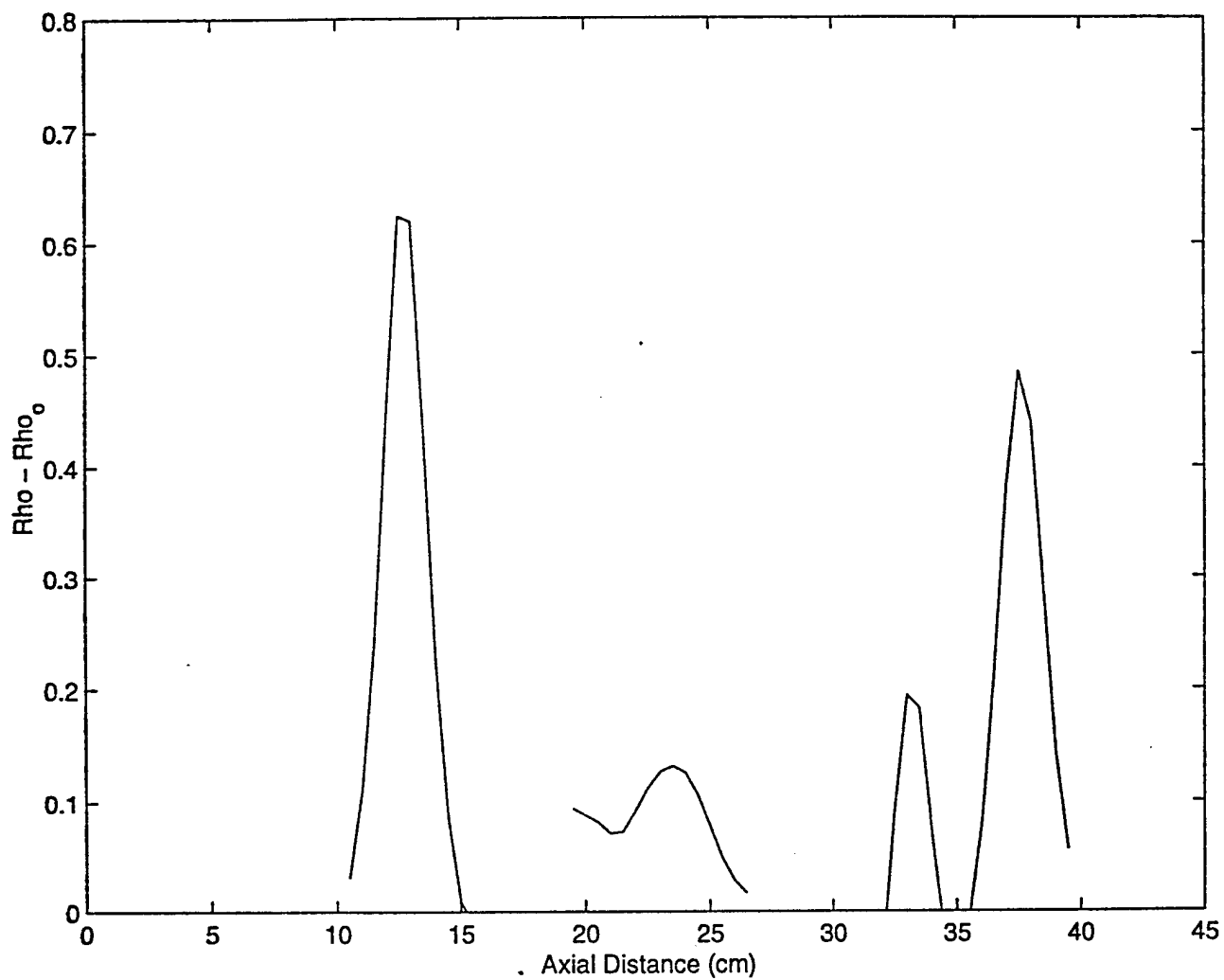


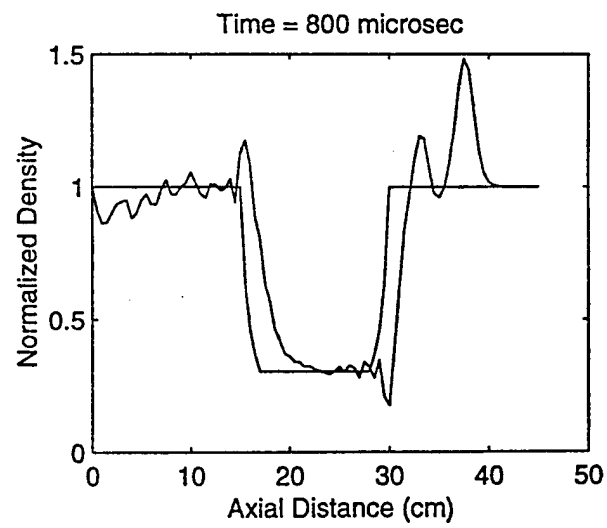
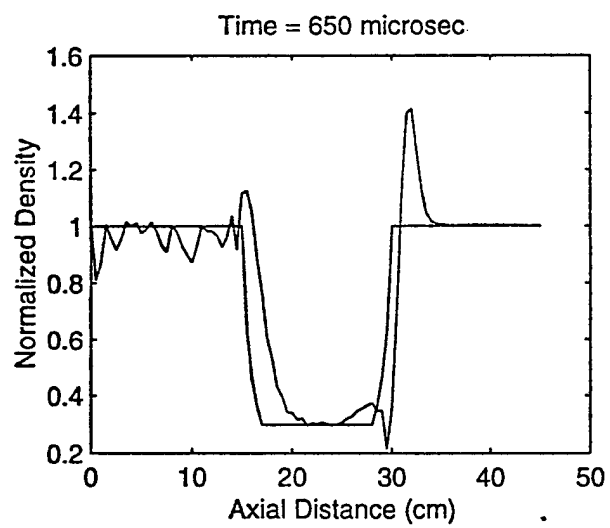
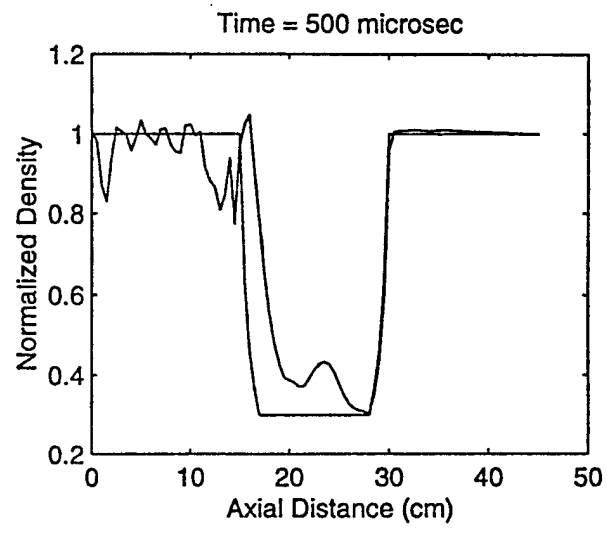
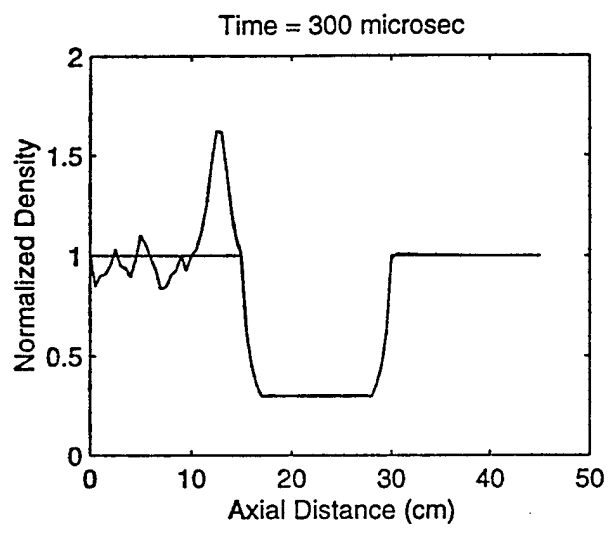
Density Profiles

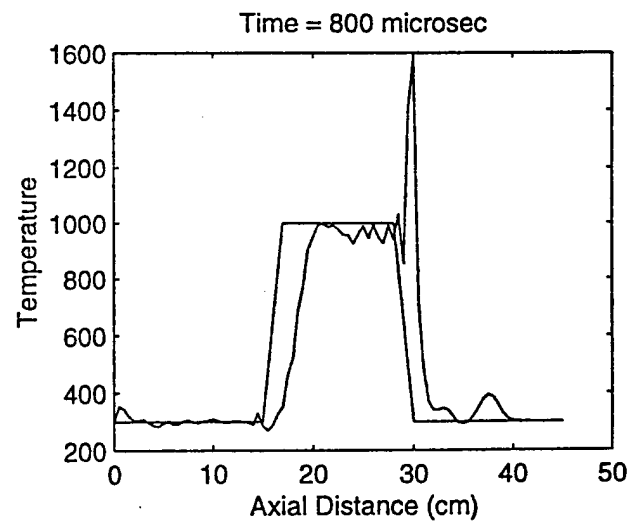
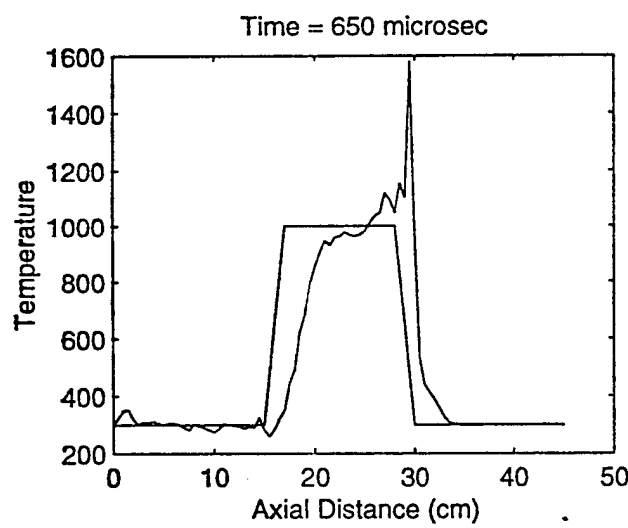
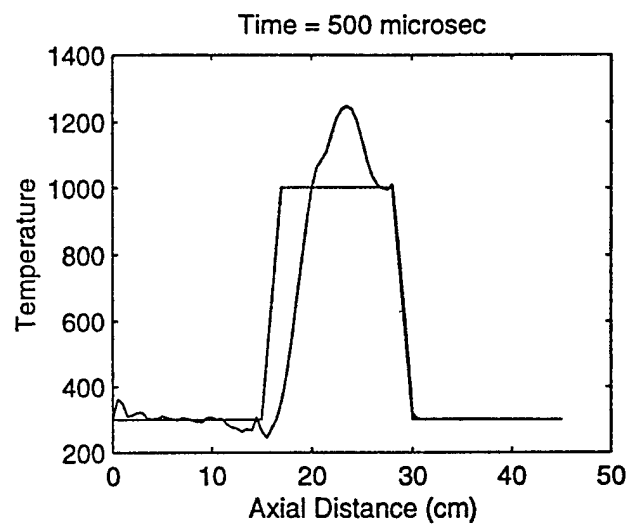
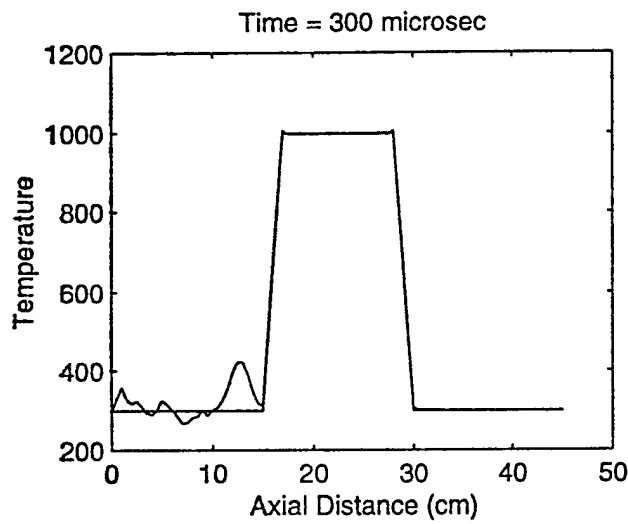
contact surfaces

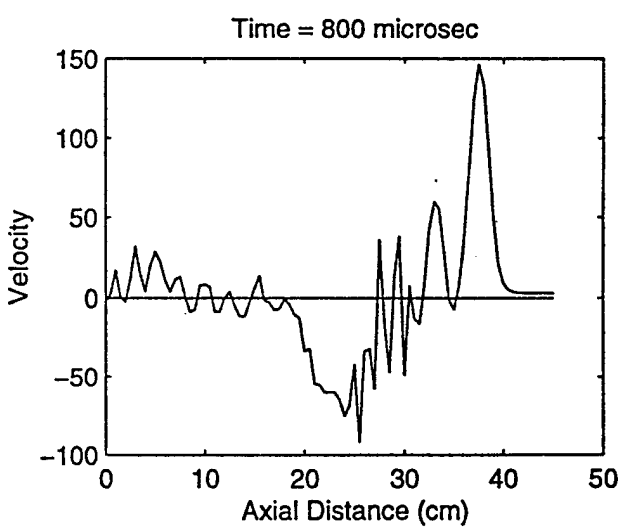
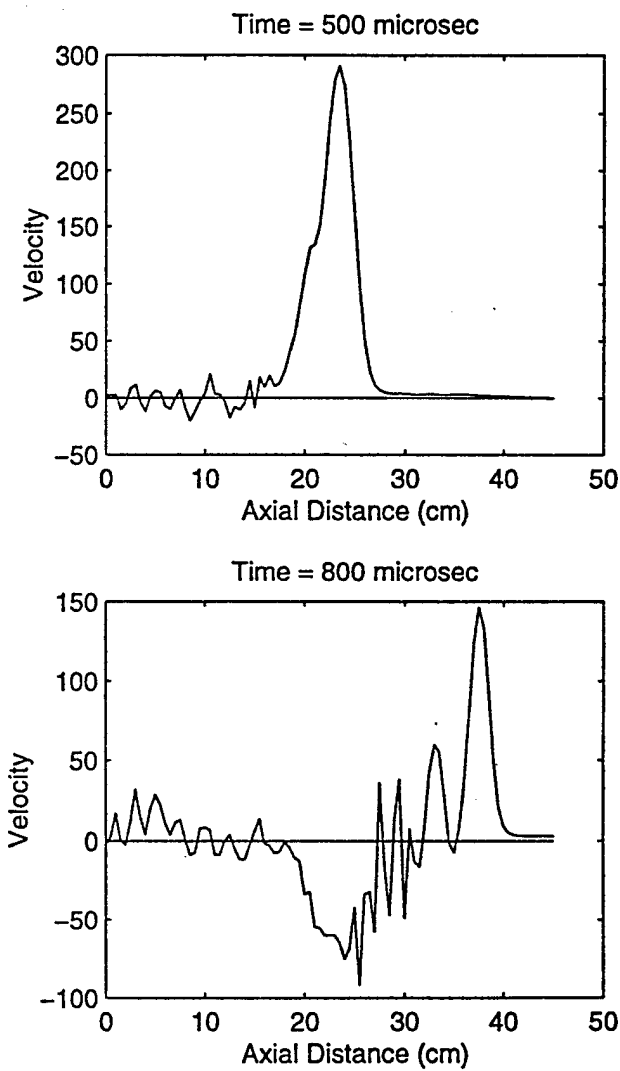
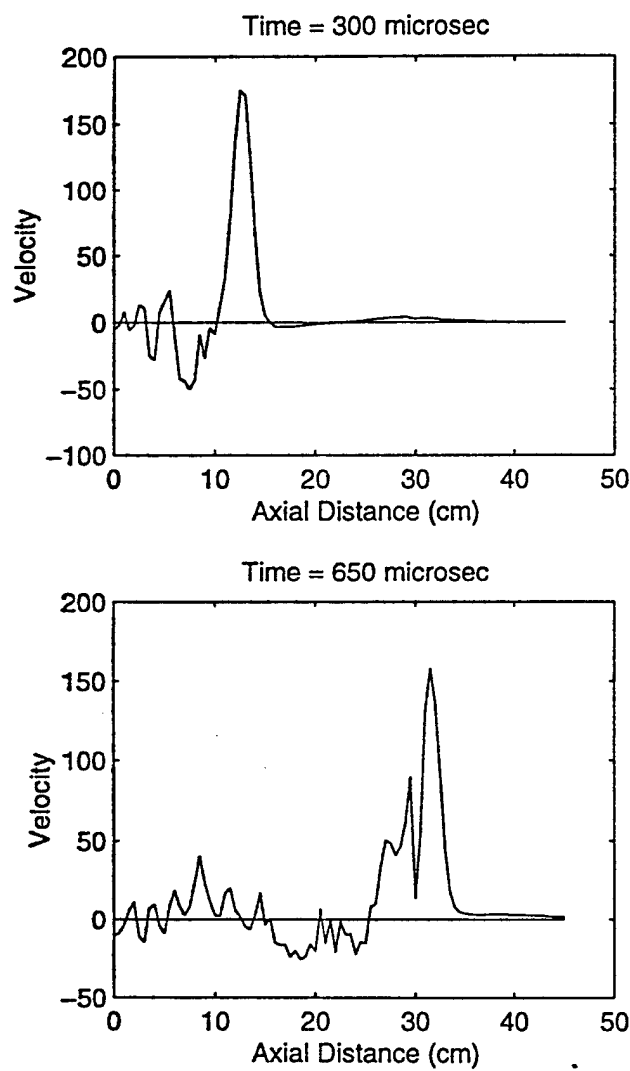


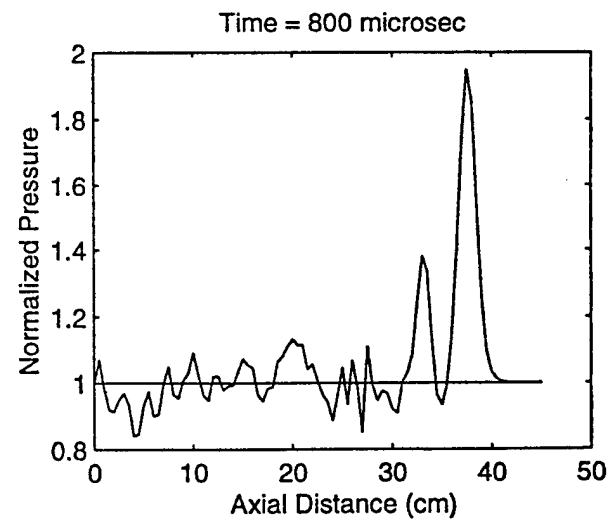
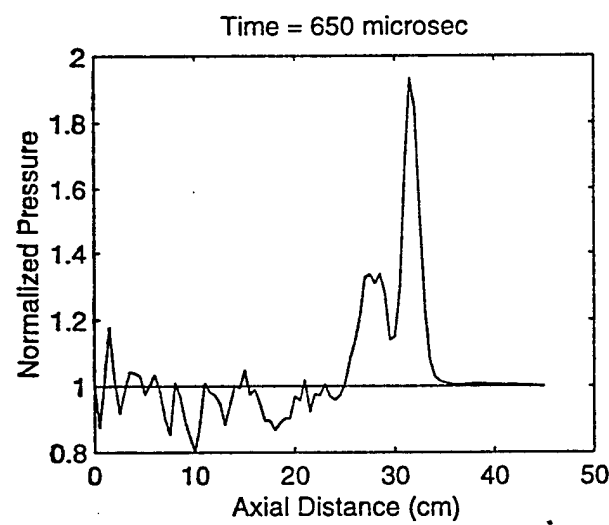
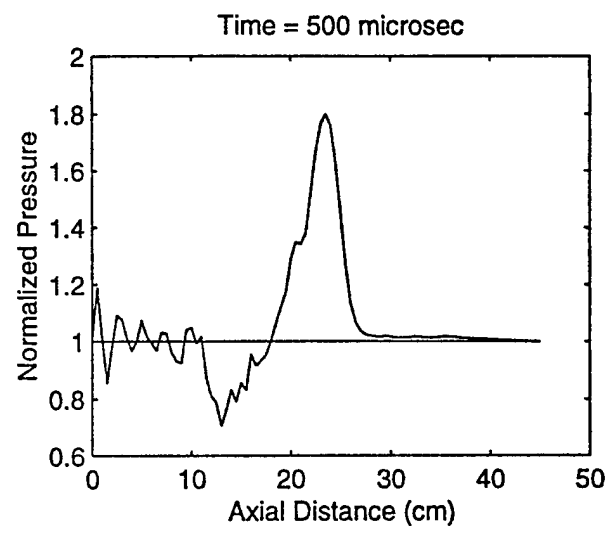
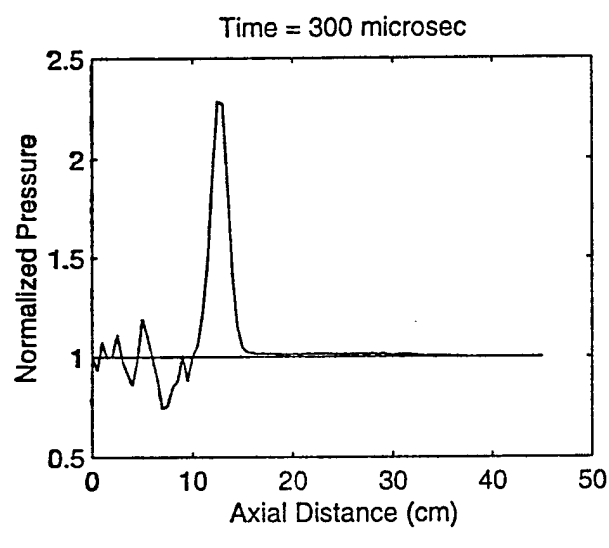


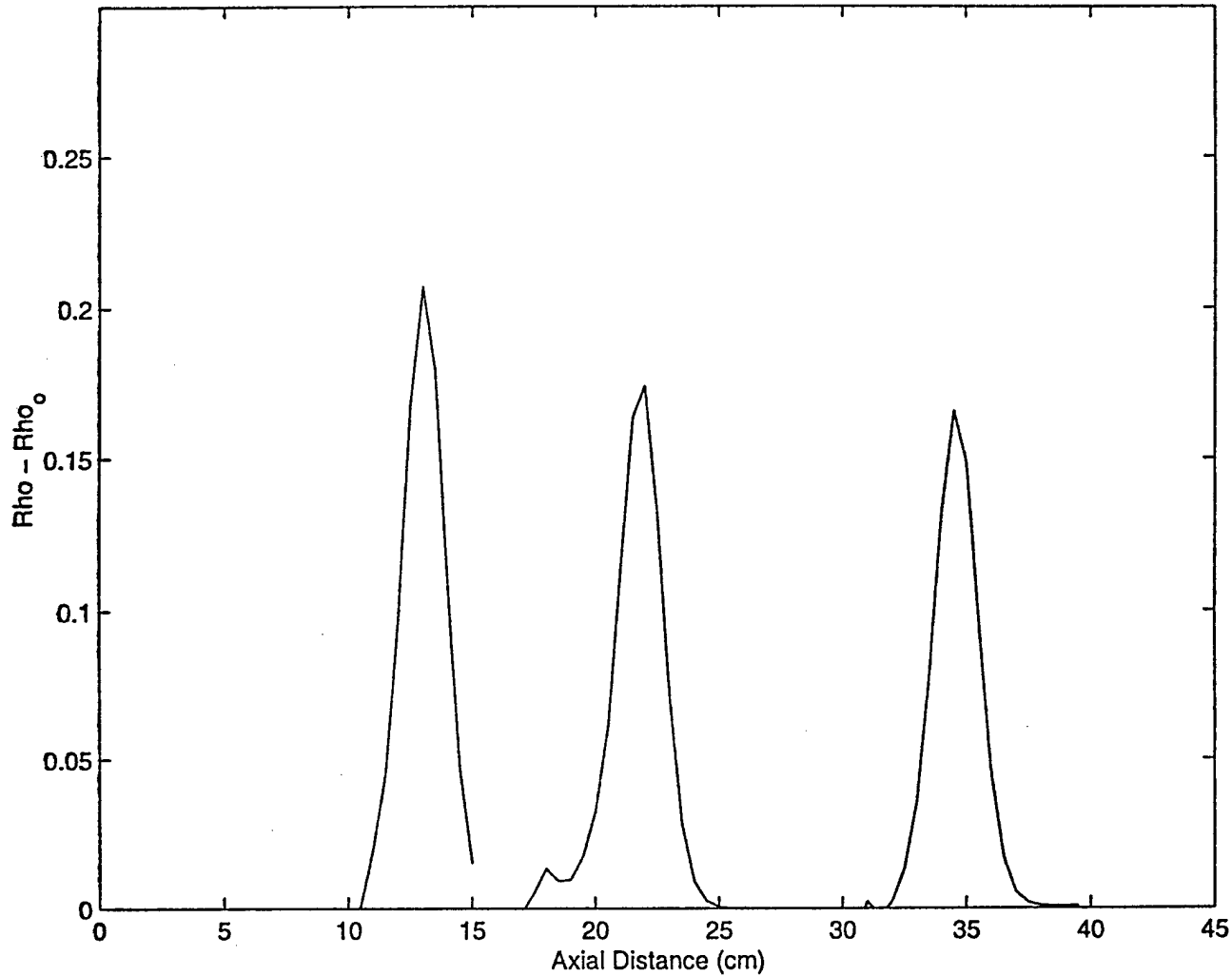




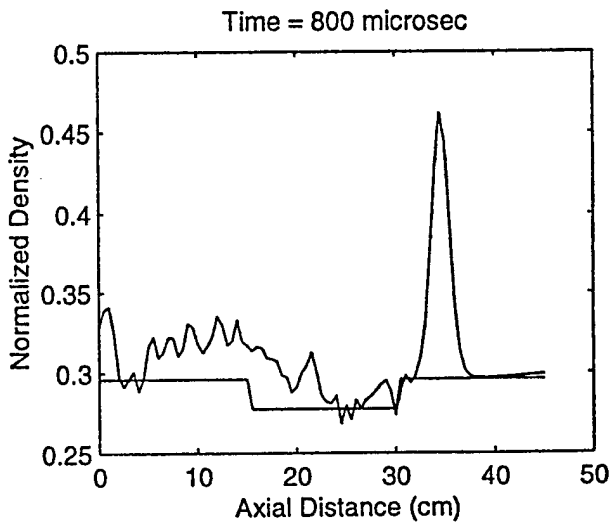
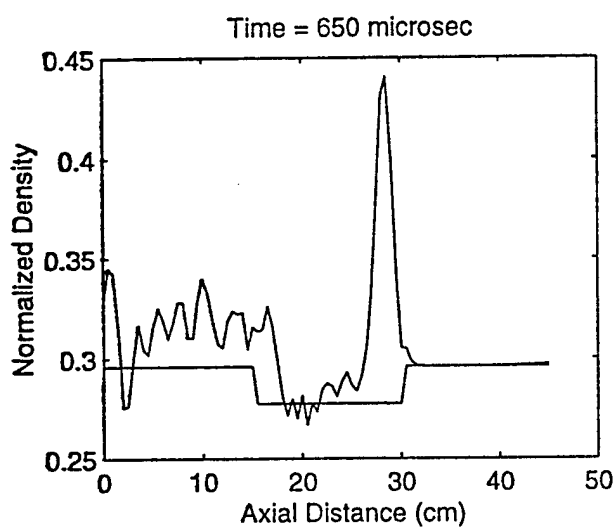
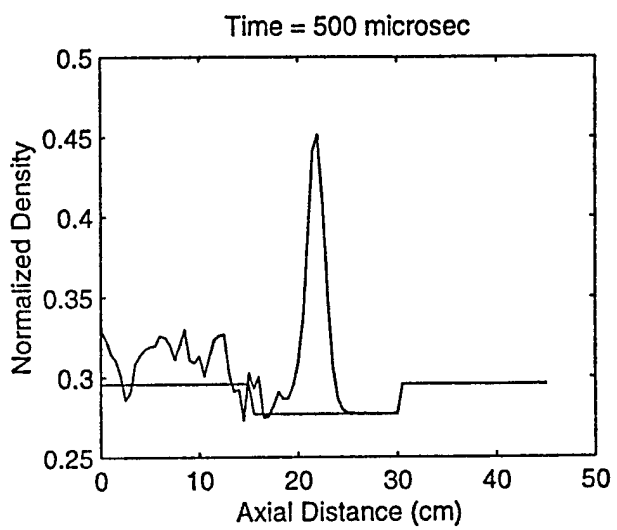
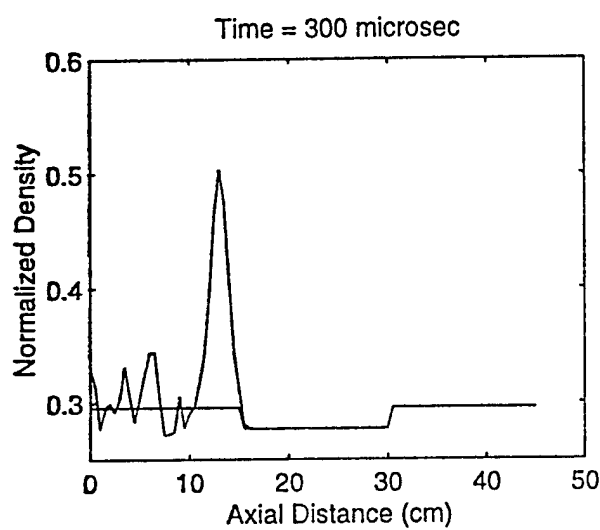


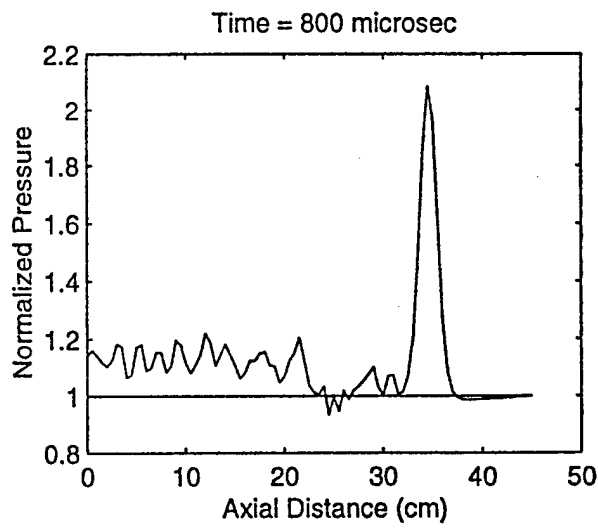
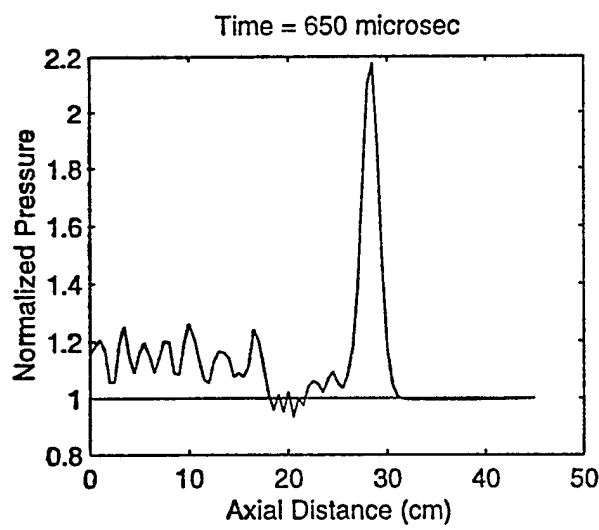
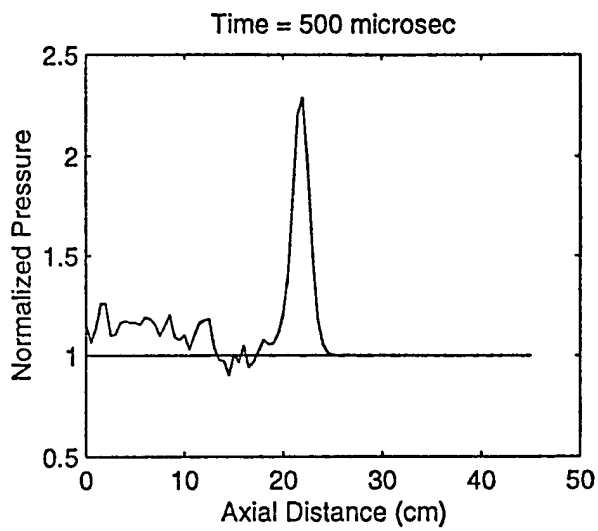
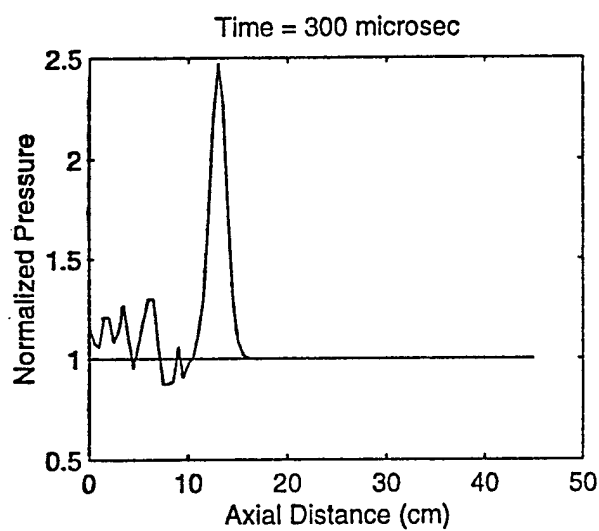


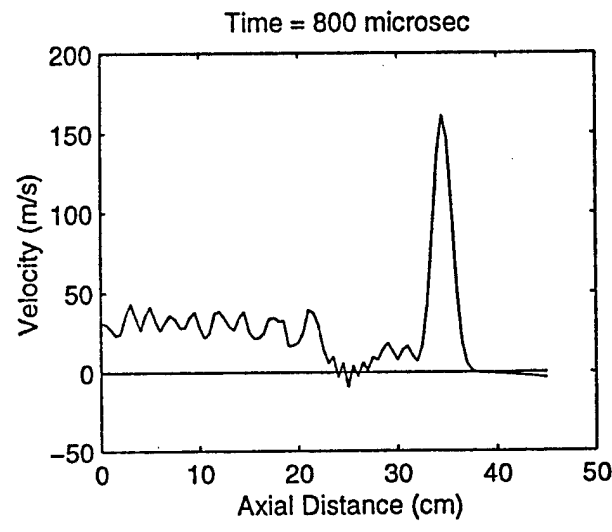
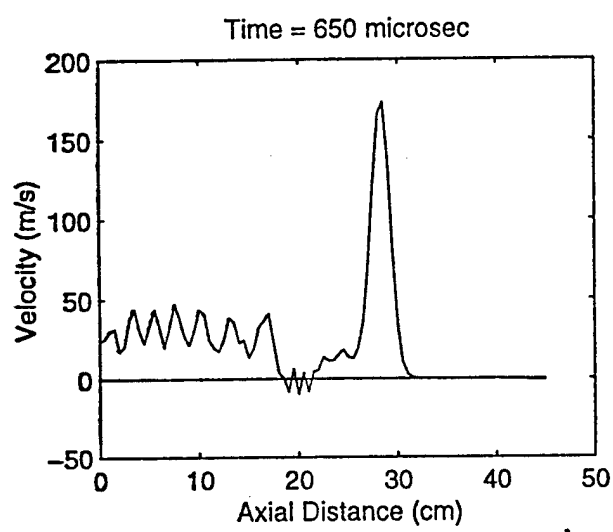
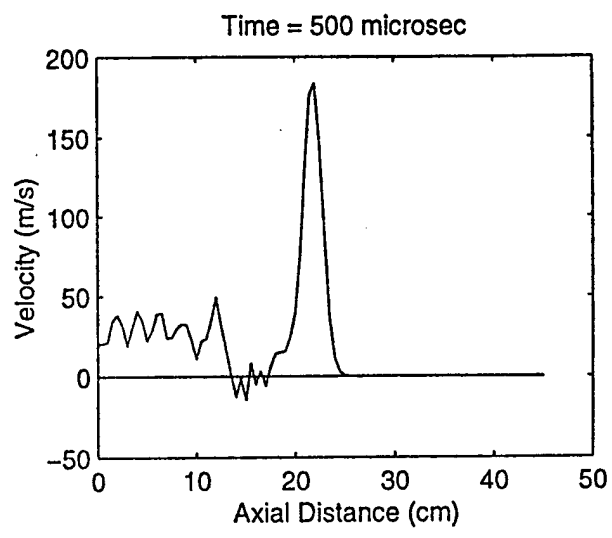
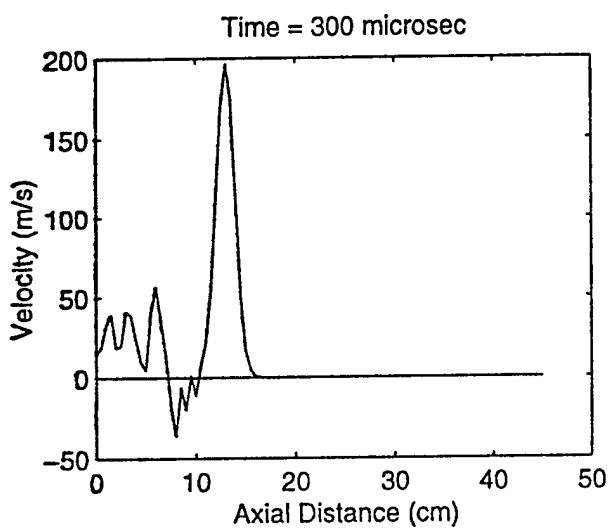


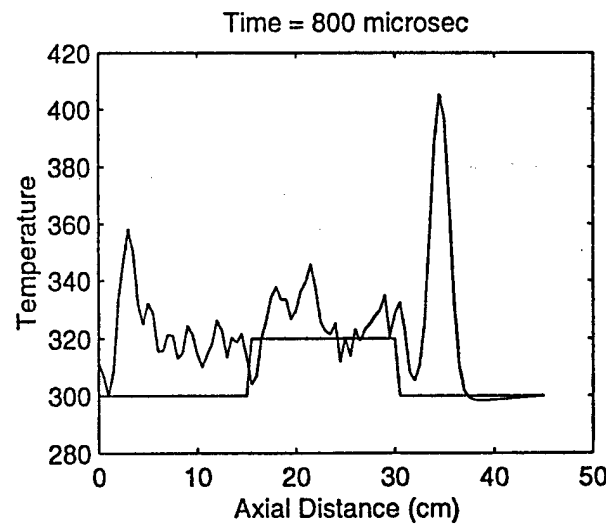
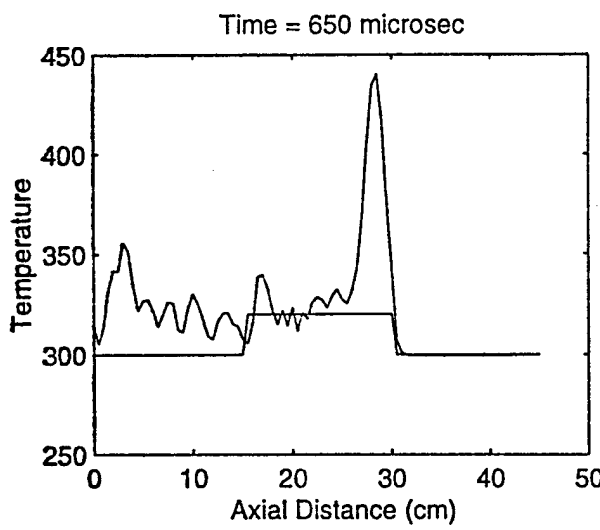
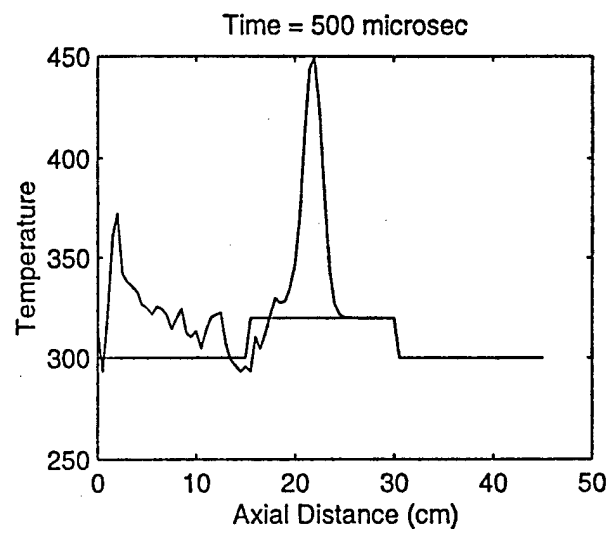
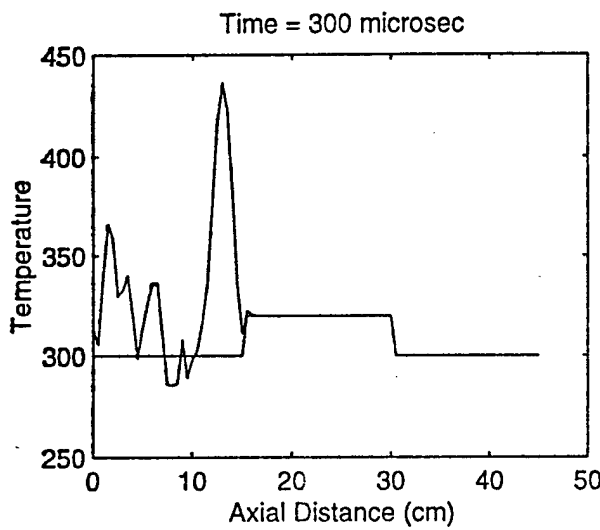


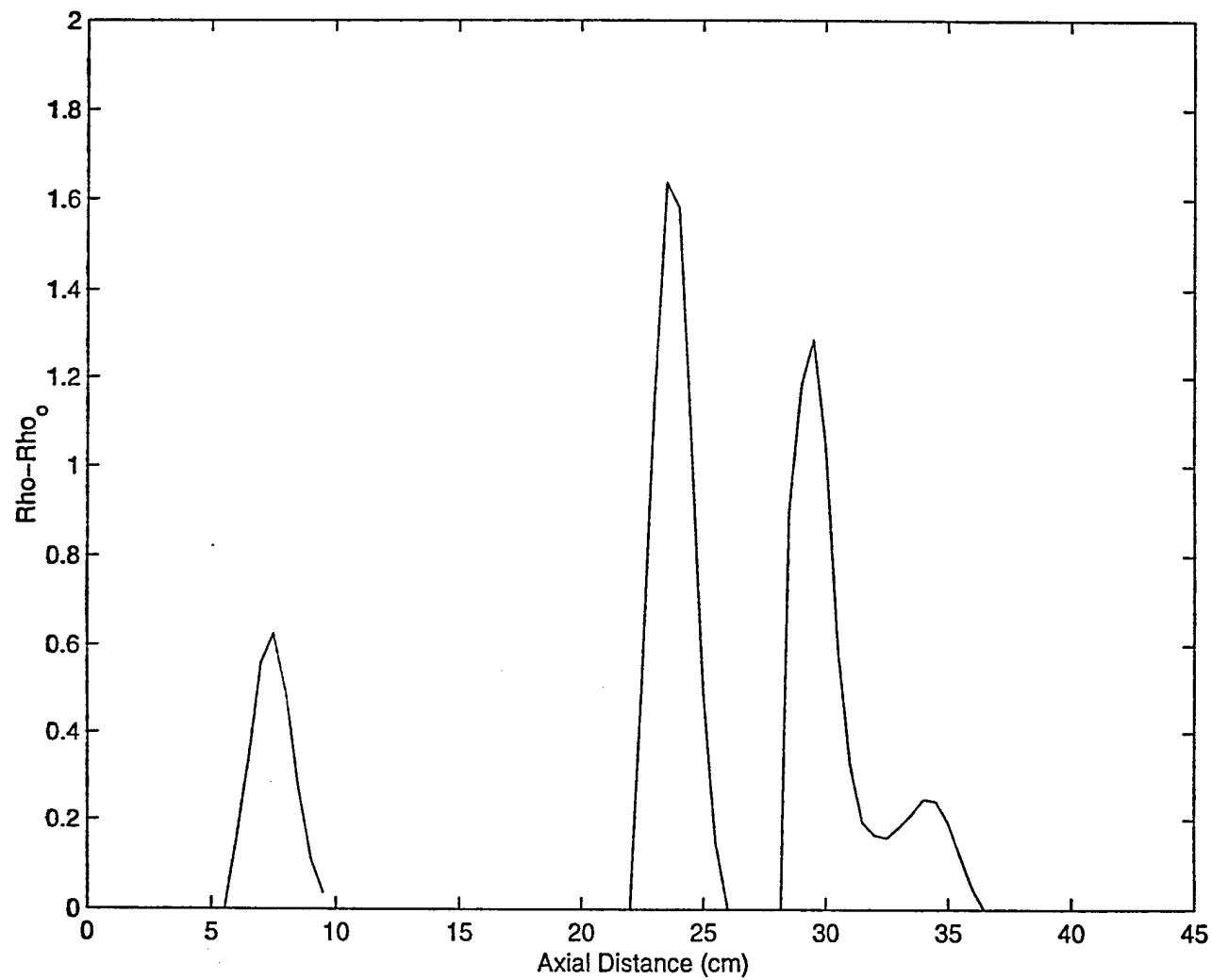
300/320/350

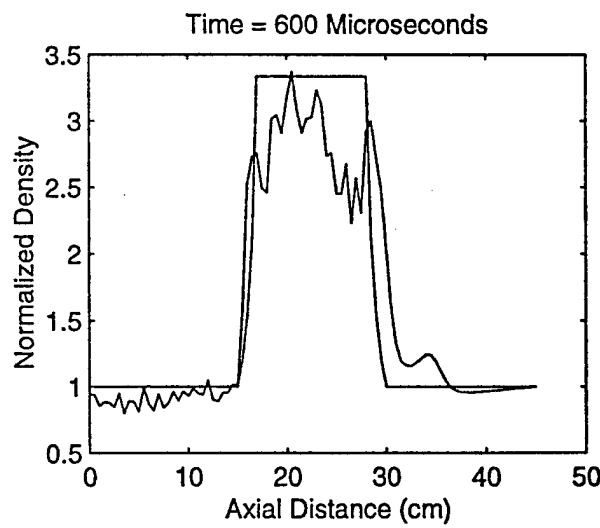
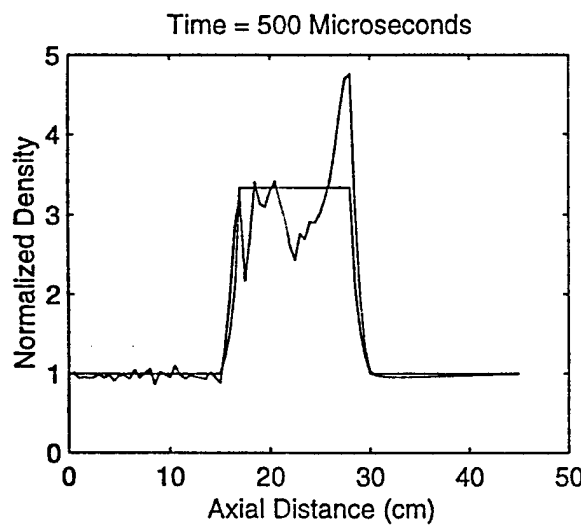
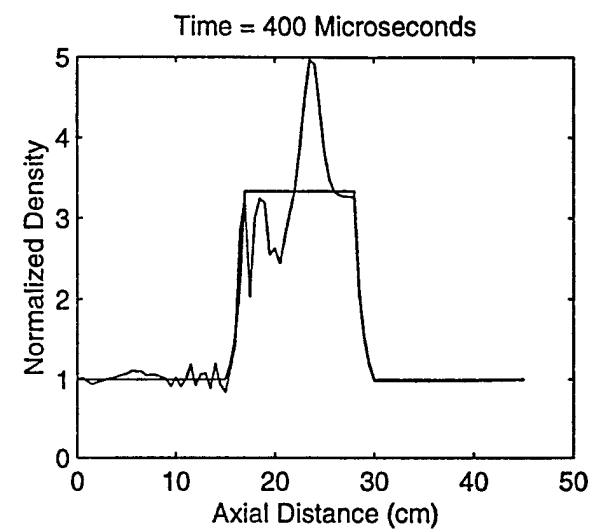
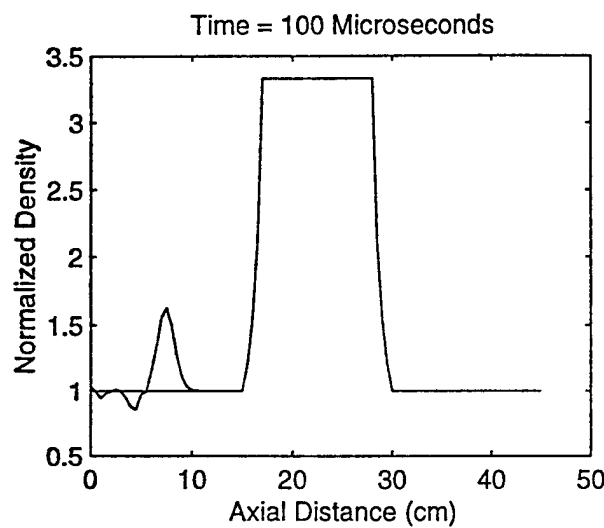


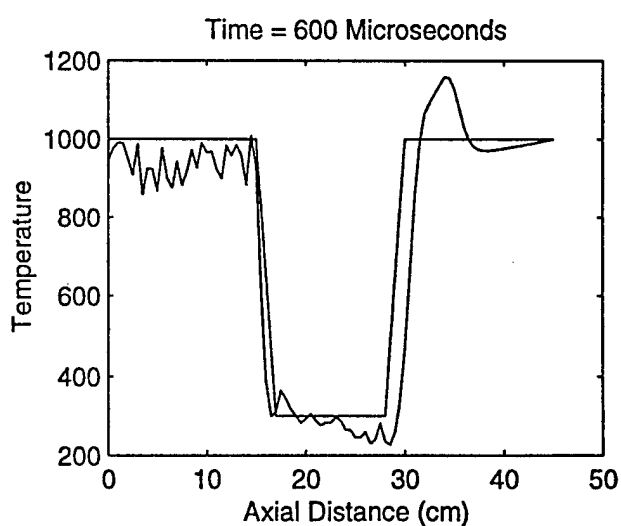
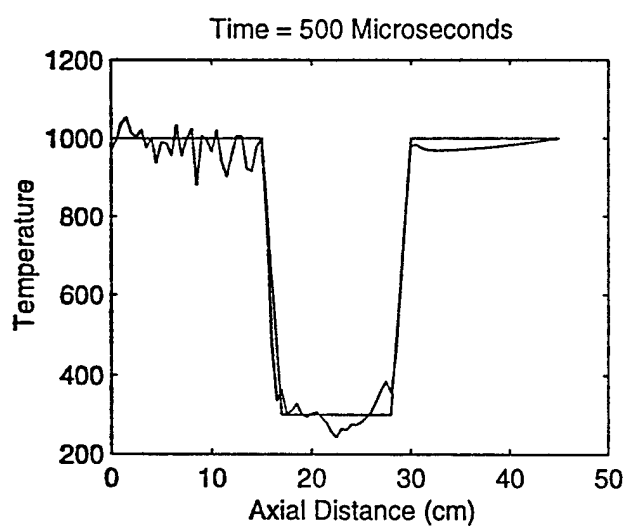
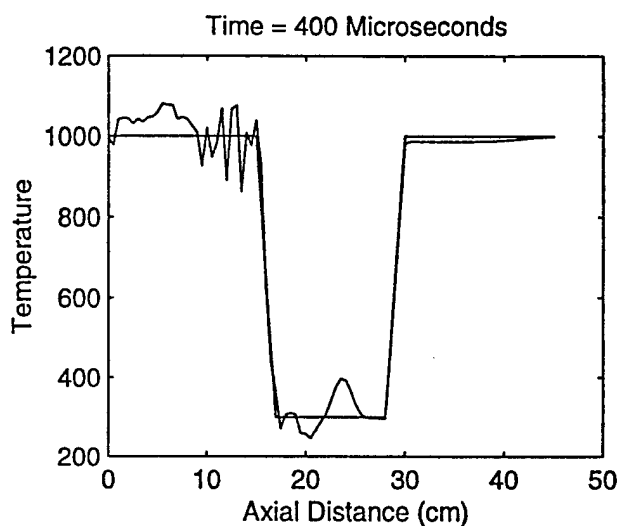
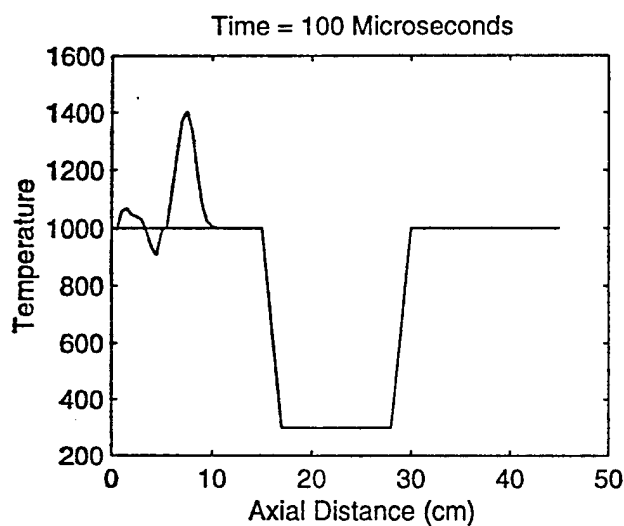


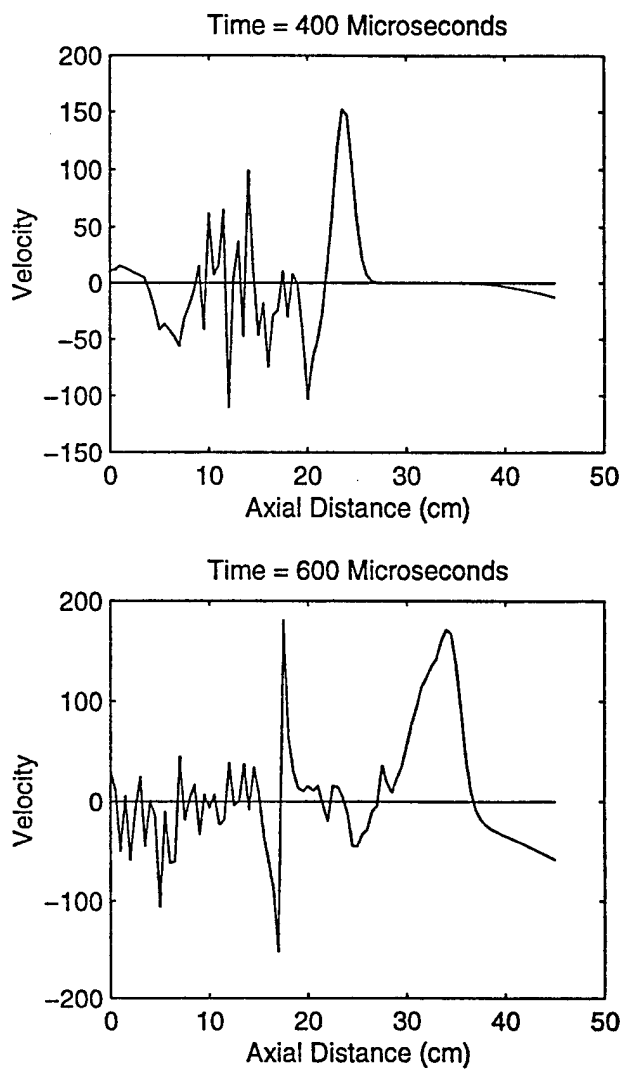
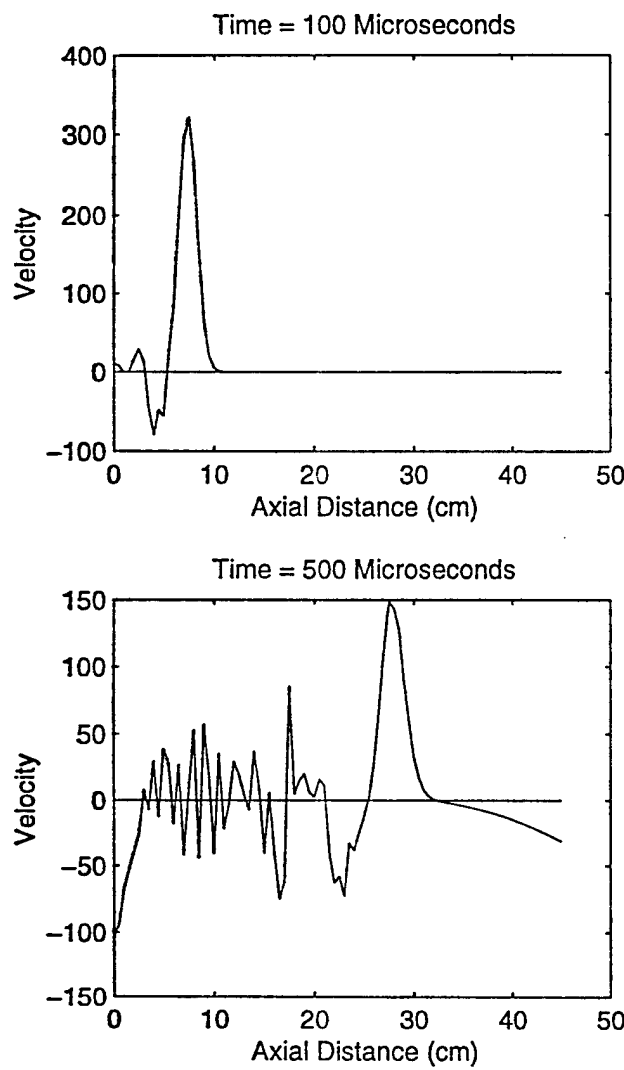


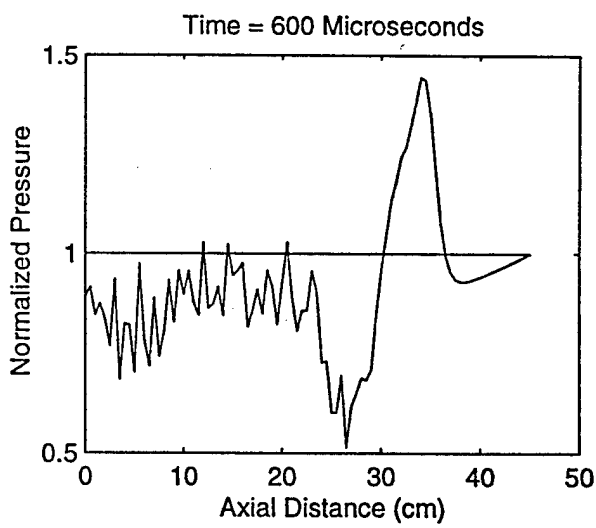
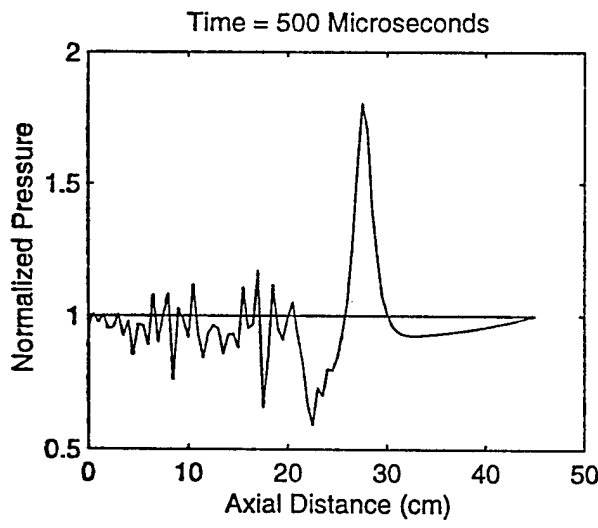
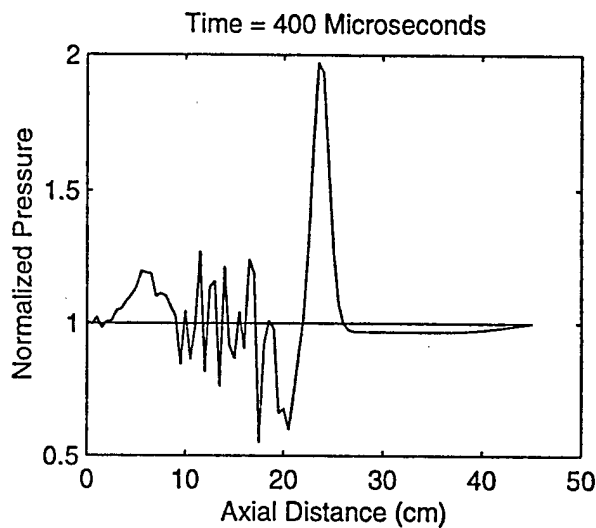
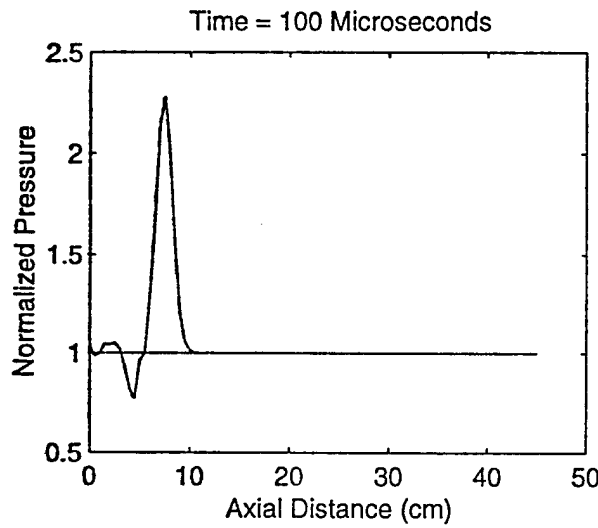








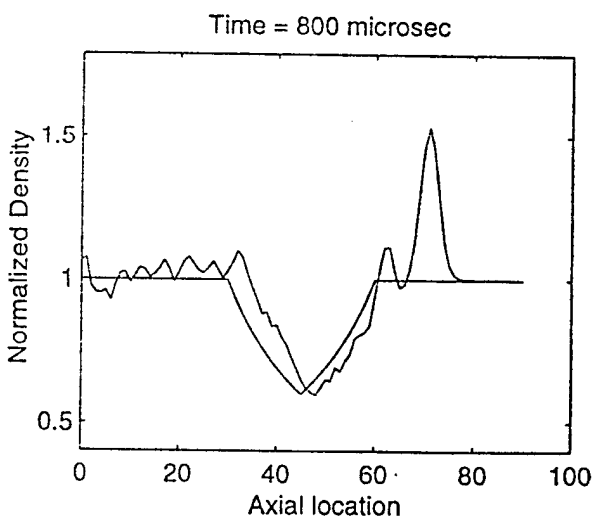
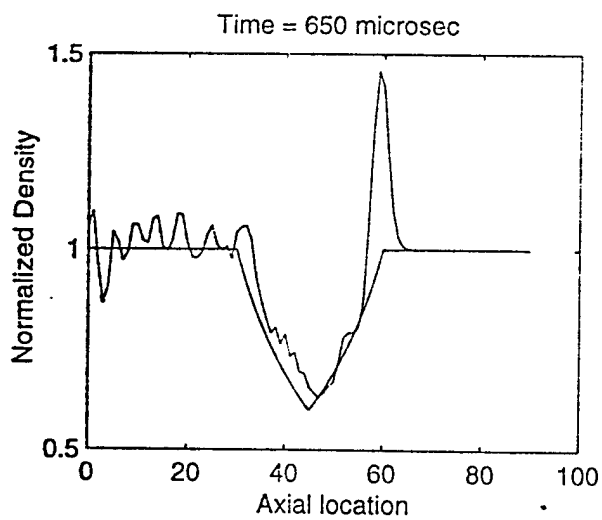
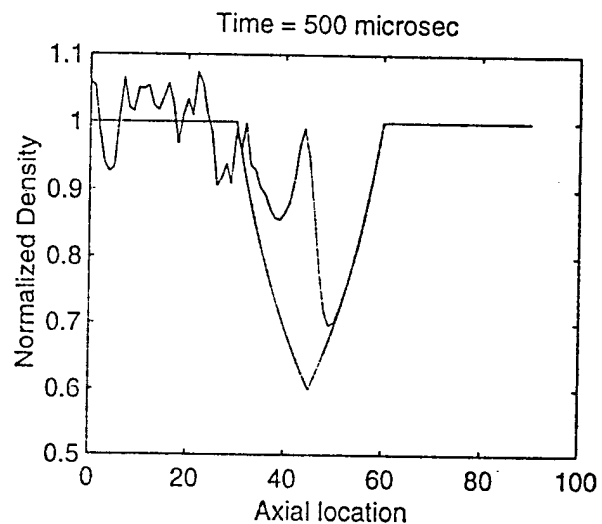
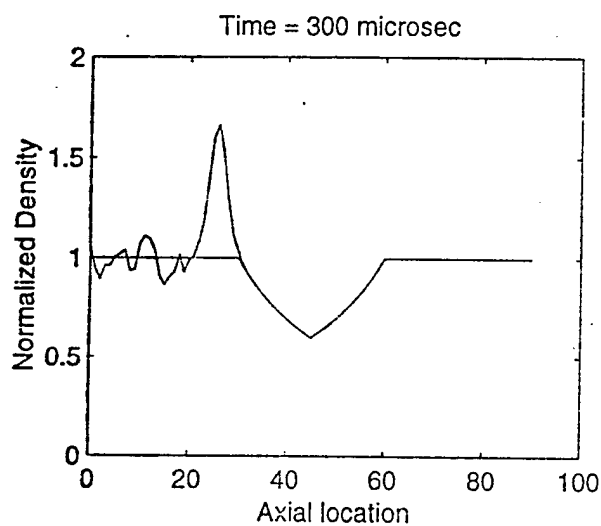




8/98

1) No radial ^{temp} grad
2) Triangular axial ^{temp} grad
3) NO plasma.

CASE III



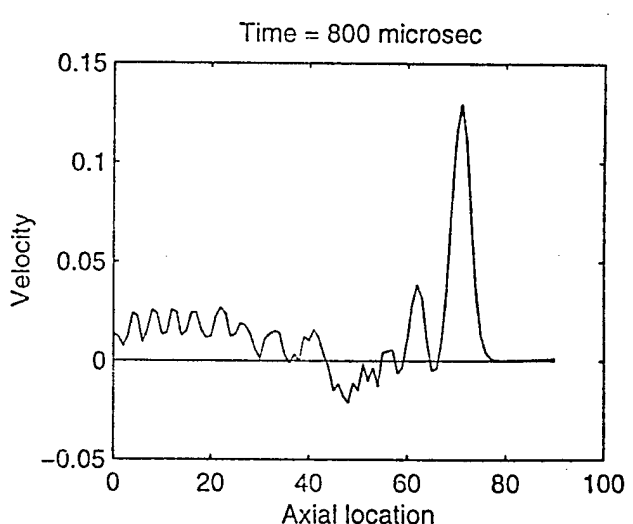
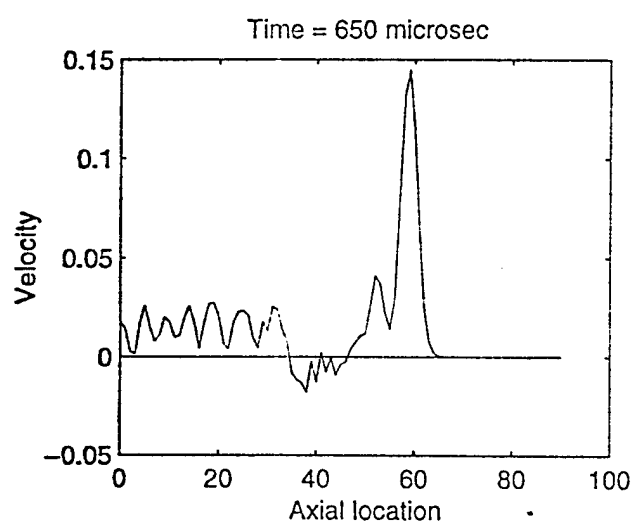
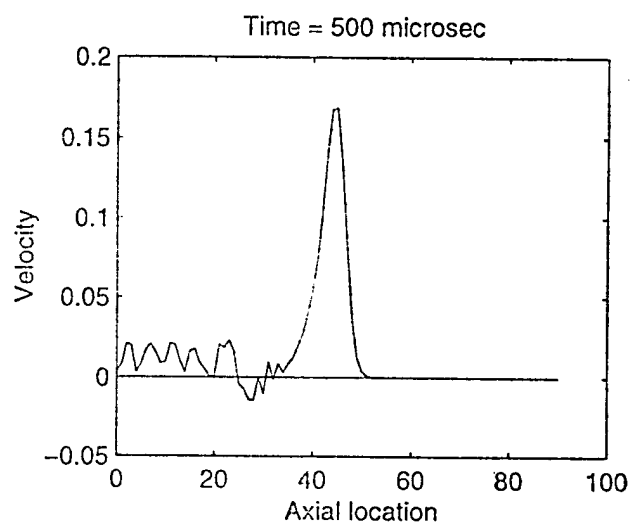
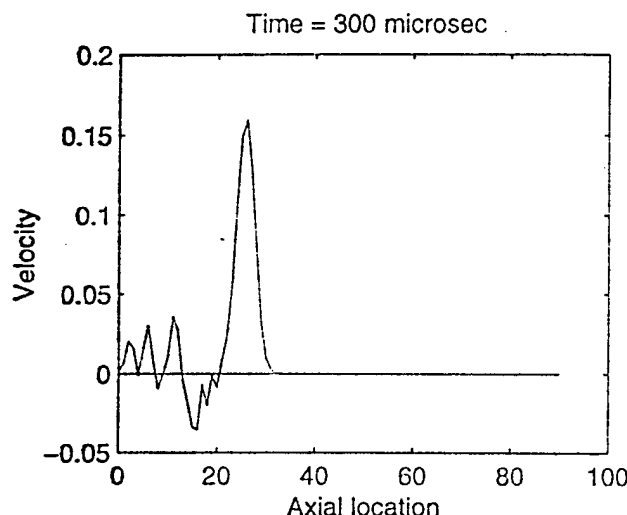
1/8/98

1) No radial term
grac

2) Triangular
axial temp gr

3) No plasma.

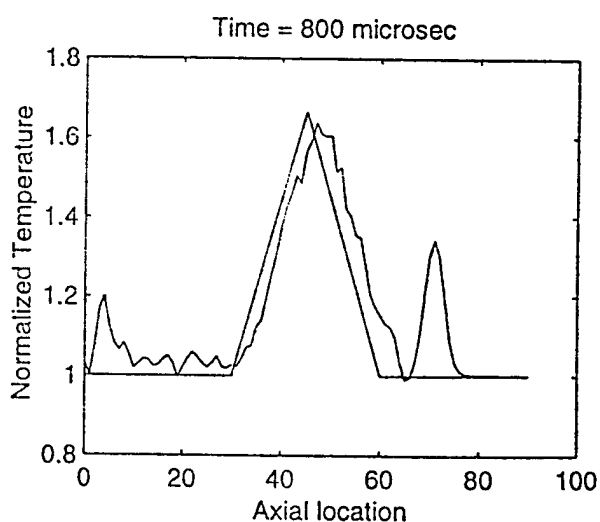
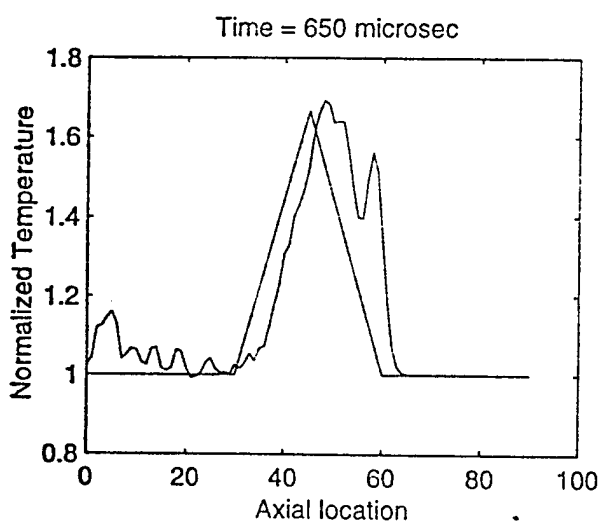
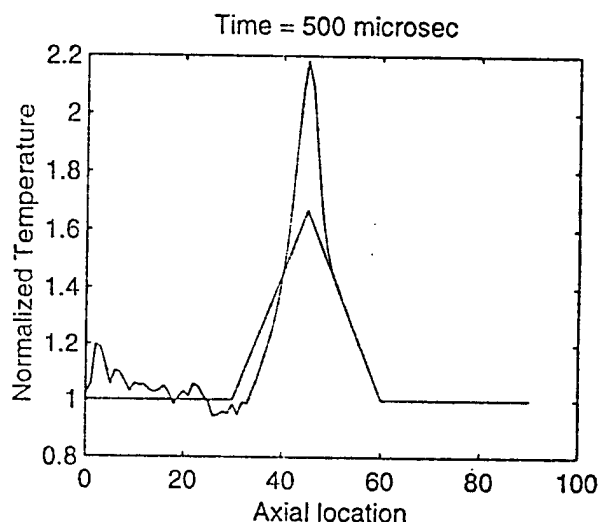
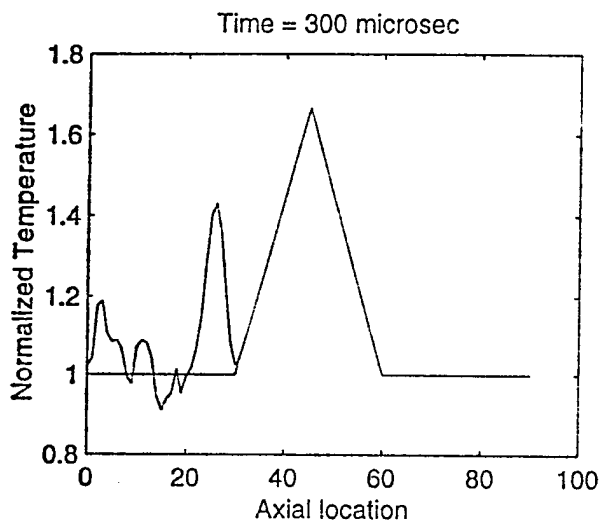
CASE III



1/8/98

- 1) No radial temp gr.
- 2) Triangular axial temp gra
- 3) No plasma

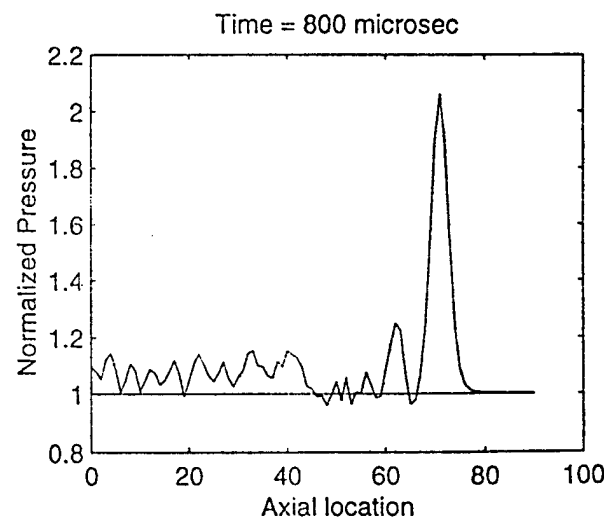
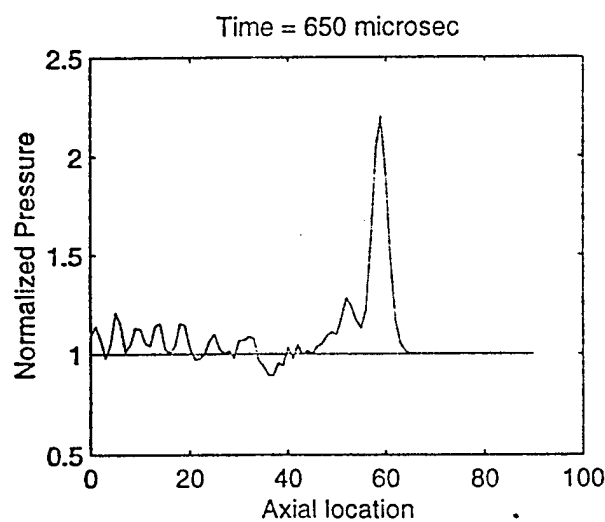
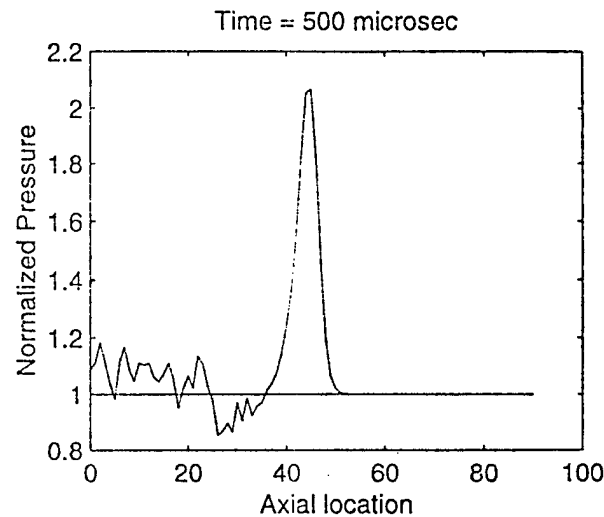
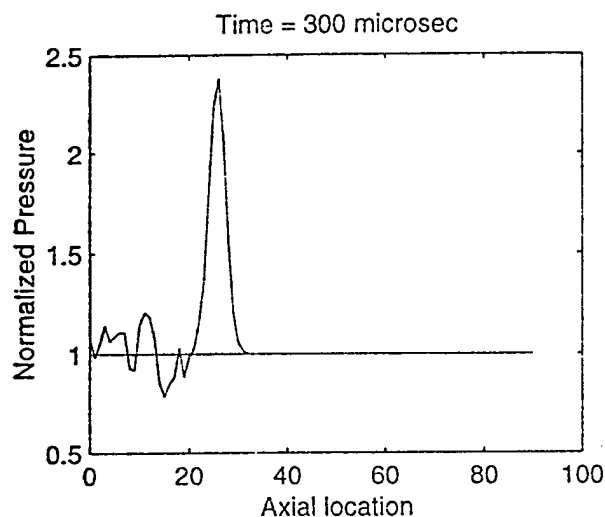
CASE III

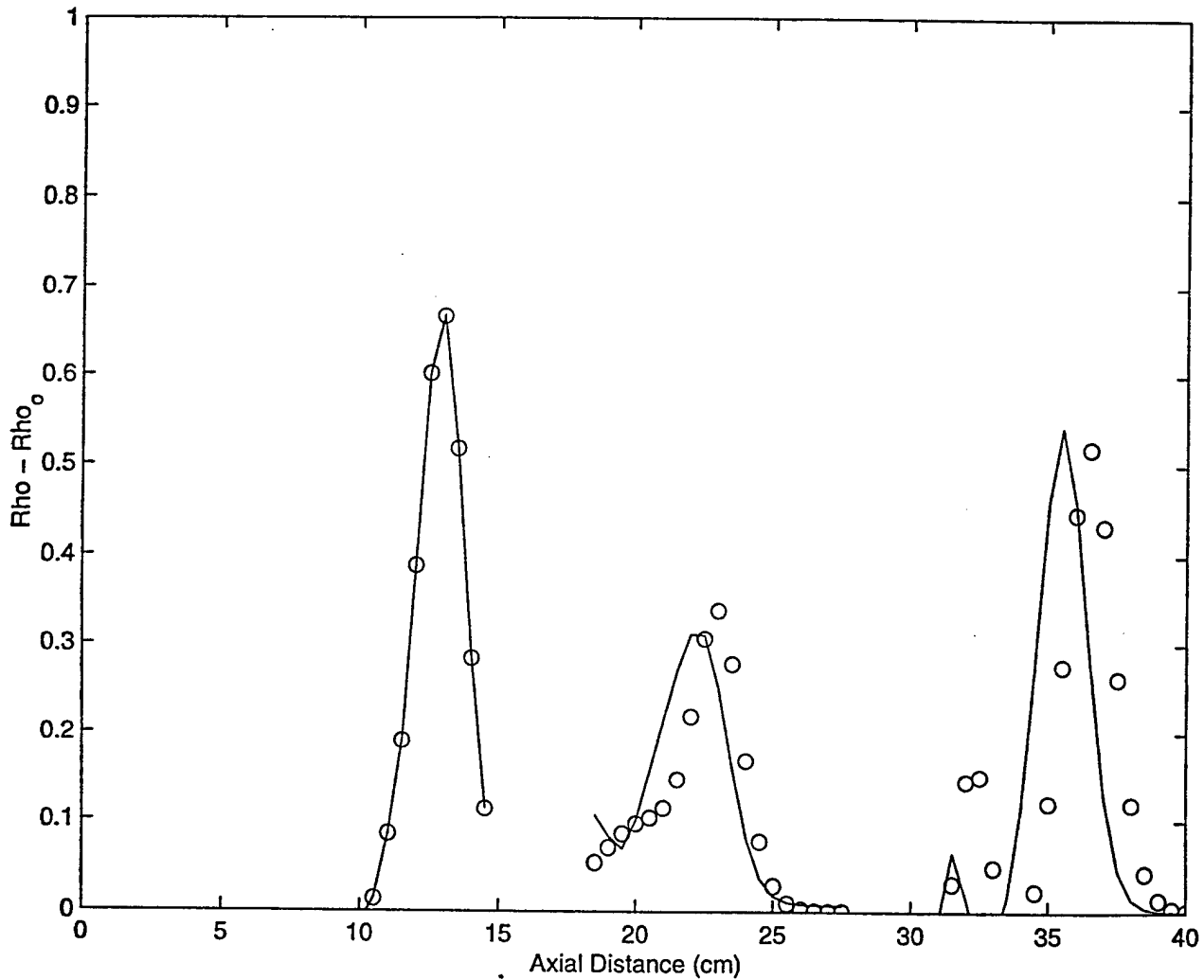


1/8/98

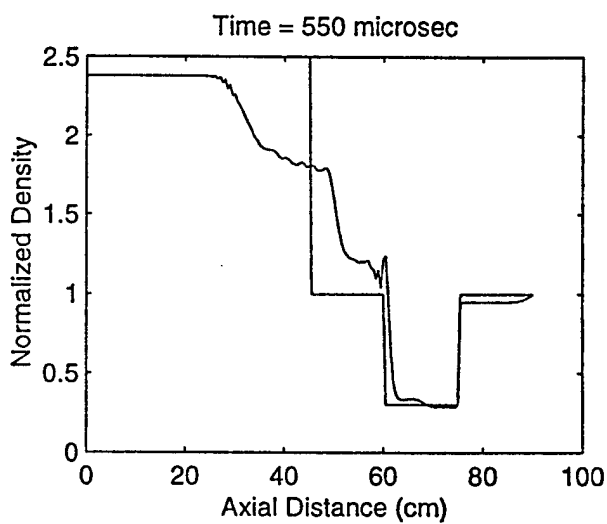
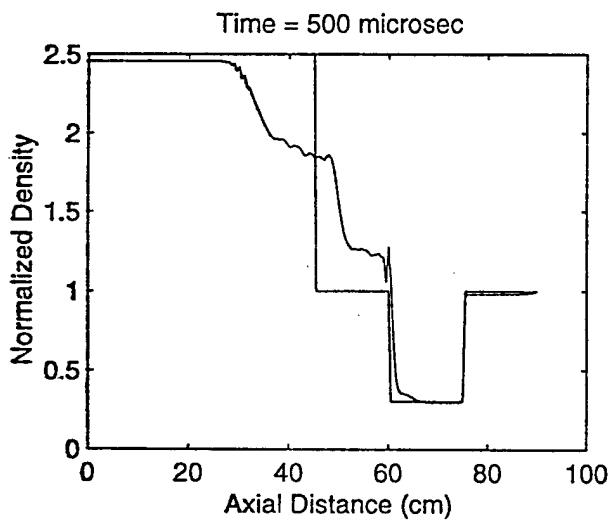
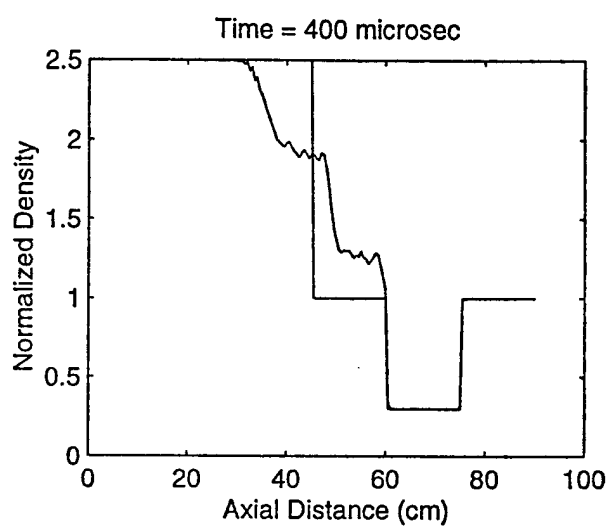
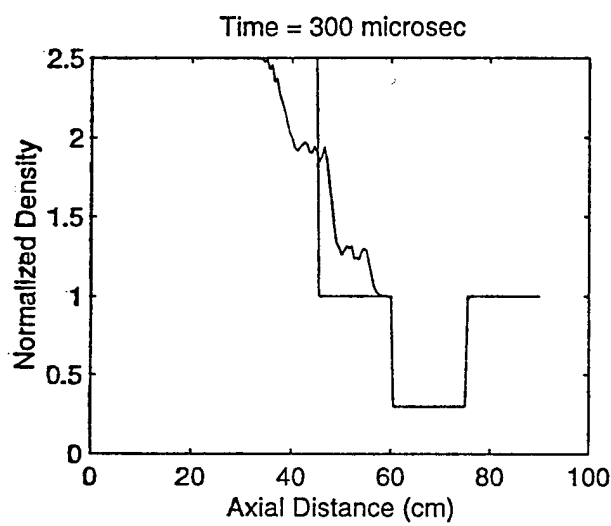
CASE III

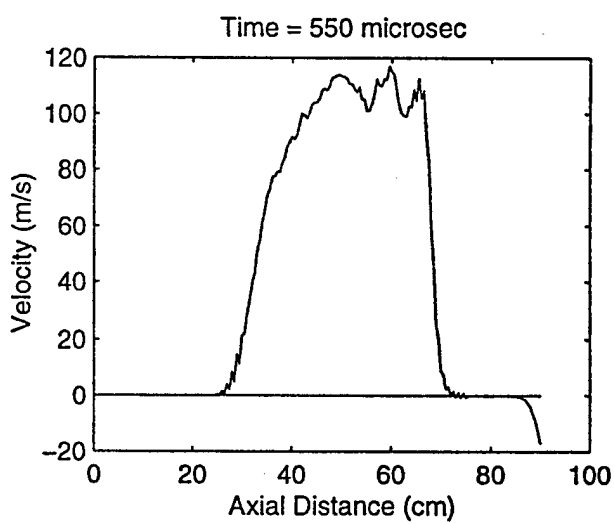
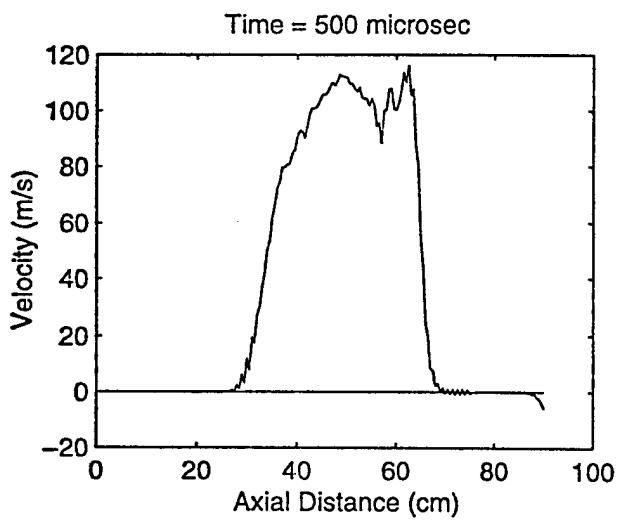
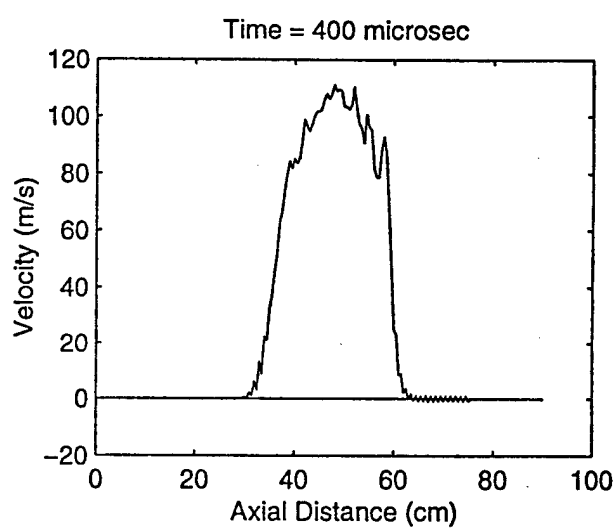
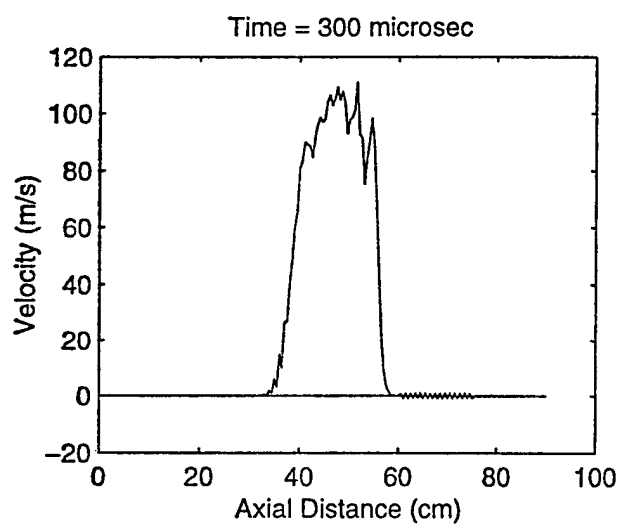
- 1) No radial temp gradient
- 2) Triangular axial temp grad
- 3) No plasma

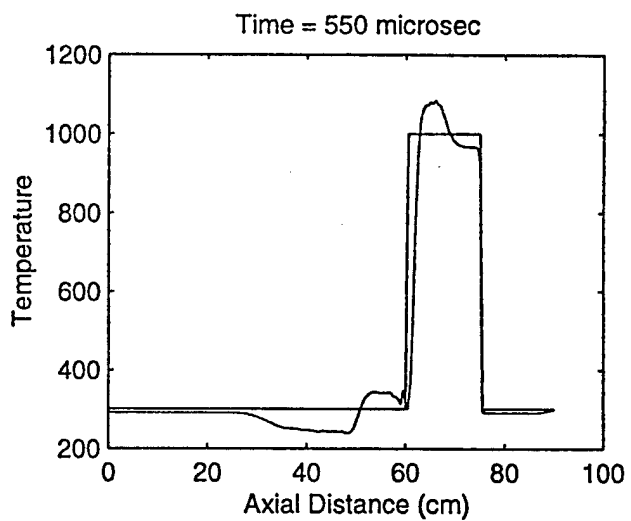
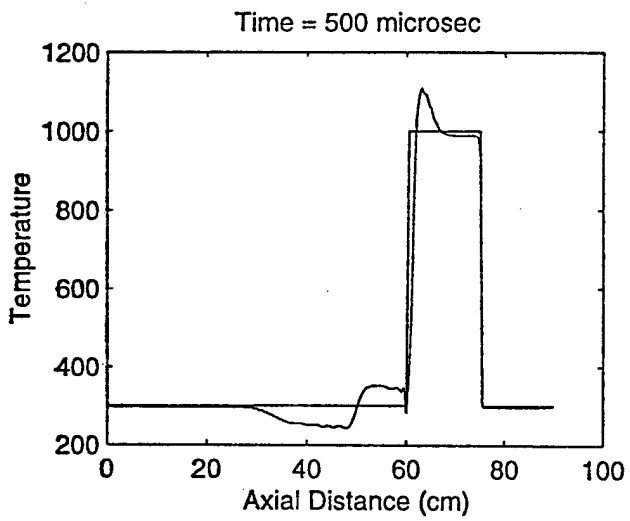
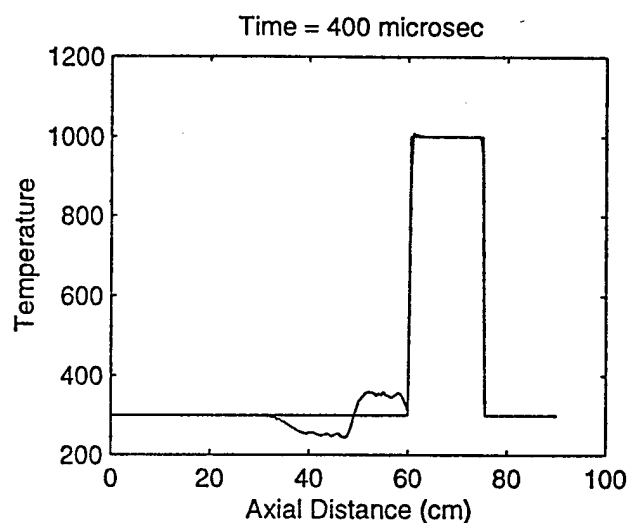
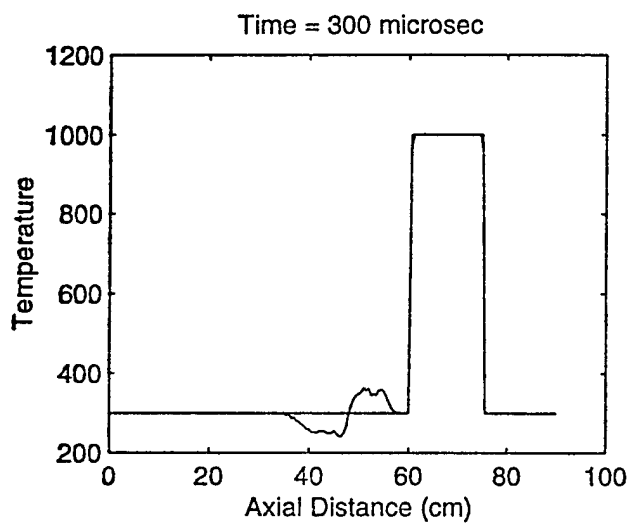


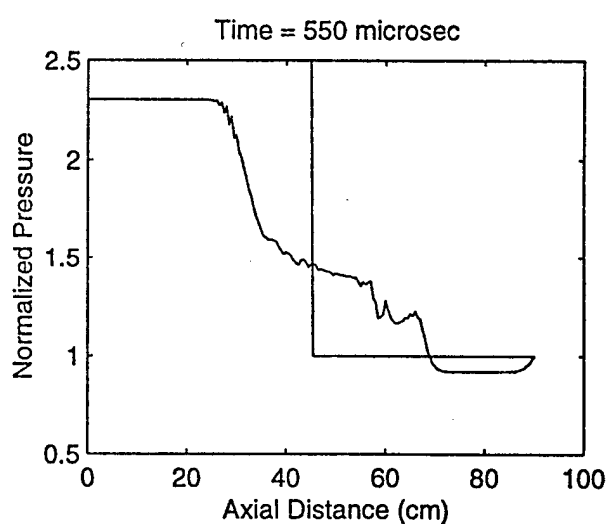
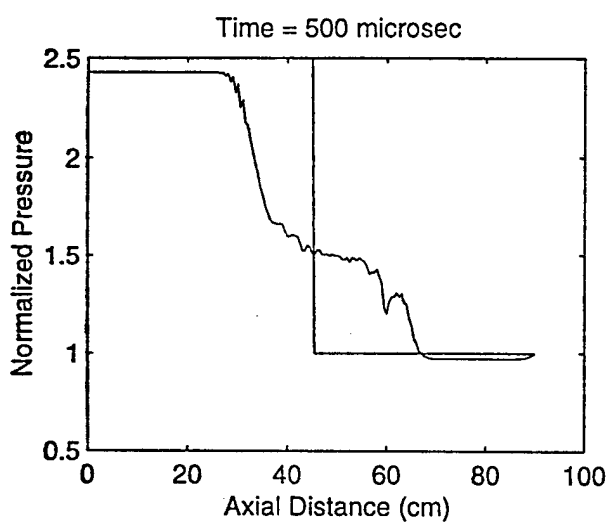
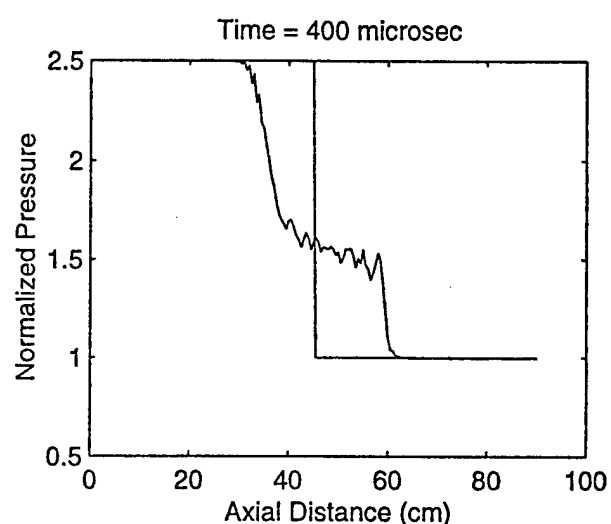
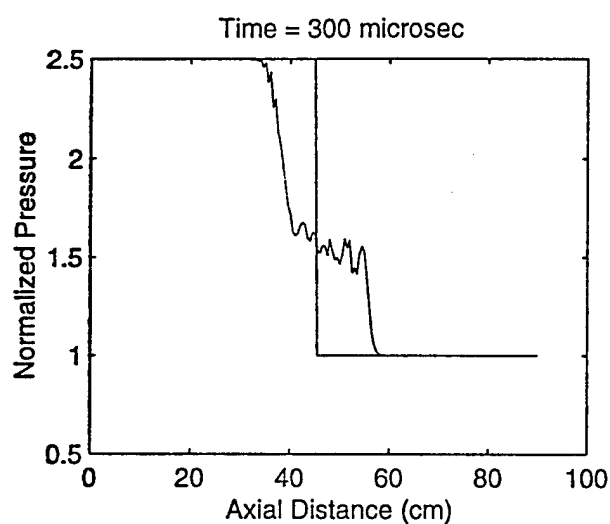


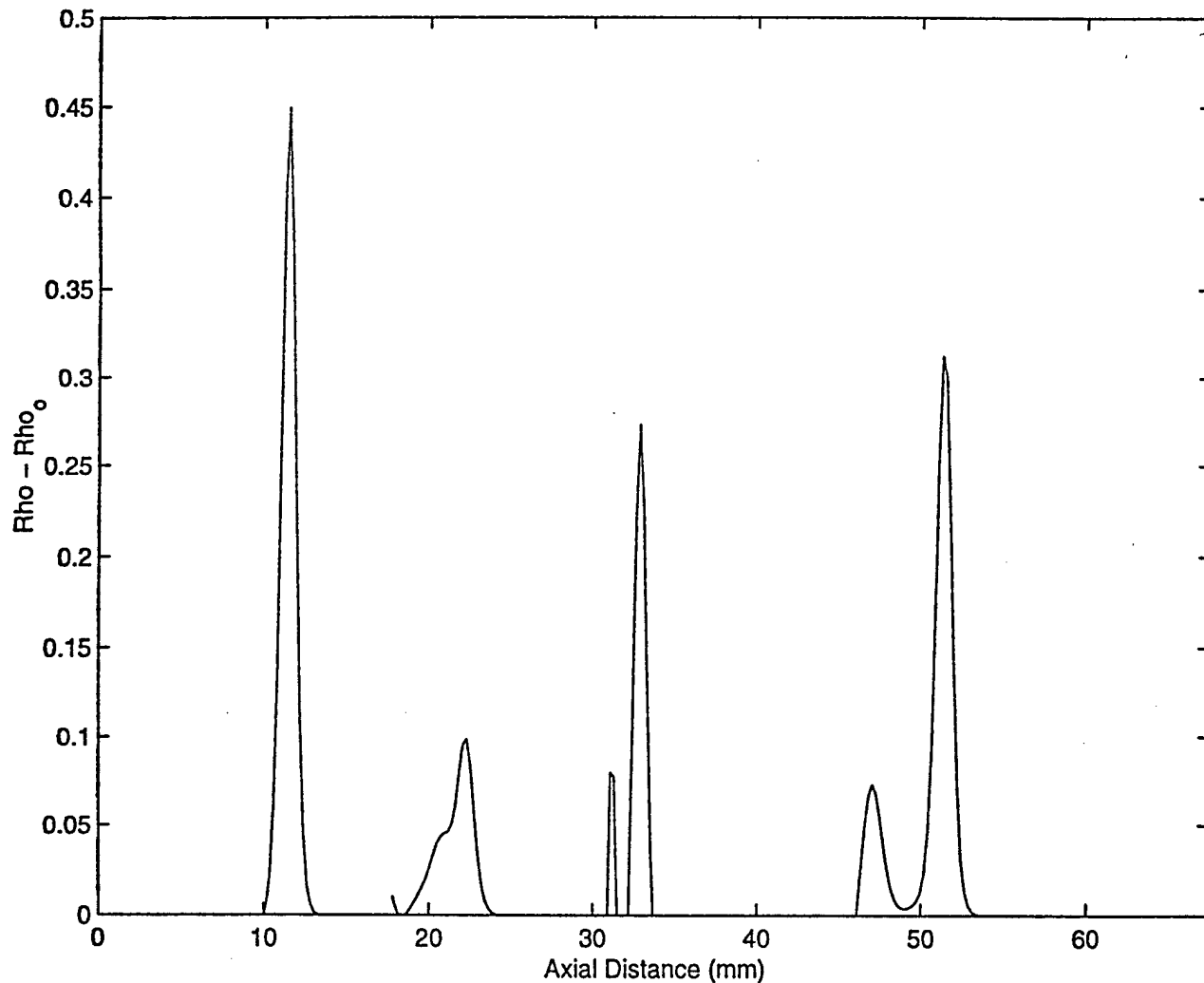
DIAPODUM/Piston - D2170N Shock

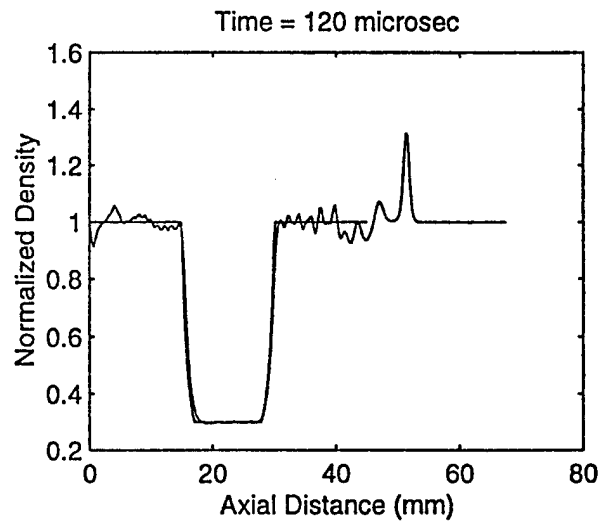
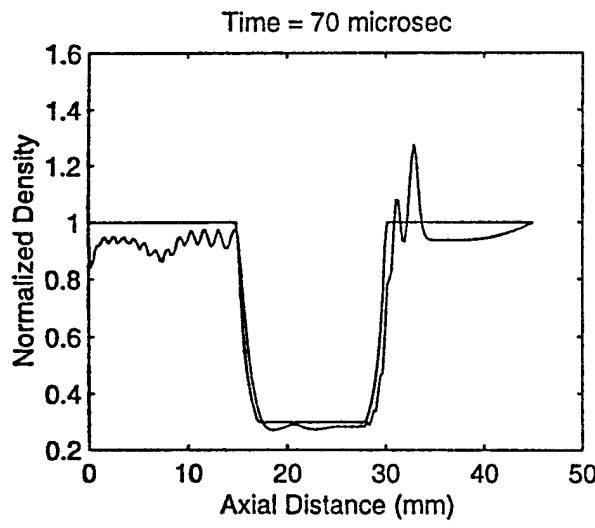
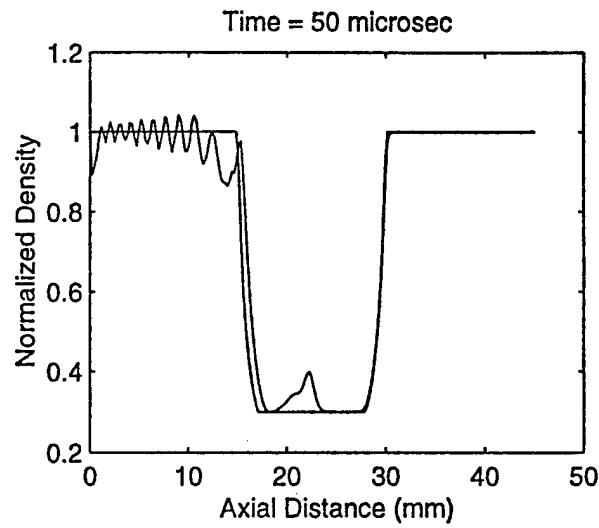
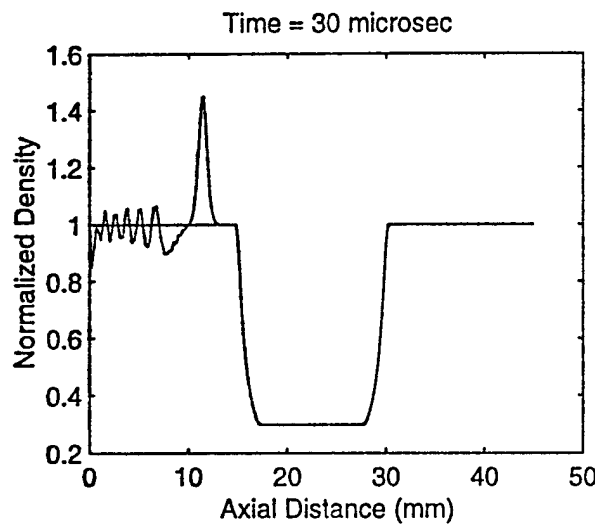


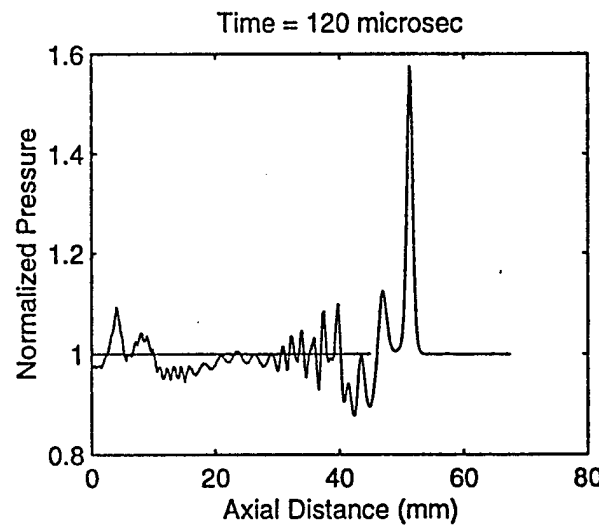
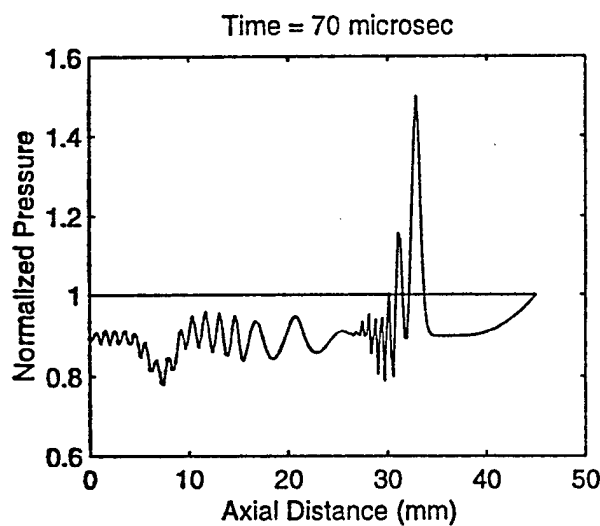
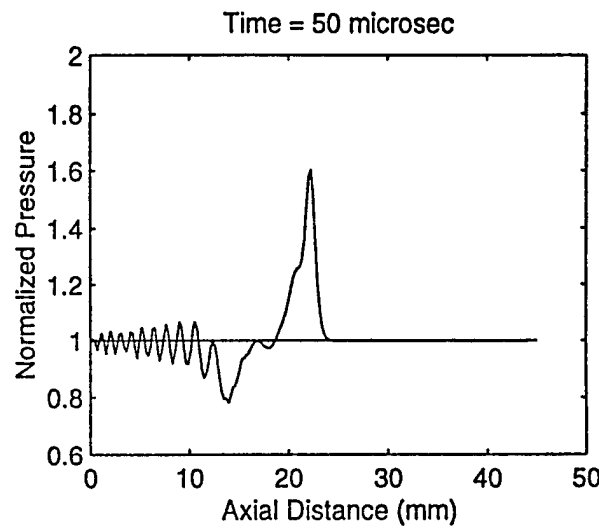
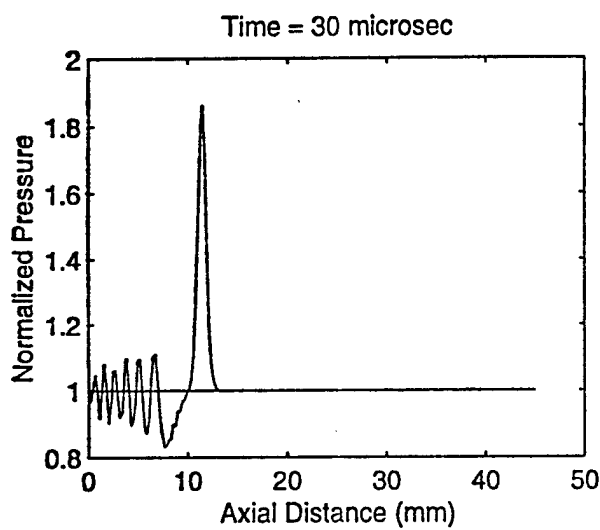


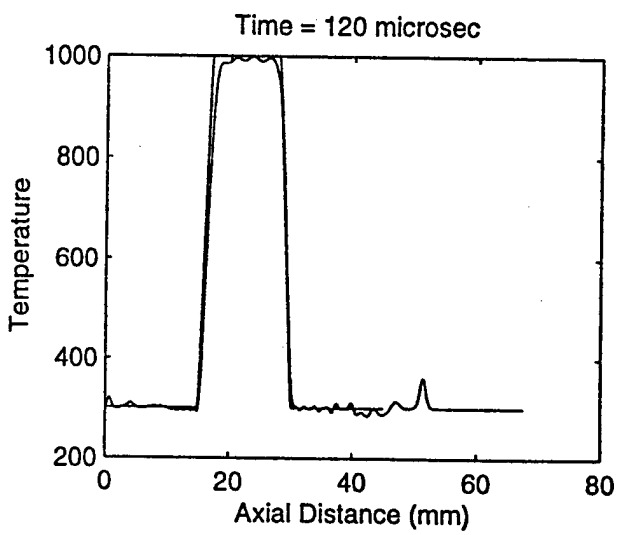
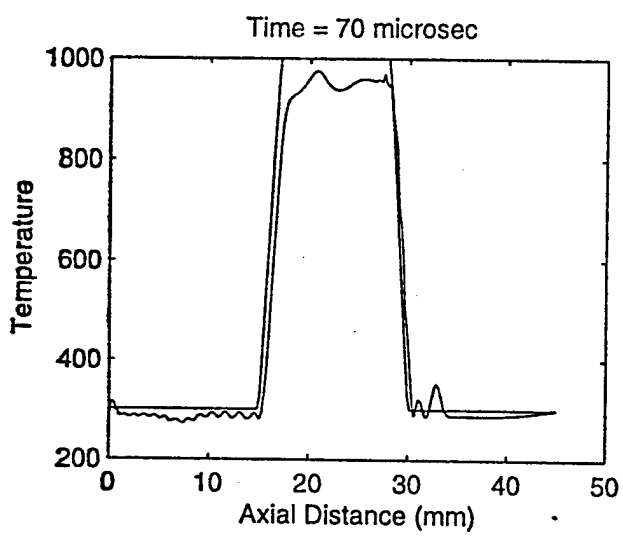
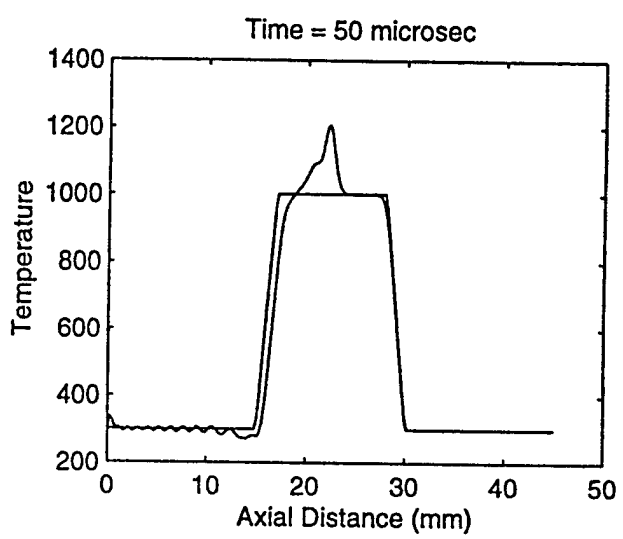
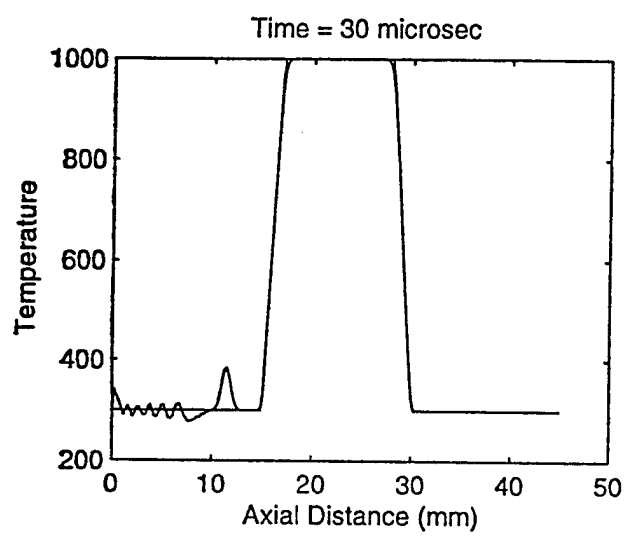


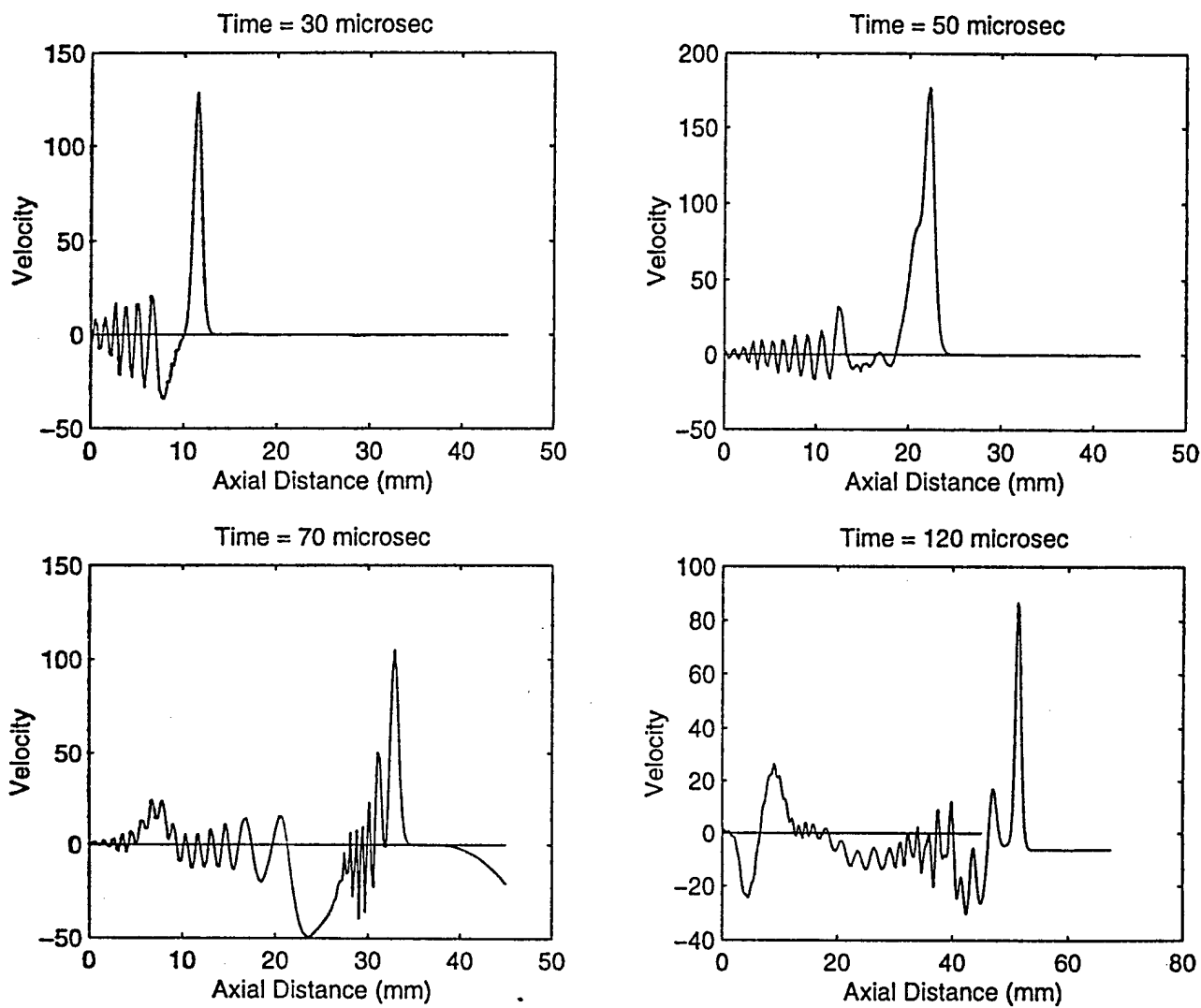


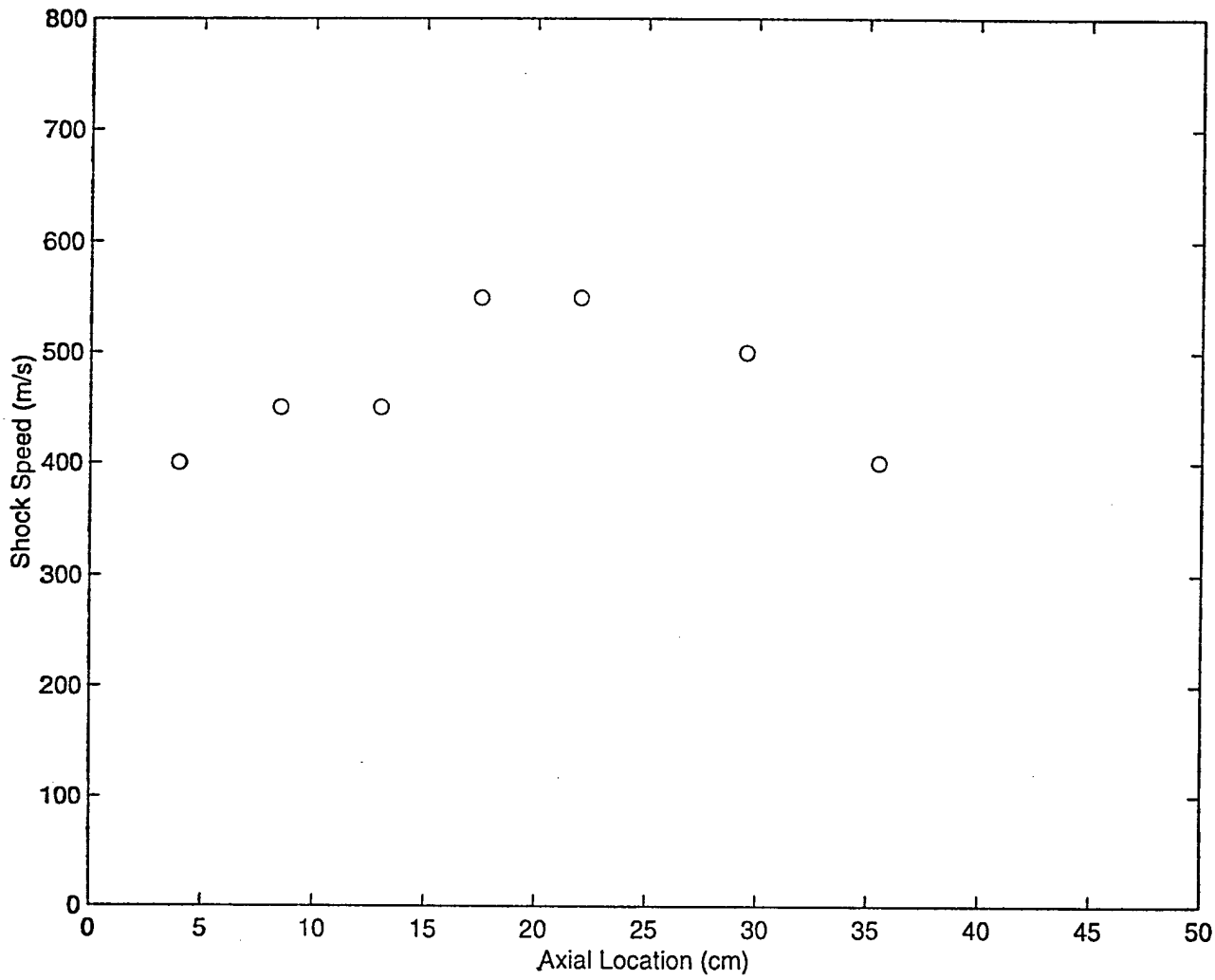


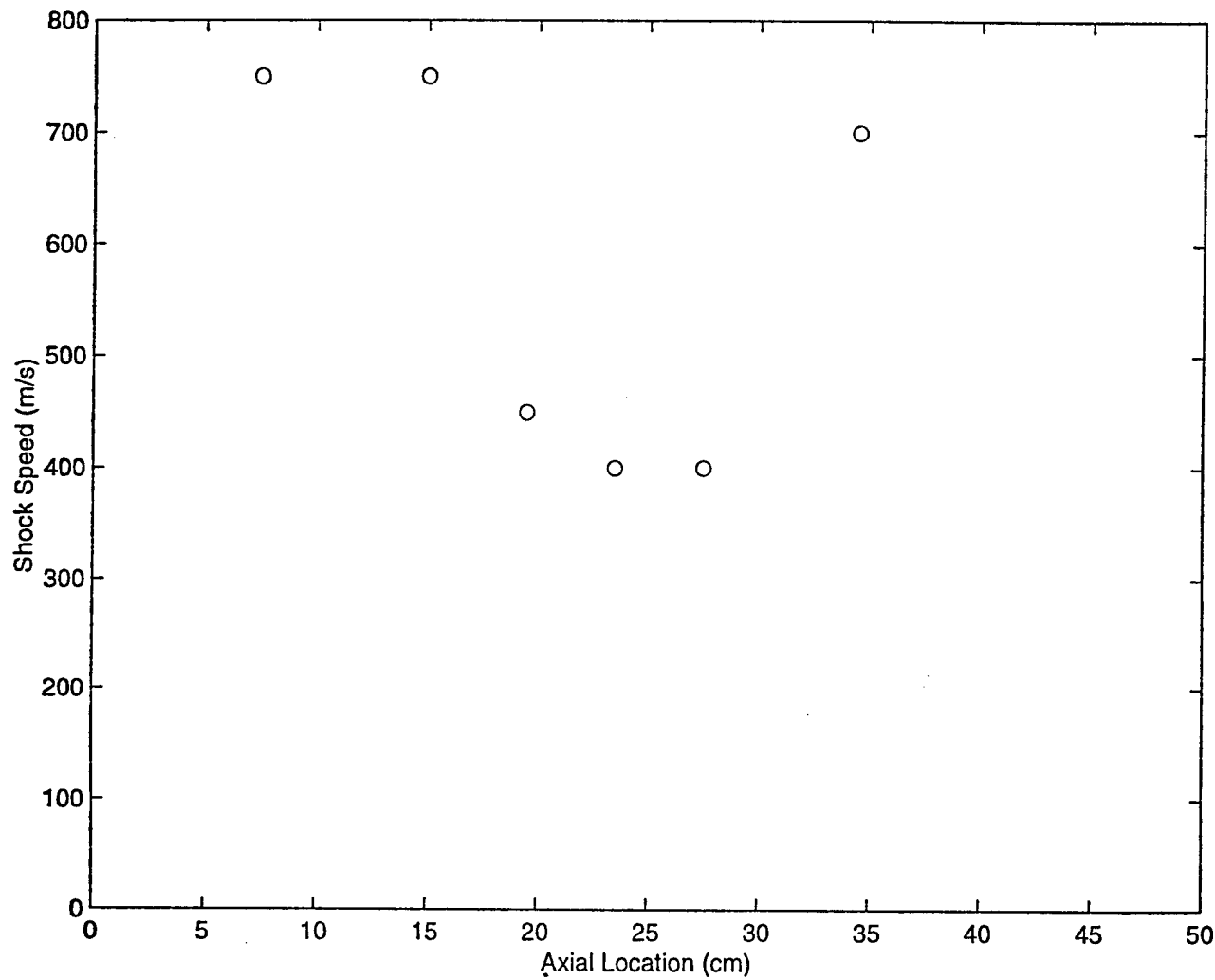








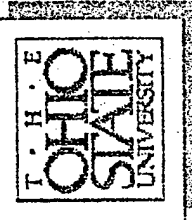




Summary of Thermal Effects

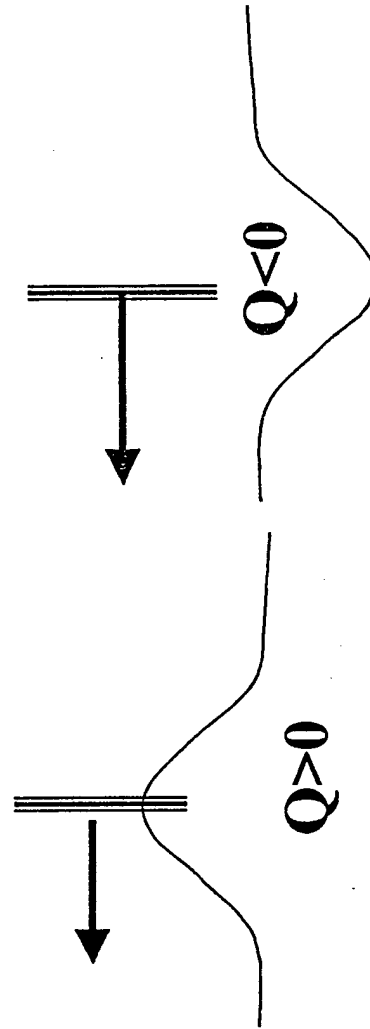
- Axial temperature gradients cause splitting of an impulsive load into two distinct waves, a strong leader, and a weak follower.
- Radial gradients affect results quantitatively, but are not the cause of this splitting.
- Shock recovery is almost immediate, whereas they vary from 10 cm to 20 cm in the Ganguly-Bletzinger experiments.

∴ THERMAL EFFECTS CANNOT SOLELY EXPLAIN OBSERVED EXPERIMENTAL RESULTS.

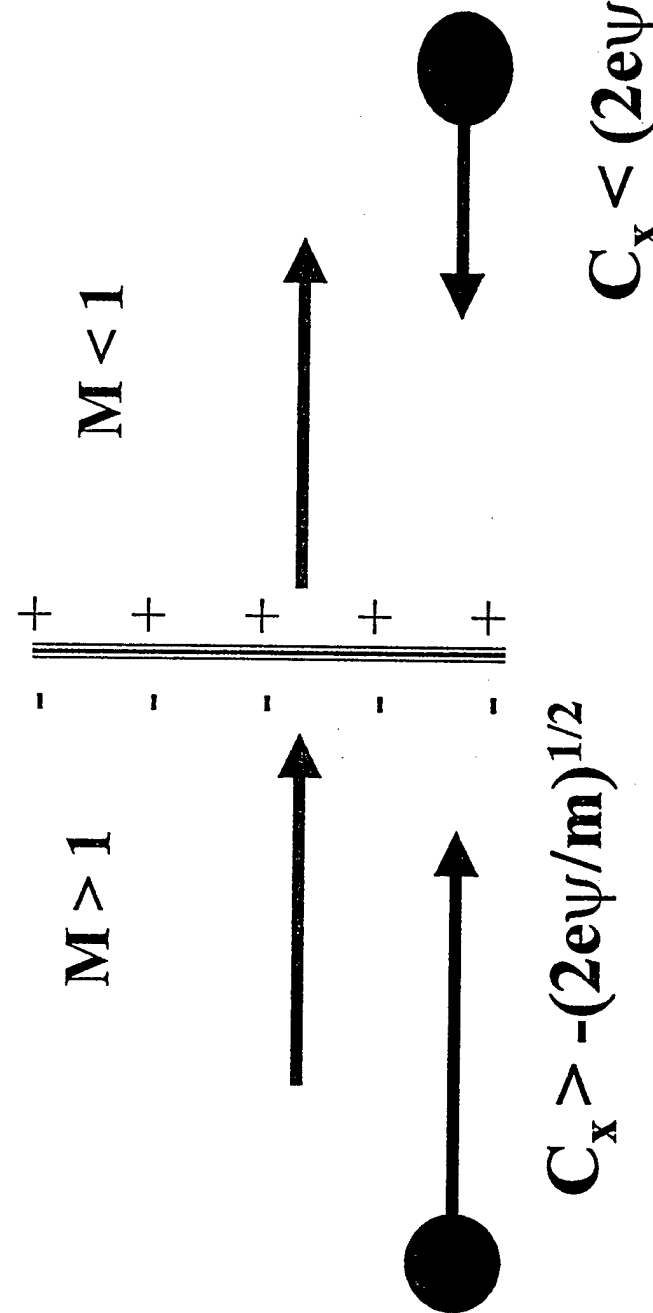


- Previous analysis (Adamovich et. al.) shows:

- (1) In order to change shock structure, an agent must have energy comparable to the incident kinetic energy density of the incident flow
- (2) Two globally adiabatic shocks, able to exchange energy among themselves reproduces experimental observations:

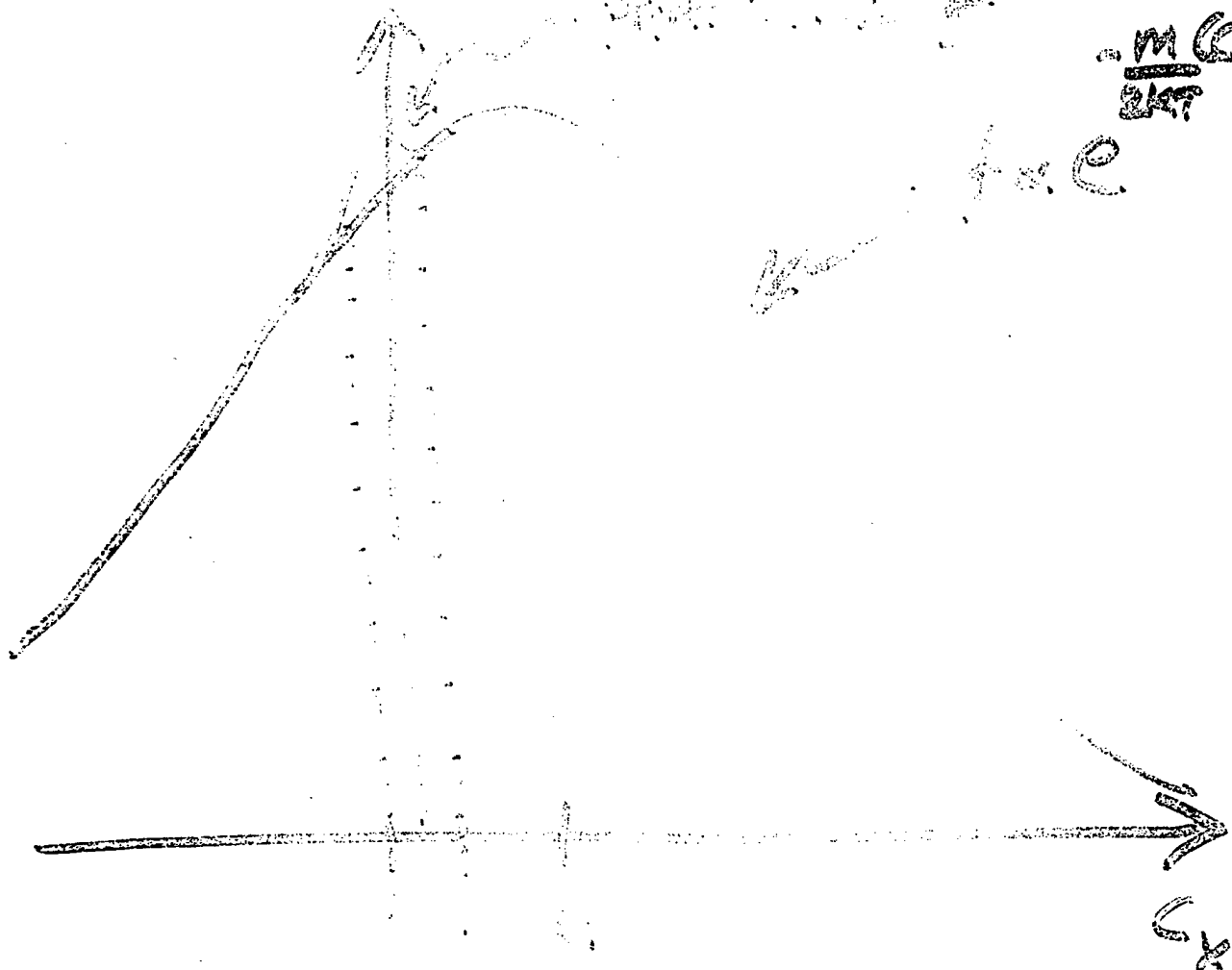


Suppose that space charge layer induces a potential in the neutral gas, because neutrals are polarizable:



M($C_x = 14$)
EKF

f.e.



CONTRIBUTION
TO
LEFTWARD FLUX

Consequences

- Let the force experienced by the neutral particles be:

$$F_x = -e \left[\frac{\partial \Psi}{\partial x} \right] \left[\sqrt{\frac{2e\Psi}{m}} - C_x \right] \bar{s}(x - x_0) + \bar{s} \left[\sqrt{\frac{2e\Psi}{m}} + C_x \right] \bar{s}(x_0 - x)$$

where

$\bar{s}(z) = \begin{cases} 0, & z < 0 \\ 1, & z > 0 \end{cases}$ is the Heaviside step function,
and C_x is the x -component of the absolute
particle velocity

What would be the corresponding macroscopic equations to lowest order?

- Continuity

$$\frac{\partial n}{\partial t} + \frac{\partial}{\partial x} (nu) = N = \begin{cases} \frac{ne}{m} \left(\frac{\partial \psi}{\partial x} \right) \sqrt{\frac{m}{2\pi kT}} e^{-\left(\sqrt{\frac{e\psi}{kT}} - u \sqrt{\frac{m}{2kT}} \right)^2} ; & x > x_0 \\ - \frac{ne}{m} \left(\frac{\partial \psi}{\partial x} \right) \sqrt{\frac{m}{2\pi kT}} e^{-\left(\sqrt{\frac{e\psi}{kT}} + u \sqrt{\frac{m}{2kT}} \right)^2} ; & x < x_0 \end{cases}$$

Source terms in continuity equation

$$\begin{aligned}
 N_1 &\approx \frac{en_1}{m} \left(\frac{\partial \psi}{\partial x} \right) \Big|_1 \sqrt{\frac{m}{2\pi kT_1}} e^{-\frac{\gamma}{2} M_1^2} \\
 N_2 &\approx -\frac{en_2}{m} \left(\frac{\partial \psi}{\partial x} \right) \Big|_2 \sqrt{\frac{m}{2\pi kT_2}} e^{-\frac{\gamma}{2} M_2^2} \\
 \frac{N_2}{N_1} &\approx -\frac{n_2}{n_1} \frac{(\partial \psi / \partial x)|_2}{(\partial \psi / \partial x)|_1} \sqrt{\frac{T_1}{T_2}} e^{\frac{\gamma}{2} (M_1^2 - M_2^2)} \\
 &\Rightarrow N_2 > N_1
 \end{aligned}$$

X-momentum

$$\frac{\partial(nu)}{\partial t} + \frac{\partial}{\partial x} \left(nu^2 + \frac{nkT}{m} \right) = M = \begin{cases} \frac{en}{m} \left(\frac{\partial \psi}{\partial x} \right) \sqrt{\frac{e\psi}{\pi kT}} e^{-\left(\sqrt{\frac{e\psi}{kT}} - u \sqrt{\frac{m}{2kT}} \right)^2} \\ \quad - \frac{1}{2} \left[1 - erf \left(u \sqrt{\frac{m}{2kT}} - \sqrt{\frac{e\psi}{kT}} \right) \right] & ; x > x_0 \\ \frac{en}{m} \left(\frac{\partial \psi}{\partial x} \right) \sqrt{\frac{e\psi}{\pi kT}} e^{-\left(\sqrt{\frac{e\psi}{kT}} + u \sqrt{\frac{m}{2kT}} \right)^2} \\ \quad - \frac{1}{2} \left[1 - erf \left(-u \sqrt{\frac{m}{2kT}} - \sqrt{\frac{e\psi}{kT}} \right) \right] & ; x < x_0 \end{cases}$$

Source term in momentum equation

$$\begin{aligned}
 M_1 &\approx -\frac{en_1}{m} \left(\frac{\partial \psi}{\partial x} \right) \Big|_1 e^{-\frac{\gamma}{2} M_1^2} \\
 M_2 &\approx -\frac{en_2}{m} \left(\frac{\partial \psi}{\partial x} \right) \Big|_2 e^{-\frac{\gamma}{2} M_2^2} \\
 \Rightarrow \frac{M_2}{M_1} &\approx \frac{n_2}{n_1} \frac{(\partial \psi / \partial x)|_2}{(\partial \psi / \partial x)|_1} e^{\frac{\gamma}{2} (M_1^2 - M_2^2)}
 \end{aligned}$$

⇒ Net Force is upstream

• Energy

$$\frac{\partial}{\partial t} \left(\frac{3}{2} nkT + \frac{1}{2} mn u^2 \right) + \frac{\partial}{\partial x} \left(\frac{5}{2} n k T + \frac{1}{2} m n u^3 \right) = S$$

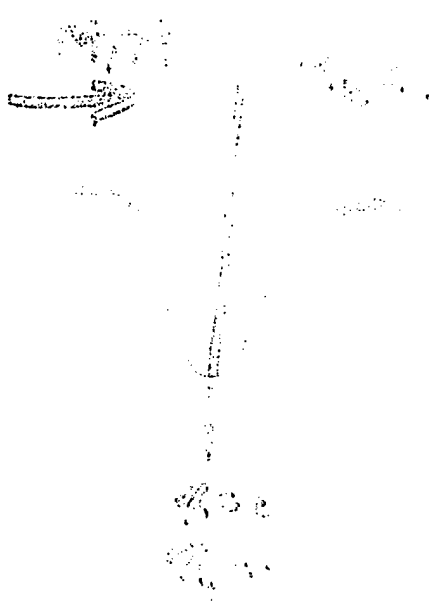
$$where \quad S = \begin{cases} ne \left(\frac{\partial \psi}{\partial x} \right) \left[\left(\frac{2kT}{m\pi} \right)^{1/2} + \left(\frac{e\psi}{kT} \right) \left(\frac{kT}{2\pi m} \right)^{1/2} \right] e^{-\left(\sqrt{\frac{e\psi}{kT}} - u \sqrt{\frac{m}{2kT}} \right)^2} \\ - \frac{n e u}{2} \left(\frac{\partial \psi}{\partial x} \right) \left[1 - \operatorname{erf} \left(u \sqrt{\frac{m}{2kT}} - \sqrt{\frac{e\psi}{kT}} \right) \right] ; \quad x > x_0 \\ - ne \left(\frac{\partial \psi}{\partial x} \right) \left[\left(\frac{2kT}{m\pi} \right)^{1/2} + \left(\frac{e\psi}{kT} \right) \left(\frac{kT}{2\pi m} \right)^{1/2} \right] e^{-\left(\sqrt{\frac{e\psi}{kT}} + u \sqrt{\frac{m}{2kT}} \right)^2} \\ - \frac{n e u}{2} \left(\frac{\partial \psi}{\partial x} \right) \left[1 - \operatorname{erf} \left(-u \sqrt{\frac{m}{2kT}} - \sqrt{\frac{e\psi}{kT}} \right) \right] ; \quad x < x_0 \end{cases}$$

Source term in energy equation

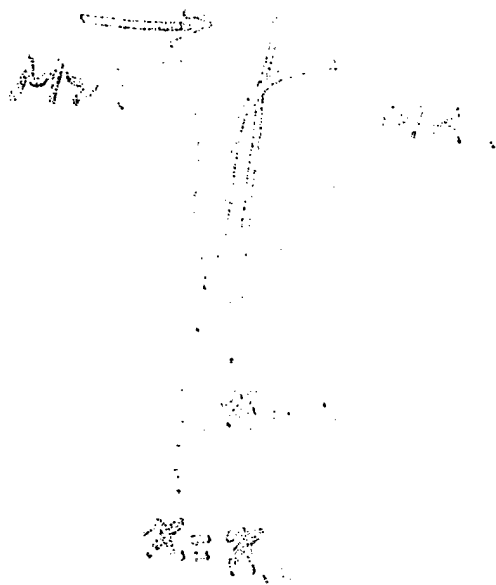
$$\begin{aligned}
 S_1 &\approx en_1 \left(\frac{\partial \psi}{\partial x} \right) \left|_1 \right. \left(\frac{\gamma k T_1}{m \pi} \right)^{1/2} \left[\sqrt{\frac{2}{\gamma}} - M_1 \right] e^{-\frac{\gamma}{2} M_1^2} \\
 S_2 &\approx -en_2 \left(\frac{\partial \psi}{\partial x} \right) \left|_2 \right. \left(\frac{\gamma k T_2}{m \pi} \right)^{1/2} \left[\sqrt{\frac{2}{\gamma}} + M_2 \right] e^{-\frac{\gamma}{2} M_2^2} \\
 \Rightarrow \frac{S_2}{S_1} &\approx \frac{n_2}{n_1} \frac{(\partial \psi / \partial x)|_2}{(\partial \psi / \partial x)|_1} \sqrt{\frac{T_2}{T_1} \left[\sqrt{\frac{2}{\gamma}} + M_2 \right]} e^{\frac{\gamma}{2} (M_1^2 - M_2^2)} \\
 \Rightarrow &\text{Note change in sign when } M_1 = \sqrt{\frac{2}{\gamma}}
 \end{aligned}$$

THREE CASES

(A)



(B)



(C)



Case(B): Potential well ahead of shock

- Just upstream of the shock, for $x_0 < x < 0$, $S > 0$, provided M_1 in the region is less than $(2/\gamma)^{1/2}$ while $S \rightarrow 0$ for $x > 0$ (downstream of the shock) since $\partial \psi / \partial x \rightarrow 0$ there
 \Rightarrow SPLITTING ?
- For $M_1 > (2/\gamma)^{1/2}$, $S < 0$ in the same region
 \Rightarrow STABLE
- Further, $\tilde{M} < 0$ for $x > x_0 \Rightarrow$ a body force driving shock upstream is present
 \Rightarrow LARGER STAND-OFF DISTANCE

- Distribution function will be non-M-B in the neighborhood of the shock
 - steep thermal, and density gradients will induce additional mass, momentum, and energy transfer from downstream region to upstream region.
- Questionable as to whether a steady state can exist when sources are present in continuity, momentum, and energy equations.

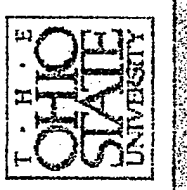
Summary

- Classical gas dynamics predicts splitting of a pulse in the presence of a streamwise temperature gradient - But, split structure appears different from that observed in experiments.
- There may be special circumstances under which induced dipole effects cause the presence of local adverse thermal gradients at the shock front, by affecting the distribution function.



Introduction

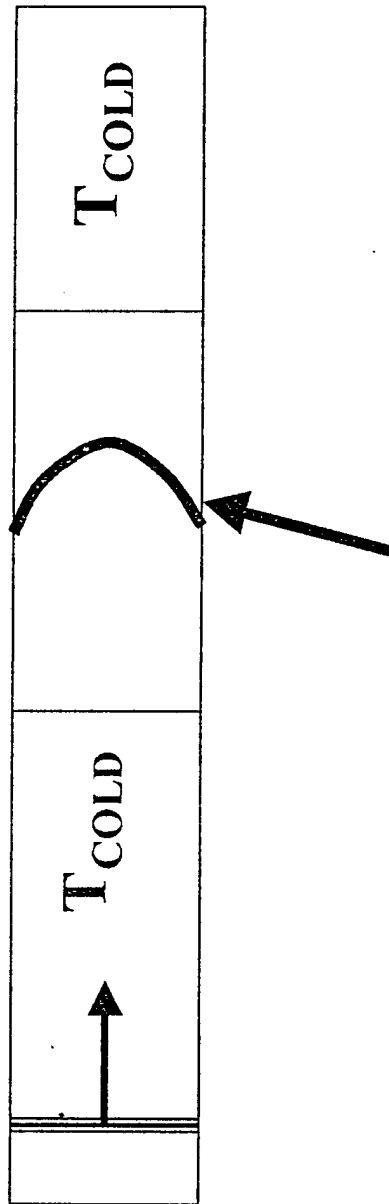
- Anomalous behavior of shock waves in weakly ionized plasmas:
 - shock wave accelerates
 - stand-off distance increases
 - shock splits into two or more structures
 - shock strength (as measured by density differences) diminishes
 - results occur in atomic and molecular gases
 - shock nearly recovers its original strength well downstream of the discharge.



- Previous simulations (Bailey & Hillbun, Macheret & Martinelli) show radial thermal gradients can alter density profiles:
 - in piston-driven shock tubes
 - and when there is a curved boundary initially separating the hot and cold regions of a gas
- Thermal effects have been invoked to explain some experimental observations, but cannot explain others (such as shock recovery distance).



Effects of Radial Thermal Gradients (2-D axi-symmetric Navier-Stokes solution for Argon)



Initial parabolic temperature profile
varying from T_{HOT} at the centerline to
 T_{COLD} at the wall.

Flow Control via MHD and EMHD

George Em Karniadakis

Division of Applied Mathematics

Center for Fluid Mechanics, Turbulence and Computation

Brown University

Providence, RI 02912

<http://www.cfm.brown.edu/CRUNCH>

AFOSR Workshop on

Understanding and Control of Ionized High-Speed Flows

February 26–27, 1998

Princeton, NJ

High-Speed Flow Features

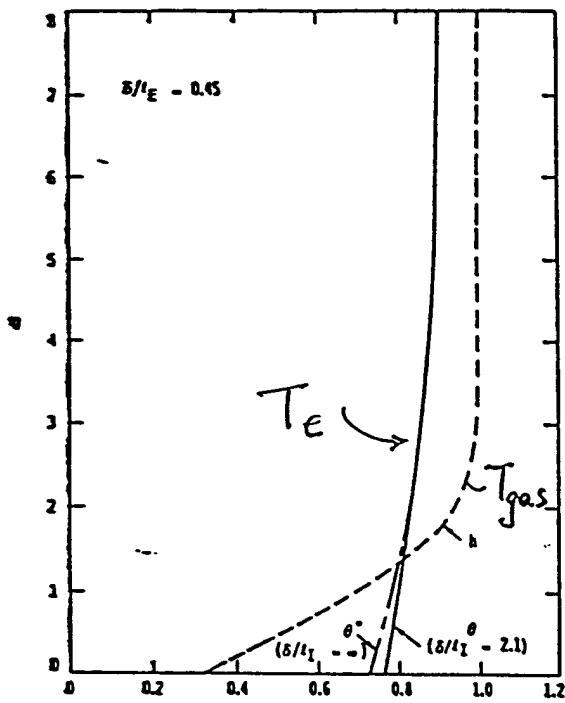
- Strong shock wave effects/interactions
 - thin layers, small detachment distance, entropy layer
- Strong viscous effects/interactions
 - $\delta \sim \frac{M^2}{\sqrt{Re}}$
 - increased drag, heating at leading edge
- Transitional flow
 - $Re_c \sim 10^8$ vs. 10^5 (subsonic)
 - C_f and C_H are $3\times$ laminar
 - $Re_c^\theta \sim 100M_e$
- Nonequilibrium
 - thermal, chemical
 - introduction of length scale
 - multi-rate physics
- Ionization
 - 4000 K to 6000 K: $NO \rightarrow NO^+ + e^-$ (mild)
 - > 9000 K: $N \rightarrow N^+ + e^-$
 $O \rightarrow O^+ + e^-$
 - Above 20kM + 10 km/s
 - External B, E , frequencies
- Multiple boundary layers
 - hydrodynamics, thermal, species
 - electric conductivity, entropy layers

∴ - Multi-Rate Physics

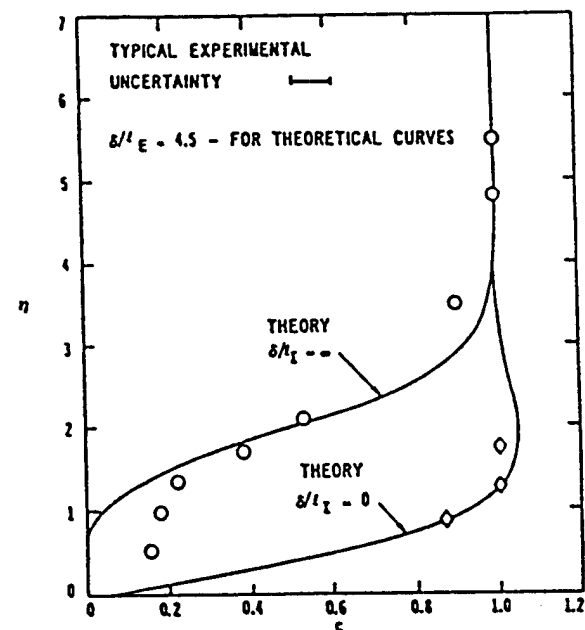
- Multiple BLs

Non-Equilibrium Plasma Boundary Layer

- Effects on T_e, σ
- atmospheric-pressure potassium-seeded argon plasma



Normalized Temperature



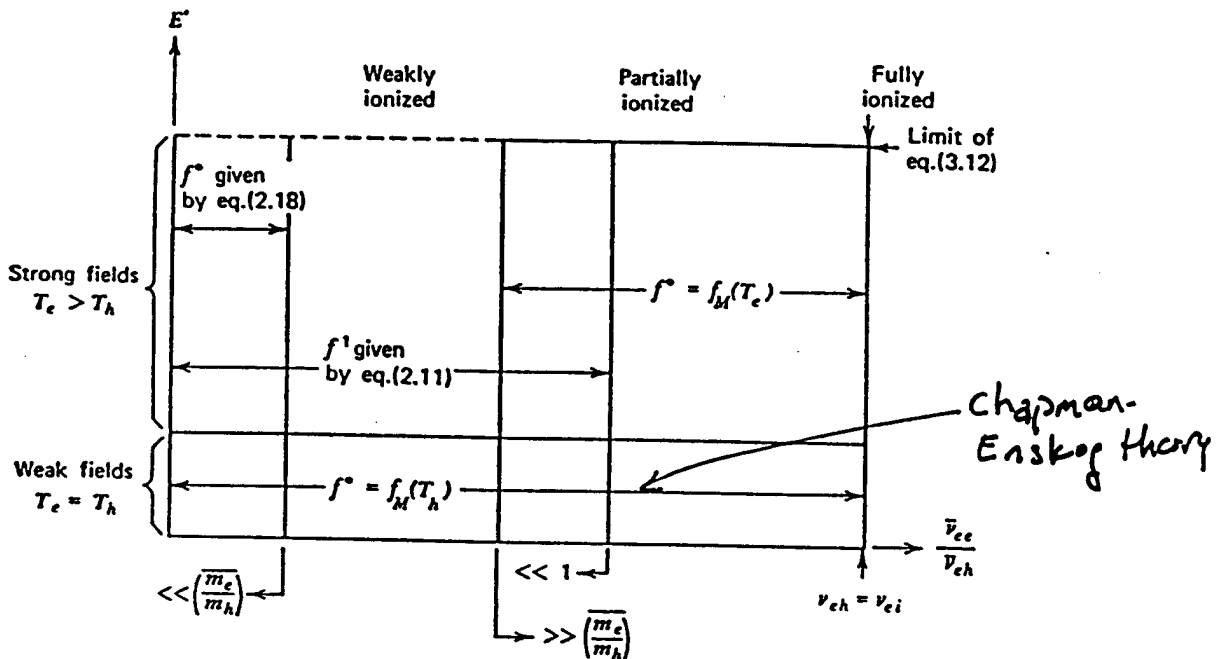
Normalized Conductivity

Ref: Brown & Mitchner (1971)

“... Even in plasma which is strongly collision dominated, significant nonequilibrium may be present in the boundary layer adjacent to a cooled solid surface...”

Note: Joule heating due to E could further increase conductivity.

Electrical Conductivity



Electric Field vs. Ionization

- In constant E, B fields tensor conductivity

$$\text{Weakly-ionized} \left\{ \begin{array}{l} \sigma_{||} = \mathcal{F}(n_e, m_e, \nu_{eH}, f^0) \\ \sigma_{\perp} = \mathcal{F}(n_e, m_e, \nu_{eH}, f^0, \omega_e) \\ \sigma_H = \mathcal{F}(n_e, m_e, \nu_{eH}, f^0, \omega_e) \end{array} \right.$$

- If $B = 0 \Rightarrow \sigma_{\perp} = \sigma_{||} = \sigma$

- If $E \sim e^{-i\omega t} \Rightarrow$ dependence of σ on ω , i.e. pulsing via tiles!

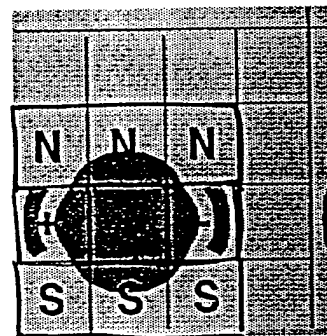
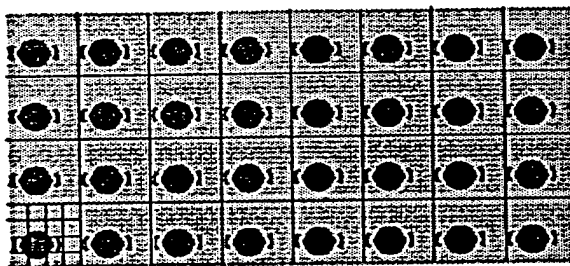
Note: $f^0 = \mathcal{F}(E_{||}^0, E_{\perp}^0, \nu_{eH}, T_H, m_e, m_H)$

Lorentz Force: Numerical Modeling

- Governing Equations for \vec{B} and \vec{E}
- Boundary Conditions - The Motz problem

Example 1: Electromagnetic Tiles

$$\text{Dirichlet: } \vec{F}_\perp \sim \frac{1}{3} \vec{F}_\parallel; \text{ Neumann: } \vec{F}_\perp \sim \vec{F}_\parallel$$



Example 2: Alternate stripes of electrodes/magnets $F_\mu \sim e^{-\frac{\pi}{\alpha} \lambda y}$? penetration

Dirichlet	Neumann	D-N	Mixed
$\lambda = 4$	$2 \neq$	8	8

Lorentz Force

- MHD Assumptions ($t_c > \omega_p^{-1}$)

- Convection current neglected: $\frac{\rho_c U}{J} \ll 1$

- Force due to net charge neglected: $\frac{\rho_c E}{|J \times B|} \ll 1$

Then:

$$\left. \begin{array}{l} \vec{F}_L = \vec{J} \times \vec{B}; \quad E_0 = \text{external} \\ \vec{J} = \sigma(\vec{E} + \vec{u} \times \vec{B}) + \sigma \vec{E}_0 \end{array} \right\} \text{simple Ohm's law}$$

MHD-Control

- Apply \vec{B}
- $E = -\nabla \Phi$
- $\nabla^2 \Phi = \nabla \cdot (\vec{u} \times \vec{B})$
- $I_{\text{induced}} = \frac{\sigma B^2 L}{\rho U}$

EMHD-Control

- Apply \vec{B} and \vec{E}
- $J \sim \sigma E_0$
- $I_{\text{applied}} = \frac{\sigma E_0 B L}{\rho U^2}$

where $R_{em} = \mu \sigma U L \ll 1$ in lab scale

(neglect induced fields)

- But Ohm's law for partially ionized gas:

$$\underline{\vec{J}} + \beta_e \vec{J} \times \vec{b} + s \vec{b} \times (\vec{J} \times \vec{b}) = \underline{\sigma(\vec{E} + \vec{u} \times \vec{B})} + \frac{\sigma}{en_e} \nabla p_e$$

↑ "Generalized Ohm's Law"
ion-slip

Discontinuous Galerkin Method - NekTar

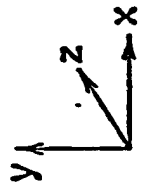
- dynamical Direct Numerical Simulation (dDNS)
- • MHD, Compressible & Incompressible flows
- Full 3D Configurations - Arbitrary Geometric Complexity
- • Unstructured/Hybrids Grids

→ • High-Order/Spectral Accuracy

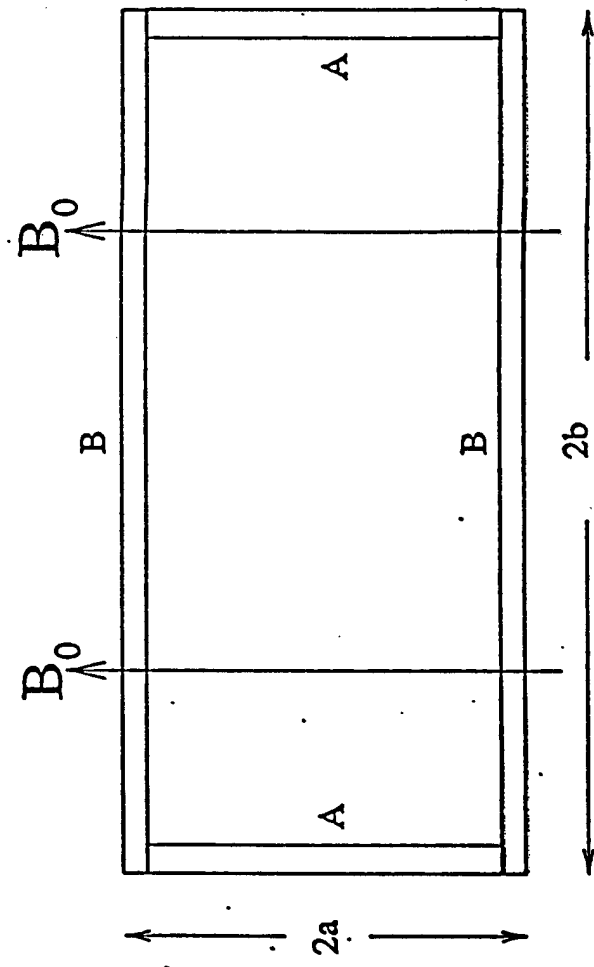
- Conservative Formulation
- h-refinement for shocks/discontinuities
- ALE Algorithm for Moving Rotating Subdomains
- METIS/MPI-based Parallelization

∴ Convergence of $(FV + FE + \text{Spectral}) \rightarrow \underset{\approx}{DG}$

- MACH 2/3 prototype - but high-order...



Hartmann-Hunt Flow : 3D



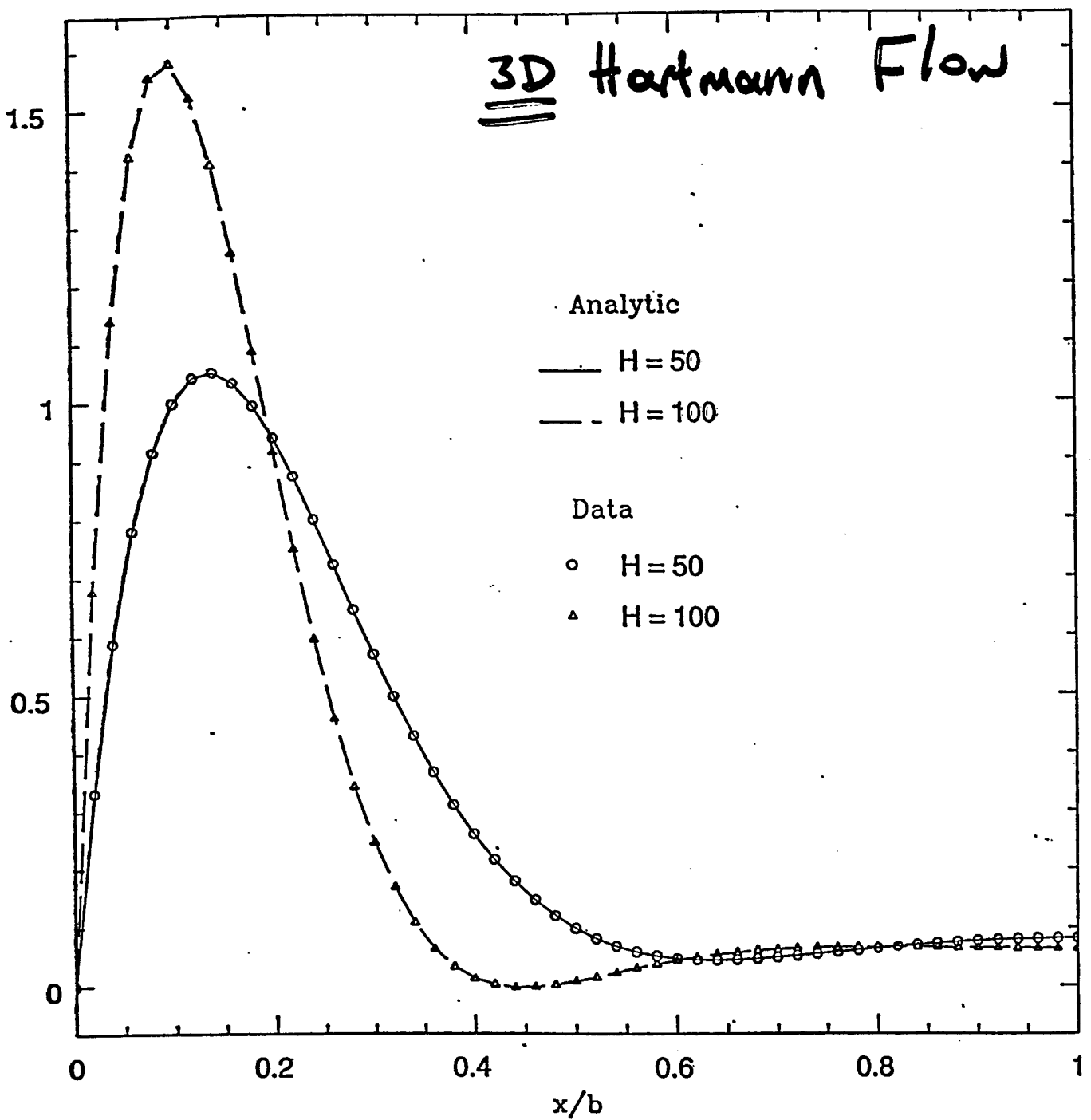
AA: Perfect Insulators

BB: Perfect Conductors

Flow is into the page

$Re = 100$, $Re_{mag} = 1$, $N = 9$

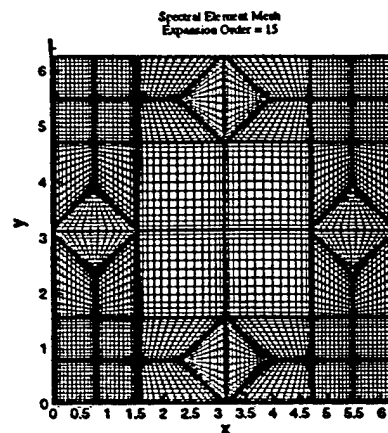
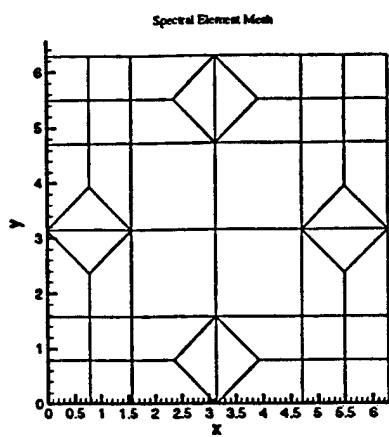
3D Hartmann Flow



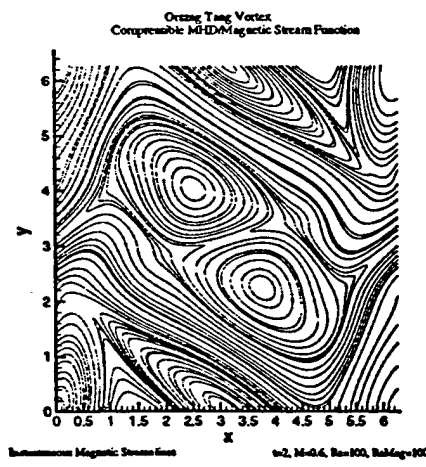
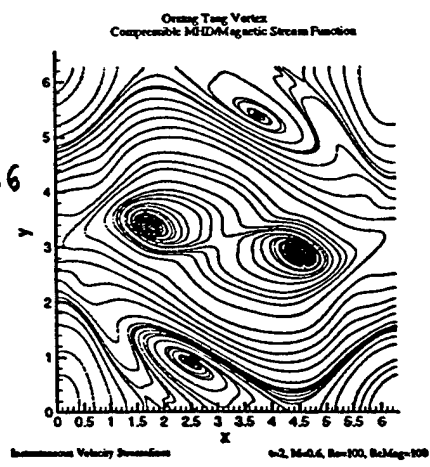
* Spectral/hp on Unstructured Grids.
(AFOSR)

Orszag-Tang MHD-Vortex

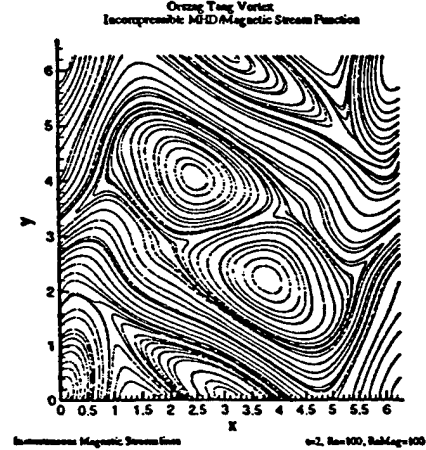
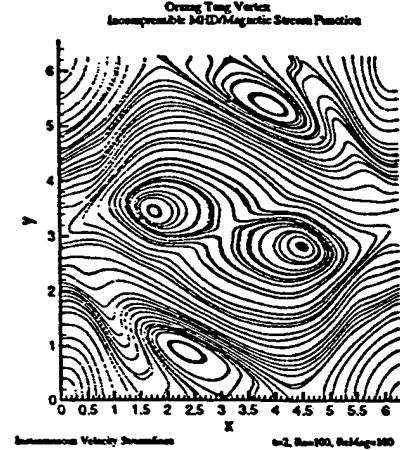
• Hybrid Grid



$M_1 = 0.6$



$M_1 = 0$



H-P Adaptive Refinement: Viscous Supersonic Flows

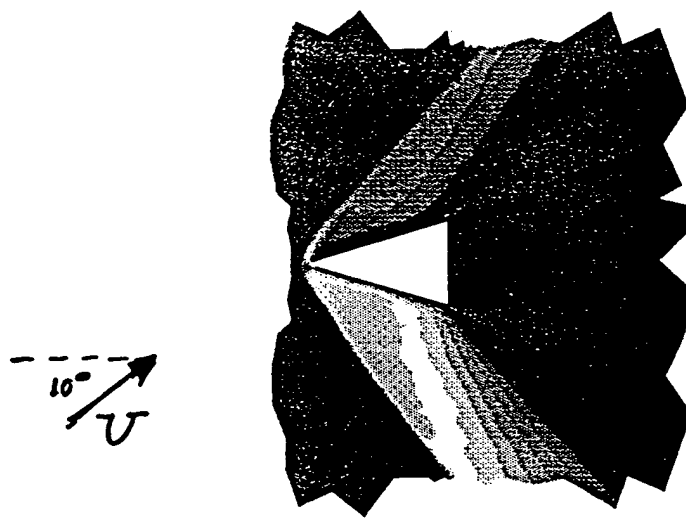


Figure 1: Discontinuous Galerkin Simulation: Density contours

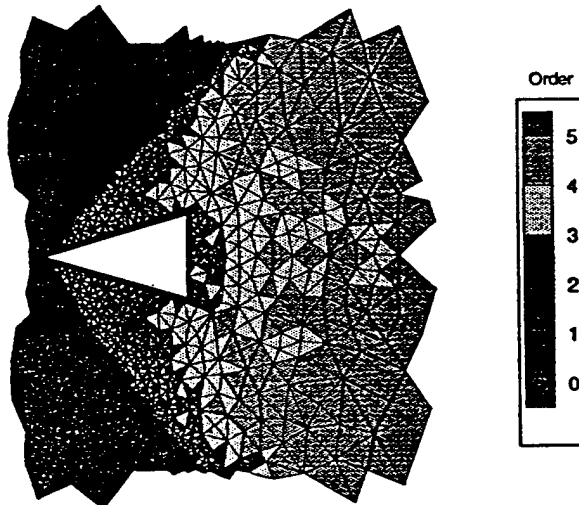
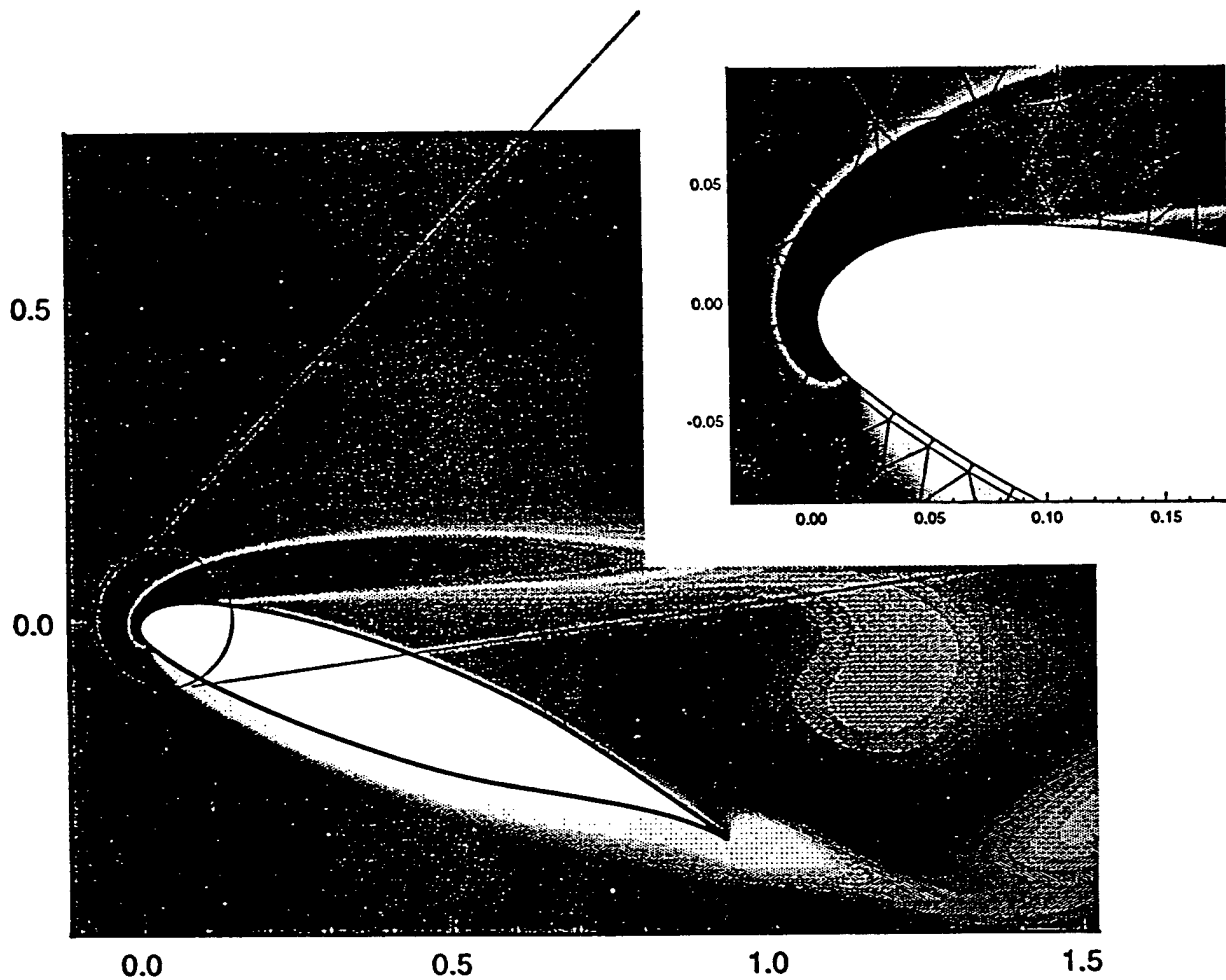


Figure 2: Unstructured grid and variable-order per element

* HYBRID APPROACH:

- DNS - near wall / structured
- LES in equilibrium regions

Hybrid-Element Boundary Layer Resolution



PhD Thesis: T.Warburton

Plan: $\left\{ \begin{array}{l} \text{• DNS with } h-p \text{ refinement.} \\ \text{• LES in equilibrium with } h-p \text{ refinement} \end{array} \right.$

\rightarrow high Re #, Complex Geometries

MHD/EMHD-Simulations

I. Laminar & Turbulent Wakes

- - vortex street suppression
- phase/frequency control

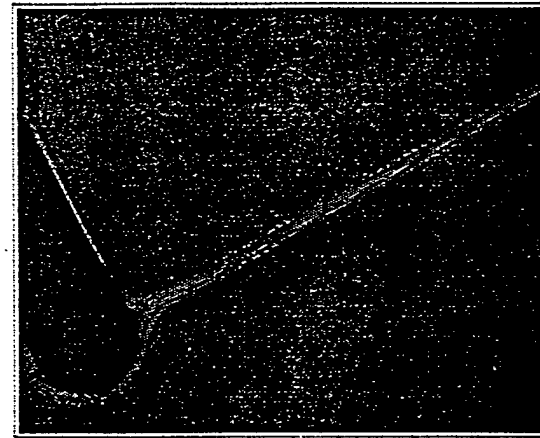
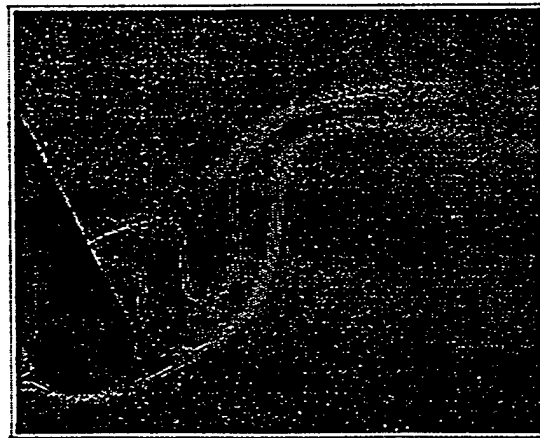
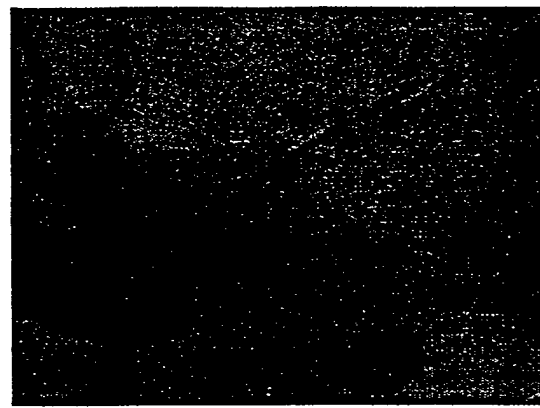
II. Wall Turbulence

- High σ , spanwise forcing/MHD
- Low σ , streamwise forcing
- - Low σ , "normal" forcing

Method: Parallel DNS - The *NekTar* Code

Experiments: Conflicting results

EMHD control of the flow around a circular cylinder

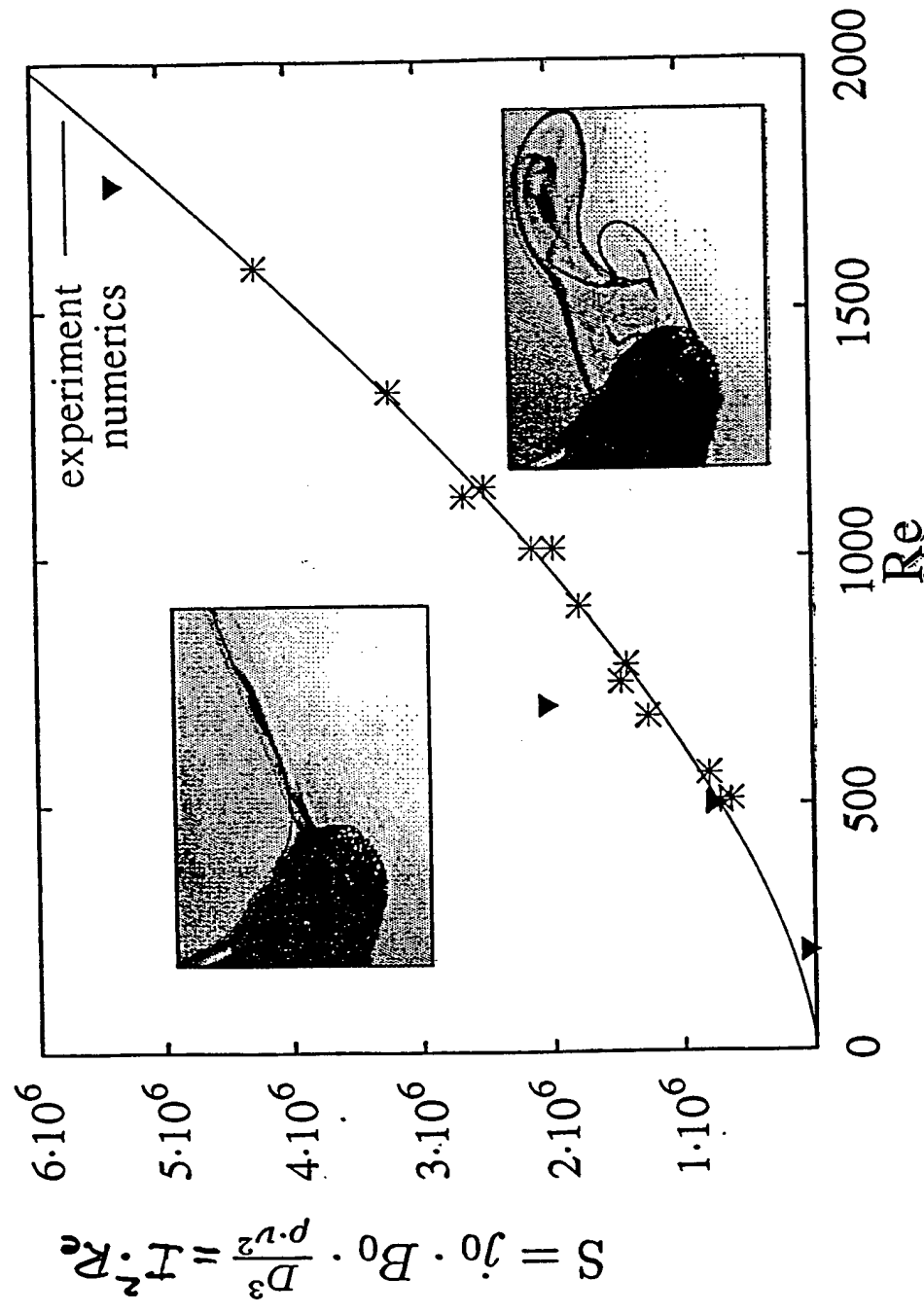


Dimensionless numbers:

$$Re = \frac{v_\infty d}{\nu} \quad - \text{Reynolds number}$$

$$N = \frac{j_0 B_0 d}{\rho v_\infty^2} \quad - \text{Interaction Parameter}$$

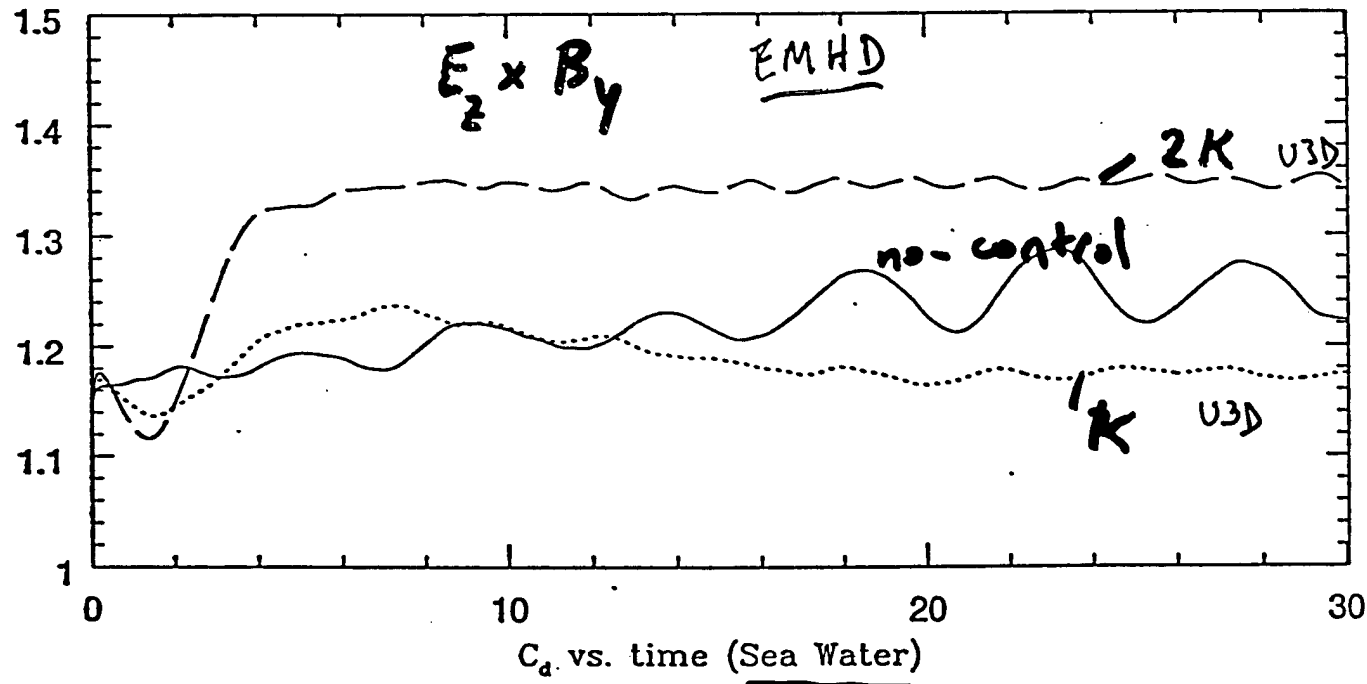
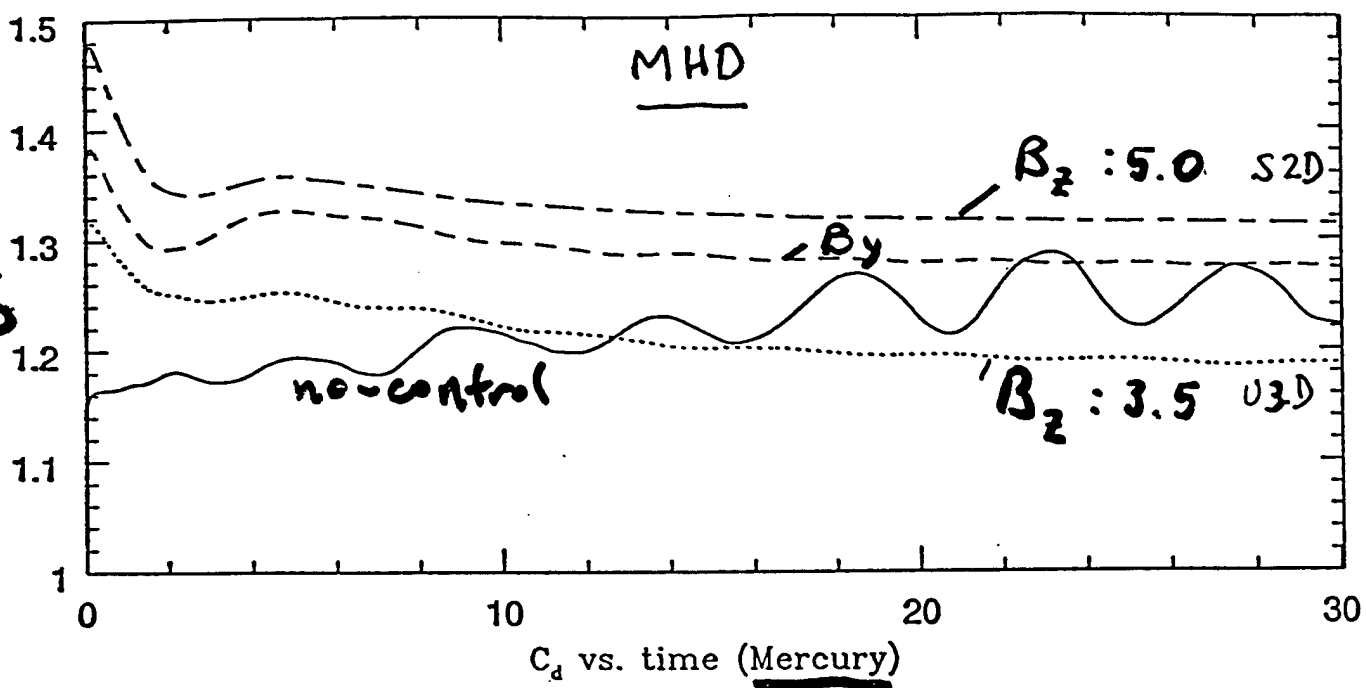
Suppression of the Kármán vortex street



TURBULENT WAKES

AIAA-95

Cylinder, $Re = 500$



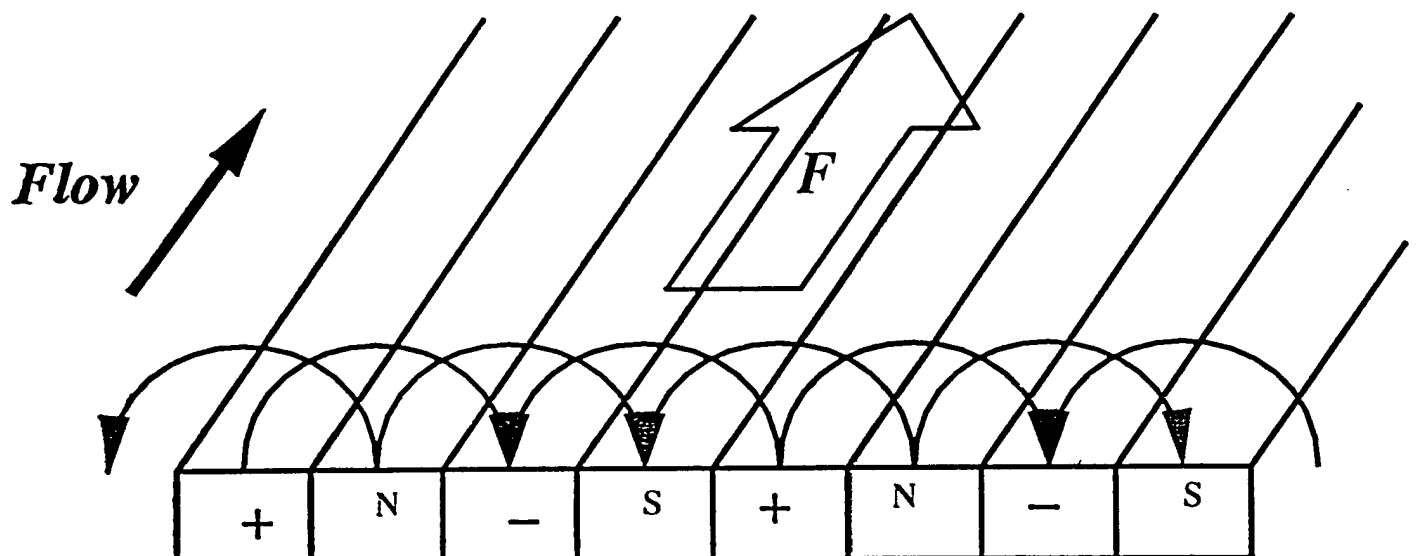
∴ Changes are non-Monotonic!

Active Control: Lorentz Body Force

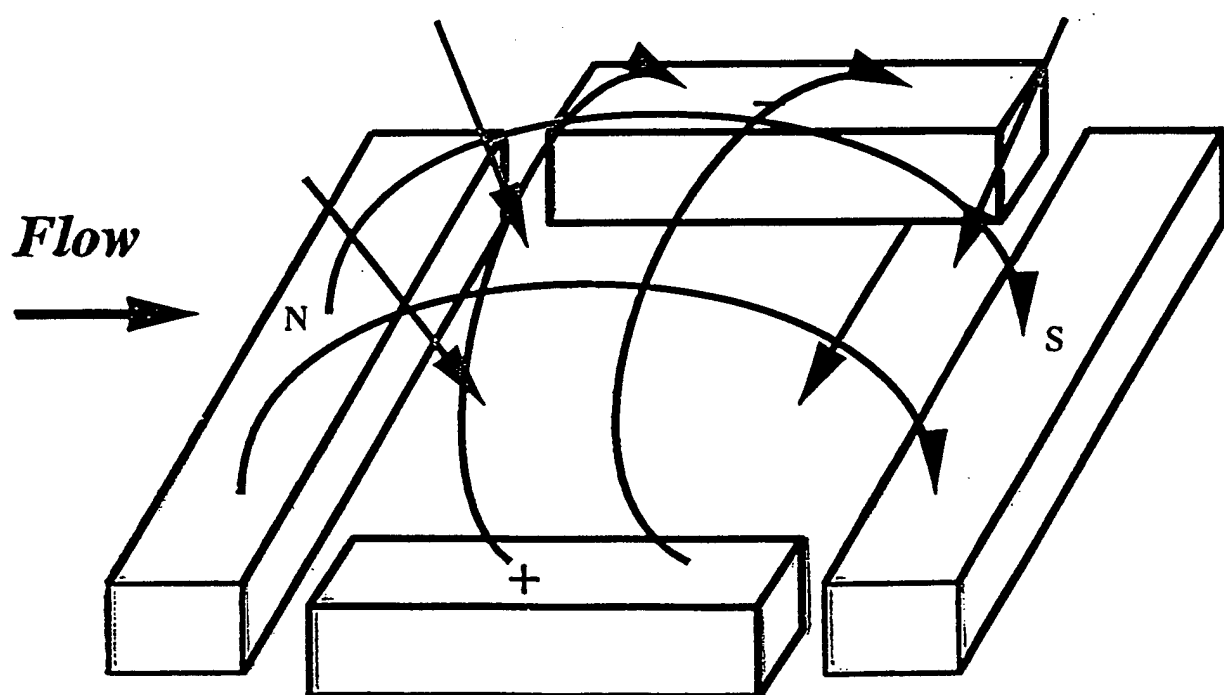
Ph.d.S
Crawford
Y. du

→ Electric Field
→ Magnetic Field
→ Lorentz Force

* DOE
* AFOSR

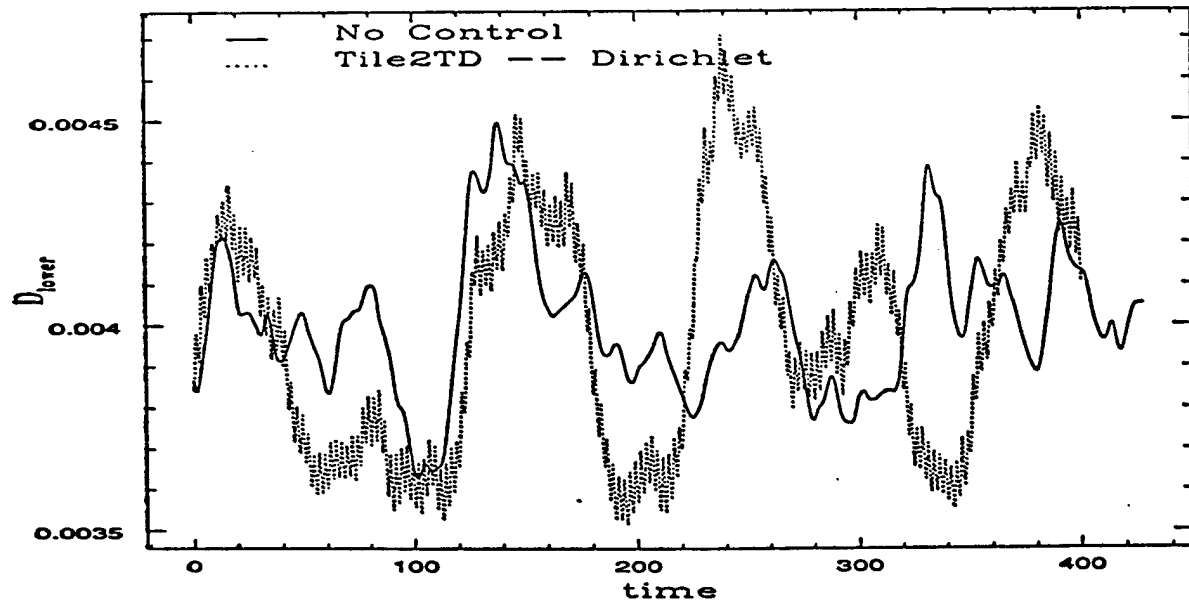
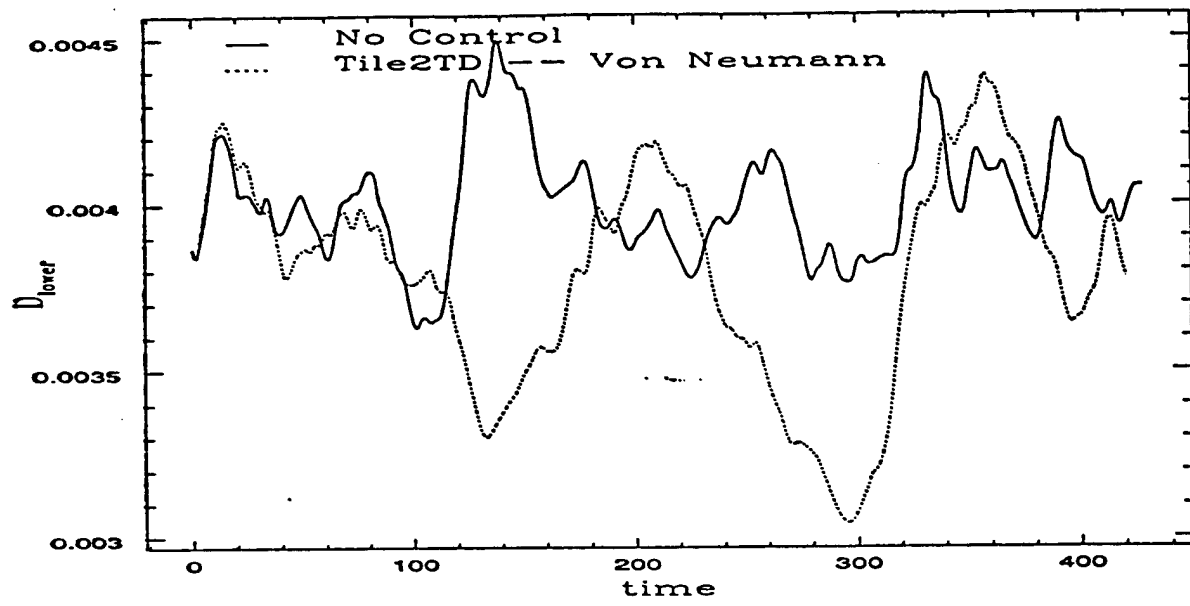


Henoch & Stace, 1995



Nosenchuck & Brown, 1994

EMHD: Shear Stress History – Effects of BC



NEAR-WALL TURBULENCE and LAMB VECTOR

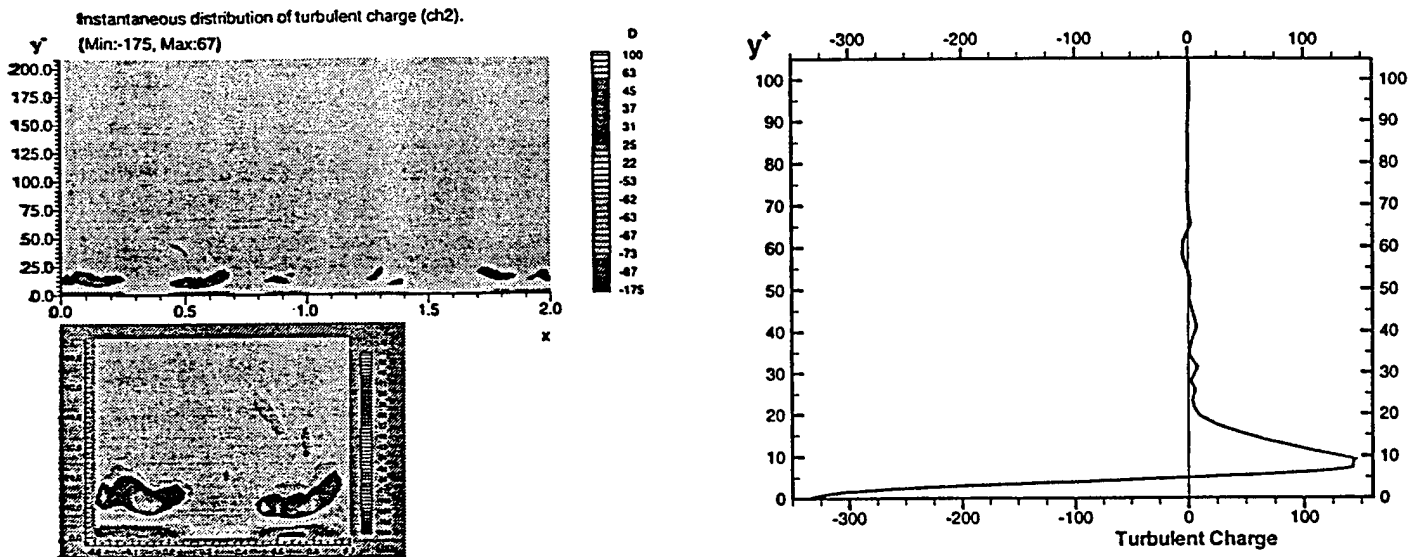


Figure 1: Dipole structure of the divergence of the Lamb vector: turbulent charge

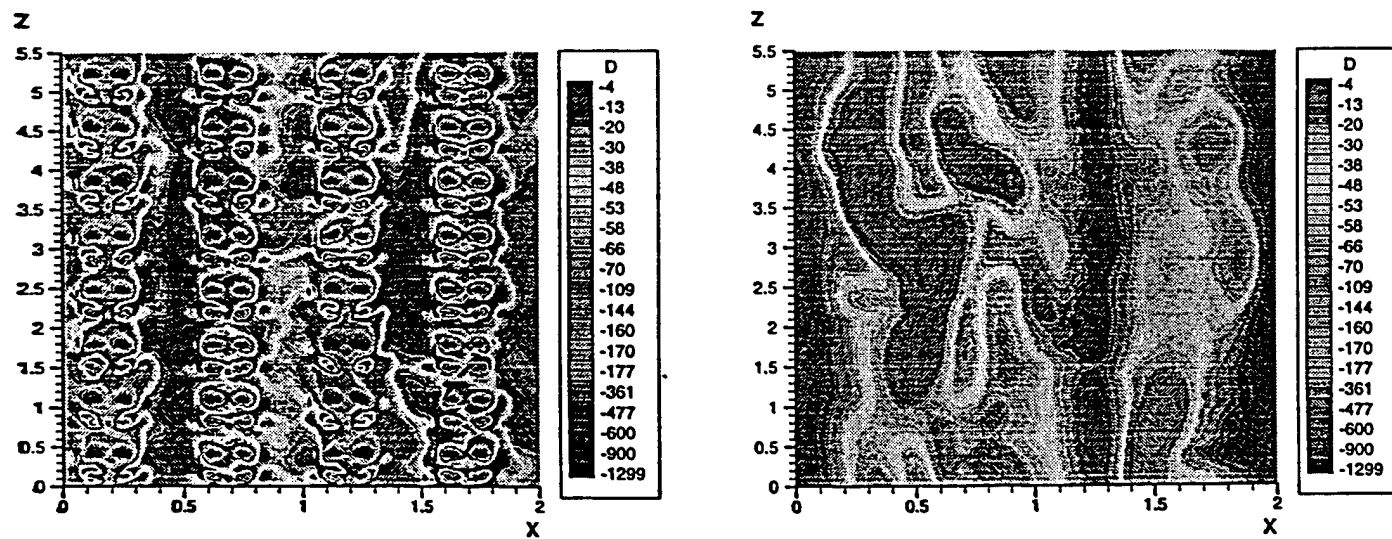


Figure 2: Footprint of the turbulent charge: LEFT - EMHD on; RIGHT: EMHD off

Summary

- Explore MHD, EMHD and EHD
- Strong electrical conductivity non-uniformity
- Selection of physical model is application-dependent
 - degree of ionization
- Transitional Flow - No *ad hoc* models
- Numerical Model ($\mathcal{N}\varepsilon\kappa\mathcal{T}\alpha r$):
 - High order
 - Hybrid grids
- Benchmark Experiments

2D vortex dynamics associated with shock splitting

Kremeyer, Nazarenko, Newell (Arizona).

Is observed shock splitting due
largely to plasma electromagnetics
or due solely to gas heating
which accompany the introduction
of non-equilibrium plasmas into a
gas flow?

Shock wave attenuation in argon plasmas

Ganguly, Bletzinger & Garscadden 1997

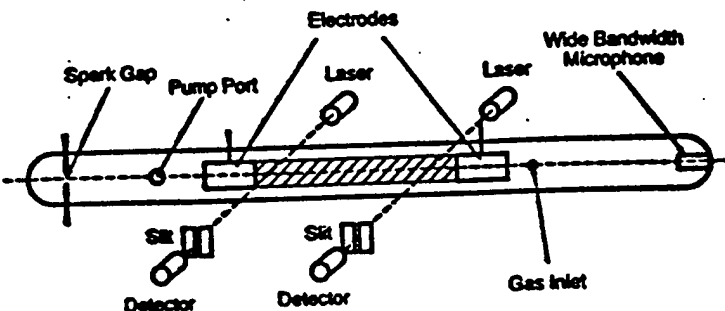


Fig. 1. Schematic of the experimental set-up.

- Shock attenuation & acceleration
1D effects ∇T .
- Shock splitting. ???

Ionisation unimportant, $\alpha \ll 1$?

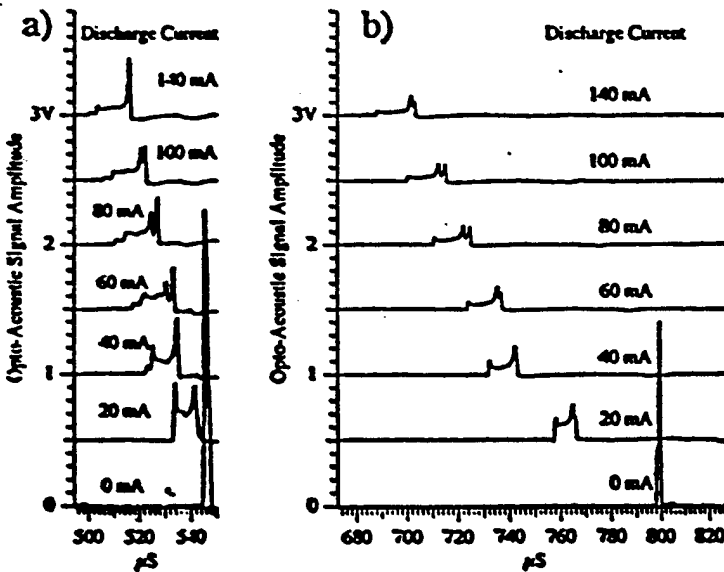
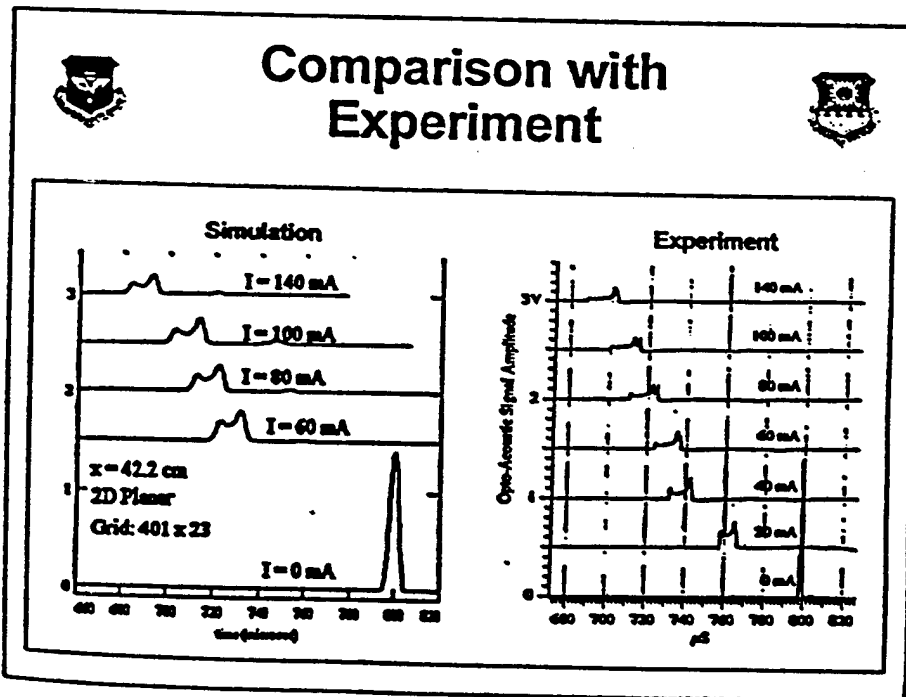
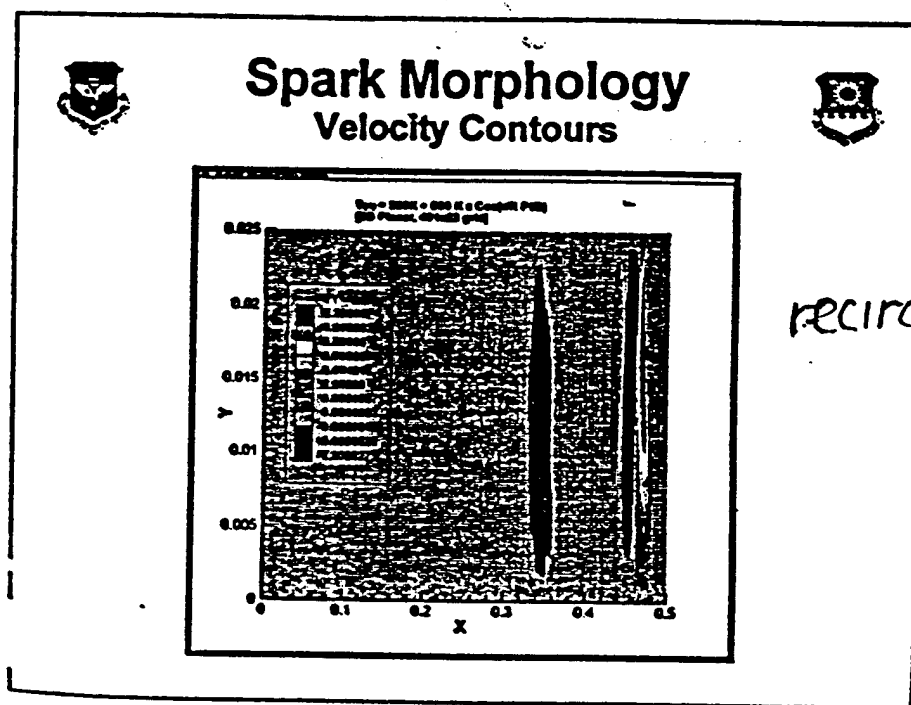


Fig. 2. Shock induced opto-acoustic signals in a 30 Torr argon discharge. (a) 30.2 cm from the spark source, (b) 42.2 cm from the sp source.

2D effects.

CFD of thermal effects,

Bailey & Hilburn '1997

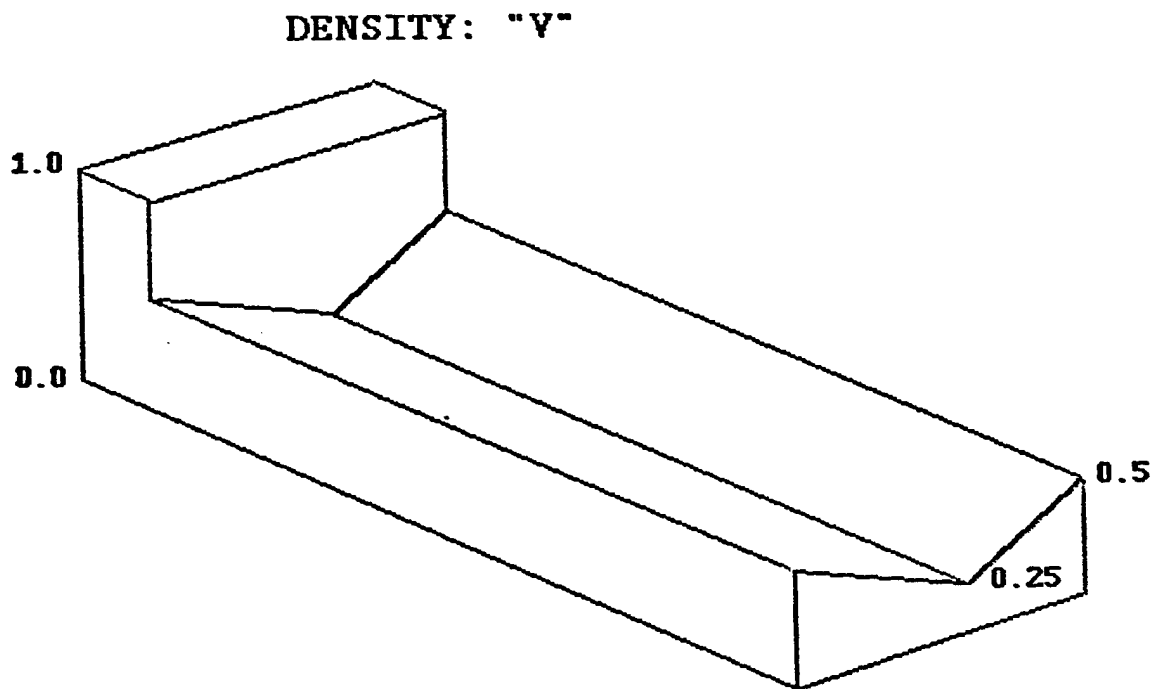


2D Shock Tube Simulation

Left Boundary: $p = 1.0$; $d = 1.0$; $u = v = 0$

Right Boundary: $p = 0.1$; $d = "V"$; $u = v = 0$
(top and bottom B.C's are "reflecting slip")

**Initially, these two states
meet at a discontinuity.**

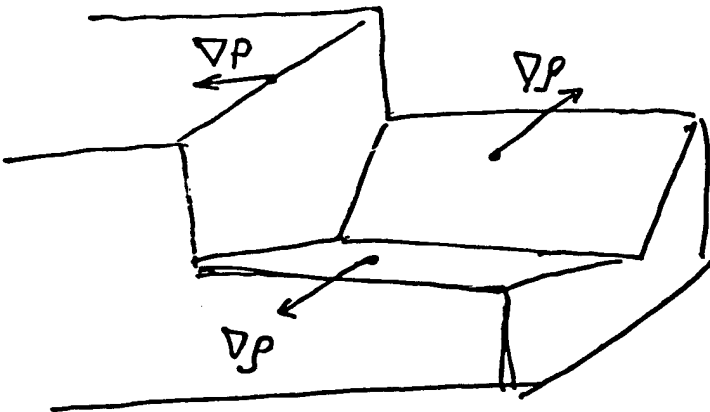


Baroclinic Vorticity Generation

$$\underline{\omega} = \nabla \times \underline{u} \quad \text{vorticity}$$

$$[\partial_t + (\underline{u} \cdot \nabla)] \underline{\omega} - (\underline{\omega} \cdot \nabla) \underline{u} = - \underline{\omega} \nabla \cdot \underline{u} - \underline{\nabla \frac{1}{\rho} \times \nabla p}$$

baroclinic term



Potential Vorticity Conservation

2D Barotropic ($\rho = \rho(p)$) fluid

$$[\partial_t + (\underline{u} \cdot \nabla)] \frac{\omega}{\rho} = 0$$

Potential vorticity $\frac{\omega}{\rho}$ is conserved by each fluid element.

SIMULATION METHOD:

(of the 2D Euler equations)

PHYSICAL ASPECT RATIO (x:y) = 100:1

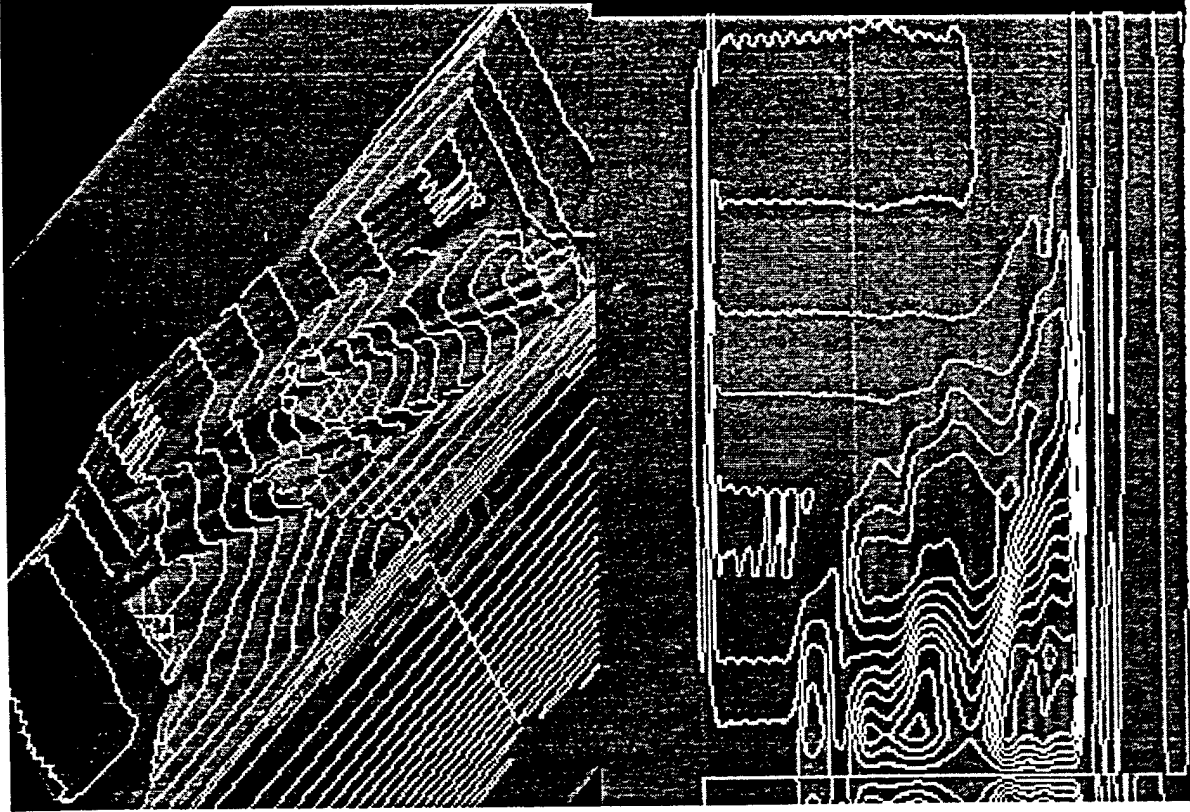
of gridpoints in x direction = 400

of gridpoints in y direction = 20

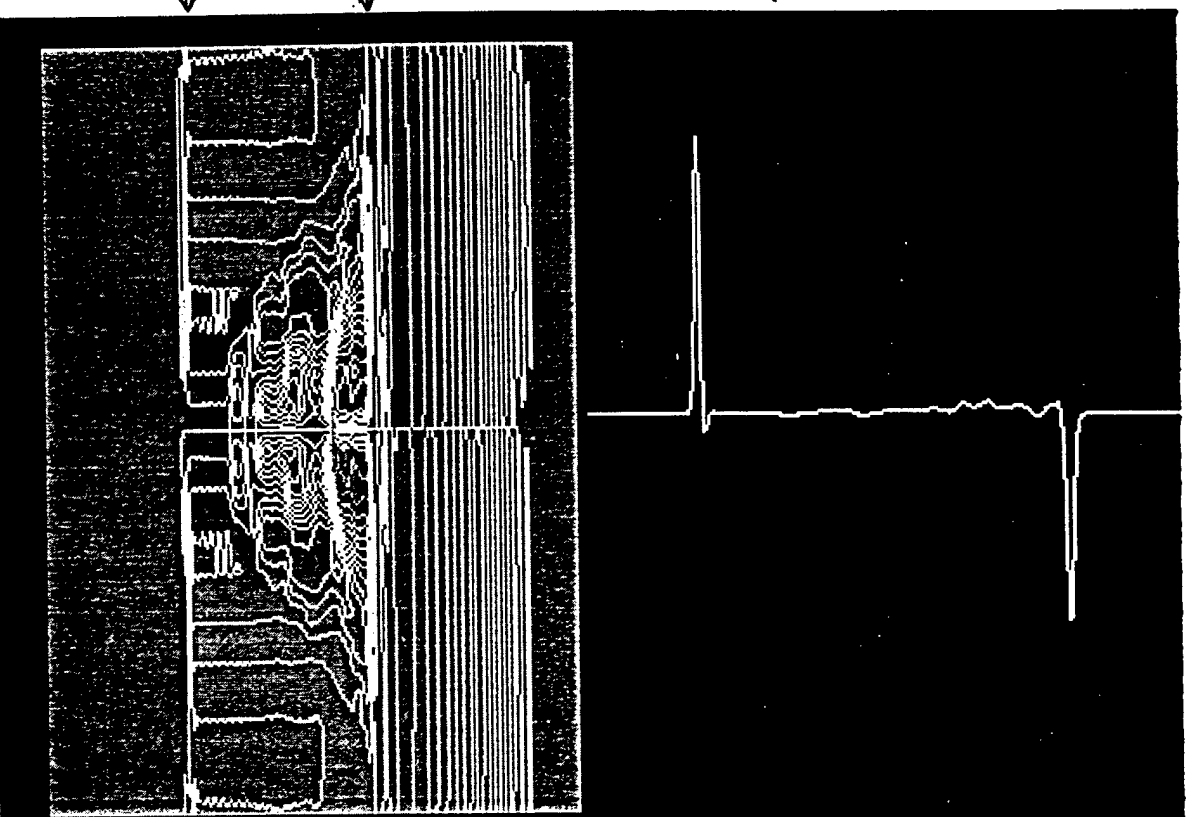
of ghostpoints = 3 (on each side)

- 1: Given the fluid parameters at each gridpoint, find the eigenvectors to Roe's matrices.
- 2: Use a 5th order weighted ENO scheme to find the flux eigenvectors at half gridpoints.
- 3: Use a 3rd order Runge Kutta routine to propagate the half gridpoint fluxes and find the new fluid parameters at the real gridpoints.
- 4: Repeat.

(1) Vorticity landscape

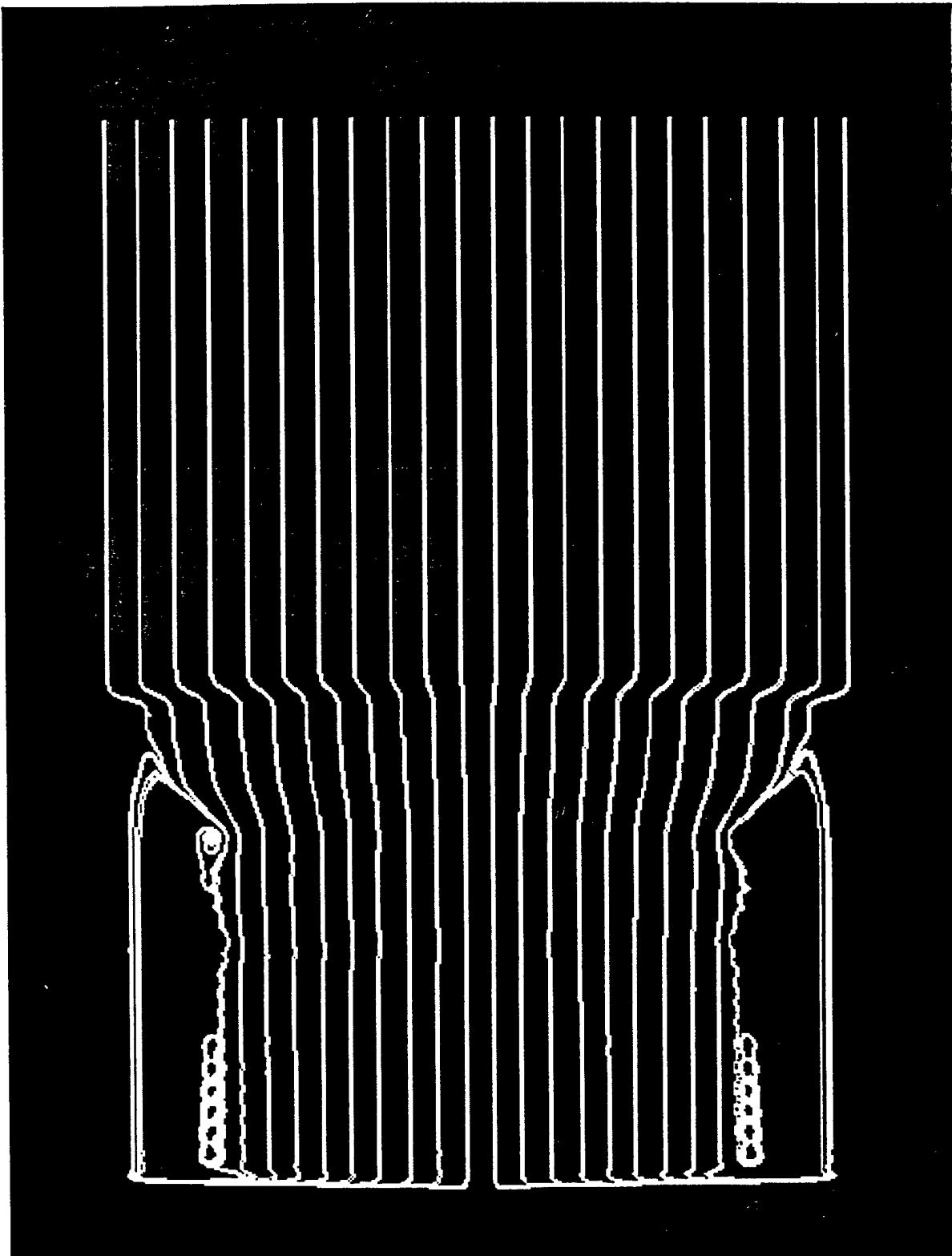


(2) Vorticity Contours

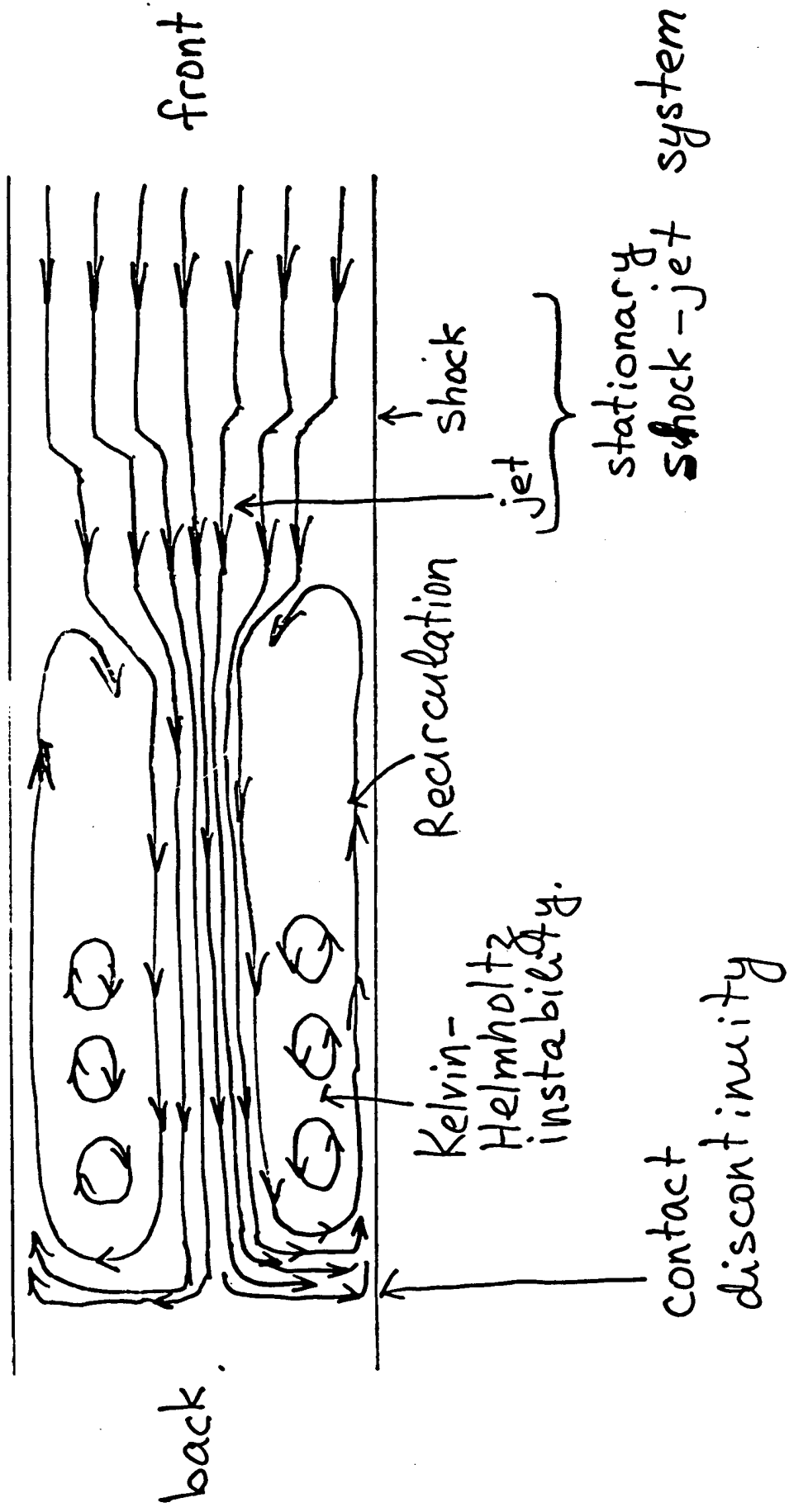


→ front jump
→ back

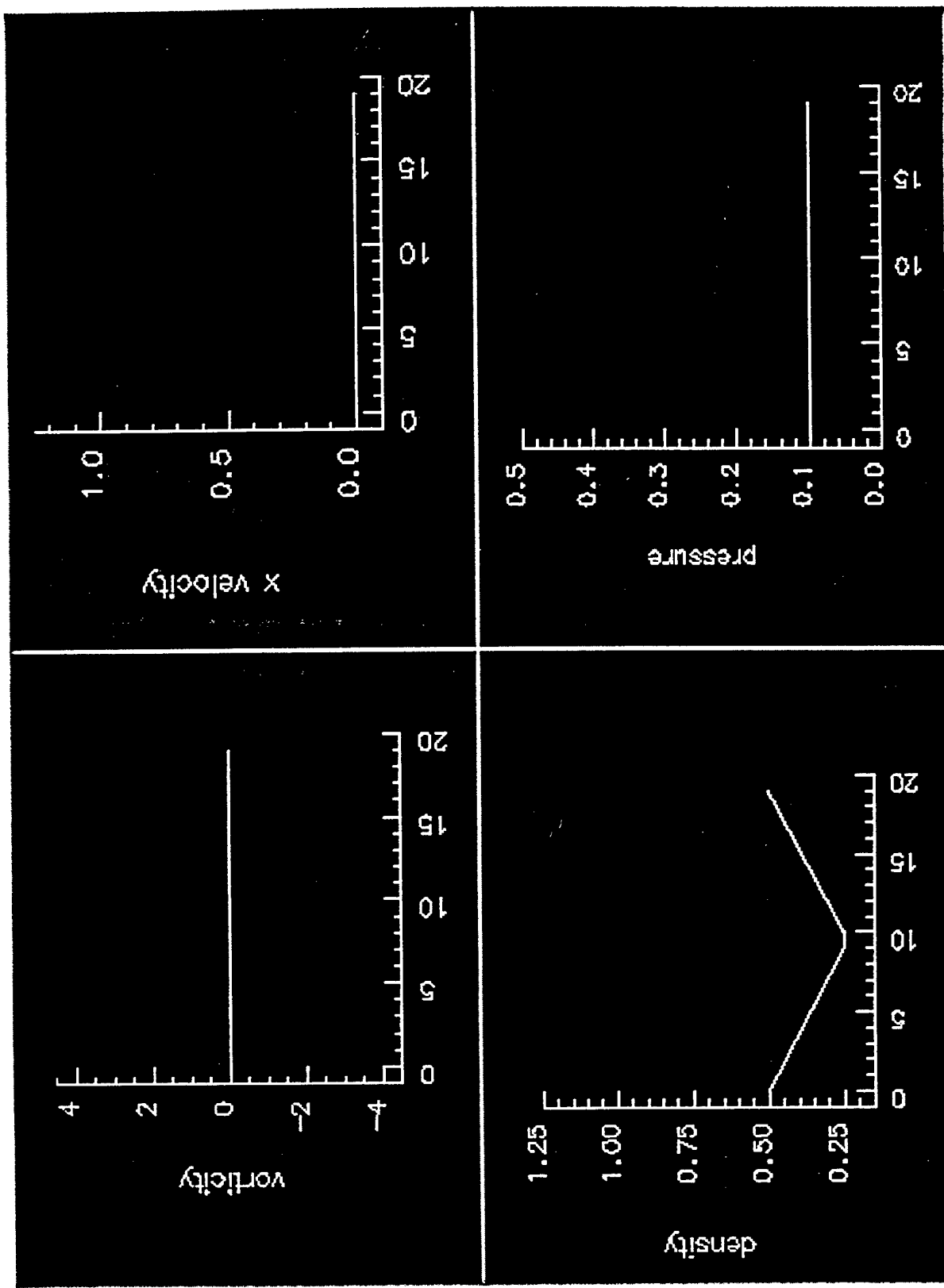
Streamlines



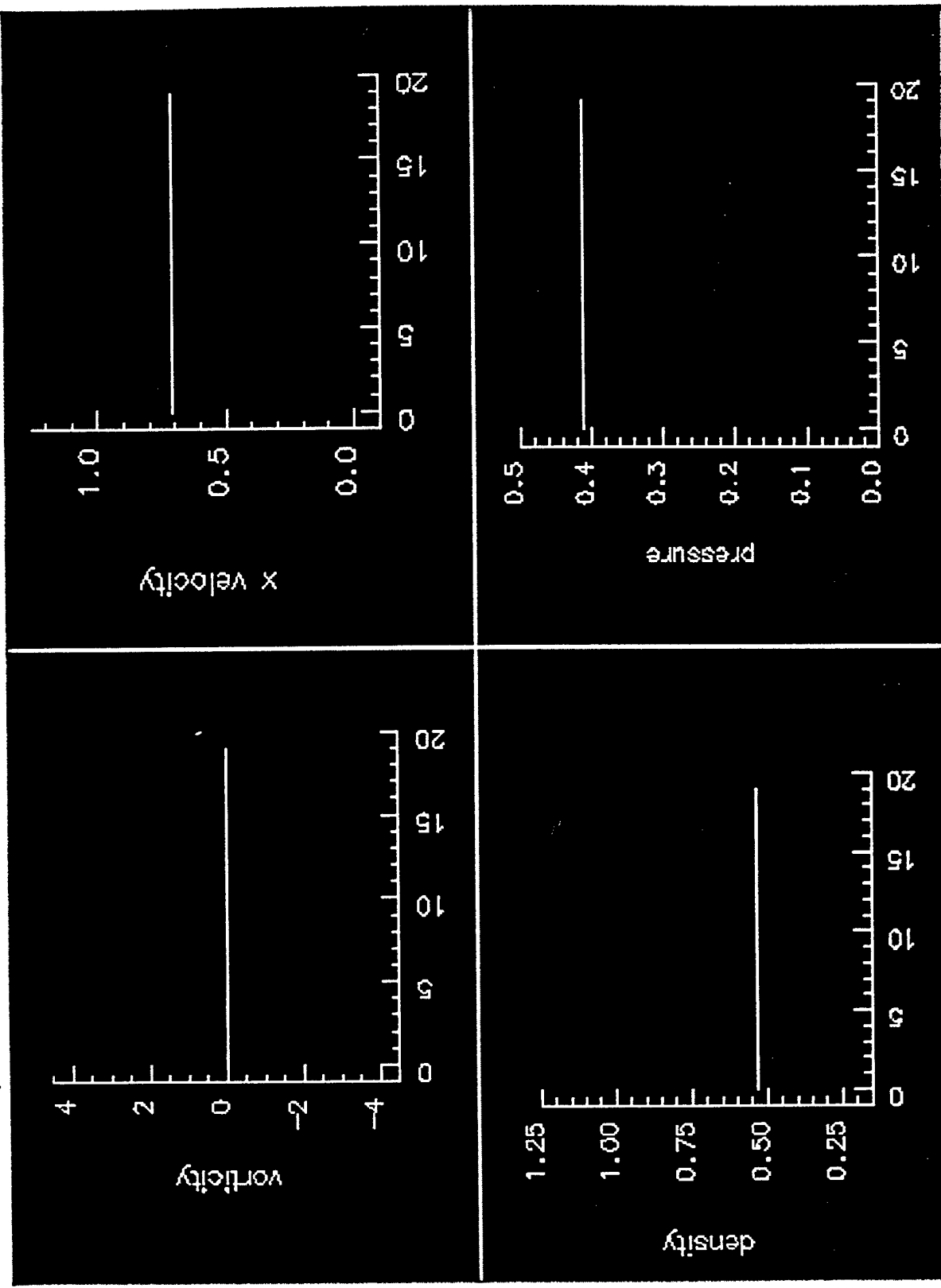
Flow Structure



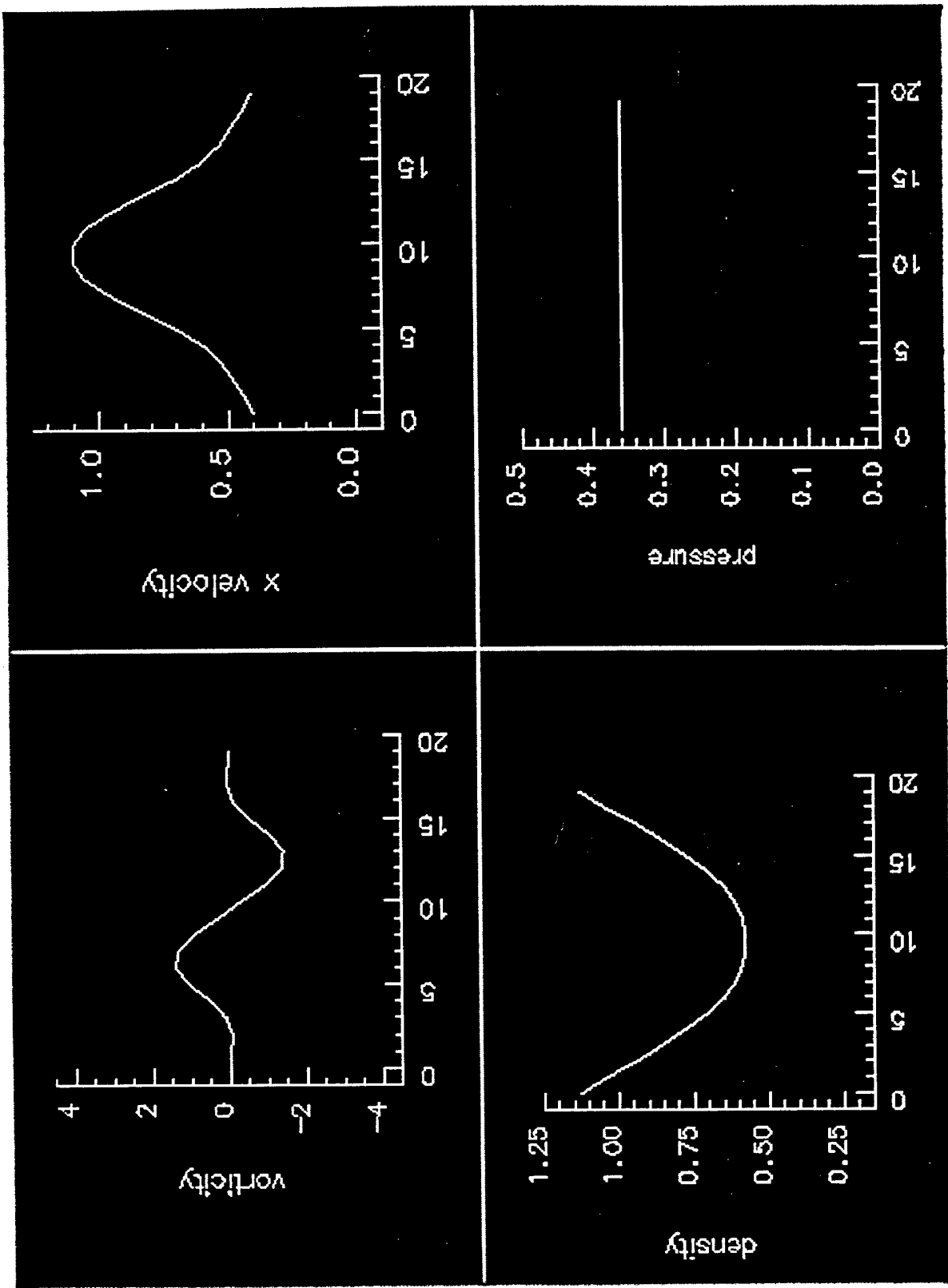
Profiles in front of the Shock



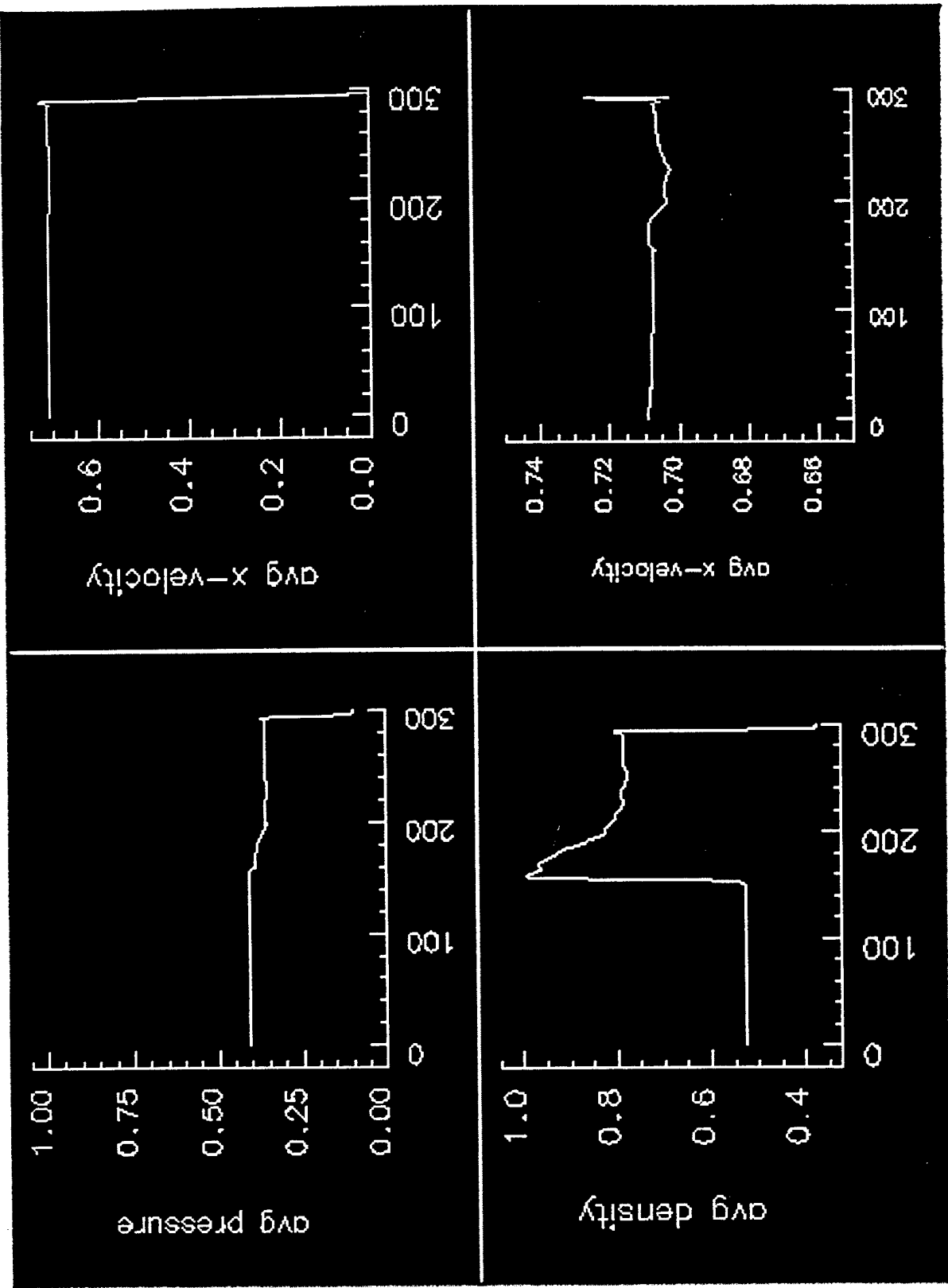
Profiles behind the contact discontinuity.



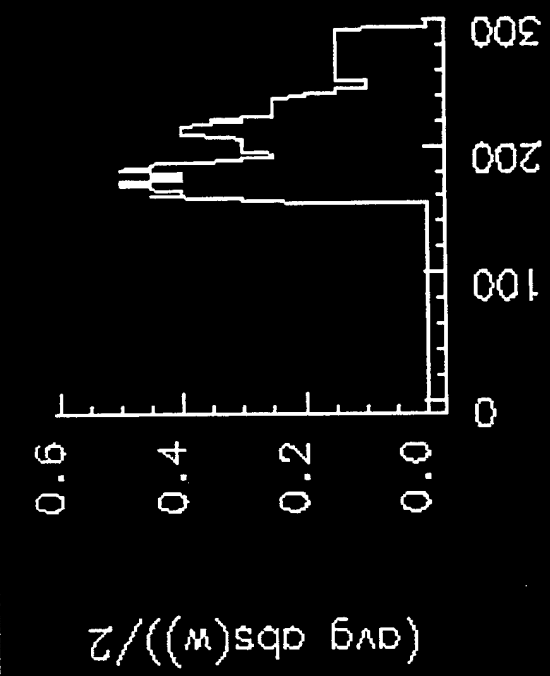
Shock - Jet System



Averaged P , u_x , β

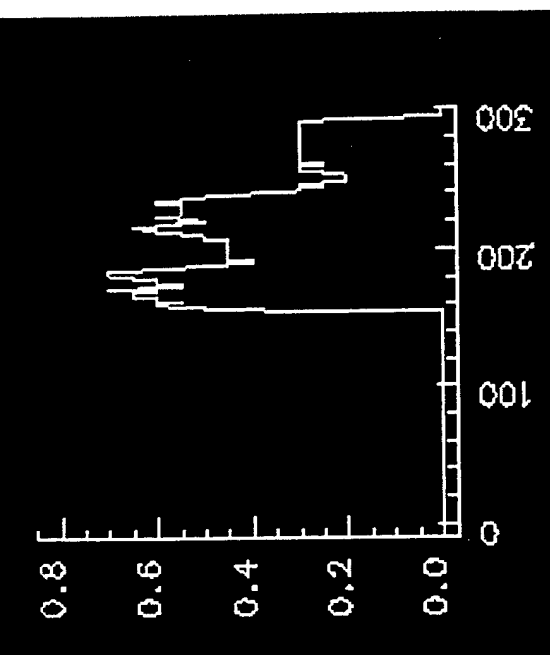


averaged vorticity

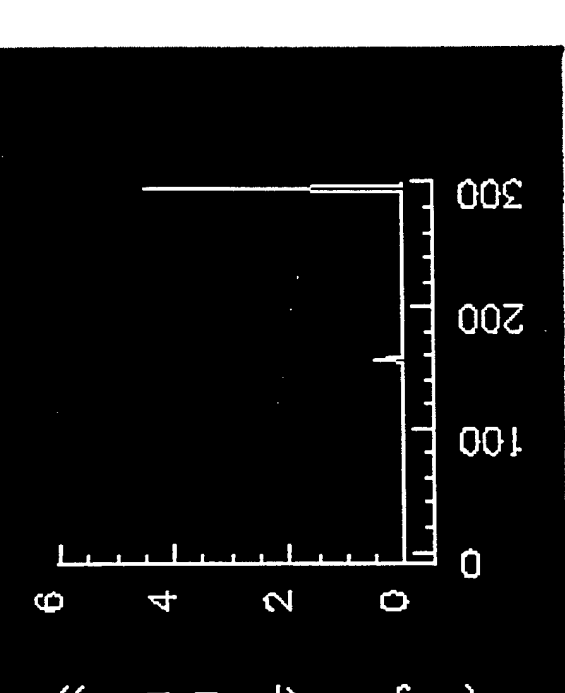


(avg abs(w))/2

averaged potential vorticity

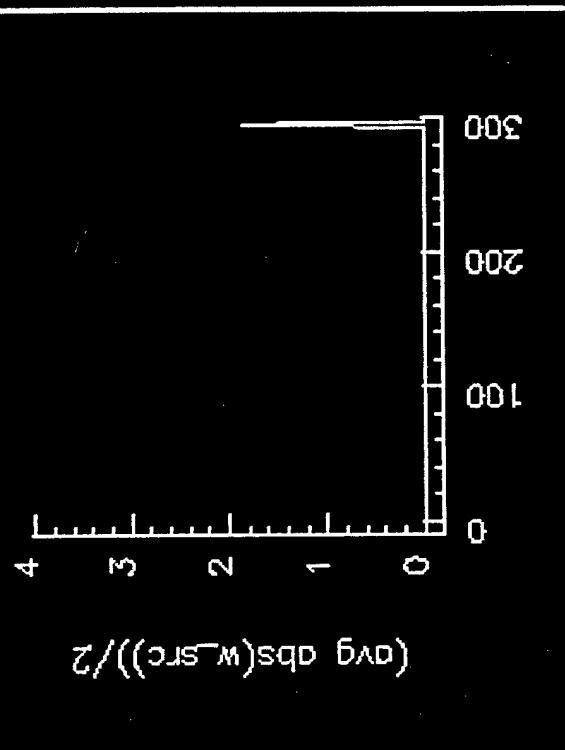


(avg abs(pot_w))/2



(avg abs($\text{pot}_w\text{-src}$))/2

avg. rate of vorticity generation



(avg abs($w\text{-src}$))/2

avg. rate of pot. vorticity generation

RSI
Research
Support
Instruments

**Further Investigation of Large Volume PIA
(Persistent Ionizationin Air) Plasmas at
Atmospheric Pressure**

Mr. John F. Kline

Dr. John E. Brandenburg

Research Support Instruments

Lanham, Maryland

**Presented at the Understanding and Control of
Ionized High-Speed Flows Workshop
Session IV: Plasma Generation and Maintenance**

Princeton University

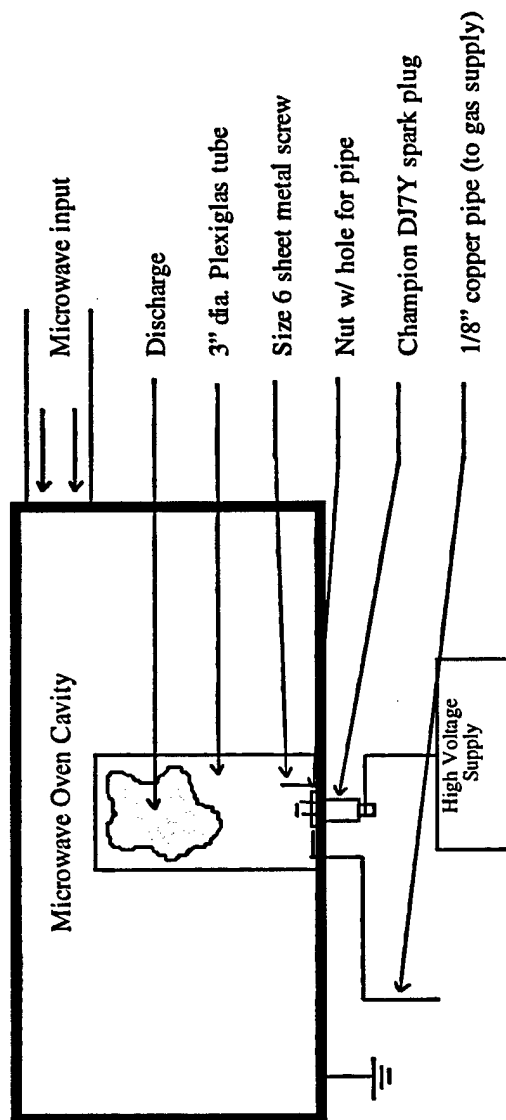
February 26, 1998

RSI

Research
Support
Instruments

Materials and Methods 2.45 GHz (1)

- Untuned cavity
- Field Enhancer
- Gas supply
- UV source
- Containment vessel

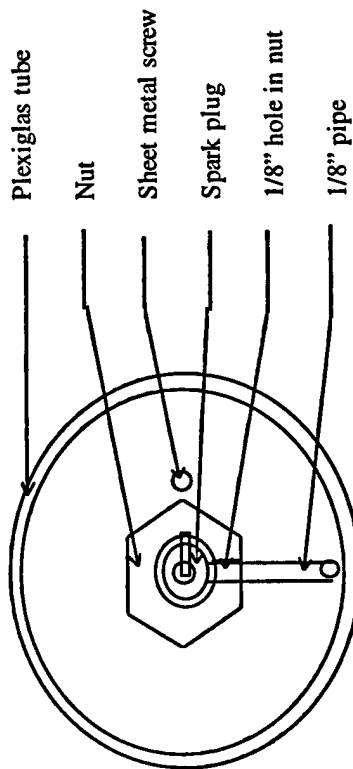


RSI

Research
Support
Instruments

Materials and Methods 2.45 GHz (2)

- Top view of apparatus
- Gases - stagnant air, nitrogen, argon, and helium
- Langmuir single probe
- Videocamera - frame counting
- Microwave detector
- Photocell to measure light decay time



RSI

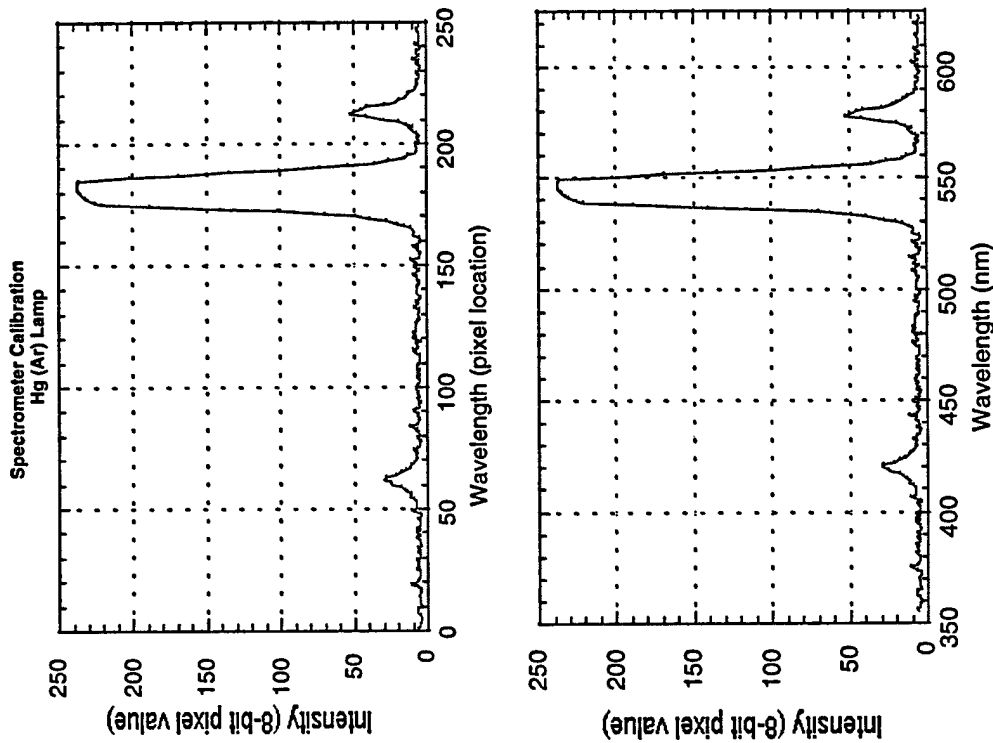
Research
Support
Instruments

Materials and Methods 2.45 GHz (3)

- Replacement of spark plug by laser induced breakdown
 - » 1.06 μm , 0.3 - 1 J, 10 Hz Nd-Yag laser
 - » Field enhancement still necessary for microwave breakdown
 - » Elimination of field enhancer by using TM₀₁₂ resonant cavity
- Vortex ring generator to provide local E/P enhancement
 - » Loudspeaker with plastic cone using voltage pulses
 - » Shapes plasma into flat disc that follows vortex ring
- Emissions spectra measurements
 - » 8-bit CCD viewing exit aperture of spectrometer
 - » Pixel values over a line give a time-resolved measurement over a broad range

Materials and Methods 2.45 GHz (4)

- Time-resolved emissions spectra
- Broad range of wavelengths
- Pixel depth vs. position yields intensity vs. wavelength
- Calibration using Hg (Ar) source

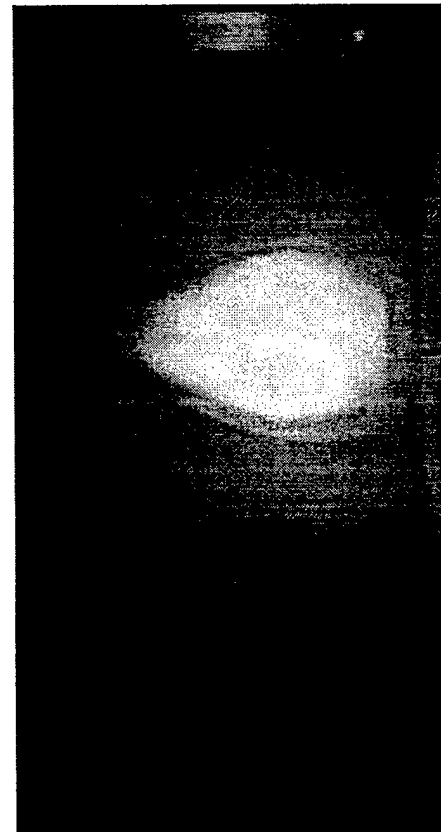
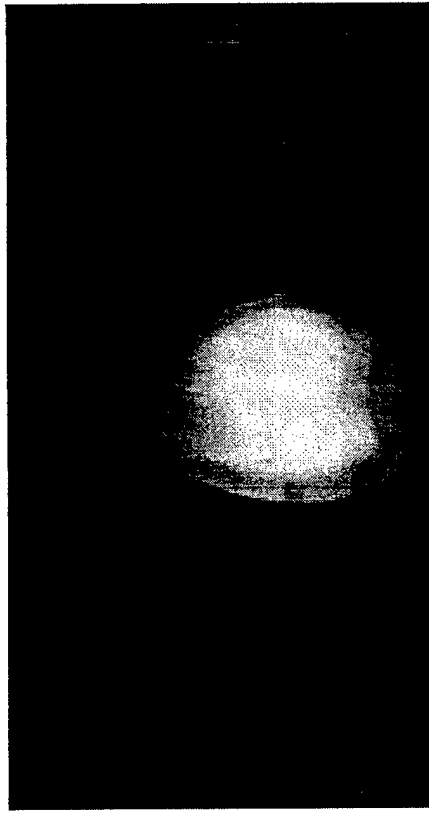


RSI

Research
Support
Instruments

Results (1)

- Temperature - 0.67 eV
- Density - 10^{10} cm^{-3}
- Low neutral gas temperature
- Turbulent, with toroidal core
- Optimal flow rate - 1.2 LPM
- Volume - 280 cm^3 average
- Microwave shielding - 1 order of magnitude increase with plasma (indicates 10^{11} cm^{-3})

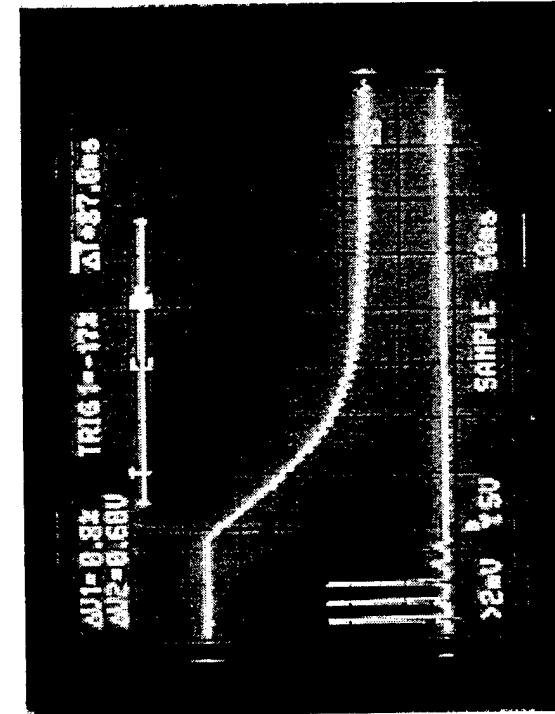


RSI

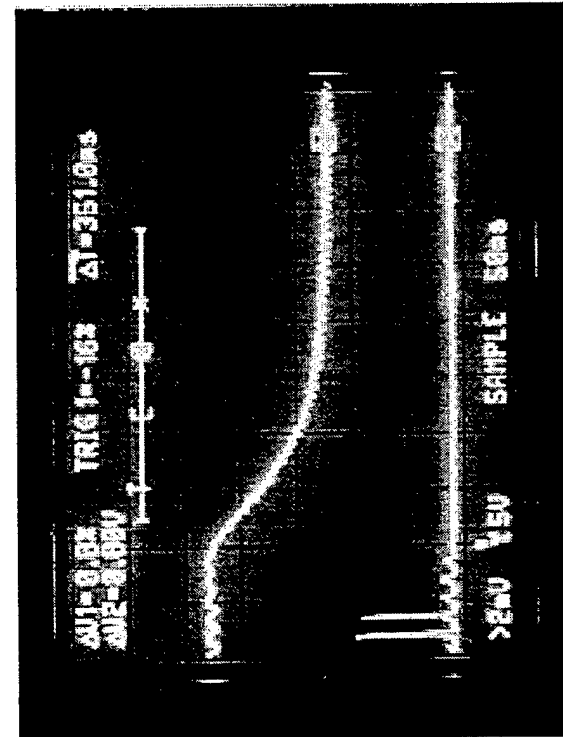
Research
Support
Instruments

Results (2)

- Unpowered lifetime - 200 ms average (3 e-folds at 60ms decay time)
- Upper channel shows photocell output
- Lower channel shows microwave detector output



Argon



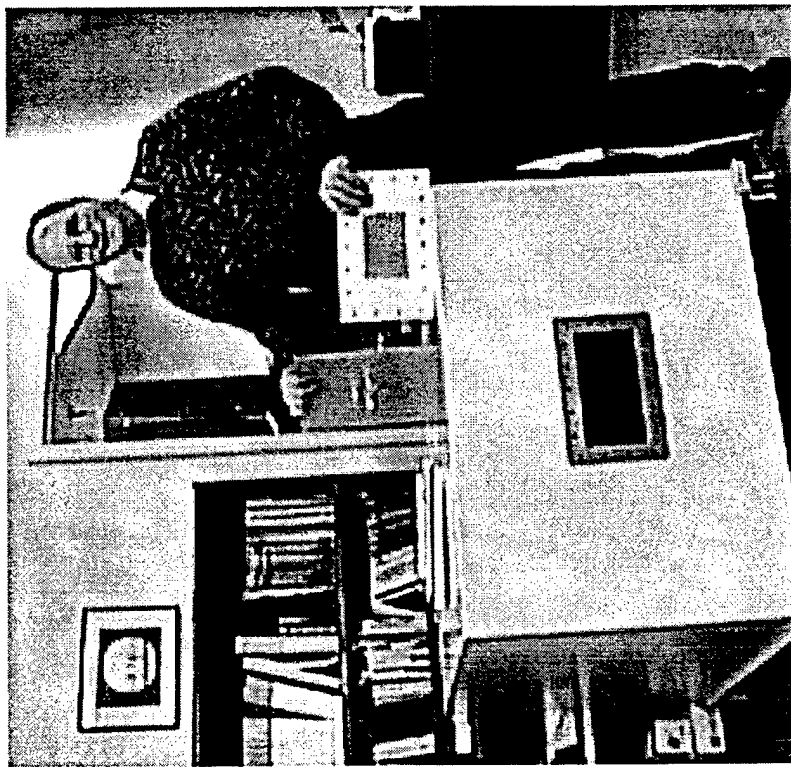
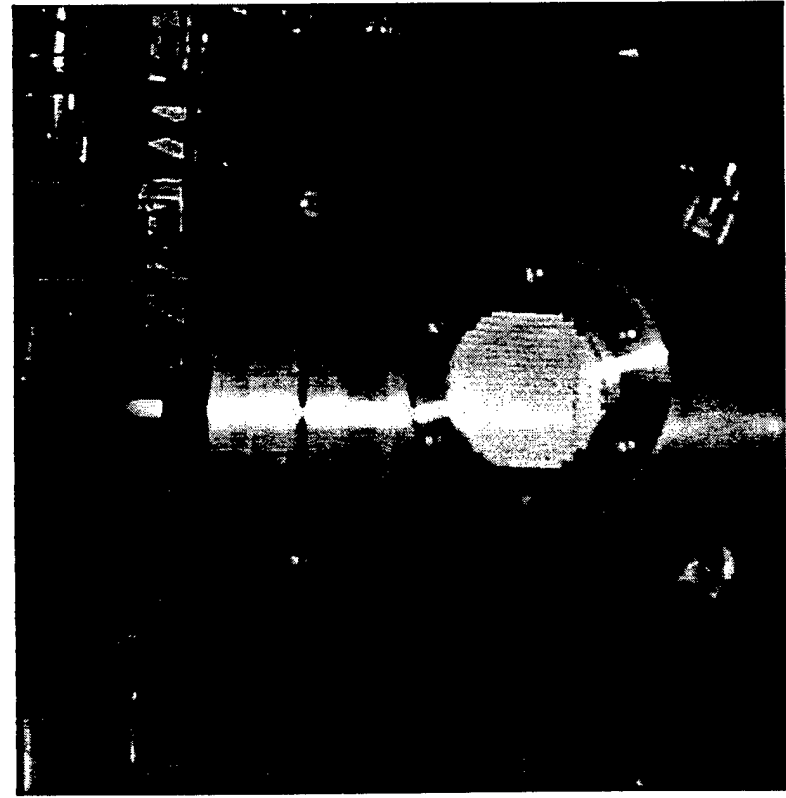
Air

RSI

Research
Support
Instruments

Results (3)

- Scaling of TM_{011} resonant cavity to 0.915 GHz
- 45 kW operation using vortex-stabilized compressed air

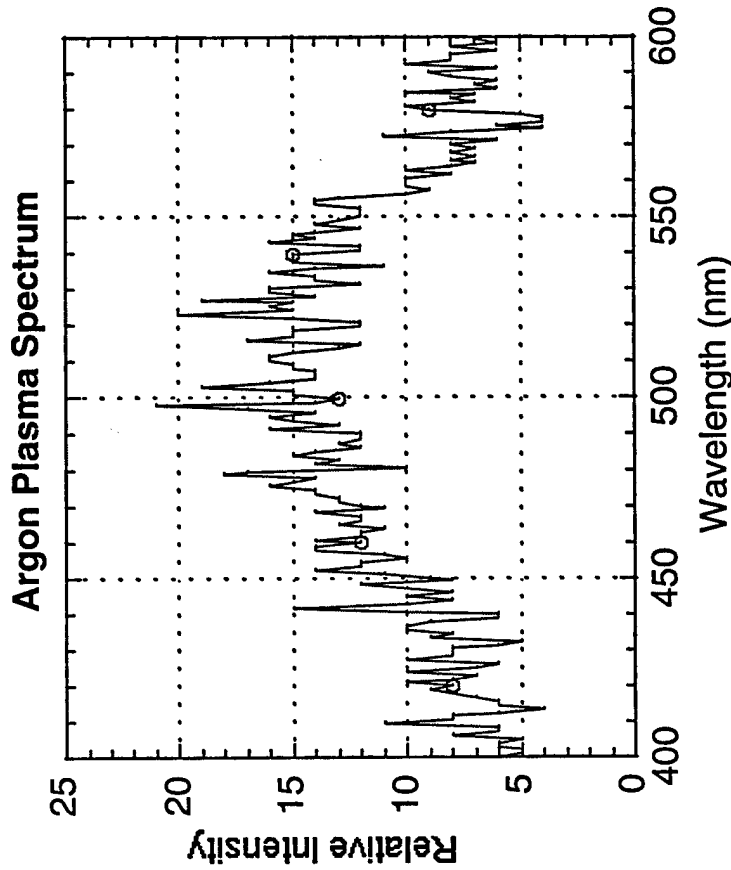


RSI

Research
Support
Instruments

Results (4)

- Initial data on argon mixture
- Shows broad continuum (previously seen at Stanford)
- Can acquire time history data



RSI

Research
Support
Instruments

Discussion

- Shared Electron Orbital (SEO) Hypothesis
 - » Decoupling of electrons from collisions with neutrals
 - » Long collisional energy transfer times
 - » Long recombination times
 - » Electrons shared between orbitals
 - » Resemble conduction bands in liquid metals
 - » Vorticity suggests trapped magnetic fluxes and dynamo action (as in liquid metals)

RSI

Research
Support
Instruments

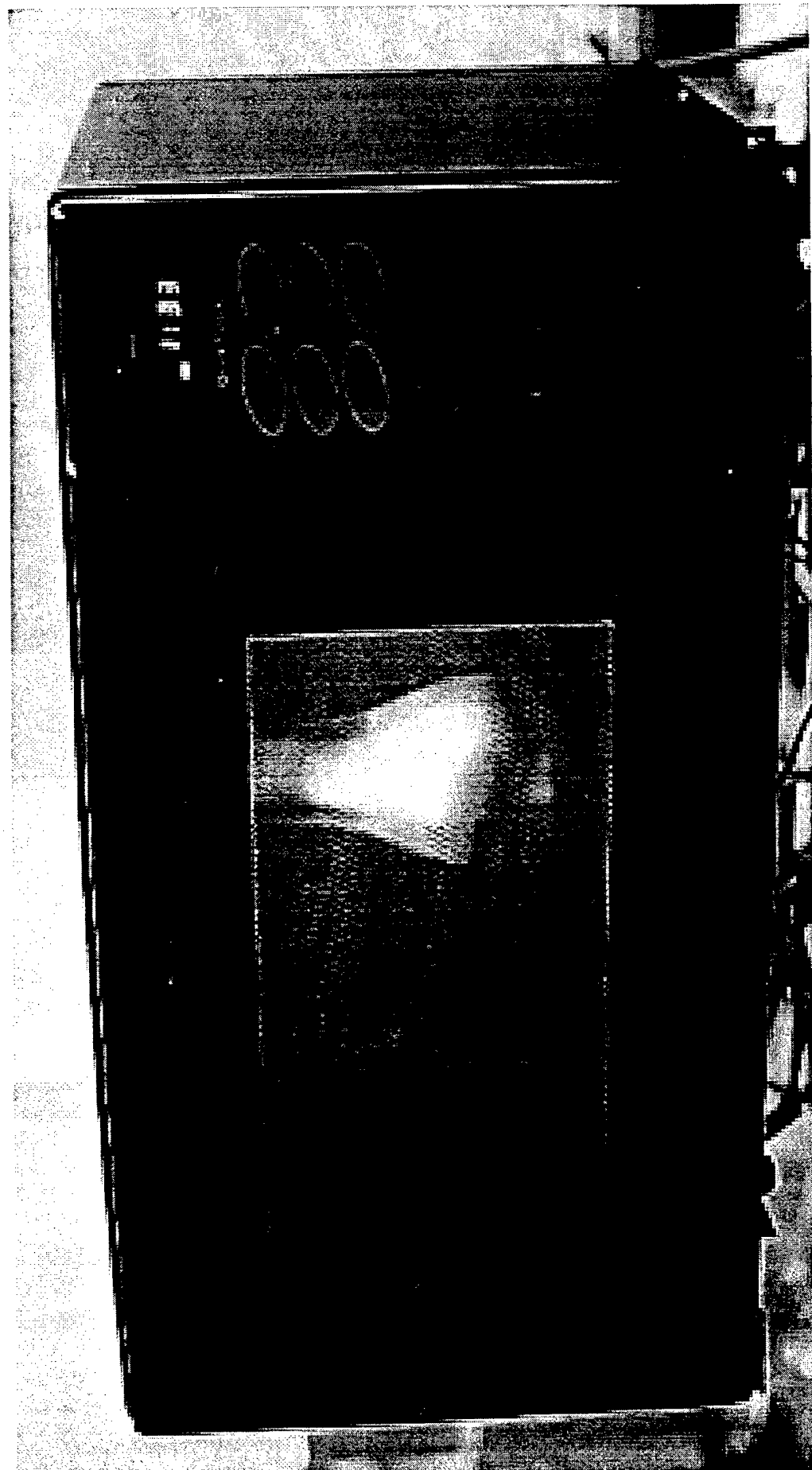
Future Work

- Advanced diagnostics
 - » Continuing work on emissions spectra
 - » Triple probe with digital oscilloscope and function generator
- Investigate vorticity
 - » Pulsed power vortex ring generator
 - » Optically measure rotation

RSI

Research
Support
Instruments

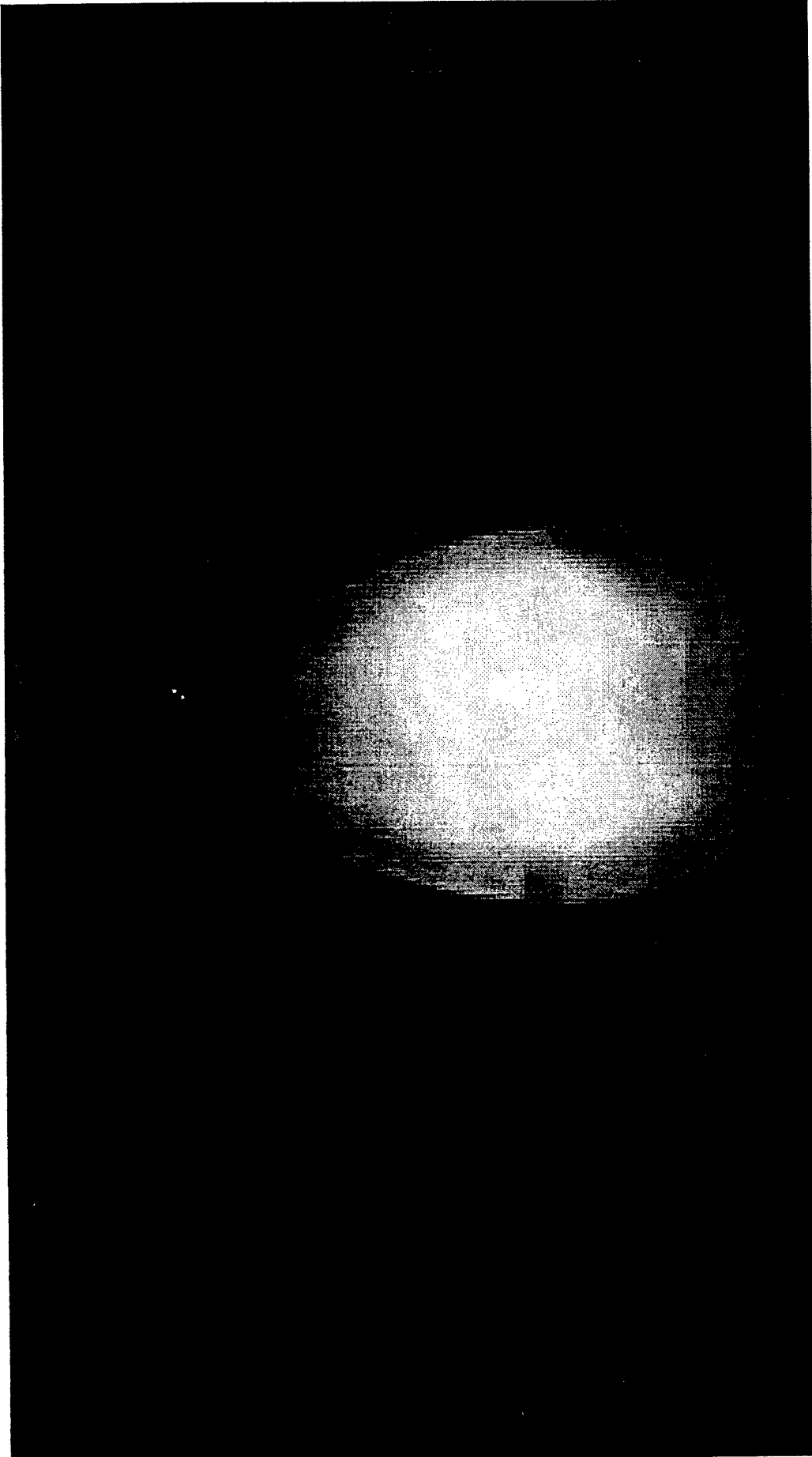
Nitrogen Plasma - Low Flow



RSI

Research
Support
Instruments

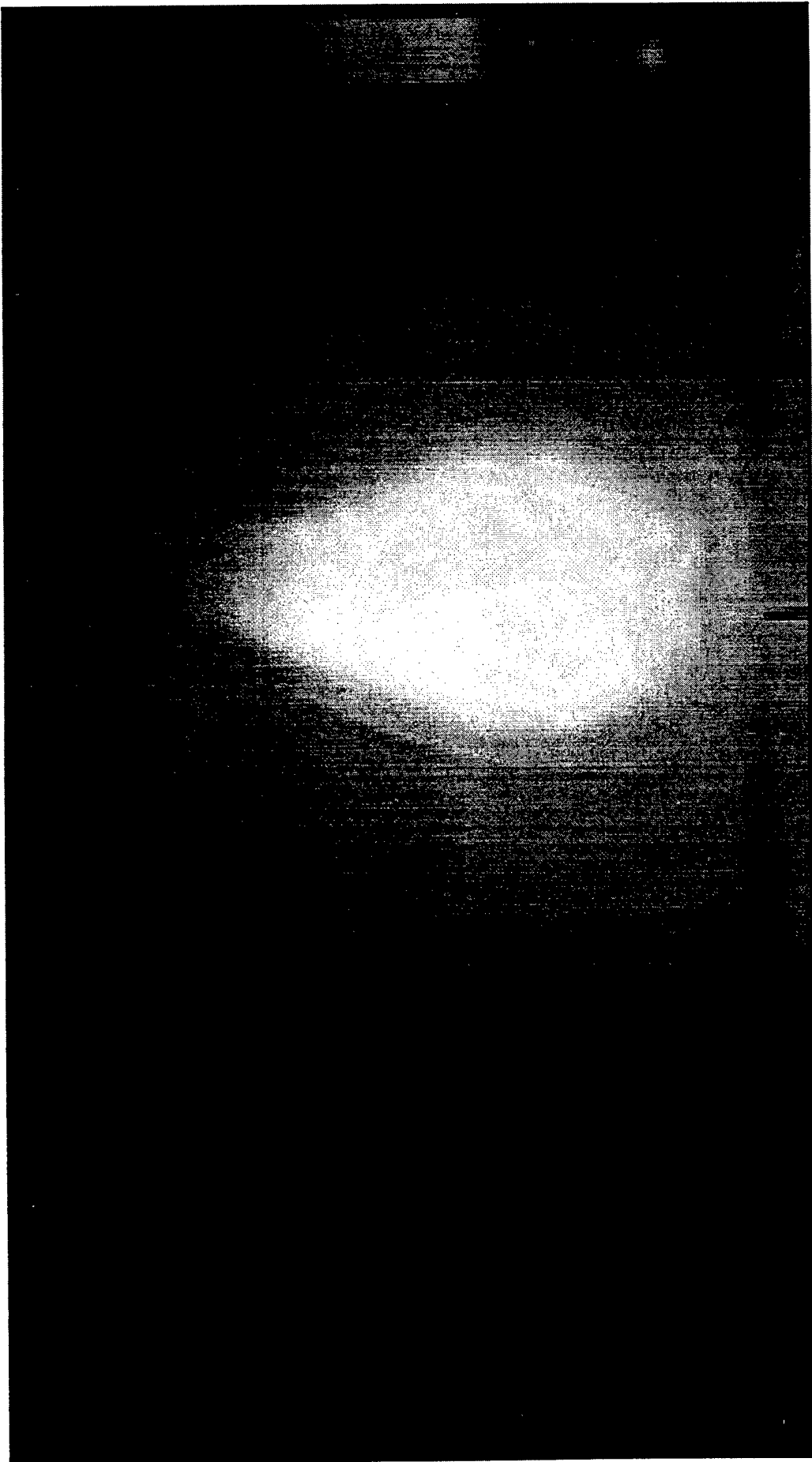
Nitrogen Plasma - Stable



RSI

Research
Support
Instruments

Argon Plasma - Stable



Plasma Torches and Their Demonstration

Spencer P. Kuo and Edward Koretzky

**Department of Electrical Engineering
Polytechnic University**

***Work supported by the AFOSR**

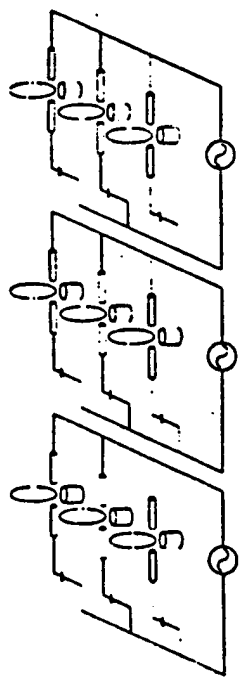


Figure 1.1: A schematic of the current arrangement for an array (3×3) of plasma torches. Tungsten electrodes are used. Each electrode pair is facilitated with an air jet nozzle.

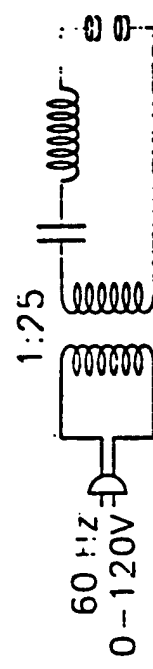
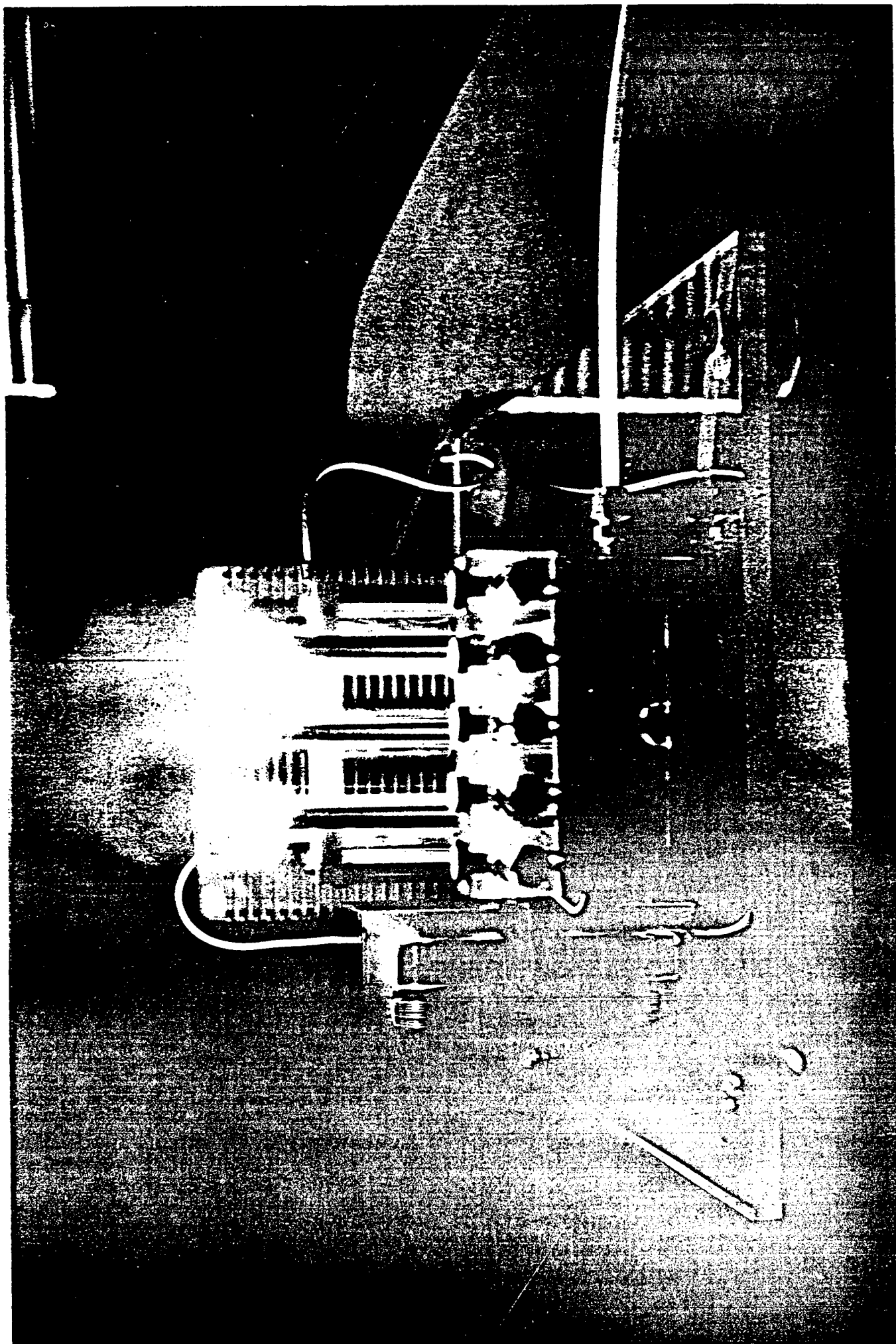
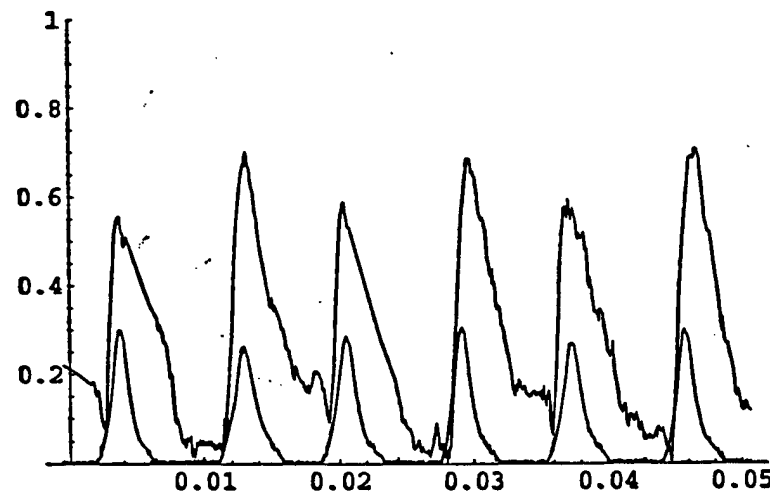
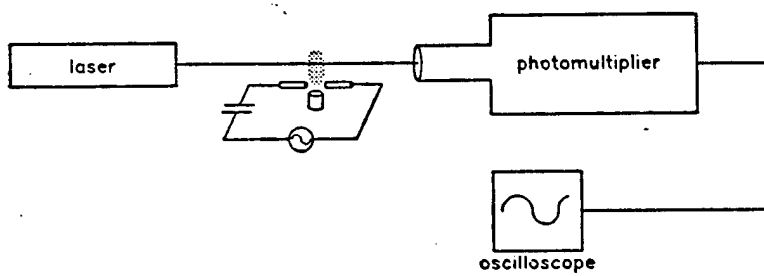
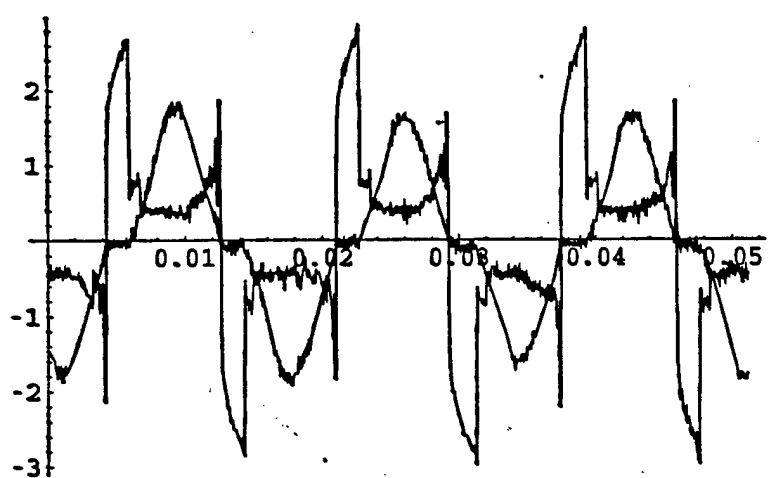


Figure 1.2: Circuit diagram of the plasma torch.

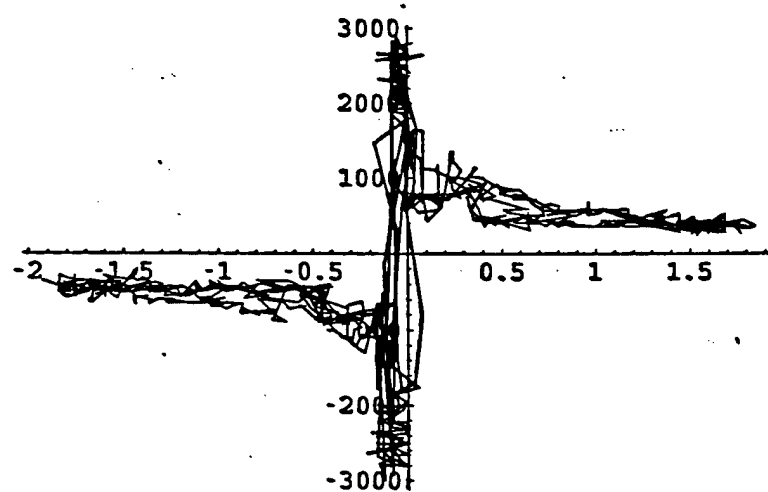
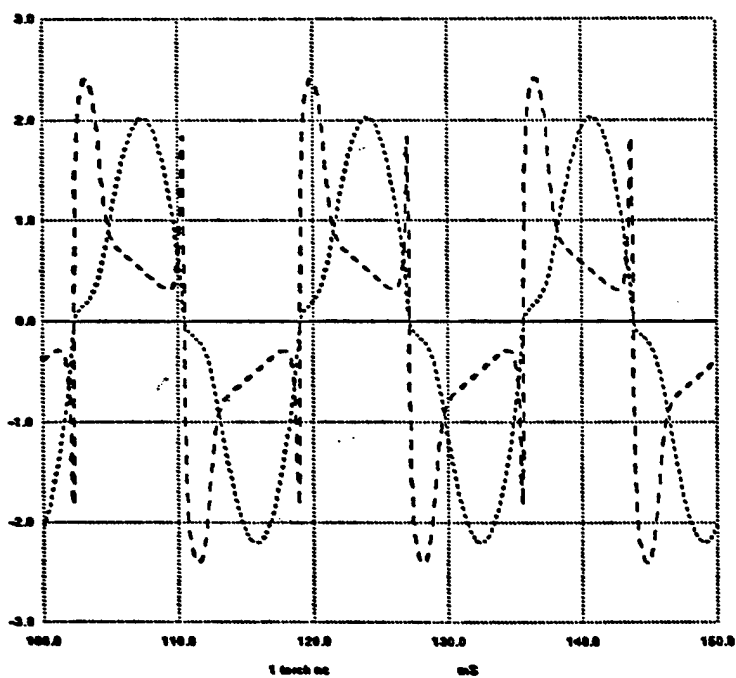


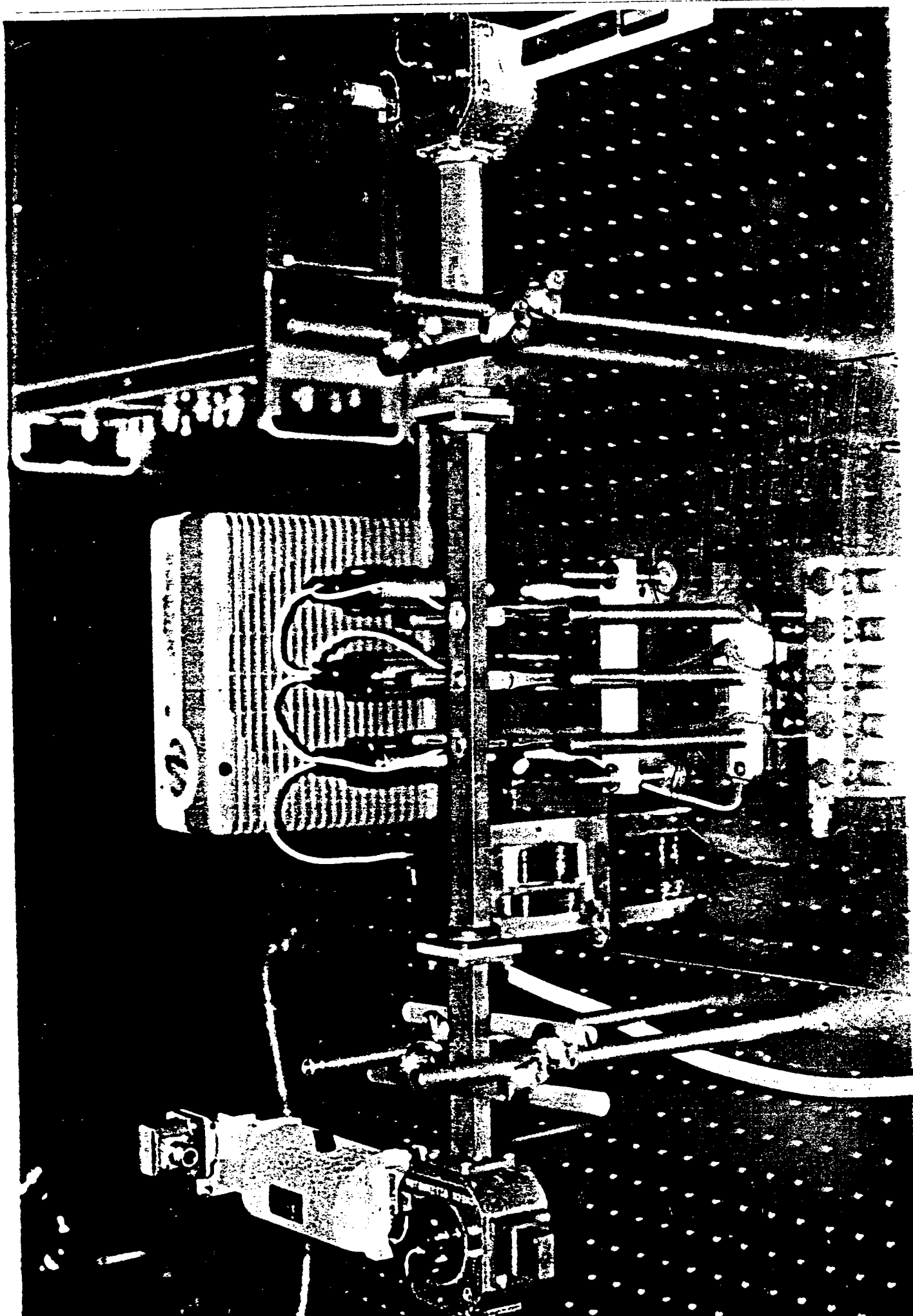


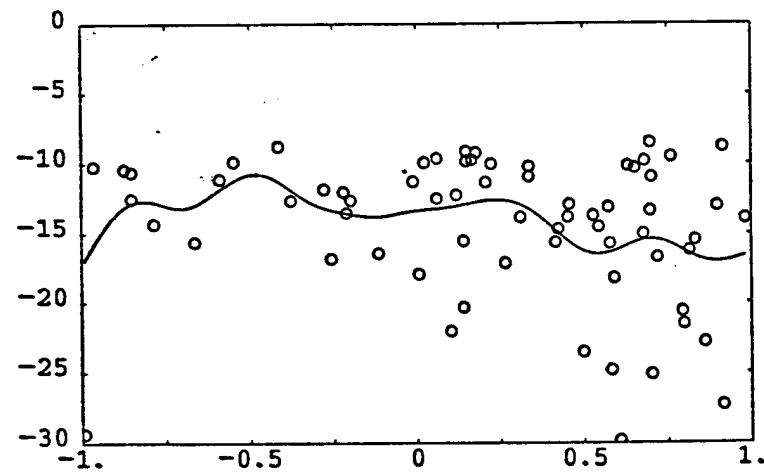
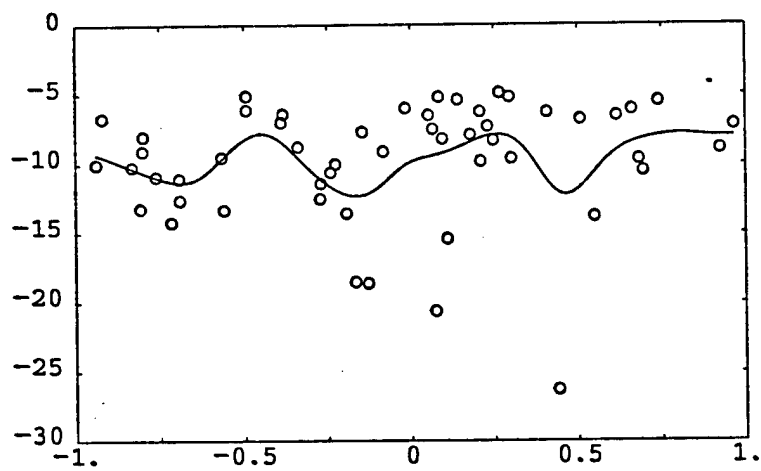
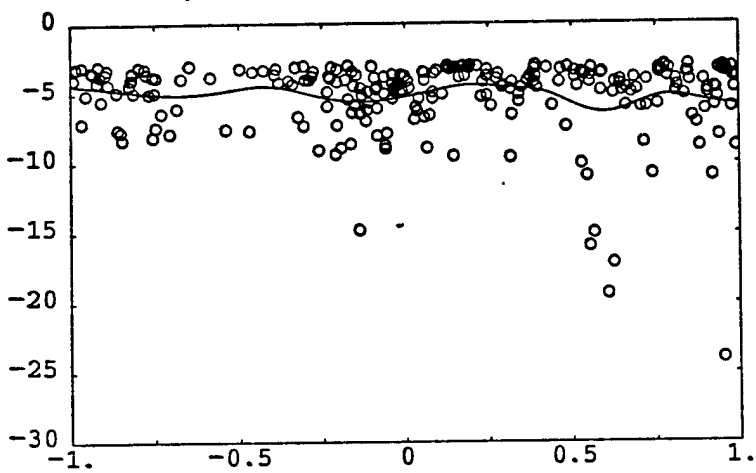


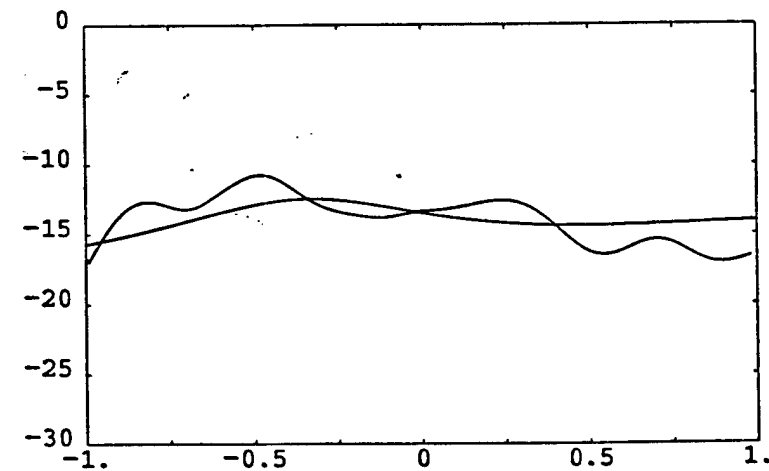
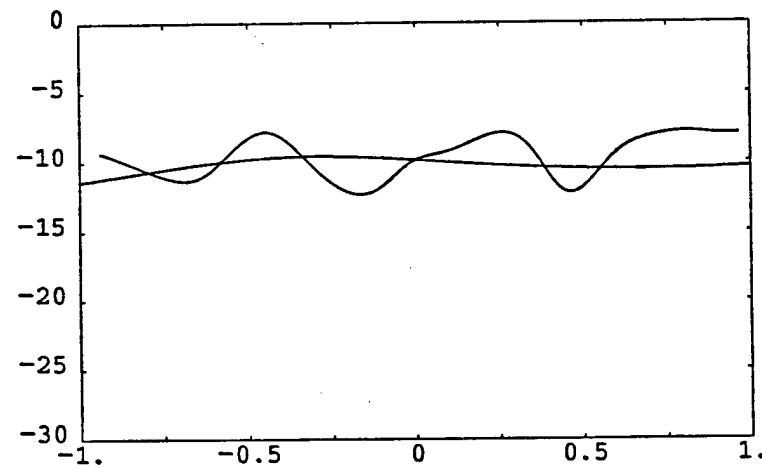
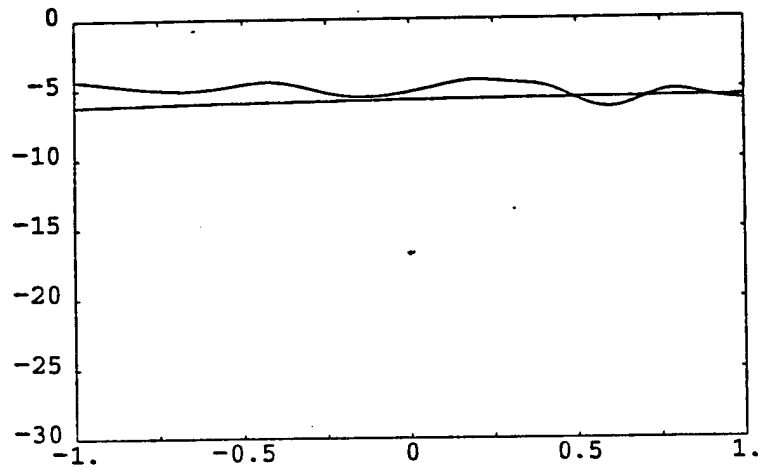


Units: ---- v16branch - - - v(21)/1000









Plasma Torch

Pressure: 1 ATM

Density: 1.5×10^{13} (deduced from measurements based on two independent methods)

Temperature: $1200^{\circ}K$

Dimensions: cylindrical shape having 1 cm radius and 7 cm length

Volume: $20 \text{ cm}^3/\text{torch}$

Power Consumption: 600 W/torch

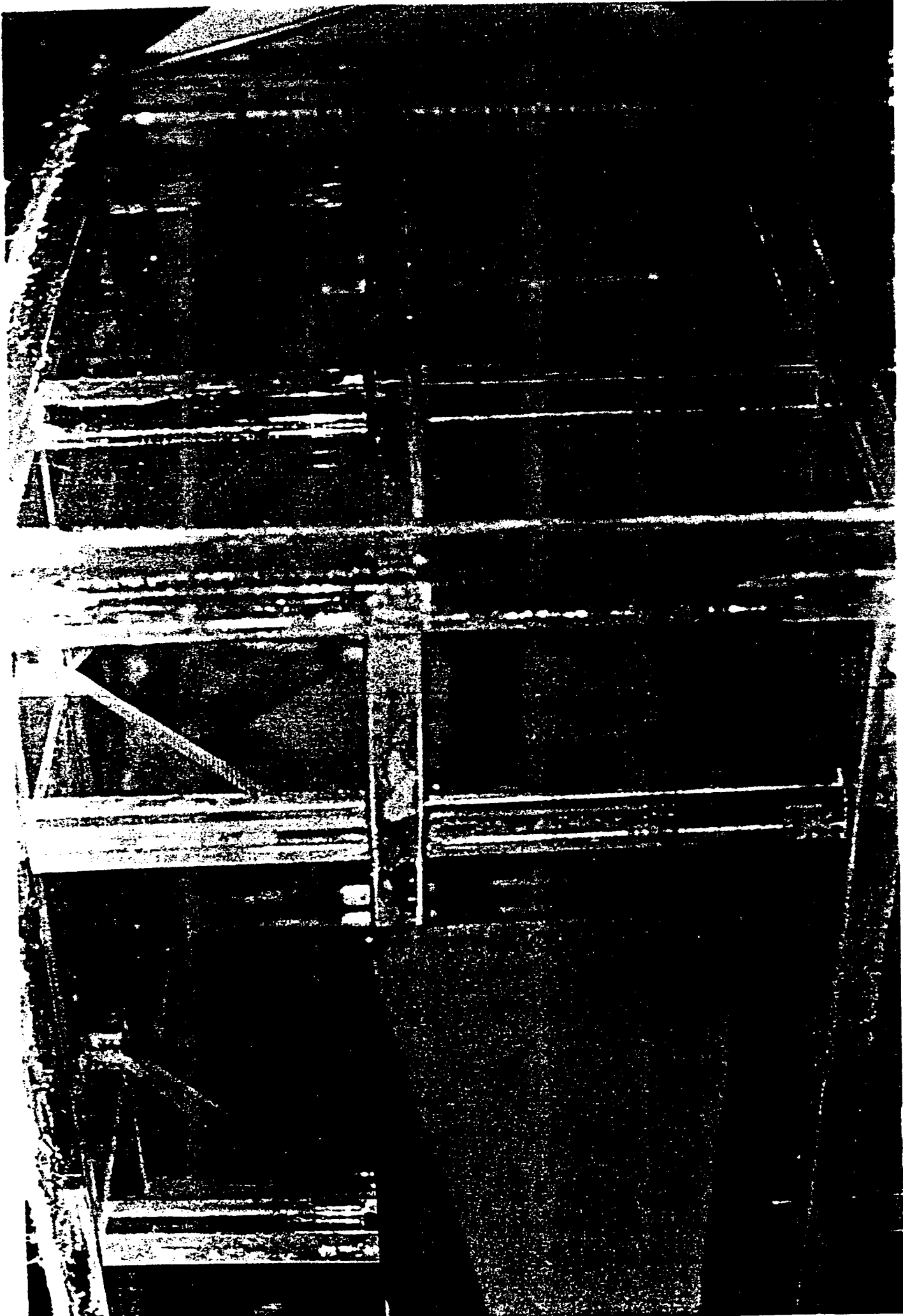
Peak Voltage and Current: 2.8 kV and 2 A

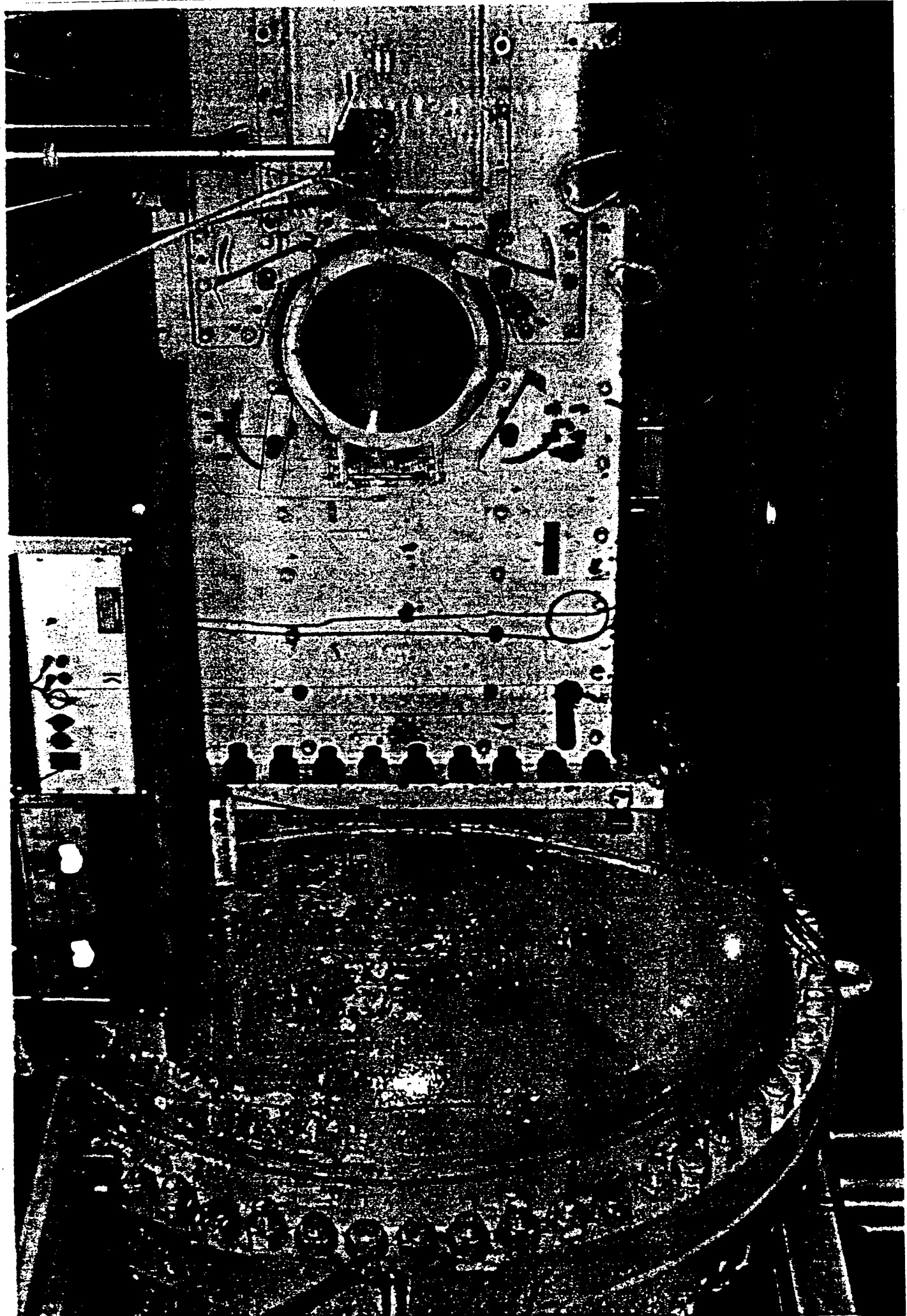
Microwave Plasma Layers

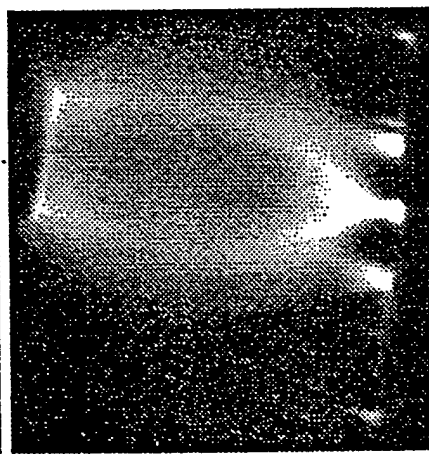
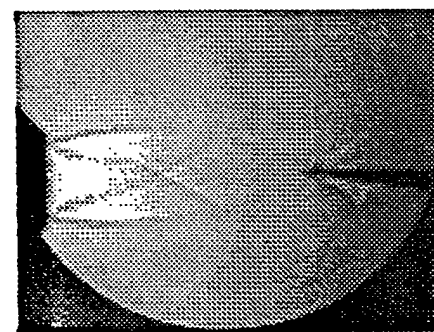
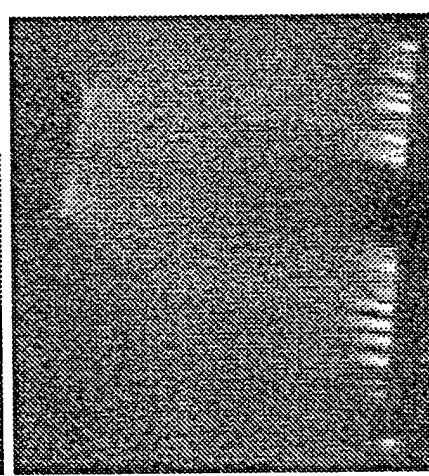
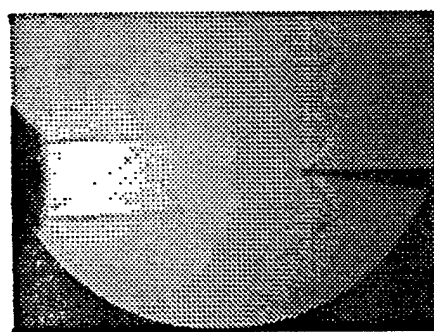
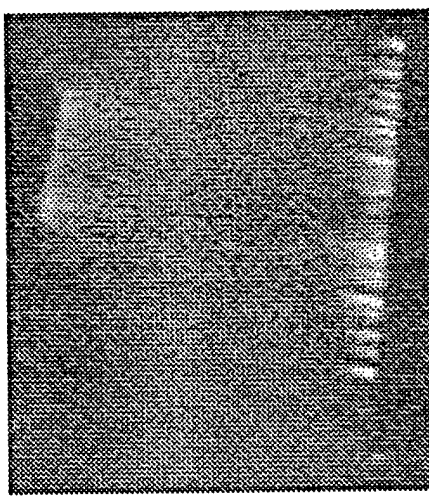
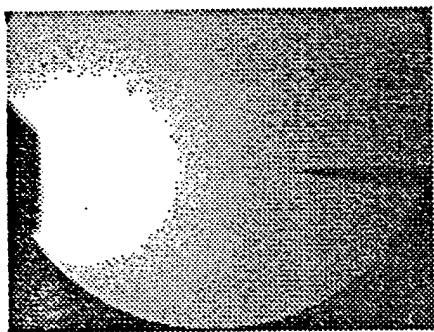
Pressure: 20 torr

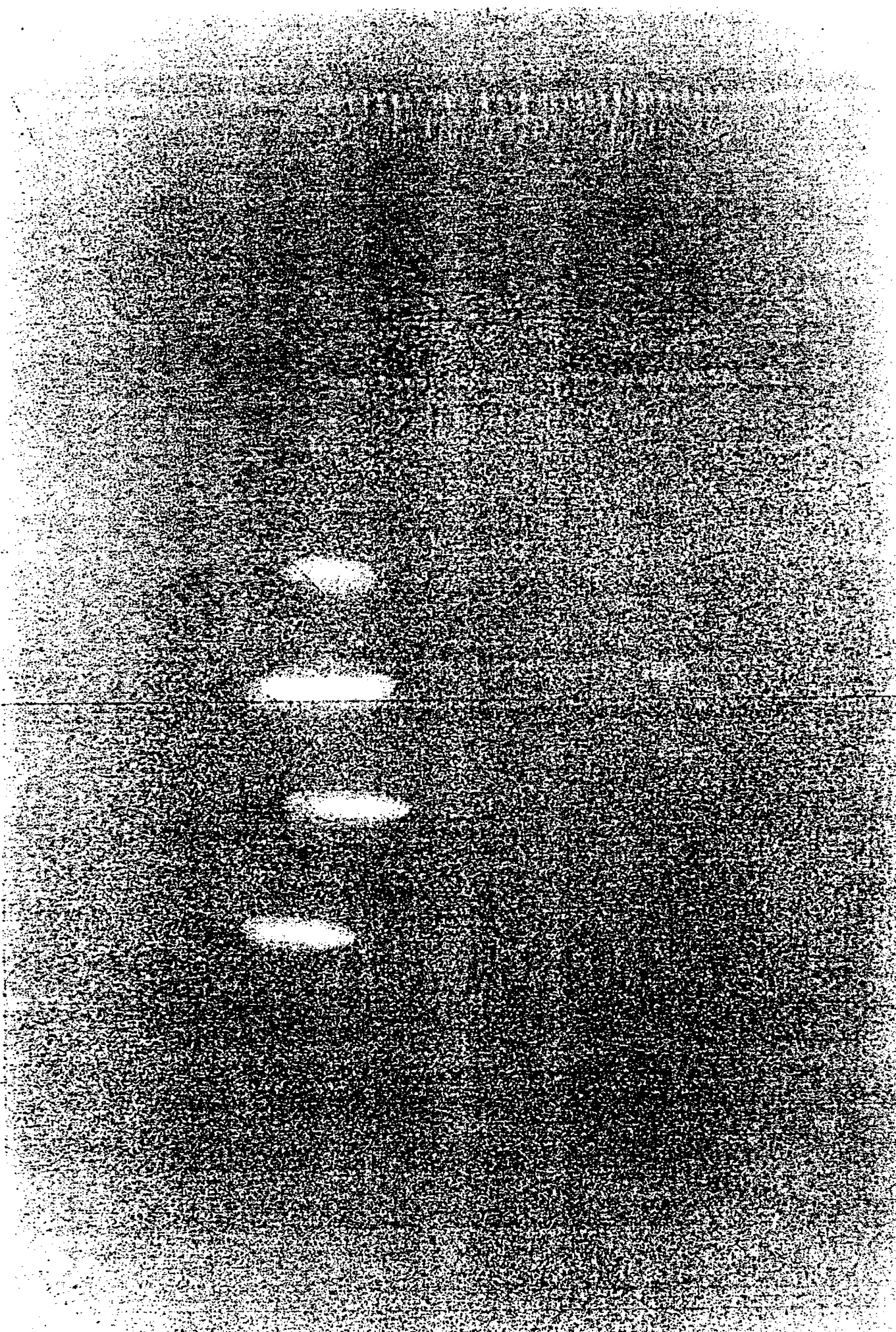
Density: 10^{11} cm^{-3}

Microwave Power: 1 MW peak, 1 μs pulse, 40 rps









Plasma Ramparts Using Metastable Molecules

MURI Program

**The Ohio State University
Princeton University**

"Optically Pumped Nonequilibrium Plasmas"

I. Adamovich, V. Subramaniam, W. Rich

Presented at

**AFOSR Workshop
"Understanding and Control of
Ionized High-Speed Flows"**

**Princeton University
Feb. 26-27, 1998**

**Work funded by the Director of Defense Research &
Engineering (DDR&E) within the Air Plasma Ramparts
MURI Program managed by AFOSR**

Program Objectives:

- Create large volume ($O[m^3]$) free air plasma
- One atmosphere
- Free electron densities 10^{13} cm^{-3} or greater
- Gas temperature less than 2,000 K
- Energy efficient method

Approaches:

A. Thermal Plasmas (High Temperature Arcs, Reentry Plasmas)

Problems:

I) High Temperature

B. NonThermal Plasmas (Glow Discharges, Optically Pumped Plasmas)

Problems:

I) Requires thermodynamic work (electrical work, laser work)

II) Stability

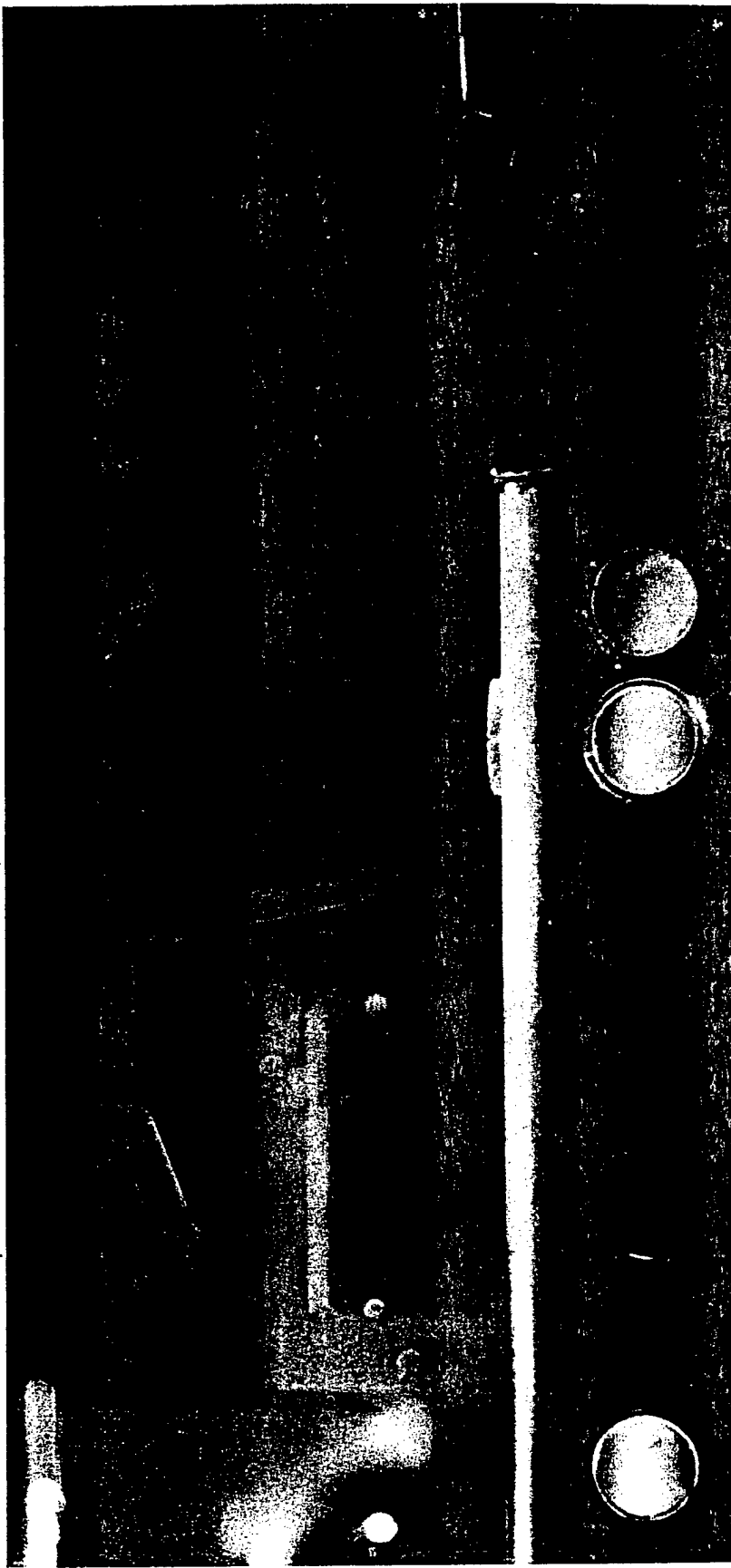
OSU/Princeton Approach: Laser Pumped Metastable State Plasmas.

92 W cw broad-band lasing conditions

Date: 10-26-1992			
Gas	Partial Pressure (Torr)	mass flow rate (10^3 g/min)	
He internal purge	4.15	18.9	
He	9.00	75.5	
N ₂	2.75	138	
CO	1.60	6.61	
Air	.01	.89	
Total	17.5	239	

He:CO:N ₂ molar ratio 751:92:157	
Discharge Conditions	
Current mA DC	45
Voltage kV DC	18
Laser Power Broad Band W	92
Physical Efficiency	30.3%

The Ohio State University



Nonequilibrium Thermodynamics Laboratories

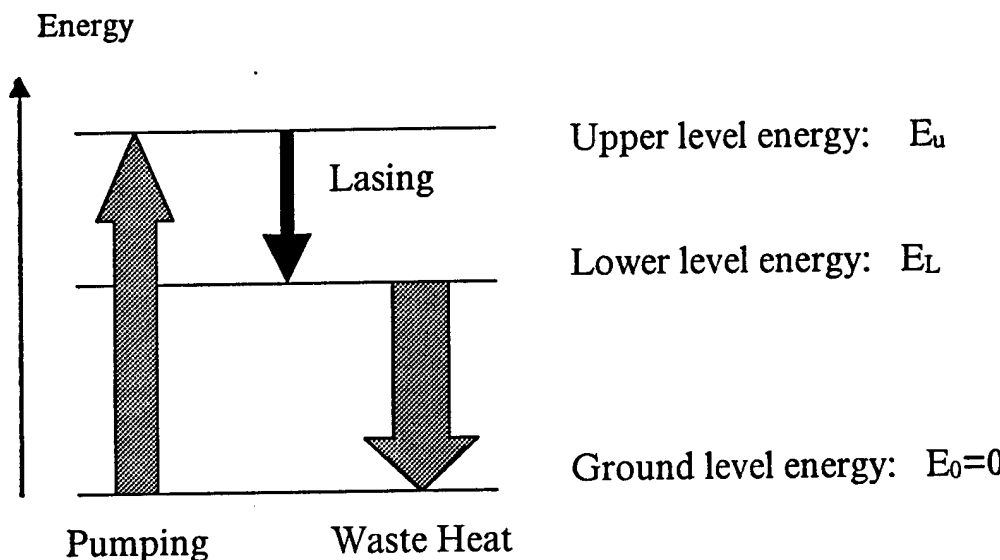
Advantages:

- **Stable, large volume**
- **High pressure**
- **Low gas temperatures**

Problems:

- **Electron density**
- **Efficiency**
- **Non-air species**

Three Level Laser



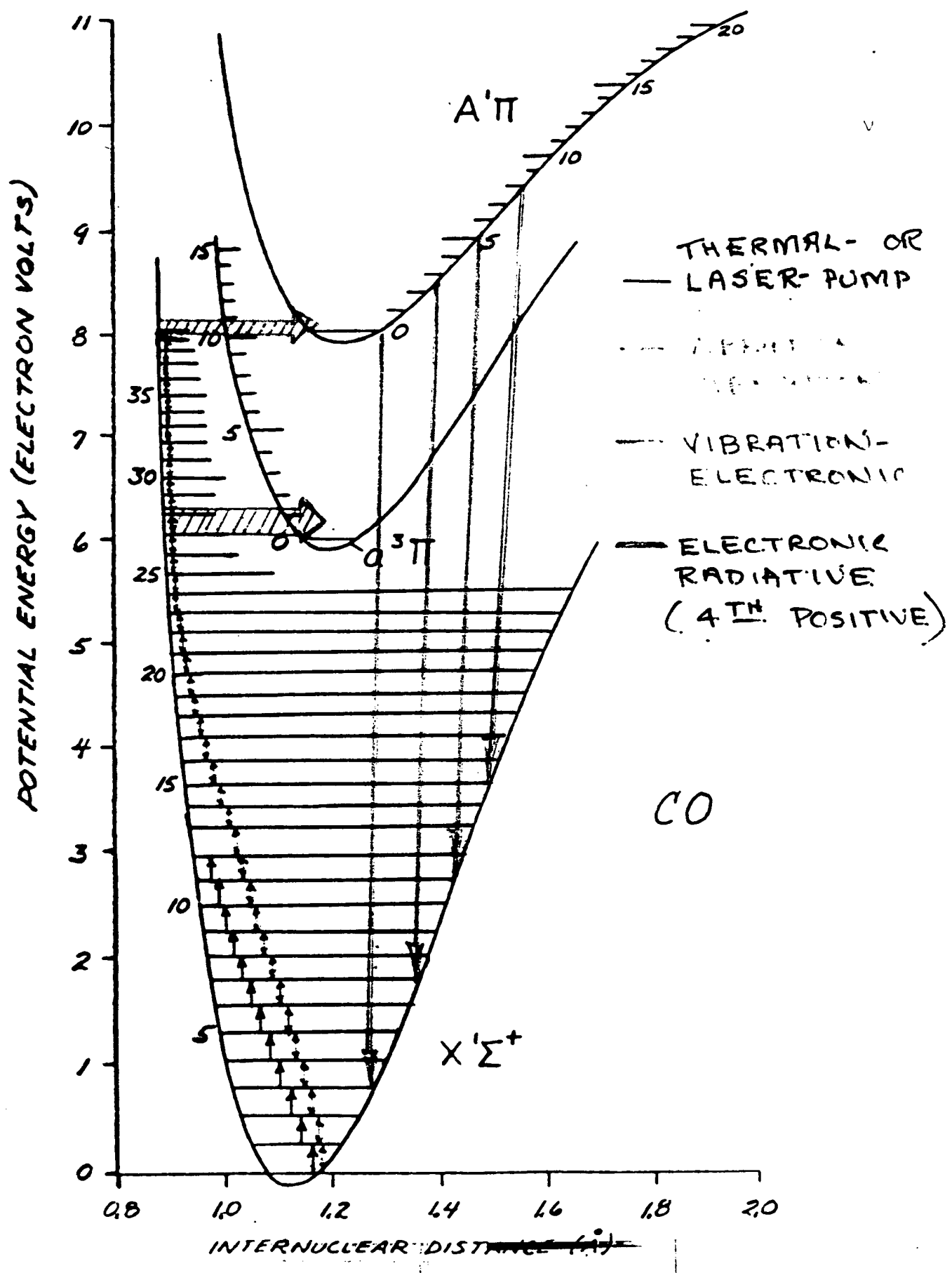
Quantum Efficiency

$$\eta_{\text{quantum}} = \frac{E_u - E_L}{E_L}$$

$\sim 40\%$ for CO_2/N_2

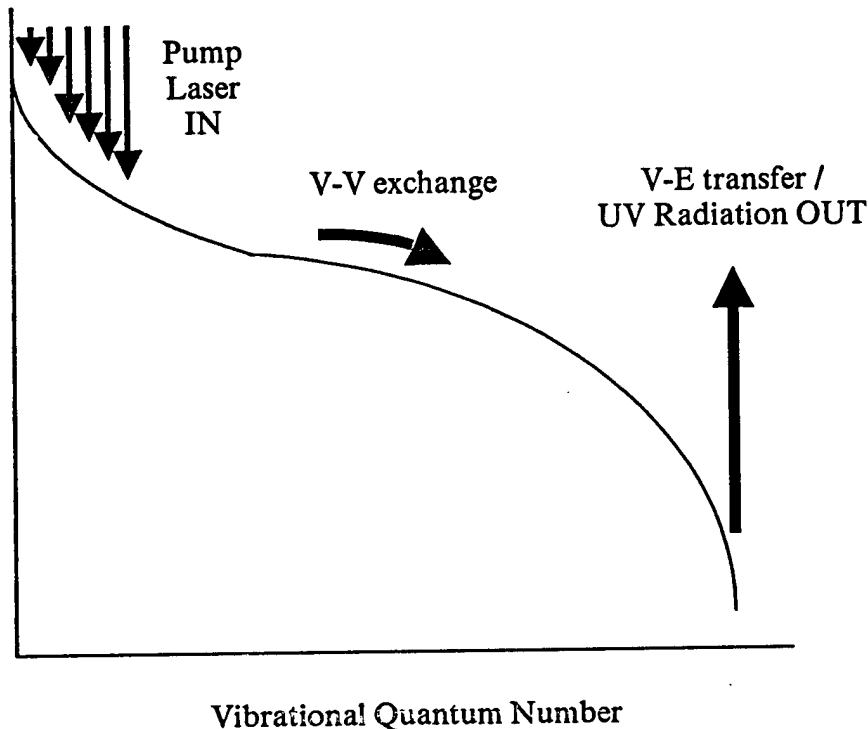
$\sim 95\%$ for CO/N_2

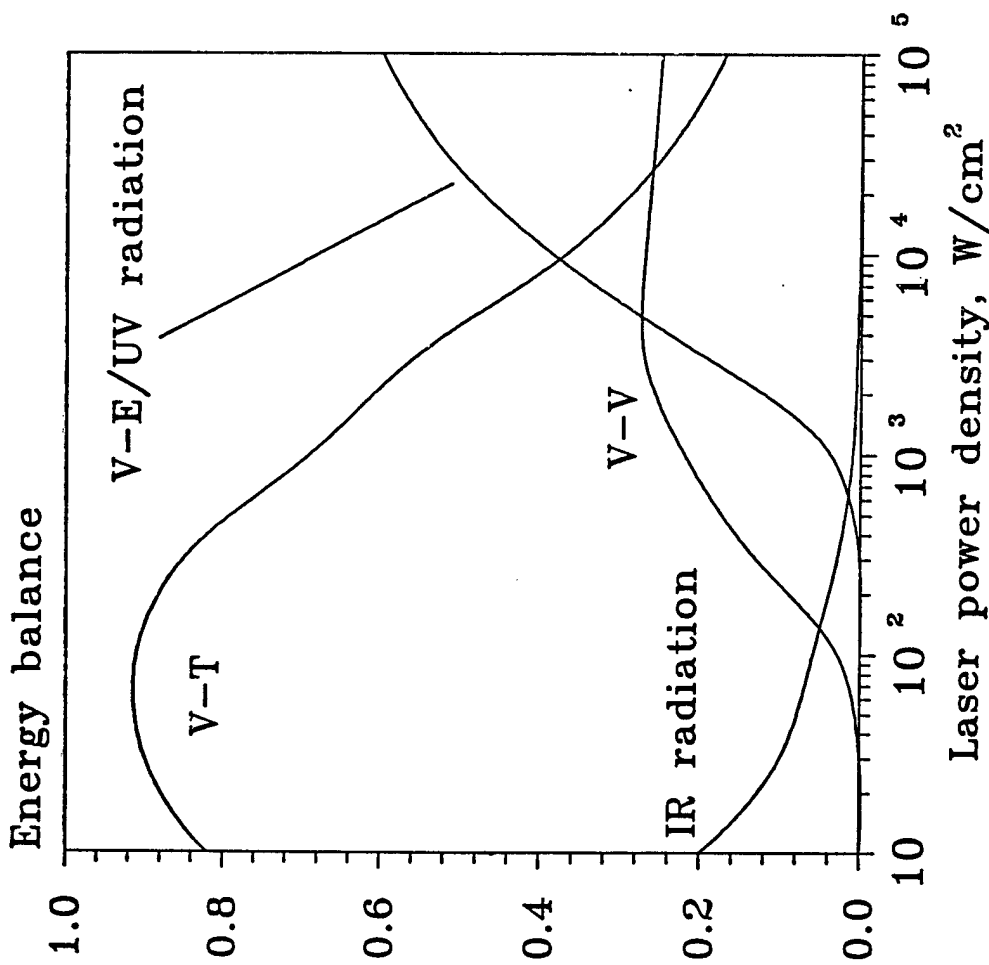
Scoville, 1954 showed equivalence
with reversible engine efficiency

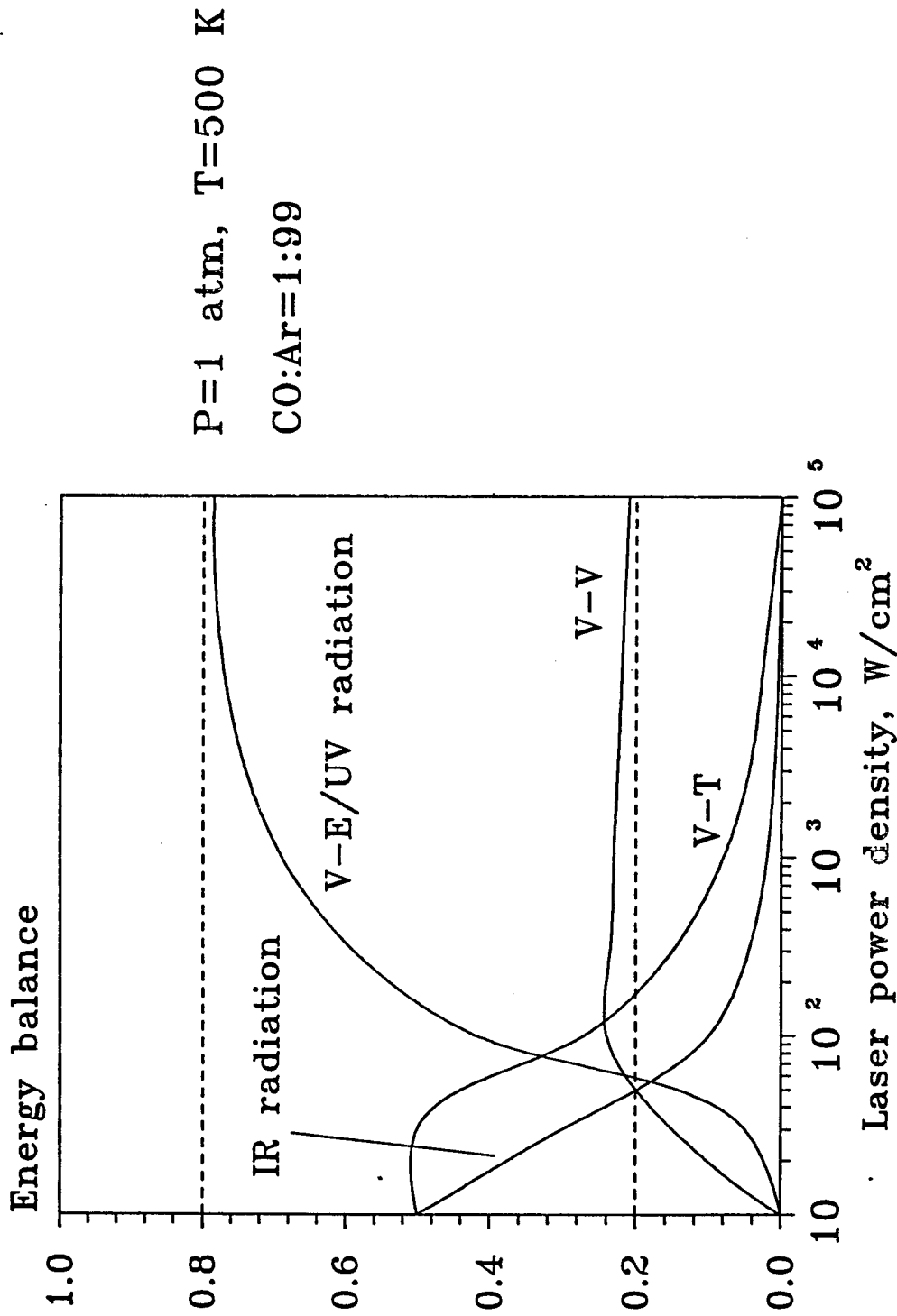


IR/UV Radiation Conversion in Optically Pumped CO-Ar Plasma

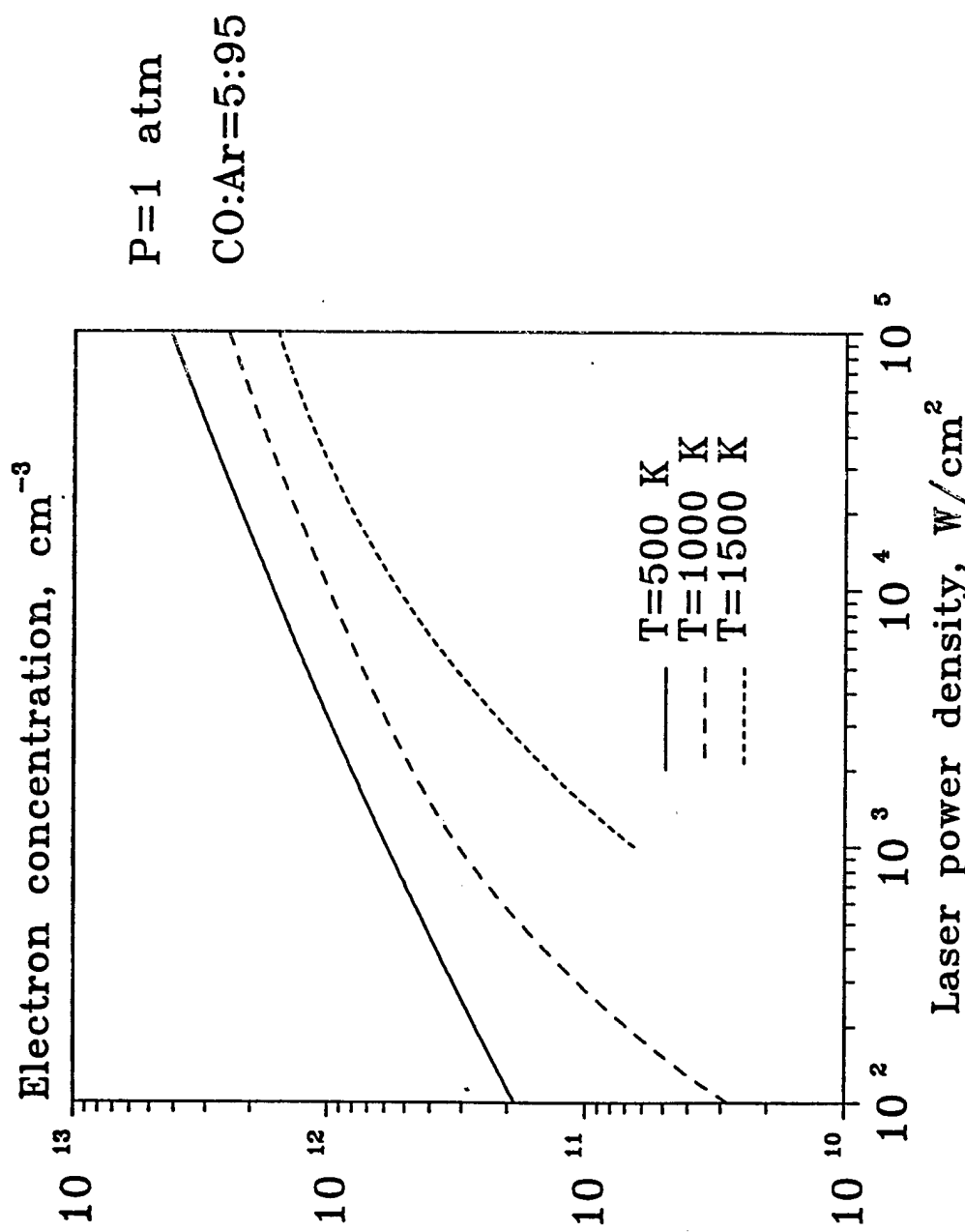
Relative population





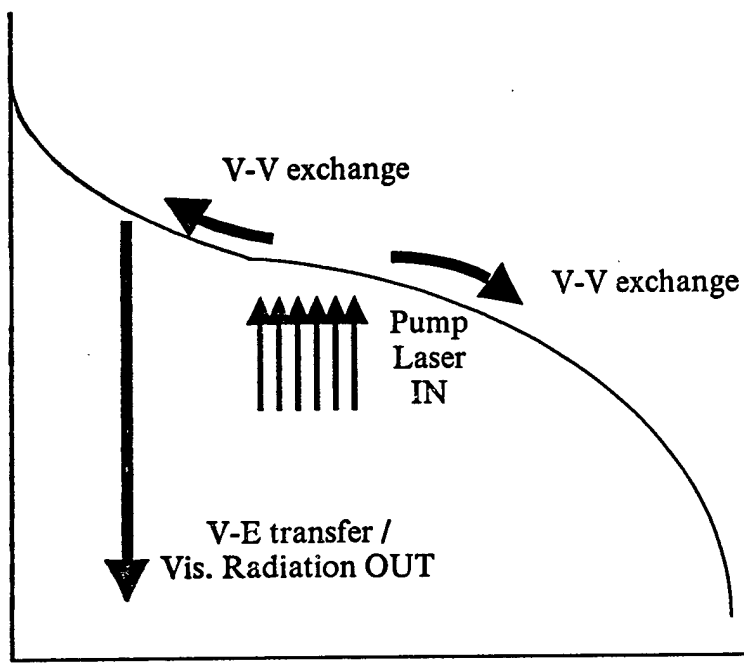


Nonequilibrium Thermodynamics Laboratories

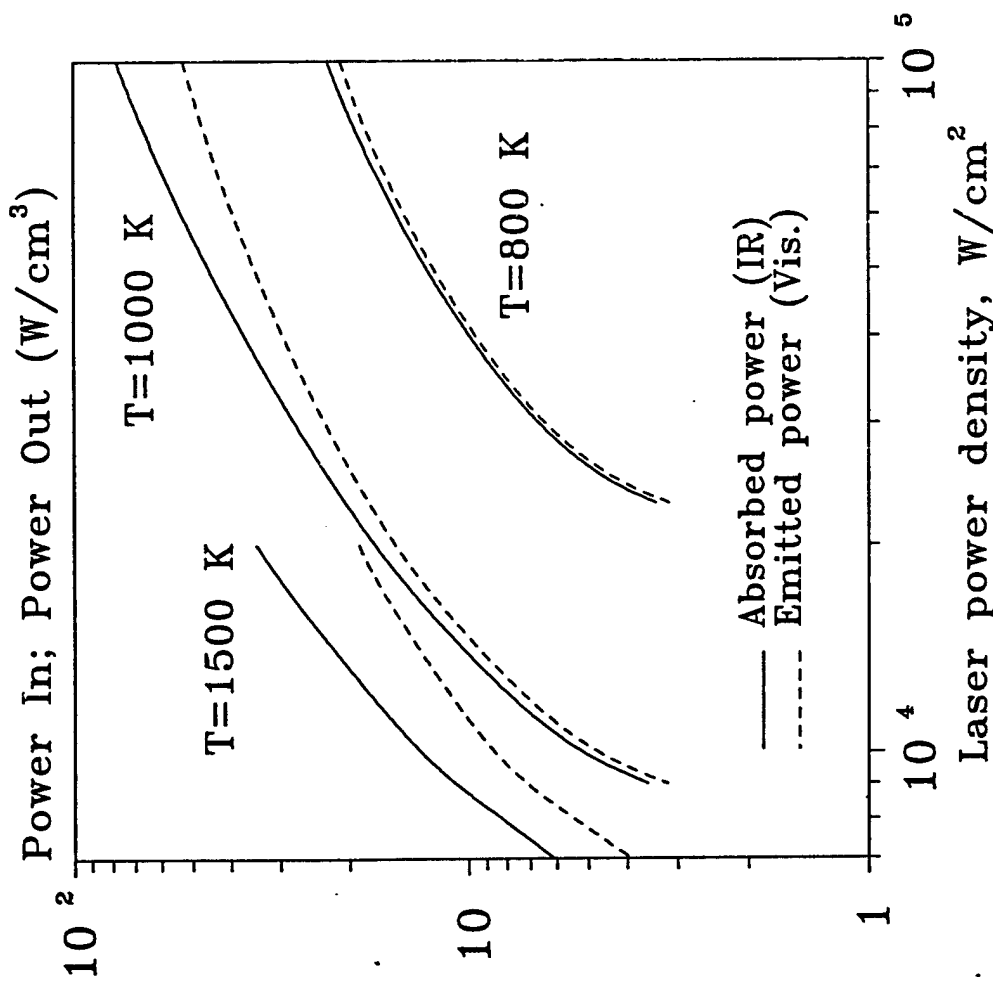


IR/Visible Radiation Conversion
in Optically Pumped CO-N₂-Na Plasma

Relative population



Vibrational Quantum Number



The Ohio State University

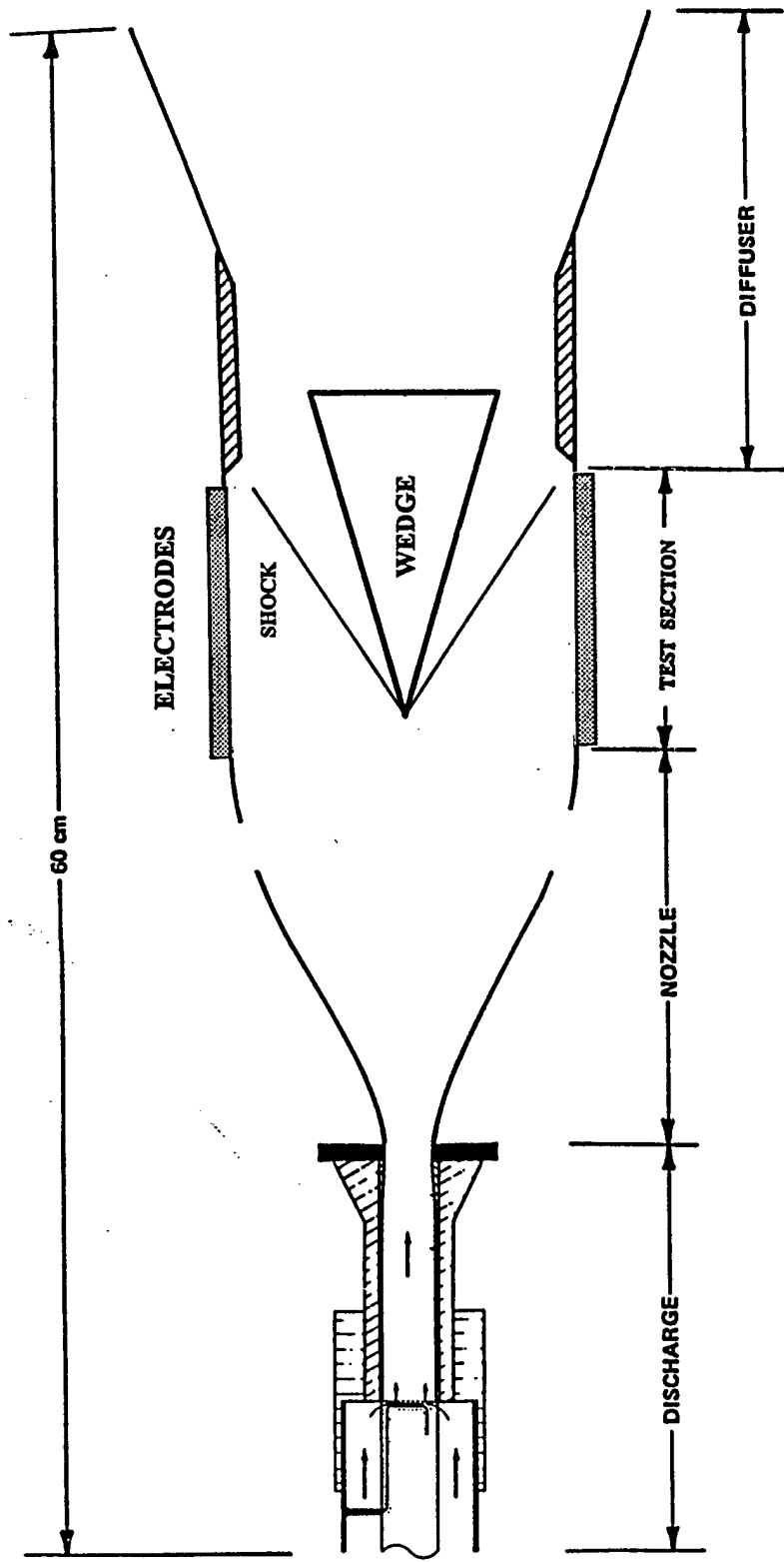
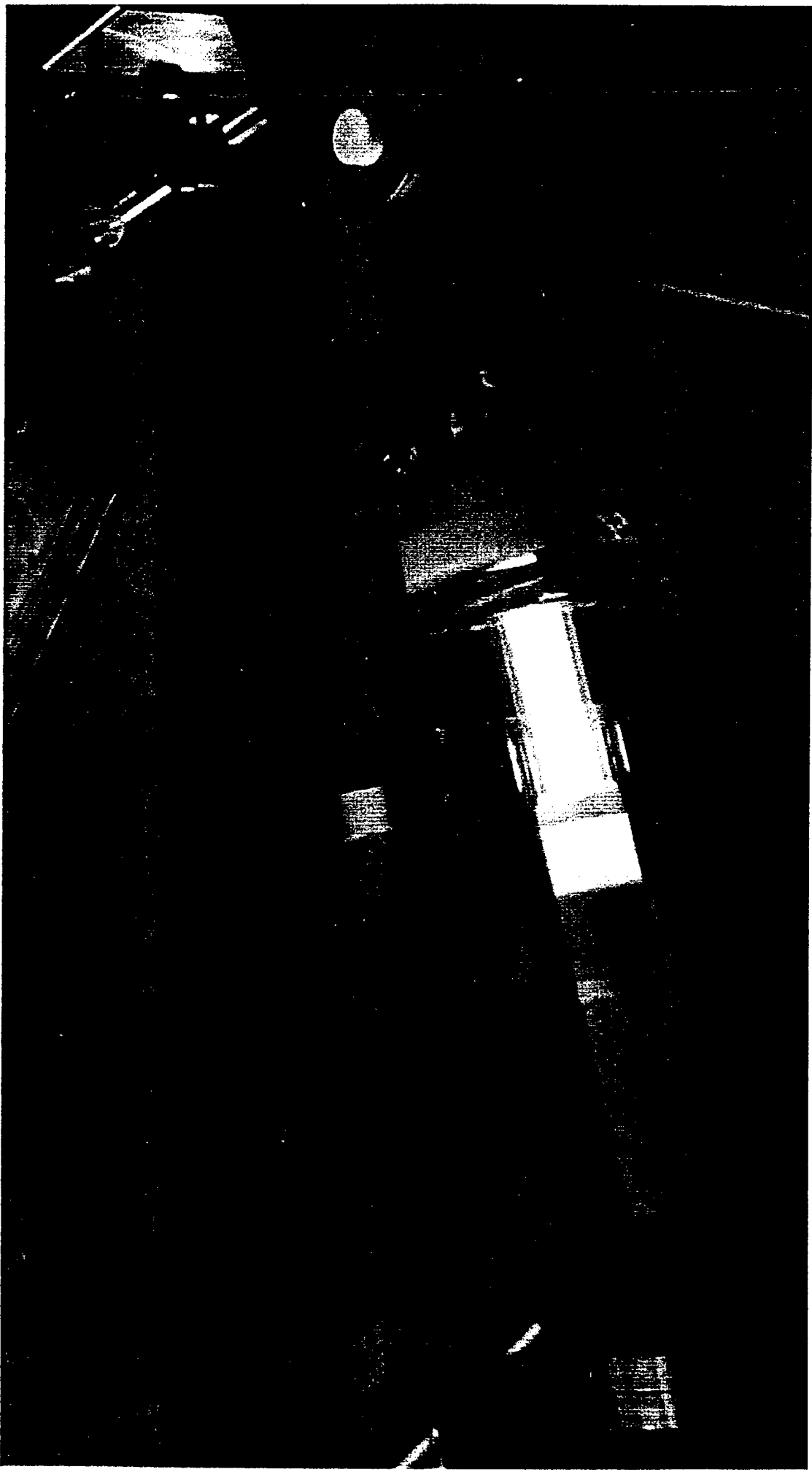


Figure 1. The schematic of the flowing afterglow experiment.

Nonequilibrium Thermodynamics Laboratories



GRADIENT DISTORTION EXPERIMENT

- Transverse temperature gradient is created by absorption of CO laser radiation (1-2% CO is added to the flow to enable absorption and as a thermometric element).

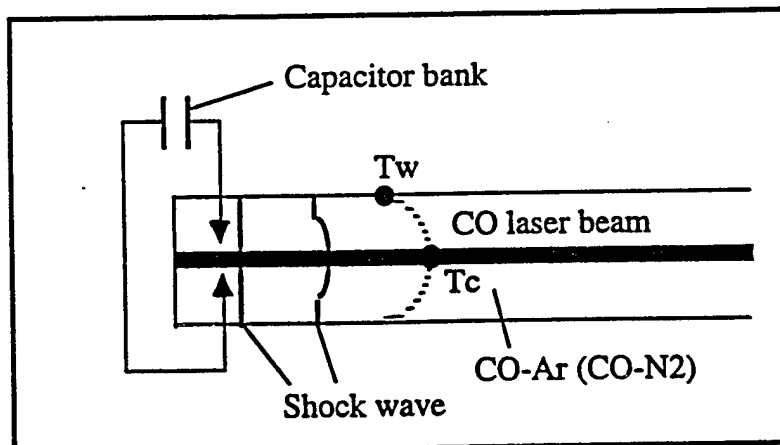
At P=100 Torr, $dT/dr \sim 100 \text{ K/cm}$

Routinely used in CO and NO optical pumping kinetic experiments.

- Plane shock wave created by a capacitor bank discharge.

Measurements of:

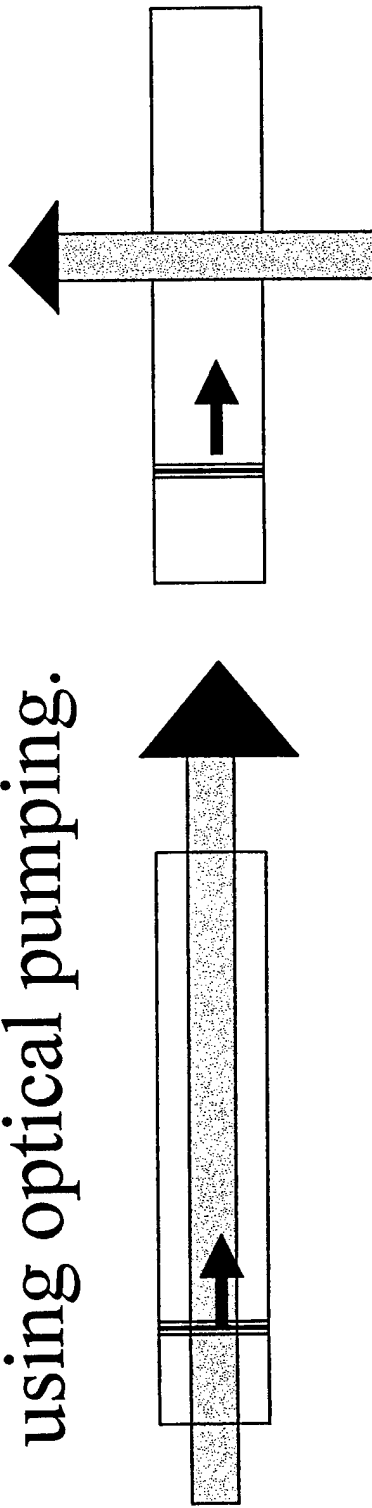
- flow density distribution
- Gas temperature and transverse temperature gradient before the shock arrival



- Radial temperature profile is parabolic:
$$T(r) = T_c - (T_w - T_c)(r/R)^2$$

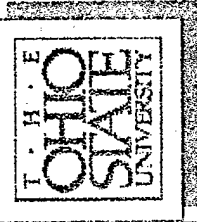
Experimental verification

- Repeat Ganguly-Bletzinger experiment with thermal effects alone - pure, non-intrusive gas heating induced in CO-seeded Argon, using optical pumping.



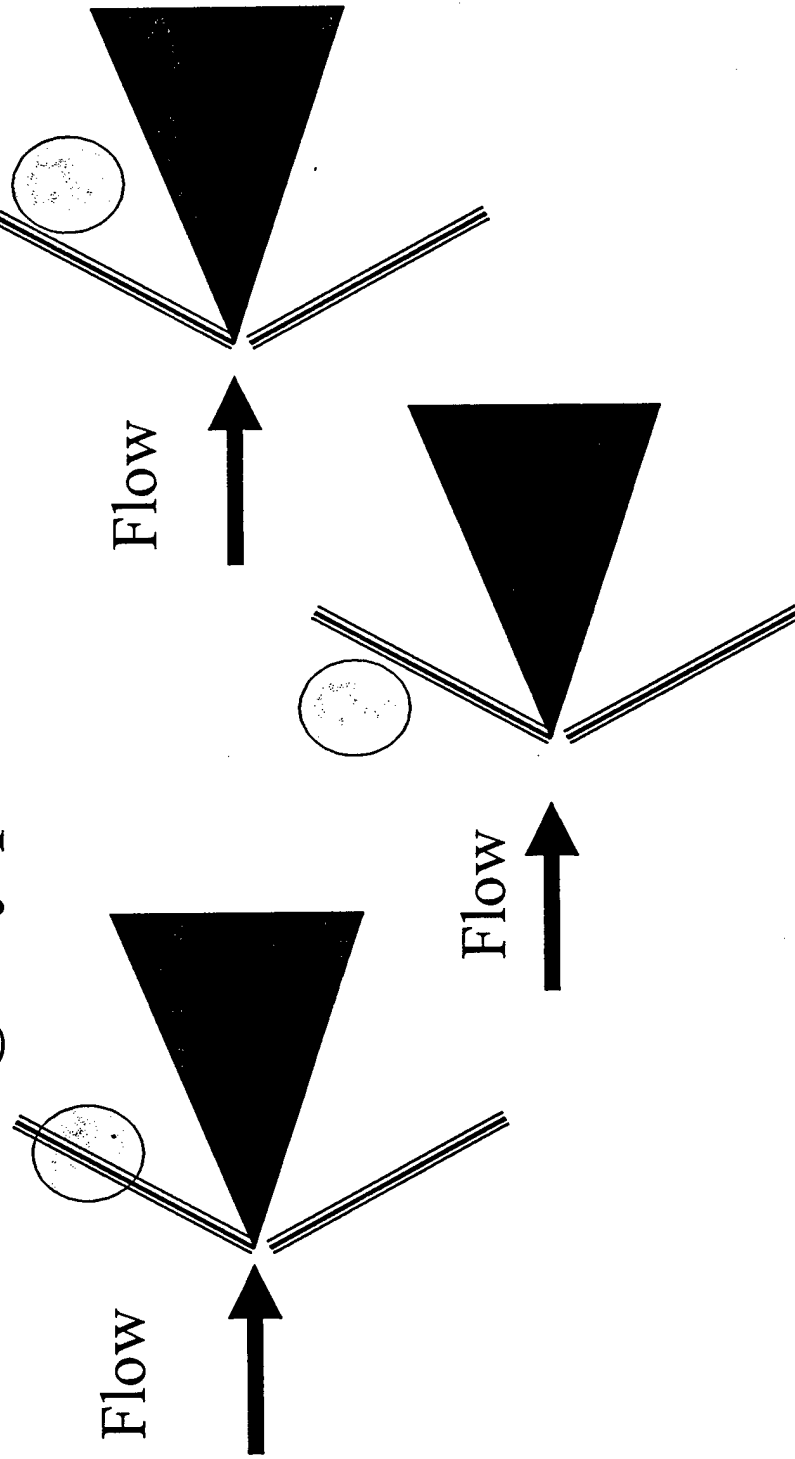
Axially directed CO laser beam

Transverse directed
CO laser beam



Experimental Validation

- Body in wind-tunnel; Thompson discharge by photo-ionization



COMPRESSION
OF A
FIELD-FREE,
NON-HOMOGENEOUS
PLASMA

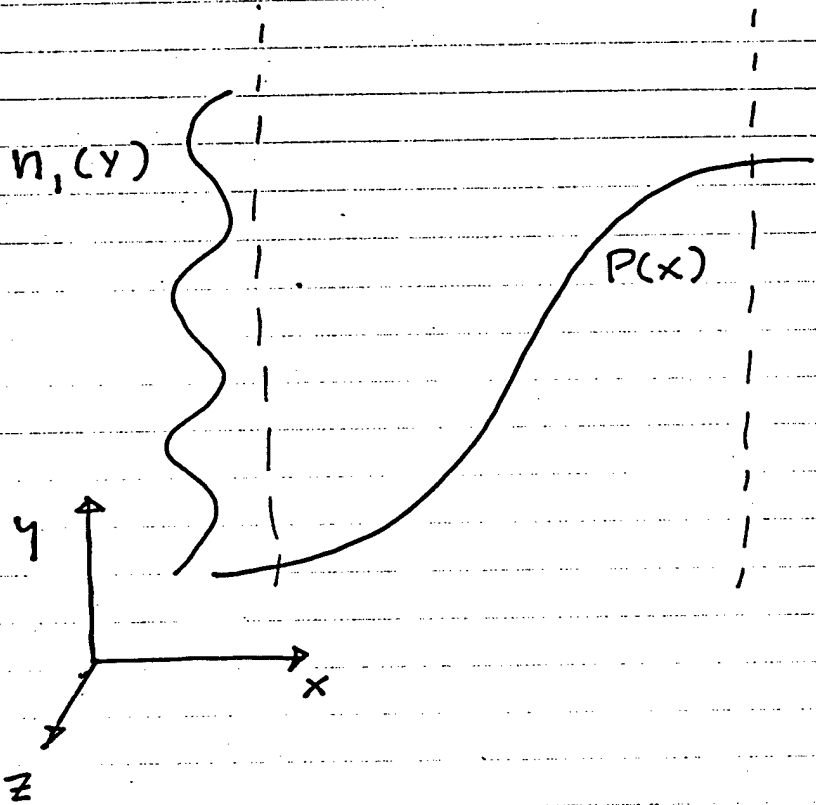
P. J. TURCHI *

AFRL/DE

KIRTLAND AFB, NM

* PROFESSOR OF AEROSPACE ENGINEERING,
THE OHIO STATE UNIVERSITY.

BASIC FORMULATION



OHM'S LAW IN LIMIT
OF HIGH DENSITY
AND LOW CONDUCTIVITY

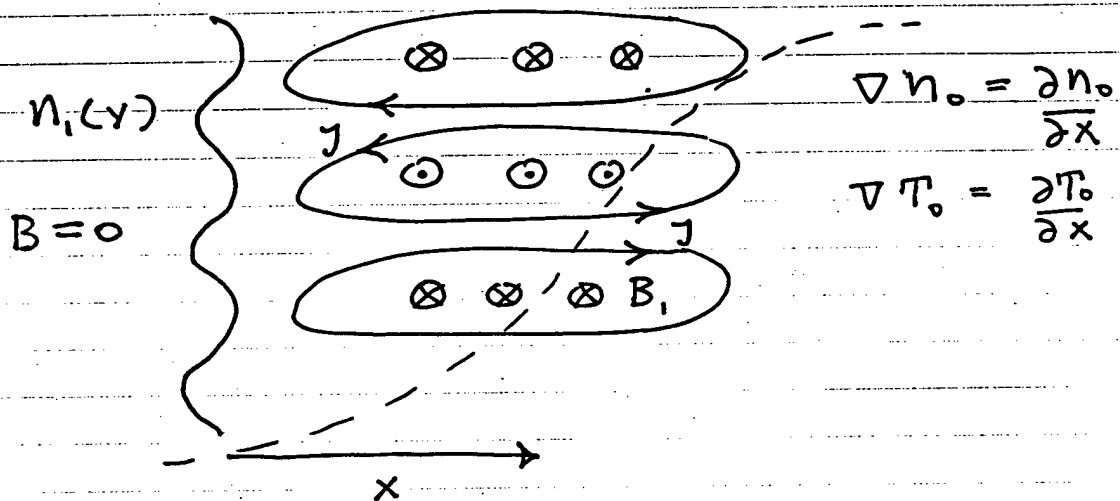
$$\Omega_e \rightarrow 0, R_m \rightarrow 0$$

$$\vec{E} = \gamma \vec{j} - \frac{1}{n_e e} \nabla P_e$$

(EXPECTATION THAT PLASMA IS TOO RESISTIVE
INITIALLY TO PERMIT FLUX CONVECTION)

$$\frac{\partial \vec{B}}{\partial t} = -\nabla \times (\gamma \vec{j}) - \left(\frac{k}{e}\right) \frac{\nabla n_e \times \nabla T_e}{n_e}$$

QUALITATIVE BEHAVIOR



$\nabla n \times \nabla T$ TERM CAUSES GROWTH

OF MAGNETIC FIELD INTO AND OUT OF PLANE

AND ASSOCIATED IN-PLANE CURRENTS

TENDENCY TO TRANSFER AND CONCENTRATE

ENERGY FROM REGIONS OF GENERATION

TO REGIONS OF DISSIPATION

$$P_d = -\vec{E} \cdot \vec{J}$$

(CURRENT DENSITY DIRECTION ALTERNATES
MAIN PRESSURE-GRADIENT INDUCED
ELECTRIC FIELD MAINTAINS DIRECTION)

POSSIBLE NONLINEAR EFFECTS

RESISTIVE HEATING MAY CHANGE PLASMA

$$\gamma j^2 \rightarrow \frac{dP_e}{dy}$$

CHANGING PLASMA MAY CHANGE TRANSPORT

$$\gamma = \gamma(n_e, T_e)$$

$$\lambda = \lambda(n_e, T_e)$$

THESE CHANGES GREATLY COMPLICATE THE

ARITHMETIC, BUT MAY BE CRITICAL

FOR DESCRIBING EXPERIMENTAL BEHAVIOR

- FURTHER CONCENTRATION OF
CURRENTS AND IONIZATION

- OPPORTUNITY FOR HEAT TRANSPORT
AT SHOCK VIA HOT COLUMNS

LINEARIZED ANALYSIS

LOOK FOR ELEMENTS OF BEHAVIOR
WITH SIMPLIFIED ARITHMETIC

LET MAIN FLOW CARRY PRESSURE GRADIENT

IN X-DIRECTION

$$\frac{\partial P_0}{\partial x}$$

TRANSVERSE VARIATION OF DENSITY

AND TEMPERATURE AT FIXED PRESSURE

$$\frac{\partial n}{\partial y}, \frac{\partial T}{\partial y} \quad \text{WITH} \quad \frac{\partial P_1}{\partial y} = 0$$

SOLVE FOR VARIATION OF (WEAK) MAGNETIC

FIELD AS FUNCTION OF BOTH X AND Y

$$\vec{B} = B \hat{k} = B_0 + \epsilon B_1(x, y)$$

$$\text{WITH } B_0 = 0 \quad \epsilon \ll 1$$

LINEARIZED ANALYSIS (CONTINUED)

SPECIFY

$$n(x, y) = n_0(x)(1 + \epsilon \sin Ky)$$

AT $\frac{\partial P}{\partial y} = 0$, THEN

$$T(x, y) \cong T_0(x)(1 - \epsilon \sin Ky)$$

WHERE $P_0(x) = n_0 R T_0$ ('0' REFERS TO
ZEROTH ORDER,
NOT STAGNATION)

Also, RESISTIVITY

$$\gamma = \gamma_0 + \epsilon \gamma_1$$

SUBSTITUTION INTO FARADAY'S LAW YIELDS AT $O(\epsilon)$:

$$\frac{\partial B_1}{\partial t} = \frac{1}{\mu} \left\{ \gamma_0 \left(\frac{\partial^2 B_1}{\partial x^2} + \frac{\partial^2 B_1}{\partial y^2} \right) + \frac{\partial B_1}{\partial x} \left[\left(\frac{\partial \gamma_0}{\partial n_e} \right) \frac{\partial n_0}{\partial x} + \left(\frac{\partial \gamma_0}{\partial T_e} \right) \frac{\partial T_0}{\partial x} \right] \right.$$

$$\left. + \frac{K \cos Ky}{en_0} \frac{\partial P_0}{\partial x} \right\}$$

STEADY STATE, $\frac{\partial B_1}{\partial t} = 0$,

$$\left(\frac{\gamma_0}{\mu} \right) \left[\frac{\partial^2 B_1}{\partial x^2} + \frac{\partial^2 B_1}{\partial y^2} \right] + \frac{1}{\mu} \frac{\partial B_1}{\partial x} \left[\left(\frac{\partial \gamma_0}{\partial n_e} \right) \frac{\partial n_0}{\partial x} + \left(\frac{\partial \gamma_0}{\partial T_e} \right) \frac{\partial T_0}{\partial x} \right]$$

$$= - \frac{K \cos Ky}{en_0} \frac{\partial P_0}{\partial x}$$

LINEARIZED ANALYSIS (CONTINUED)

TRY SOLUTION OF FORM:

$$B(x, y) = b(x) \cos k y$$

WHICH PROVIDES EQUATION:

$$\left(\frac{\gamma_0}{\mu}\right) \left[\frac{d^2 b}{dx^2} - k^2 b \right] + \frac{1}{\mu} \frac{db}{dx} \left[\left(\frac{\partial \gamma_0}{\partial n_e}\right) \frac{\partial n_0}{\partial x} + \left(\frac{\partial \gamma_0}{\partial P_e}\right) \frac{\partial P_0}{\partial x} \right]$$
$$= -K \frac{dP_0}{dn_0} \frac{dP_0}{dx}$$

EXPLORE SIMPLER CASE: LET $\gamma_0 = \text{CONSTANT}$

$$\left(\frac{\gamma_0}{\mu}\right) \left[\frac{d^2 b}{dx^2} - k^2 b \right] = -\frac{K}{\gamma_0 e n_0} \frac{dP_0}{dx}$$

OR

$$\frac{d^2 b}{dx^2} - k^2 b = -\frac{\mu K}{\gamma_0 e n_0} \frac{dP_0}{dx}$$

NORMALIZED EQUATIONS

LET $P_0(x) = \frac{b_c^2}{2m} \beta(\alpha)$ WHERE $\alpha = x/\lambda$
AND $k = 2\pi/\lambda$

$$b(x) = b_c f(\alpha)$$

$$n_0(x) = \frac{P_0(x)}{k T_0(x)} = \frac{b_c^2}{2m k T_0} \frac{\beta(\alpha)}{\theta(\alpha)}$$

SUBSTITUTION THEN PROVIDES:

$$\frac{d^2f}{d\alpha^2} - 4\pi^2 f = -\left(\frac{2\pi m k T_0}{\gamma_0 e b_c}\right) \frac{\theta(\alpha)}{\beta(\alpha)} \frac{d\beta}{d\alpha}$$

WHICH FURTHER SIMPLIFIES TO:

$$\frac{d^2f}{d\alpha^2} - 4\pi^2 f = -\frac{\theta(\alpha)}{\beta(\alpha)} \frac{d\beta}{d\alpha}$$

BY DEFINING $b_c = \frac{2\pi m k T_0}{\gamma_0 e}$

SOLUTION OF NORMALIZED EQUATION

HOMOGENEOUS PART:

$$\frac{d^2 f_H}{d \alpha^2} = 4\pi^2 f_H$$

$$f_H = C_1 e^{2\pi\alpha} + C_2 e^{-2\pi\alpha}$$

PARTICULAR SOLUTION, WITH FURTHER SIMPLIFICATION $\theta=1$,

$$\frac{d^2 f_p}{d \alpha^2} - 4\pi^2 f_p = -\frac{1}{\beta} \frac{df}{d\alpha}$$

TRY FORM OF $f_p(\alpha)$ THAT PROVIDES USEFUL FORM

FOR $\beta(\alpha)$:

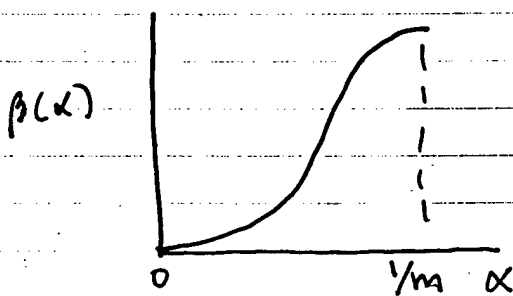
$$f_p(\alpha) = a \sin(m\pi\alpha)$$

THIS GIVES (BY SUBSTITUTION AND INTEGRATION):

$$\beta(\alpha) = \beta_1 e^{\frac{a\pi(m^2-4)}{m}[1-\cos(m\pi\alpha)]}$$

$$\alpha = 0, \beta = \beta_1$$

$$\alpha = y_m, \beta = \text{MAXIMUM}$$



THICKNESS OF
PRESSURE RISE:

$$\gamma = \lambda/m$$

(WHICH GIVES m)

SOLUTION OF NORMALIZED EQUATION
(CONTINUED)

WITH $b_1 = 0$ AT $x = 0$ ($f(0) = 0$)

AND $\frac{db_1}{dx} = 0$ ALSO $\frac{df}{dx} = 0$)

THE FULL SOLUTION IS:

$$B_1(x, y) = \frac{\mu k T_0}{\gamma_0 e} \cos\left(\frac{2\pi y}{\lambda}\right) \frac{(\lambda/\zeta) \ln \gamma}{\left[\left(\frac{\lambda}{\zeta}\right)^2 - 4\right]}$$

$$\left\{ \sin\left(\frac{\pi x}{\zeta}\right) - \frac{\lambda}{2\zeta} \sinh\left(\frac{2\pi x}{\lambda}\right) \right\}$$

WHERE λ IS THE WAVELENGTH OF
TRANSVERSE PERTURBATIONS OF PLASMA

ζ IS THE COMPRESSION THICKNESS

AND γ IS THE PRESSURE RATIO

THE SOLUTION IS RESTRICTED TO

$$0 \leq x \leq \zeta \quad \lambda/\zeta > 2$$

(AND LINEARIZED ANALYSIS)

IT CAN MATCH TO $x \geq \zeta$ WITH UNIFORM PRESSURE,
FOR WHICH B DECREASES EXPONENTIALLY WITH x/λ .

CONCLUDING REMARKS

- INTERACTION OF COMPRESSION WAVE WITH FIELD-FREE, NONHOMOGENEOUS PLASMA CAN GENERATE CURRENT CONCENTRATIONS DUE TO $\nabla n \times \nabla V$ PROCESS.
- MAGNITUDES OF CURRENT DENSITIES INCREASE EXPONENTIALLY AS x/λ (FOR LINEARIZED SOLUTION) THROUGH THE THICKNESS OF COMPRESSION
- NONLINEAR EFFECTS IN PLASMA MAY RESULT IN FURTHER CONCENTRATION AND INCREASED TRANSPORT
- THE RESULT OF SUCH CONCENTRATION OF ENERGY AND * INCREASED TRANSPORT MAY BE CHANGE IN FLOW STRUCTURE AND RELATED AERODYNAMIC DRAG